Étude du développement des racines protéoïdes chez le lupin blanc

Cécilia Gallardo

THÈSE POUR OBTENIR LE GRADE DE DOCTEUR DE L'UNIVERSITÉ DE MONTPELLIER

En Biologie du Développement

École doctorale n°584 GAIA : Biodiversité, Agriculture, Alimentation, Environnement, Terre, Eau

Unité mixte de recherche BPMP : Biologie et Physiologie Moléculaire des Plantes

Étude du développement des racines protéoïdes chez le lupin blanc

Présentée par CECILIA GALLARDO

Le 06 décembre 2019

Sous la direction de Dr. Benjamin Péret

Devant le jury composé de

Stéphanie Robert, Associate Professor, Umeå, Suède	**Rapporteur**
Florian Frugier, Directeur de Recherche, CNRS, Paris	**Rapporteur**
Sandra Bensmihen, Chargé de Recherche, CNRS, Toulouse	**Examinateur**
Laurent Laplaze, Directeur de Recherche, IRD, Montpellier	**Examinateur**
Pascal Gantet, Professeur, Université de Montpellier, Montpellier	**Président du Jury**
Benjamin Péret, Chargé de Recherche, CNRS, Montpellier	**Directeur de thèse**

Abstract in English

Cluster roots (CRs) are striking root developmental adaptations to soils with scarce nutrient avaibility. The development of these spectacular structures, made of dozen of short packed small roots named rootlets, is mainly triggered in phosphate-deprived conditions. These particular secondary root stuctures are dedicated to improve phosphate acquisition by the plant, and are of interest for plant nutrition. Surprisingly, even though white lupin (*Lupinus albus*) is a model species for the study of CRs, little information can be found about their formation and the molecular mechanisms behind it.

To better understand rootlet formation in white lupin, an anatomical description was performed. Starting with a tissular study, 8 stages in rootlet primordium development were defined by analogy with the model plant *Arabidopsis thaliana*. Due to the major role of the phytohormone auxin in the formation of lateral roots, the work was next focussed on auxin response. The expression of the DR5:GUS auxin reporter showed that an auxin maximum was gradually established at the tip of the rootlet primordium.

With the aim to improve the description of rootlet primordium development, cell divisions dynamic and tissue differentiation were studied. Using tissue-specific markers (AtCYCB1 ;1, LaWOL, LaSCR, LaPEP), cell divisions were observed not only in the pericycle, but also in the endodermis and the cortex, suggesting a contribution of these tissues to the formation of the rootlet primodium. Following these divisions, tissues started to differentiate to form a higly-organized meristem, whose cellular organization was described with the same set of molecular markers.

Lastly, a transcriptomic approach was performed on two detailed transcriptomics datasets describing rootlet development in a spatial and temporal manner. Analysis of gene expression profiles during the early steps of rootlet formation enabled the identification of specific expression profiles and the selection of candidate genes for functional analyses. Inhibiting the activity of 9 transcription factors (by fusing them with the SRDX repressor domain) allowed the identification of three genes for which repression prevented rootlet formation, suggesting a crucial role for *LaLBD16*, *LaERF12* and *LaSTY1* during rootlet organogenesis.

This thesis work suggests that a lateral root developmental program may have been recycled for the formation of cluster roots. The molecular mechanisms governing the massive induction of rootlets at the origin of the developmental curiosity that are cluster roots remain to be determined. In the future, this work may allow to transfer the ability to produce these structures to other crop species to expand their soil exploration capacity and improve their phosphate nutrition.

Keywords: cluster root, rootlet, development, white lupin, auxin.

Résumé en français

Les racines protéoïdes (RPd) sont une des adaptations développementales les plus frappantes du système racinaire exposé à des sols pauvres en nutriments. Le développement de ces structures spectaculaires, composées de dizaines de petites racines nommées rootlettes, se déclenche principalement en réponse à une carence en phosphate (Pi). Ces racines particulières sont dédiées à améliorer l'acquisition du Pi par la plante et sont importantes pour sa nutrition. De façon surprenante, bien que le lupin blanc soit considéré comme une espèce modèle pour la formation des RPd, très peu d'informations sont actuellement disponibles sur leur formation et sur les mécanismes moléculaires qui contrôlent ce processus développemental.

Afin de mieux comprendre comment se forment les rootlettes chez le lupin blanc, une description anatomique a été réalisée. Une étude tissulaire a permis de définir 8 stades dans le développement du primordium de rootlette, par analogie avec la formation des racines latérales chez *Arabidopsis*. Du fait du rôle majeur de l'auxine dans la formation des racines latérales, l'étude s'est focalisée sur les mécanismes reliés à cette hormone. L'expression du rapporteur auxinique DR5:GUS, chez le lupin blanc, a montré l'existence d'un maximum d'auxine, graduellement établi à l'apex du primordium de rootlette.

Dans le but de générer une description détaillée du développement du primordium de rootlette, la dynamique des divisions cellulaires et la différenciation des tissus ont été étudiées. L'utilisation de marqueurs spécifiques des tissus de la racine protéoïde (CYCB1 ;1, LaWOL, LaSCR, LaPEP) a identifié des divisions non

seulement dans le péricycle, mais également dans l'endoderme et le cortex, suggérant une contribution de ces tissus à la formation du primordium. A la suite de ces divisions, les tissus commencent à se différencier pour former un méristème dont l'organisation cellulaire a été décrite grâce au même jeu de marqueurs moléculaires.

Enfin, une approche de transcriptomique a été réalisée sur deux jeux de données détaillés décrivant le développement des rootlettes de façon spatiale et temporelle. L'analyse de l'expression des gènes au cours des étapes précoces de la formation des rootlettes a permis de dresser des profils types d'expression et de sélectionner des gènes candidats pour des analyses fonctionnelles. De plus, le blocage de l'activité de 9 facteurs de transcription (par fusion avec le domaine répresseur SRDX) a permis d'identifier 3 gènes dont la répression bloque la formation des racines protéoïdes, suggérant un rôle important de *LaLBD16*, *LaERF12* et *LaSTY1* dans l'organogénèse des rootlettes.

Ce travail de thèse suggère que le programme développemental de la racine latérale a pu être recyclé pour la formation des racines protéoïdes. Il reste à déterminer les mécanismes moléculaires qui gouvernent l'induction massive des rootlettes à l'origine de la curiosité développementale que sont les racines protéoïdes. Ces travaux permettront peut-être de transférer la capacité à produire ces structures à d'autres espèces cultivées pour élargir leur capacité à explorer le sol et améliorer leur nutrition phosphatée.

Mots clés : racine protéoïde, rootlette, développement, lupin blanc, auxine.

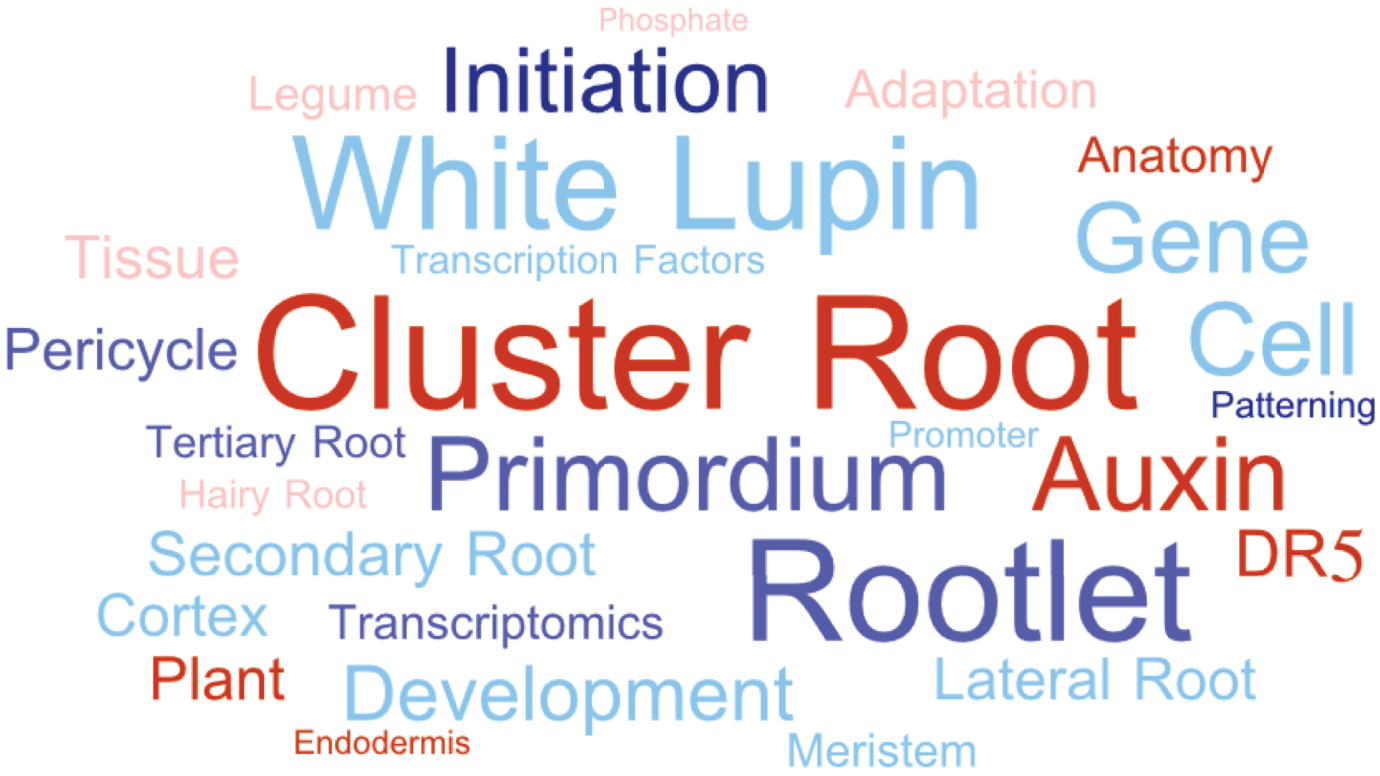
Phosphate
Legume
Initiation
Adaptation
White Lupin
Anatomy
Gene
Tissue
Transcription Factors
Pericycle
Cluster Root
Cell
Patterning
Tertiary Root
Promoter
Primordium
Auxin
Hairy Root
Secondary Root
DR5
Rootlet
Cortex
Transcriptomics
Plant
Development
Lateral Root
Endodermis
Meristem

A mon père, A David

Remerciements

Avant tout, je tiens à remercier chaleureusement Benjamin Péret, plus communément appelé « Chef », pour m'avoir donné l'opportunité de réaliser ce travail de thèse, mais surtout de m'avoir encouragée pendant ces trois années (et demi). Merci de m'avoir accompagnée et guidée, tout en me laissant une grande liberté dans la réalisation de ce projet. Je n'aurai jamais pu réussir sans ta patience, tes qualités humaines et scientifiques, mais aussi ton enthousiasme. Pour tout cela, un grand merci chef !

Je tiens également à remercier Bárbara Hufnagel, pour son encadrement, ses conseils et son aide. Je te remercie d'avoir toujours été disponible et à l'écoute, mais également pour ta gentillesse et tes encouragements continus. Merci encore Barbara ! Cela a été un plaisir de travailler avec toi.

J'adresse mes remerciements aux membres de mon comité de thèse : Sandra Bensmihen, Philippe Nacry, Valérie Hocher et Alain Gojon. Merci pour vos conseils et toutes les riches discussions qui ont beaucoup apporté à ce projet. Un merci particulier à ma référente Valérie Hocher qui a su m'aiguiller avec beaucoup de tact et de bienveillance.

J'adresse également mes remerciements les plus sincères à toutes les personnes de l'équipe qui ont largement contribué à ce projet pour leur aide scientifique, mais aussi pour leur bonne humeur quotidienne.

Merci donc à Laurence Marquès et à Patrick Doumas d'avoir toujours été présents pour des discussions enthousiastes, ainsi que pour leur aide dans la correction de ce manuscrit. Je remercie également Fanchon Divol pour son aide au quotidien, ses conseils et son dynamisme contagieux.

Je remerciement également Carine Alcon de m'avoir formée à l'histologie et pour son aide précieuse en microscopie, mais aussi pour tous les fous rire que l'on a pu avoir ensemble.

Merci aux Pérettes pour leur soutien précieux et pour toutes nos conversations autour d'un thé. Merci à Célia Casset pour sa sympathie, sa patience et son aide précieuse en clonage, et à Fanny Garcia pour sa joie de vivre.

Merci à Alexandre Soriano d'avoir participé à ce projet avec beaucoup de sympathie et d'enthousiasme.

Je remercie également tous les autres membres de l'équipe pour leur soutien et leur générosité. Merci à Tamara Le Thanh, André Marquès, Virginia Fernandez, Laurent Brottier et François Jobert.

Je remercie aussi mon stagiaire Quentin Rigal pour son aide au cours de nos longues heures de CIV et nos petits papotages botaniques. Je remercie également tous les autres stagiaires pour tous les moments de partage et les petits gateaux cuisinés. Merci à Cuong, Eva, Claire, Pauline, Laure, Malika, Louis et Marion.

Un grand merci également à tous les chercheurs, ingénieurs, post-doctorants, doctorants, techniciens et autres personnels du laboratoire BPMP avec qui j'ai pu échanger et qui m'ont permis de réaliser ce travail dans de bonnes conditions et avec le sourire.

Merci à tous de m'avoir épaulé tant sur le côté scientifique qu'humain. J'ai énormément appris à vos côtés et je vous remercie infiniment pour ça. J'ai été très heureuse de passer ces trois années avec des gens aussi passionnées que vous (et gourmands) !

Je salue également les équipes pédagogiques du module de Biologie Cellulaire (HLBI101) et du module base de la physiologie végétale (HLBI303) dans lesquelles j'ai effectué mon monitorat. Un grand merci à Laurence Marquès et Anne-Sophie Gosselin-Grenet qui m'ont permis de découvrir l'enseignement. Merci également à Olivier Rodriguez pour sa patience et sa disponibilité. Merci à Fabrice Merezegue et Lydia Gamet, de m'avoir permis de travailler dans des conditions agréables. Une dernière petite pensée pour tous les étudiants à qui j'ai tenté de transmettre ma passion pour la biologie.

Je remercie Florian Frugier, Stéphanie Robert, Sandra Bensmihen, Pascal Gantet et Laurent Laplaze d'avoir accepté de faire parti de mon jury de thèse.

Je remercie avec gratitude l'Université de Montpellier d'avoir financé cette thèse.

J'adresse un remerciement spécial à ma famille pour leur soutien inconditionnel, en particulier mon Papa, qui m'a transmis sa curiosité et son amour de la nature.

Un dernier merci à mon David, qui a été là jour après jour et qui m'a soutenu avec amour en toutes circonstances. Un grand merci pour tous ces moments incroyables et pour tous les moments à venir !

Tables des matières

Liste des abréviations

ABC	ATP Binding Cassette
AIA	acide indole 3-acétique
AUX/LAX	AUXIN1/LIKE-AUXIN1
AUX/IAA	auxin/indoleacetic acid
AuxRE	auxine response element
ARF	auxine response factor
At	*Arabidopsis thaliana*
cDNA	complementary DNA
CYC	cycline
CR	cluster root
CWR	cell wall remodeling enzymes
DNA	deoxyribonucleic acid
DR5	direct repeat 5
EDTA	ethylenediaminetetraacetic acid
EXP	expansine
GFP	green fluorescent protein
GH3	GRETCHEN HAGEN 3
GUS	ß-glucuronidase
HCl	hydrochlor*ic* acid
La	*Lupinus albus*
LR	lateral root
LRP	lateral root primordium
LUC	luciférase
AS2/LOB	ASYMMETRIC LEAVES2/LATERAL ORGAN BOUNDARIES
OZ	zone d'oscillation
P	phosphore
PAR	photosynthetically active radiation
PCR	polymerase chain reaction
Pi	phosphate inorganique
PG	polygalacturonase
PGP	P-glycoprotéine
PIN	PIN-FORMED
PILs	PIN-likes
PLT	PLETHORA
QC	quiescent center
qRT-PCR	Real-time quantitative reverse transcription polymerase chain reaction
Rpd	racines protéoïdes
RNA	ribonucleic acid
RNA-seq	RNA sequencing
SAUR	SMALL AUXIN UP RNA
RL	racine latérale
SCF	SKP, CULLIN, F-BOX

s.d.	standard deviation
TIR1/AFB	TRANSPORT INHIBITOR RESPONSE 1/AUXIN SIGNALING F-BOX PROTEIN
Tris	tris(hydroxyméthyl)aminométhane

Unités

%	percent
°C	degrees Celsius
bp	base pair
cm	centimetre
g	gramme
h	hour
L	litre
M	molar
m	metre
min	minute
s	second
µ	micro
w/v	weight by volume

Liste des figures

Introduction

Chapitre 1

Chapitre 2

Chapitre 3

Fig. S3. Top 15 enriched GO terms for the genes highly induced during early steps of cluster root formation shown in Fig.4.

Fig. S4. Silencing of *LaMAKR4* kinase expression in white lupin.

Fig. S5. Phenotype of white lupin transgenic root systems compared to untransformed plants and p35S::GUS control plants.

Fig. S6. Partial phylogenetic tree of LBDs class Ia subtype C of *Arabidopsis* and white lupin orthologs.

Fig. S7. Phylogenetic tree of SHI-RELATED SEQUENCE (SRS) family of *Arabidopsis* and white lupin orthologs.

Fig. S8. Phylogenetic tree of the AP2/EREB subfamily VIII/B2 of *Arabidopsis* and white lupin orthologs.

Liste des tables

Préface

Chez les plantes, contrairement aux animaux, le développement des organes est un processus continu qui a lieu durant l'ensemble du cycle de vie de la plante. Le corps primaire de la plante est établi dans l'embryon et produit un axe simple avec deux méristèmes : les méristèmes apicaux caulinaire et racinaire reliés par un système vasculaire. Après l'embryogénèse, de nouveaux organes se forment à partir de ces sites actifs pour bâtir l'architecture entière de la plante. Le développement des plantes est essentiellement post-embryonnaire.

Parce qu'elles font face à des conditions environnementales hétérogènes, les plantes adaptent leur développement. Cette plasticité leur permet de supporter des conditions changeantes qu'elles ne peuvent fuir. Comprendre les mécanismes moléculaires impliqués dans le développement et la plasticité du système racinaire est le domaine de recherche de l'équipe dans laquelle j'ai effectué ma thèse pendant les 3 dernières années.

L'équipe « Développement et Plasticité du Système Racinaire » utilise deux plantes modèles pour étudier ces aspects, *Arabidopsis thaliana* parce qu'elle est l'espèce modèle dans la recherche en génétique des plantes et le lupin blanc (*Lupinus albus L.*), parce qu'il produit des racines très particulières, au développement exacerbé, appelées racines protéoïdes. La présente thèse est une étude qui a pour but de décrire et de comprendre les événements précoces de la formation de ces racines.

INTRODUCTION

Développement et plasticité du système racinaire

I. Les racines protéoïdes : une adaptation développementale remarquable

I.1. Les racines protéoïdes: définition et origine

Les racines protéoïdes ont été observées pour la première fois par Adolf Engler (1894) et, plus tard, définies par Helen Purnell (1960). Cette botaniste leur a donné le nom de racines protéoïdes, car elles ont été observées chez tous les membres de la familles des *Proteaceae*, à l'exception du genre primitif *Persoonia* (Purnell, 1960). Elles ont originalement été définies comme des amas denses de rootlettes avec une croissance déterminée (« dense cluster of rootlets of limited growth »). Par la suite, les racines protéoïdes ont été décrites chez 10 familles botaniques éloignées, incluant des espèces monocotylédones et dicotylédones parmi les *Betulaceae*, *Casuarinaceae*, *Cucurbitaceae*, *Cyperaceae*, *Eleagnaceae*, *Fabaceae*, *Moraceae*, *Myricaceae* and *Restionaceae* (Dinkelaker *et al.* 1995; Skene 1998). Ainsi, le terme plus général de « cluster root » a été créé, pour définir ces structures sur la base de leur ressemblance morphologique plutôt que sur l'historique de leur découverte (Hocking and Jeffery, 2004).

Les racines protéoïdes représentent une des adaptations majeures pour améliorer la nutrition des plantes, avec les nodules symbiotiques fixateurs de N_2 et les mycorhizes qui permettent d'augmenter l'absorption du P (mycorhizes à arbuscules) (Neumann and Martinoia, 2002). En effet, les racines protéoïdes sont des organes dédiés à la remobilisation et à l'absorption du phosphate inorganique (Pi). Ces racines exsudent de grandes quantités de protons, d'acides organiques et de phosphatases afin de libérer le Pi non accessible à la plante et permettre ainsi la biodisponibilité puis le prélèvement du Pi par des transporteurs spécifiques. Les mécanismes impliqués dans la physiologie des racines protéoïdes ont été bien décrits (voir revue de Neumann and Martinoia 2002). Cependant, leur développement atypique reste peu étudié. Les racines protéoïdes (RPd) sont des racines secondaires comportant un ou plusieurs amas de racines tertiaires avec un développement déterminé, appelées rootlettes (Watt and Evans, 1999b; Dinkelaker *et al.*, 1995) (Fig. I.1). Les rootlettes sont éphémères et sont produites plus ou moins régulièrement le long des RPd lors de leur croissance (Shane and Lambers, 2005).

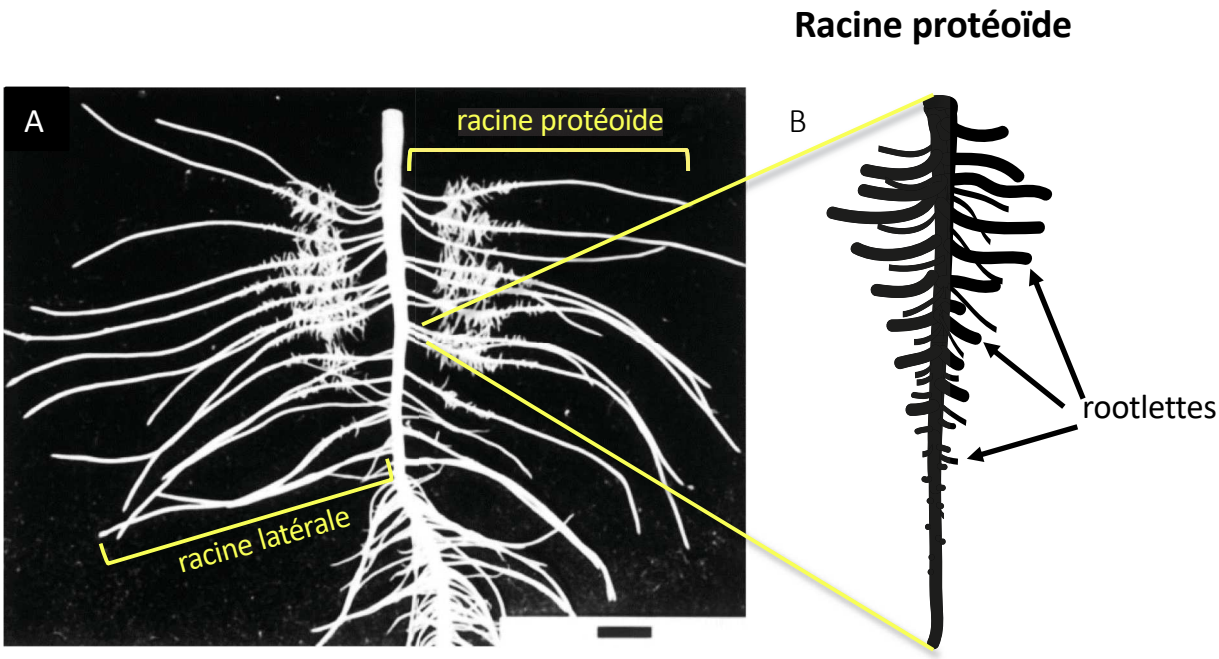

Fig. I.1. Formation des racines protéoïdes sur le système racinaire du lupin blanc. (A) En absence de phosphate inorganique dans le milieu, le lupin blanc produit deux types de racines secondaires: des racines latérales et des racines protéoïdes. Les racines latérales sont initiées sur la racine primaire dans la partie inférieure du système racinaire. Les racines protéoïdes sont des racines secondaires spécialisées et sont initiées à partir la racine primaire dans la partie haute du système racinaire (Watt 1999). (B) Ces racines secondaires portent au moins un amas dense de racines tertiaires au développement déterminé, appelées rootlettes.

La morphologie des RPd est variée chez les espèces de plantes qui les produisent. Ces racines peuvent être soit simples, soit composées (voir revue de Lambers and Shane 2007). Les RPd simples sont des racines secondaires qui portent des amas de rootlettes et sont produites par des espèces de *Proteaceae* australiennes et sud-africaines, et d'autres genres comme le lupin chez la famille des *Fabaceae* (Fig. I.2). Les racines composées sont formées quant à elles par le branchement itératif de racines protéoïdes simples et ont tendance à former de denses tapis racinaires à la surface du sol. Ces racines complexes sont produites par quelques espèces de *Proteaceae*, comme le genre australien *Banksia*, et montrent une très forte densité de rootlettes.

Une faible disponibilité de certains nutriments est le déclencheur de la formation de ces racines. Chez le lupin blanc, la formation de RPd est principalement déclenchée par une faible disponibilité du Pi dans le milieu (Gilbert *et al.*,2000). Au contraire, chez *Casuarina glauca*, la formation RPs est essentiellement déclenchée par une faible disponibilité en fer (Diem *et al.*, 2000).

I.2. Le lupin blanc : un modèle pour la formation des racines protéoïdes

Dans le but de comprendre et décrire la formation des RPd, il est important d'établir une espèce modèle. Puisque la plupart des espèces formant des RPd sont des arbustes ou des arbres, elles ne conviennent pas pour l'étude de ces racines notamment car leur culture est longue. Parmi ces espèces, le lupin blanc est une plante annuelle avec un cycle de vie relativement court (6 à 8 mois) qui produit des RPd en conditions contrôlées. Le lupin blanc peut être considéré comme un modèle pour comprendre le développement racinaire et, en particulier, l'initiation des racinaires tertiaires (voire revue: Skene 2001). En effet, cette espèce initie rapidement et massivement des RPd dans la partie supérieure de son système racinaire après 11 à 13 jours de culture, en condition de carence en Pi (Fig. I.3A). Cette induction massive de rootlettes se produit de façon localisée sur les racines secondaires et suit un patron spatial et temporel assez prédictible. Les rootlettes sont initiées de façon séquentielle dans l'axe longitudinal et produisent ainsi un organe représentatif de tous les stades de développement de la rootlette. Pour cette raison, il est possible de diviser une RPd en plusieurs zones développementales distinctes (Fig. I.3B). La zone où se forment les primordia de rootlettes est

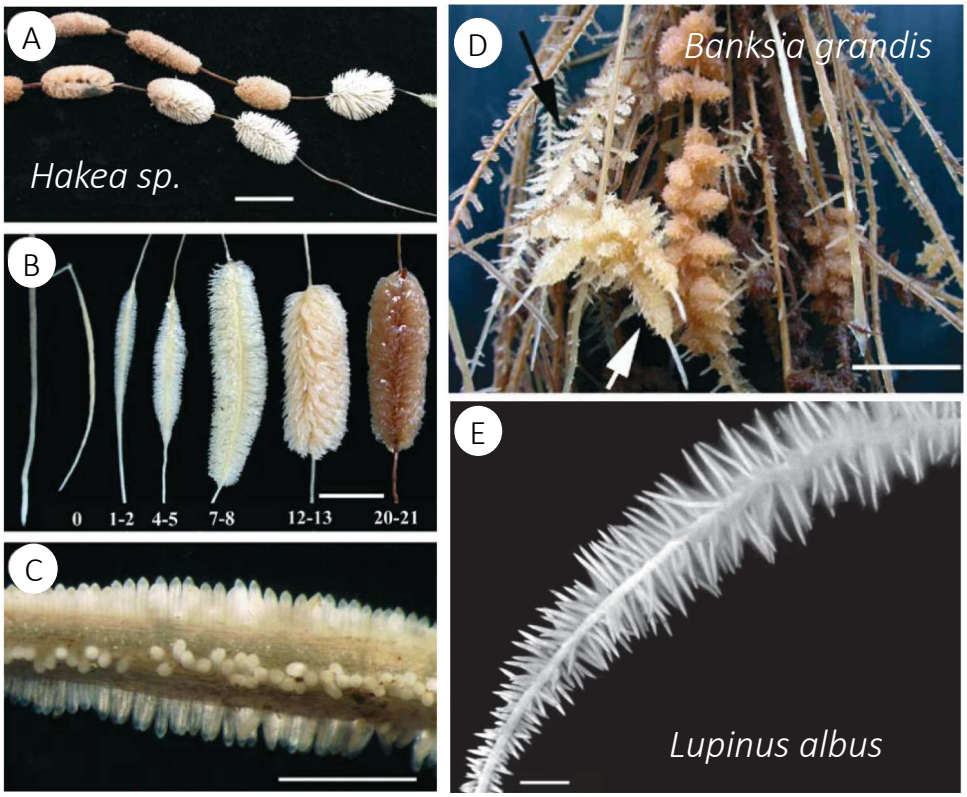

Fig. I.2. Morphologie des racines protéoïdes chez plusieurs genres. (A-C) Racines protéoïdes simples observées chez des espèces du genre *Hakea* (Shane and Lambers, 2005). (A) *Hakea petiolaris* produit des racines « en collier » chacune portant plusieurs amas de rootlettes (barre d'échelle: 20 mm). (B) Stades successifs de la formation de racines protéoïdes chez *Hakea prostrata,* de l'émergence des rootlettes au jour 0 jusqu'à la sénescence des rootlettes au(x) jour(s) 20-21 (barre d'échelle : 10 mm). (C) Jeune racine émergée d'*Hakea prostrata*. La densité de rootlettes est très élevée chez cette espèce (barre d'échelle : 5 mm). (D) Racines composées de *Banksia grandis*. Sur le système racinaire, des amas de rootlettes en développement (flèche noire) ou matures (flèche blanche) peuvent être observées (barre d'échelle : 20 mm). (E) Racine protéoïdes de *Lupinus albus*. Les rootlettes sont initiées de façon séquentielle dans la zone de l'amas (barre d'échelle : 5 mm) (Shane *et al.,* 2003).

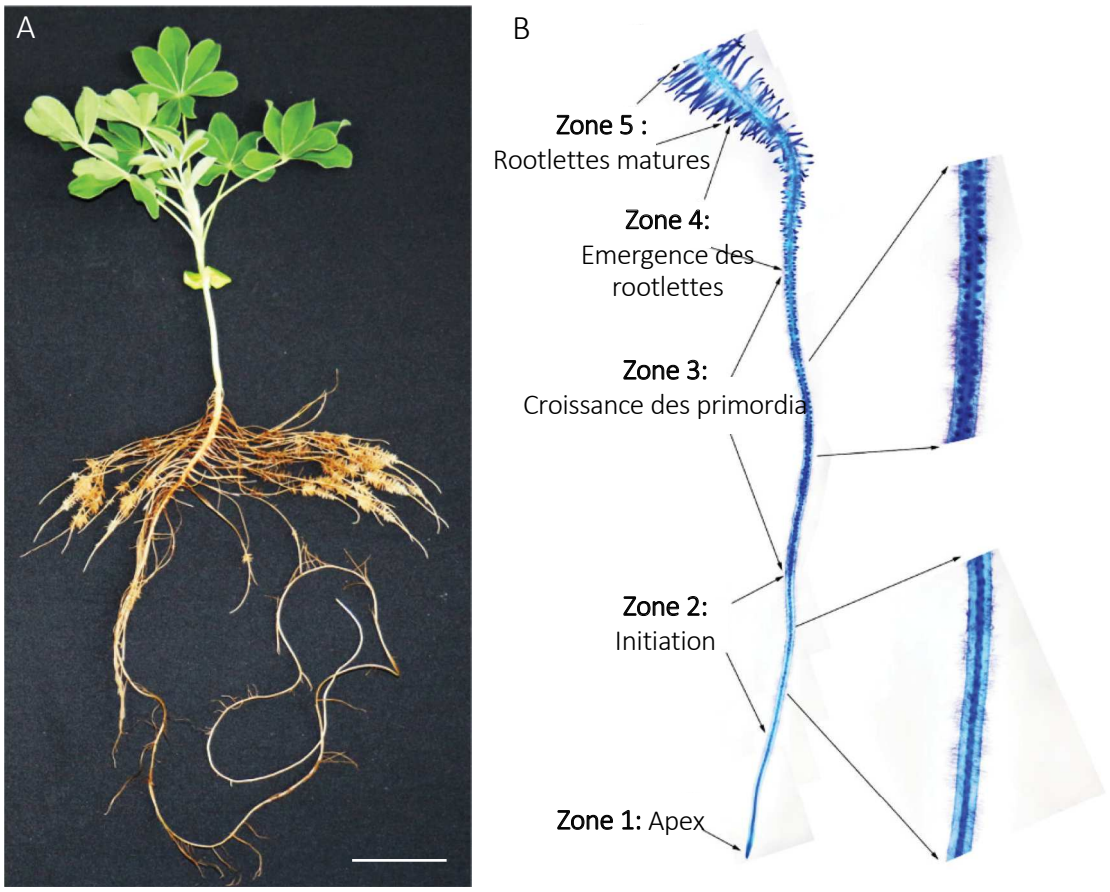

Fig. I.3. Le lupin blanc est une plante modèle pour l'étude des racines protéoïdes. (A) Chez les plantes carencées en P, des dizaines de racines protéoïdes sont formées dans la partie haute du système racinaire (barre d'échelle: 5 cm) (Müller *et al.,* 2012). (B) Les racines protéoïdes sont caractérisées par une induction massive de rootlettes. Les rootlettes sont formées de façon continue le long des racines protéoïdes et des dizaines de primordia sont initiés dans la zone d'initiation pendant leur croissance (Sbabou *et al.,* 2010).

caractérisée par de très nombreux événements d'initiations. Cela explique pourquoi les amas de rootlettes formés ont une densité qui s'élève en moyenne à 30 rootlettes/cm (Doumas *et al.*, résultats non publiés). Cette forte densité offre une quantité importante de matériel biologique pour étudier les premières étapes du développement de ces racines.

D'un point de vue développemental, les rootlettes semblent similaires aux racines latérales, mais une description très détaillée de ces racines n'a pas encore été apportée. Ces petites racines sont initiées en rangée en face des pôles de xylème (Johnson *et al.* 1996; Hagström *et al.* 2001) (Fig. I.4 A, B). Dans l'axe longitudinal, les rootlettes sont initiées très proches les unes des autres, au point que les primordia de rootlettes fusionnent parfois (Fig. I.4 C). Ainsi, les RPd peuvent être considérées comme des racines secondaires avec une initiation exacerbée, puisque la plupart des cellules du péricycle peuvent être recrutées pour participer à la formation de racines tertiaires (Skene 2000). Chez *Arabidopsis*, des mécanismes moléculaires inhibent la formation/maintenance des cellules fondatrices en face ou à proximité d'une cellule fondatrice pré-existante (Toyokura *et al.*, 2018; Himanen *et al.*, 2002). La forte induction de l'initiation chez les RPd suggère que les mécanismes moléculaires impliqués dans l'inhibition longitudinale et radiale des rootlettes sont absents ou supprimés dans la zone de formation de l'amas de racines. Ces observations soulèvent la question des mécanismes moléculaires et hormonaux à l'origine de leur formation.

Plusieurs jeux de données et outils ont été produits pour comprendre les bases moléculaires de la formation des RPd. Le développement de la transformation génétique dite « hairy root » médiée par *Agrobacterium rhizogenes* a établi une base solide pour la caractérisation fonctionnelle des gènes impliqués dans la formation de ces racines (Uhde-Stone *et al.*, 2003). En parallèle, des études transcriptomiques ont révélé les premiers acteurs moléculaires et hormonaux de leur formation (Wang *et al.*, 2015a; Secco *et al.*, 2014; O'Rourke *et al.*, 2013). Cependant, seuls quelques gènes en lien avec le développement ont été identifiés dans ces jeux de données. Le développement de nouvelles approches de génétique classique et inverse sont nécessaires pour identifier de nouveaux gènes en lien avec leur formation.

Afin d'améliorer la compréhension du développement des RPd, mon équipe d'accueil a développé plusieurs outils. A la moitié de ma thèse, le génome du lupin blanc a été séquencé

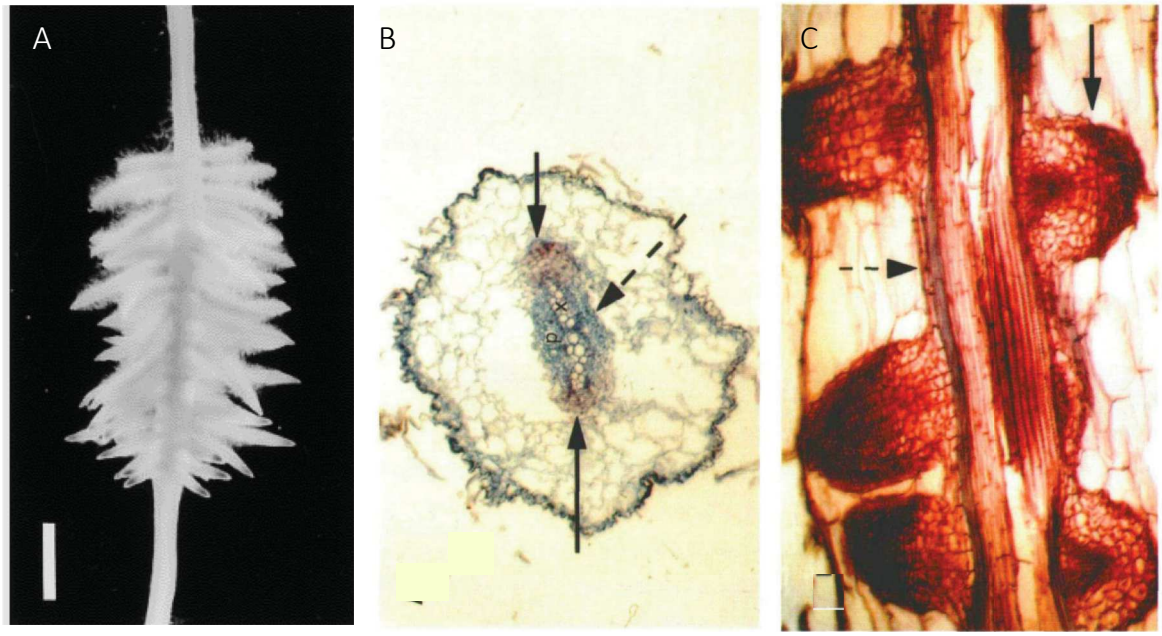

Fig. I.4. La formation des racines protéoïdes dépend de l'initiation massive de rootlettes (A) Une racine protéoïde comporte au moins un amas de rootlettes (scale bar: 3 mm) (Watt 1999). (B-C) Formation des primordia de rootlettes selon l'axe radial (B) et longitudinal (C). Les primordia de rootlettes sont initiés à partir des tissus situés en face des pôles de xylème (B) et se développent très proches les uns des autres dans l'axe longitudinal. Les flèches pleines montrent les primordia en développement, et les flèches en pointillés indiquent la position du péricycle. Le grossissement est 100X (Johnson *et al.,* 1996).

au sein de notre équipe de recherche (début 2018) apportant une base solide pour l'analyse des mécanismes moléculaires (Hufnagel *et al.*, 2019). L'équipe a également produit deux transcriptomes couvrant les différents stades de développement de la formation de RPs dans le but d'étudier les mécanismes moléculaires à l'origine de la formation des rootlettes. La présente thèse s'intéresse en particulier aux facteurs régulant les étapes précoces de la formation des rootlettes. D'autres travaux sont en cours dans l'équipe pour étudier les stades de développement plus tardifs (émergence, extinction du méristème).

I.3. Facteurs induisant la formation des racines protéoïdes

Les RPd étant des organes dédiés à la remobilisation et l'acquisition du Pi, il est couramment accepté que c'est la carence en Pi qui provoque l'induction de ces structures (Neumann *et al.* 2000; Wang *et al.* 2015). Néanmoins, il a été également observé des RPd en conditions riches en Pi, il semblerait donc que leur inhibition par ce nutriment ne soit pas complètement totale (Gilbert *et al.*, 2000; Abdolzadeh *et al.*, 2010). Dans le sol, par nature hétérogène, il est possible d'observer que les RPd apparaissent préférentiellement dans l'horizon superficiel, où la matière organique a tendance à s'accumuler (Skene, 1998).

Chez la plante modèle *Arabidopsis*, la perception de la carence en Pi provoque différents types de réponse qui ont été groupées en réponses locales et systémiques (Péret *et al.*, 2011). Les réponses locales couvrent les adaptations morphologiques et développementales (racines primaire et latérales, poils racinaires) alors que les réponses systémiques concernent la régulation de l'homéostasie du Pi (remobilisation et transport, recyclage et économie).

Des expériences de *split-root* ont démontré que la formation des RPd est induite par une faible concentration en Pi dans les parties aériennes (Marschner *et al.*, 1987; Shane *et al.*, 2003). Ces résultats suggèrent que le développement des RPd est régulé de manière systémique par le statut en Pi des parties aériennes. En plus du rôle du Pi interne, la concentration externe en Pi semble réguler la formation des RPd. Dans un sol artificiel stratifié, la présence locale de Pi favorise la formation de RPd dans ces strates, indiquant l'implication d'un signal local capable de percevoir la concentration externe en Pi (Shu *et al.*, 2007). Ainsi, la

formation de RPd est contrôlée à la fois par la concentration interne en Pi, mais aussi par sa disponibilité locale.

D'autres carences en nutriments peuvent influencer la formation des RPd. C'est notamment le cas d'une carence en azote (N) ou en fer (Fe). Lorsque la disponibilité du Pi est faible, un faible apport d'azote va favoriser la formation de RPd mais également la formation de nodules fixateurs d'azote (Dinkelaker *et al.* 1995). Les plantes qui s'engagent dans ces symbioses ont généralement un fort besoin en P. La formation de RPd permet d'améliorer l'acquisition du Pi, pour maintenir l'homéostasie du Pi dans les tissus de la plante, mais également dans les tissus symbiotiques. L'induction de la formation de RPd serait donc essentielle pour maintenir la symbiose et la croissance de la plante, en particulier lors d'une carence combinée en P et N.

Très peu d'études se sont intéressées au rôle du fer dans la formation des RPd. Une carence en fer induit leur formation, mais l'induction de ces organes est moins importante que dans le cas d'une carence en Pi (Hagström *et al.*, 2001). La carence en Pi plutôt que la carence en Fe semble donc déterminante pour induire le développement de ces racines chez le lupin blanc. Néanmoins, une étude comparative de l'architecture racinaire au sein de notre équipe, a montré qu'il existe une interaction complexe entre P et Fe dans le cadre de la formation de RPd (résultats non publiés). Ces travaux suggèrent qu'il y a un lien fort entre l'homéostasie de ces deux éléments au sein de la plante. Un tel lien semble exister puisqu'une étude récente a montré qu'*AtPHR1*, un régulateur central de l'homéostasie du P, et son proche homologue *AtPHL1*, peuvent réguler l'expression de gènes nécessaires à l'homéostasie du fer comme *AtFER1* (Bournier *et al.*, 2013). Il est probable qu'un mécanisme similaire existe pour réguler finement l'homéostasie du P et du Fe chez le lupin, et module la formation des RPd.

La faible disponibilité en nutriments modifie également le partitionnement des photoassimilats des organes sources aux organes puits (Marschner *et al.*, 1996). Pendant la carence en P, la photosynthèse est négativement affectée mais la translocation des photoassimilats au phloème, en particulier du sucrose, est maintenue pendant les 6 premiers jours de la carence (Hermans *et al.*, 2006; Lemoine *et al.*, 2013). Les sucres transportés, via le phloème, sont utilisés comme une source de carbone par les racines pour leur croissance.

Plusieurs études suggèrent également que la translocation des sucres au phloème jouerait un rôle dans la signalisation systémique à la carence en Pi (Hammond et White 2008, 2011). Chez le lupin, il a été proposé que le saccharose agisse comme un signal systémique de la carence en Pi et induise la formation des RPd (Zhou *et al.*, 2008; Wang *et al.*, 2015b). L'ajout de saccharose dans le milieu suffit pour induire la formation des RPd, même à des concentrations élevées en Pi externe, mais n'induit pas les réponses physiologiques associées (Wang *et al.* 2015). De la même manière, il a été montré que les sucres induisent la formation des racines latérales indépendamment de la concentration en Pi dans le milieu (Jain *et al.*, 2007).

Des changements dans la concentration, le transport ou la sensibilité à certaines hormones peuvent également être impliqués dans les réponses développementales du système racinaire à la carence en Pi (Rubio *et al.*, 2009). Parmi ces hormones, l'auxine est une hormone centrale qui contrôle les modifications de l'architecture racinaire lors d'une carence en Pi (López-Bucio *et al.* 2002; Nacry *et al.* 2005). Le transport polaire de l'auxine des parties aériennes aux racines est important pour la formation des racines latérales et il a été envisagé que le transport à longue distance de l'auxine soit un signal pour induire la formation des RPd (Bhalerao *et al.*, 2002; Meng *et al.*, 2013). Cependant, des expériences impliquant l'élimination des parties aériennes et l'application d'inhibiteurs du transport de l'auxine ont montré que l'auxine synthétisée dans les feuilles n'est pas la source principale d'auxine qui contrôle la formation des RPd (Meng *et al.*, 2013). Il apparaît au contraire que l'auxine synthétisée par les RPd, et sa redistribution le long de la racine, joue un rôle critique dans leur formation. Des données transcriptomiques suggèrent que l'auxine serait synthétisée dans les RPd par les enzymes YUCCA, puis redistribuée par les transporteurs AUX1 et PIN3 (Secco *et al.*, 2014; Wang *et al.*, 2014). L'implication de ces gènes dans la formation des rootlettes rappelle que ces racines sont très similaires à des racines latérales d'un point de vue développemental.

La formation des racines latérales implique une interaction entre les auxines et les cytokinines qui agissent de façon antagoniste pour réguler leur développement (Fig. 1.5). Contrairement à l'effet stimulateur de l'auxine, un traitement exogène avec des cytokinines réprime l'initiation des racines latérales et leur développement et a un effet similaire sur la formation des RPd (Laplaze *et al.*, 2007; O'Rourke *et al.*, 2013b). L'effet inhibiteur des cytokinines sur l'initiation repose sur des composants de la signalisation des cytokinines, en

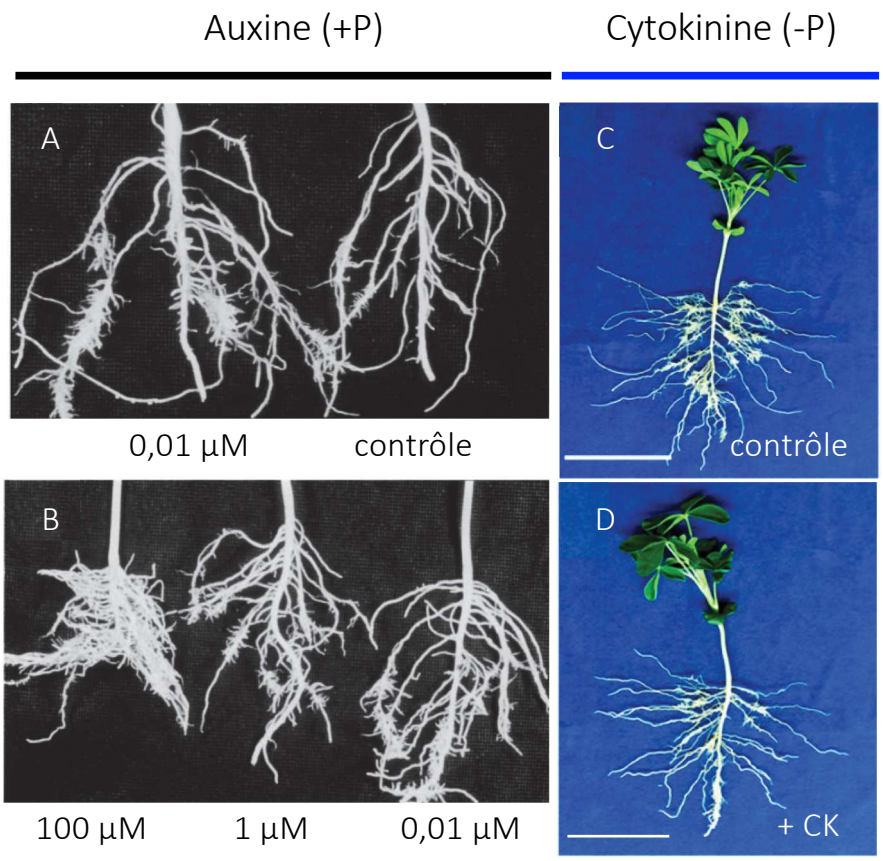

Fig. I.5. **L'auxine et les cytokinines ont un effet antagoniste sur la formation des racines protéoïdes chez le lupin blanc.** (A-B) L'application foliaire de l'auxine synthétique ANA (acide naphthoxyacétique) promeut la formation des racines protéoïdes à des concentrations en Pi qui inhibent normalement leur formation. L'ANA a été appliqué aux concentrations indiquées à 4, 8, et 12 jours après l'émergence des parties aériennes (Gilbert *et al.,* 2000). (C-D) L'application foliaire de cytokinines supprime la formation de racines protéoïdes chez des plantes carencées en P. L'auxine synthétique BAP (6-benzylaminopurine) a été appliquée à des concentrations de 1 ou 10 µM à 3, 6 et 8 jours après l'émergence des parties aériennes (O'Rourke *et al.,* 2013).

particulier leur récepteur *CRE1/AHK4* (Li *et al.*, 2006). L'expression de ce récepteur est réduite chez des plantes carencées en Pi (Franco-Zorrilla *et al.*, 2002) et cette répression a pour effet d'augmenter le nombre de racines latérales (Gonzalez-Rizzo *et al.*, 2006). La carence en Pi semble induire l'expression de *CRE1* dans des racines de lupin transgéniques, indiquant l'importance de la perception et de la signalisation des cytokinines pendant la formation des RPd (O'Rourke *et al.*, 2013b). L'augmentation de la capacité à percevoir les cytokinines dans la zone d'initiation et de formation des primordia de rootlette pourrait être ainsi impliquée dans la formation dense de ces racines le long de RPd.

La carence en Pi peut également modifier la concentration de certaines phytohormones, en altérant leur biosynthèse. Une augmentation de la production en éthylène est caractéristique des tissus carencés en Pi et est également observée dans les racines de plusieurs légumineuses dont les RPd chez le lupin (Gilbert *et al.*, 2000). Dans ces racines, une forte biosynthèse de l'éthylène est observée dans les rootlettes matures et conduirait à l'accumulation de cette hormone (O'Rourke *et al.*, 2013). Une forte concentration d'éthylène a un effet inhibiteur sur l'élongation racinaire et pourrait donc être impliquée dans la croissance déterminée de ces racines (Negi *et al.*, 2008). Au contraire, une faible concentration en éthylène est connue pour promouvoir l'initiation des racines latérales et pourrait favoriser l'initiation des rootlettes (Ivanchenko *et al.*, 2008). En accord avec cette hypothèse, il a été observé que les enzymes impliquées dans la voie de biosynthèse de l'éthylène sont faiblement exprimées dans la zone d'initiation et qu'une application d'éthylène a un effet stimulateur sur la formation de ces racines (Wang *et al.*, 2015a). L'effet de l'éthylène sur l'initiation peut s'expliquer par son rôle sur le transport de l'auxine et son accumulation locale (Muday *et al.*, 2012). Ainsi, une faible concentration en éthylène favorise l'initiation racinaire en permettant l'accumulation locale de l'auxine.

Plusieurs phytohormones impliquées dans la formation des racines latérales coordonnent également la formation des RPd (Fig. I.6), indiquant que le développement de ces racines est régulé par des mécanismes moléculaires très similaires. Ces processus développementaux sont contrôlés par l'environnement et une carence en Pi induit des réponses locales et systémiques qui gouvernent la formation de ces racines.

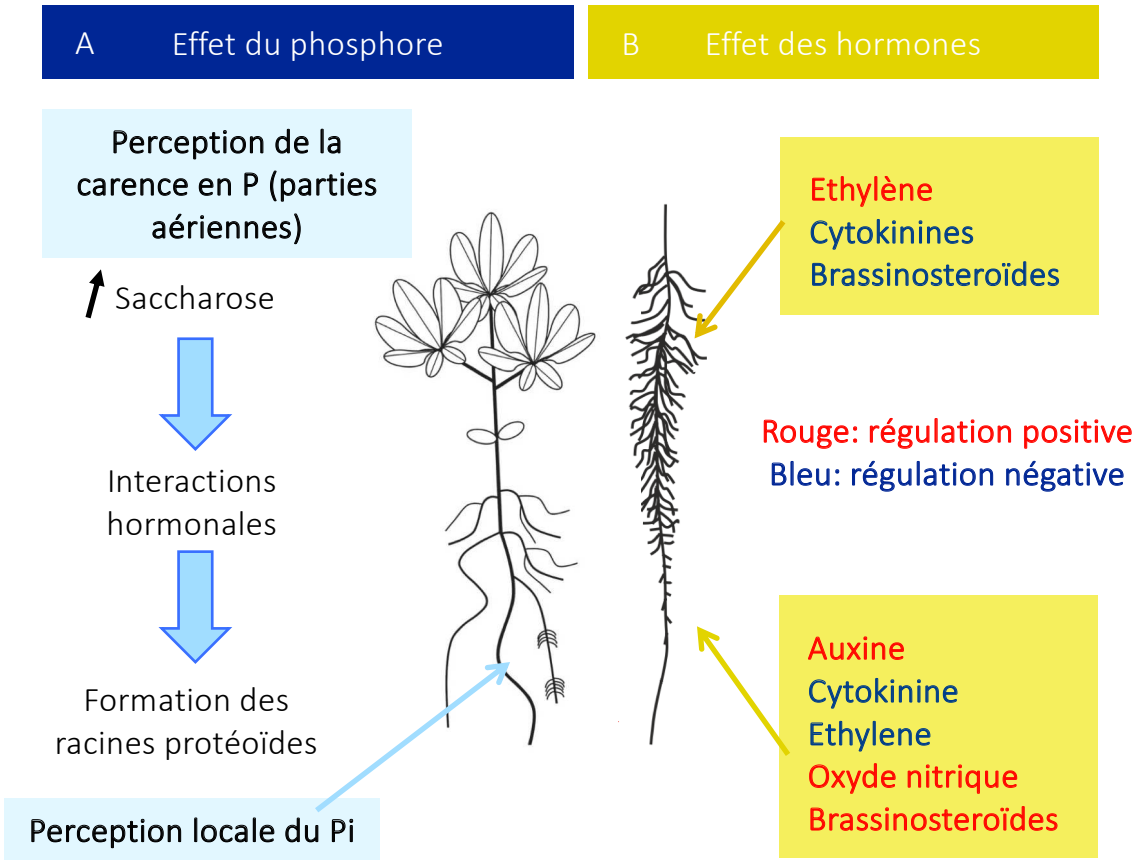

Fig. I.6. Modèle schématique montrant l'effet combiné du phosphore et des hormones dans la formation des racines protéoïdes chez le lupin blanc. (A) La formation de racines protéoïdes est déclenchée par un signal local en réponse à la perception de la faible concentration du Pi disponible dans le milieu. La carence en P dans la plante induit également le transport du saccharose des parties aériennes vers les racines. Le saccharose interagirait avec les hormones pour déclencher la formation des racines protéoïdes (Uhde-Stone *et al.,* 2017; Müller *et al.,* 2012). (B) Interactions hormonales dans la zone d'initiation et de maturation des rootlettes. L'initiation des rootlettes est coordonnée par l'interaction entre 5 phytohormones (Wang *et al.,* 2014). Le rouge indique une régulation positive, alors que le bleu indique une régulation négative.

D'un point de vue développemental et anatomique, les RPd sont comparables aux racines latérales. Afin de comprendre la formation des RPd, il apparait donc nécessaire de s'appuyer sur les données obtenues sur la formation des racines latérales, un processus développemental bien décrit chez *Arabidopsis*.

II. Formation des racines latérales

Pendant le développement post-embryonnaire, les parties aériennes des plantes sont générées à partir du méristème apical caulinaire. Ce méristème est formé de cellules indifférenciées, qui initient des feuilles à ses flancs et participent à l'élongation de la tige à sa base. A l'aisselle de chaque feuille, un ou plusieurs méristèmes secondaires aussi appelé méristèmes axillaires se développent pour former de nouvelles fleurs ou tiges (McSteen and Leyser, 2005). La formation de ces méristèmes assure la ramification du système aérien. Contrairement au méristème apical caulinaire, les cellules du méristème apical racinaire ne génèrent pas directement des méristèmes secondaires. Le branchement du système racinaire nécessite la formation *de novo* de racines secondaires, communément appelées racines latérales (RLs), à partir de cellules différenciées.

La racine primaire *d'Arabidopsis* a une organisation radiale très simple puisqu'elle est formée d'un ensemble de couches monocellulaires entourant le système vasculaire de la plante (Dolan *et al.*, 1993) (Fig. II.1). Cette simplicité se retrouve également le long de la racine primaire qui est composée de plusieurs zones développementales appelées (i) zone méristématique, (ii) zone d'élongation et (iii) zone de différenciation (Ivanov and Dubrovsky, 2013). C'est à partir de cette dernière zone, composée de cellules différenciées, que se forment les RLs.

La formation des RLs a été décrite au niveau anatomique par Malamy et Benfey (1997) et comprend huit stades (Fig. II.2). Le processus développemental est initié par des divisions asymétriques dans les cellules du péricycle situées en face des pôles de xylème. Elle se poursuit par une succession de divisions non stéréotypiques qui produisent un primordium de RL. Ce primordium croit à travers les tissus de la racine primaire, forme un méristème puis émerge

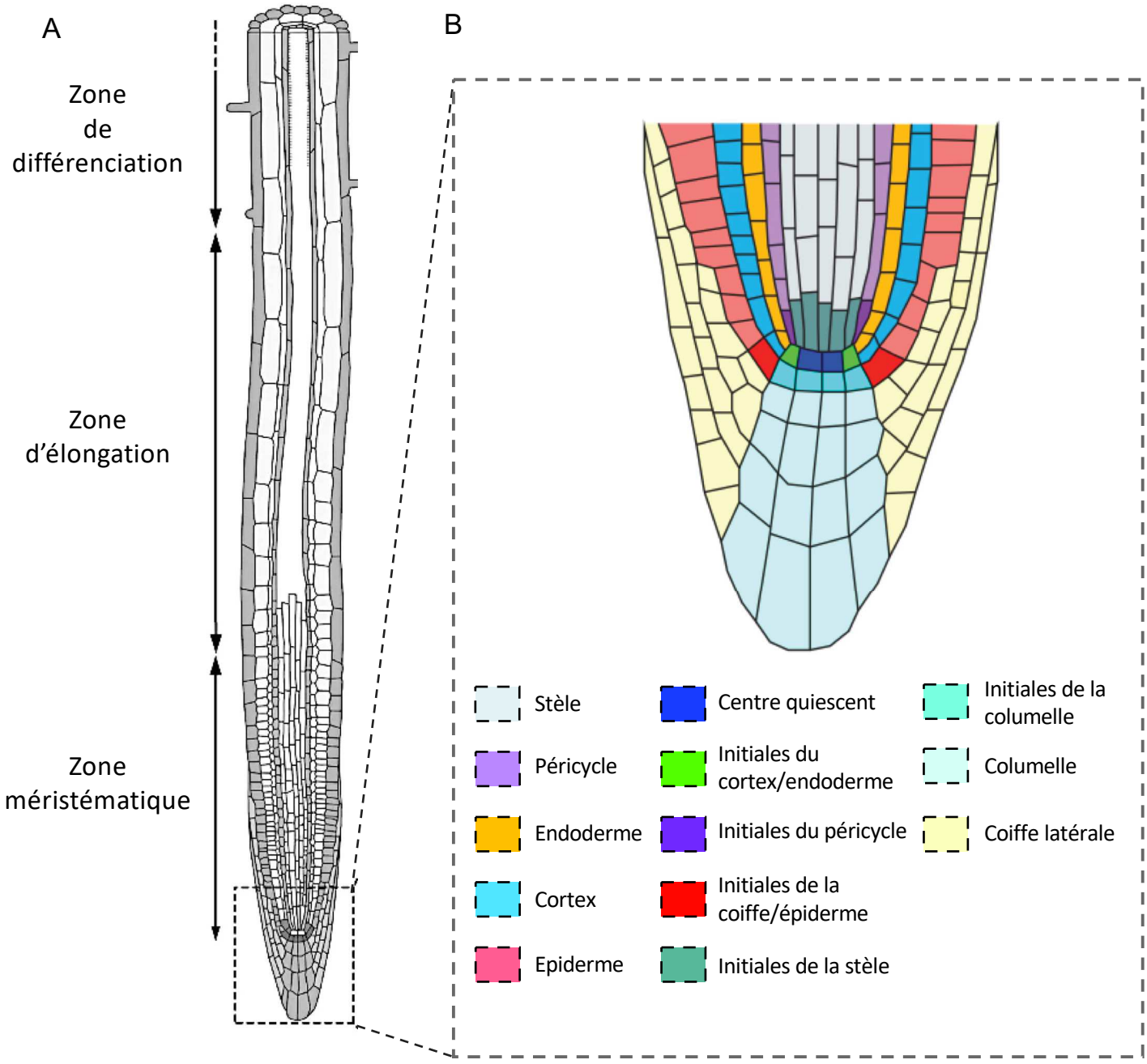

Fig. II.1. Organisation de la racine primaire d' *Arabidopsis thaliana*. (A) La racine en croissance peut être divisée en trois zones développementales le long de l'axe longitudinal. La zone méristématique comprend le méristème apical racinaire (MAR) et produit de façon continue de nouvelle cellules progénitrices pour tous les tissus de la racine (Rodriguez-Alonso *et al.,* 2018) (B) Schéma montrant l'organisation et les différents types cellulaires du MAR (Trinh *et al.,* 2018).

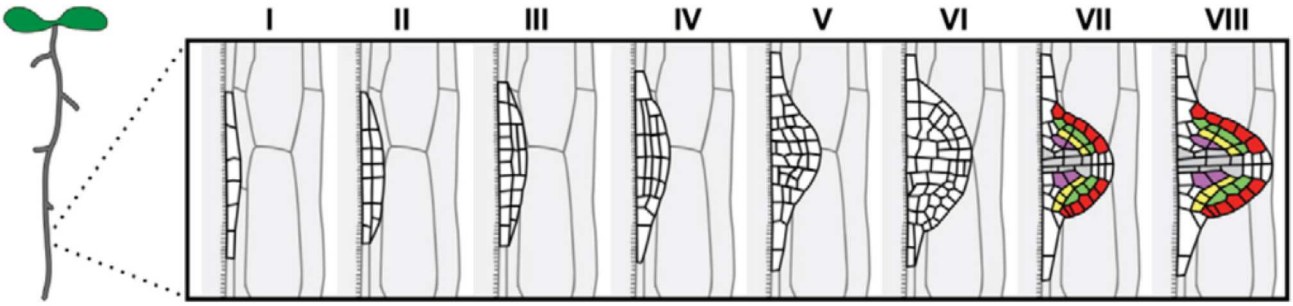

Fig. II.2. Stades développementaux de la formation du primordium de racine latérale chez *Arabidopsis thaliana*. Organisation schématique du primordium de racine latérale au cours des 8 stades successifs de sa formation. (I) L'initiation de la racine débute avec une première division asymétrique et produit deux petites cellules centrales flanquées de deux cellules plus larges. (II) Des divisions périclines dans les cellules du péricycle produisent un primordium formé d'une couche cellulaire interne (IL) et externe (OL). Ce primordium traverse l'endoderme. (III-IV) Deux séquences de divisions périclines donnent naissance à un primordium formé de trois puis quatre couches cellulaires, lequel traverse le cortex. (V-VI) La prolifération cellulaire se poursuit dans le primordium qui s'organise. (VII) Le primordium au stade VII est formé de cellules différenciées et son organisation est comparable à celle de la racine primaire (Porco *et al.,* 2016).

des tissus parentaux. Suite à son émergence, le méristème de la RL devient actif pour permettre la croissance de la RL.

II.1. Evènements précoces de la formation des racines latérales

La formation de RL commence avec la spécification des cellules du péricycle puis est suivie par l'initiation de ces racines. La spécification des cellules du péricycle correspond à l'acquisition de la compétence à former des RLs alors que l'initiation est la conséquence de l'activation de ces cellules (Chandler, 2011). Ainsi, la spécification et l'activation des cellules du péricycle peuvent être considérées comme deux processus développementaux différents et participent successivement à la formation des RLs.

Pré-initiation

Si la formation des racines latérales a lieu dans la zone de différenciation, la sélection des cellules qui vont devenir des cellules du péricycle a plutôt lieu dans une large région située en aval de la zone d'élongation de la racine primaire. Dans cette zone, les cellules sont choisies de façon périodique par un mécanisme oscillatoire nommé « priming ». Ce mécanisme oscillatoire a d'abord été visualisé par De Smet *et al.* (2007) qui ont observé des fluctuations de la réponse à l'auxine à l'aide du rapporteur synthétique *DR5* (DIRECT REPEAT 5) couplé à la β-glucuronidase. Les auteurs ont montré que des pulses de la réponse à l'auxine se produisent dans les cellules du protoxylème du méristème basal avec une périodicité de 15 h et marquent les sites où apparaissent plus tard les RLs. Ces oscillations périodiques ont également été observées *in vivo* avec le rapporteur *DR5* fusionné au gène de la luciferase (LUC) (Moreno-Risueno *et al.*, 2010). L'expression récurrente de *DR5:LUC* se produit dans une région, dénommée zone d'oscillation, couvrant la zone de transition (aussi appelée méristème basal) et le début de la zone d'élongation de la racine primaire (Fig. II.3). Les cellules qui montrent des oscillations de l'expression de ce gène rapporteur deviennent ensuite marquées par un pic stable de son expression, dans le début de la zone de différenciation. Ces pics stables, appelés sites de pré-branchement, caractérisent des régions compétentes à former des RLs. Le positionnement des RLs serait donc ainsi basé sur des oscillations de la réponse à l'auxine. Le priming permet de définir des sites de pré-branchement et donc de marquer les cellules qui

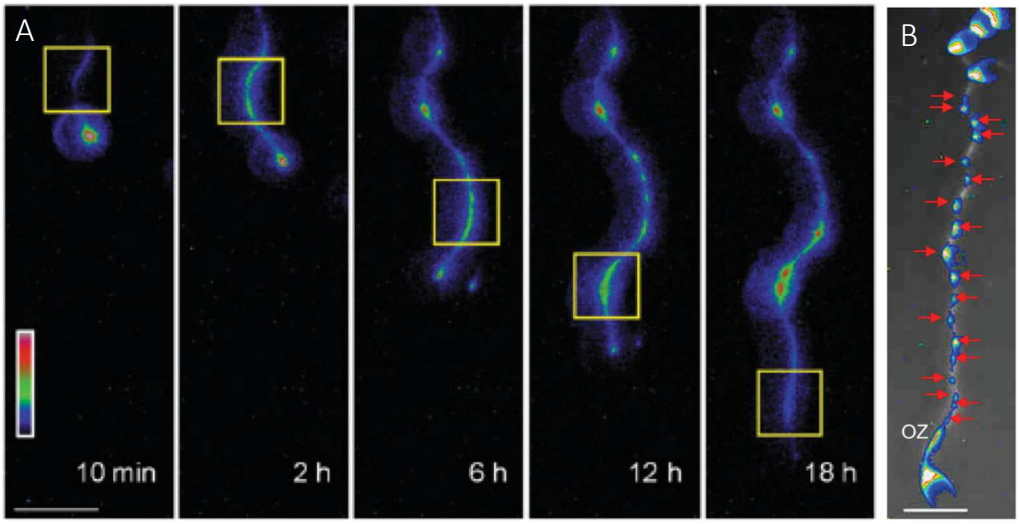

Fig. II.3. Le priming des racines latérales repose sur des oscillations de l'expression des gènes de réponse à l'auxine. (A) L'expression du gène rapporteur *DR5:luciférase* permet du suivre l'oscillation temporelle de la réponse à l'auxine qui se produit dans la zone incluant la zone de transition et le début de la zone d'élongation. Cette oscillation pré-sélectionne les cellules qui pourront devenir compétentes pour former la racine latérale (Jansen *et al.,* 2018). (B) La persistance du signal *DR5:luciférase* dans la zone de différenciation marque l'emplacement des sites de pré-branchement, où se formeront les futures racines latérales (Xuan *et al.,* 2016).

peuvent devenir compétentes pour former des RLs. Cependant, tous les sites de pré-branchement ne produisent pas des racines latérales. Les cellules du péricycle marquées par le priming ne sont donc pas toutes destinées à devenir des cellules fondatrices. Cela suggère que des mécanismes additionnels doivent être impliqués dans la spécification de ces cellules.

Spécification des cellules du péricycle

L'auxine et la signalisation auxinique participent également à la spécification des cellules du péricycle. Une accumulation locale d'auxine est observée dans les cellules du péricycle avant leur division et permettrait leur spécification (Dubrovsky *et al.* 2008). Il est possible de créer une accumulation locale d'auxine dans les cellules du péricycle en utilisant un système inductible. Dans ce système, une enzyme de biosynthèse de l'auxine est exprimée de façon aléatoire dans des secteurs de la racine et permet d'augmenter sa production dans des patchs de cellules, comme les cellules du péricycle. L'auxine synthétisée dans ces cellules permet d'induire la formation de RLs, indiquant qu'une accumulation de cette hormone est nécessaire et suffisante pour spécifier les cellules fondatrices. De ce fait, l'accumulation de l'auxine agit comme un déclencheur morphogénétique de la formation de RLs.

L'accumulation locale d'auxine dans les cellules du péricycle est à l'origine d'une cascade de signalisation de l'auxine impliquée dans la spécification de ces cellules. Cette cascade, impliquant *INDOLE-3-ACETIC ACID 28* (*IAA28*) et plusieurs *AUXIN RESPONSE FACTORS* (*ARFs*), active directement *GATA23*, un facteur de transcription exprimé dans les cellules du péricycle qui quittent la zone de transition (Fig. II.4A,B) (De Rybel *et al.*, 2010). *GATA23* est connu pour réguler le destin cellulaire des cellules de mammifères (Cripps and Olson, 2002; Chou *et al.*, 2009) et est considéré comme le premier marqueur moléculaire de la spécification des cellules fondatrices. L'expression de *GATA23* chez certaines cellules du péricycle participe ainsi à déterminer la position des RLs le long de la racine primaire.

MEMBRANE-ASSOCIATED KINASE REGULATOR 4 (*MAKR4*) est un autre gène nécessaire à la spécification des cellules fondatrices (Xuan *et al.*, 2015). Cette kinase est exprimée au niveau des sites de pré-branchement et sa protéine s'accumule au niveau de la membrane plasmique juste avant l'initiation, indiquant que cette protéine est impliquée dans la phase

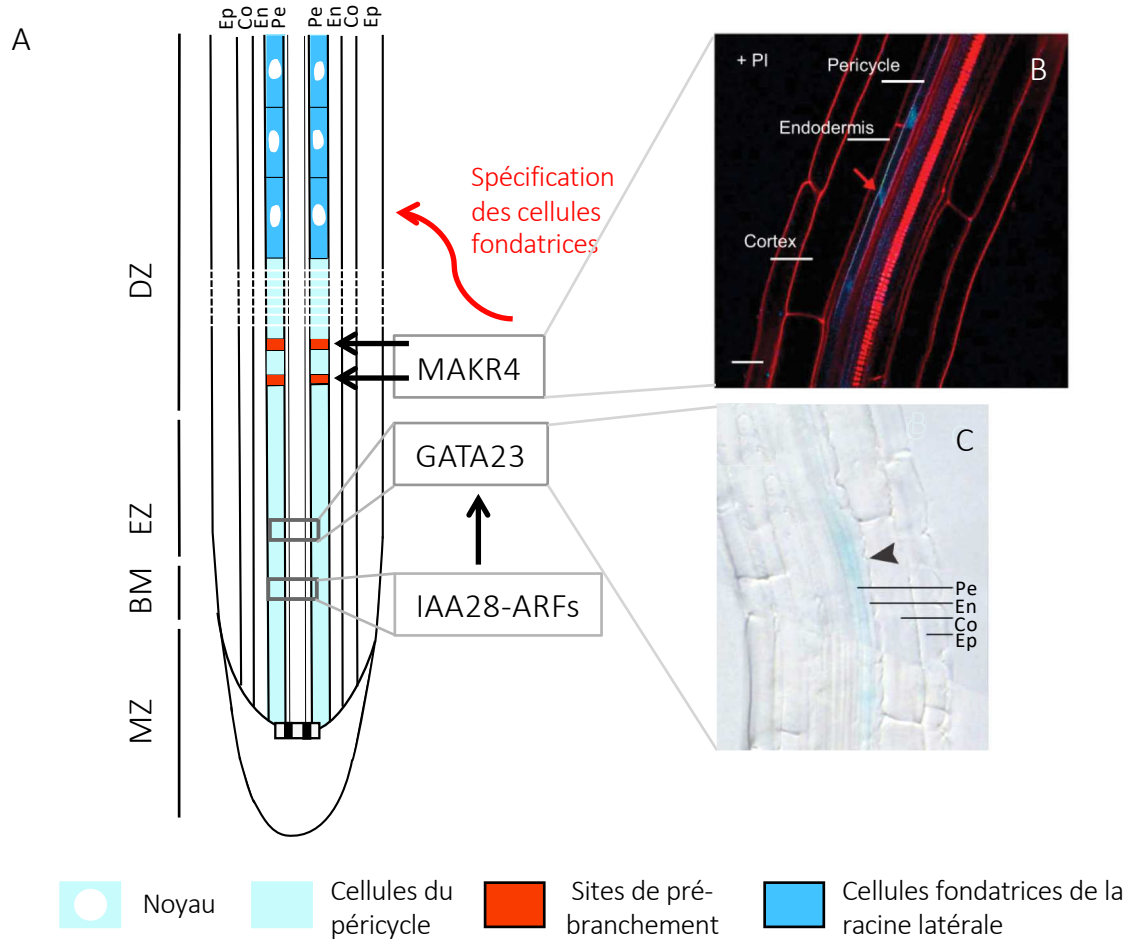

Fig. II.4. La spécification des cellules du péricycle est initiée dans le méristème basal et se poursuit dans la zone d'élongation. (A) La spécification des cellules fondatrices dépend de l'expression de *GATA23* dans la zone d'élongation (EZ) et de *MAKR4* dans la zone de différenciation (DZ). L'expression de *GATA23* spécifie les cellules du péricycle pendant ou en aval de l'oscillation, alors que *MAKR4* agit en aval de l'oscillation et son expression est requise pour convertir un site de pré-branchement en racine latérale (Du and Scheres. 2017) (B) Localisation tissulaire de la protéine pMAKR4:GFP-MAKR4 au niveau d'un site de pré-branchement chez le mutant *makr4-1,* dans une racine colorée à l'iodure de propidium (Xuan *et al.,* 2015). (C) Expression de *GATA23* dans un groupe de cellules du péricycle qui quittent le méristème basal (De Rybel *et al.,* 2010). MZ, zone méristématique; BM, méristème basal; EZ, zone d'élongation; DZ, zone de différenciation ; Ep, épiderme, ; Co, cortex; En, endoderme; Pe, péricycle.

précoce de la formation des RLs (Fig. II.4C). La perte de fonction de ce gène chez le mutant *makr4* a pour effet de réduire le nombre de RLs formées mais n'altère pas le nombre de sites de pré-branchement. *MAKR4* semble donc agir en aval de la formation des sites de pré-branchement et son expression serait nécessaire pour convertir ces sites en cellules compétentes à former des RLs.

Initiation

Les cellules fondatrices spécifiées sont compétentes à former des RLs et vont pouvoir être activées par un signal pour initier de nouvelles RLs. L'initiation de RLs désigne tous les événements conduisant à la première division asymétrique et à l'établissement du destin cellulaire des cellules filles.

Dans les cellules spécifiées, l'auxine s'accumule et crée un maximum qui contribue à l'activation de ces cellules. Cette accumulation, induit la signalisation de l'auxine, peut être visualisé à l'aide du gène rapporteur *DR5 :GUS* dans les cellules fondatrices activées (Benková *et al.*, 2003). Un composant essentiel de cette signalisation est le module *SOLITARY-ROOT (SLR)/IAA14-ARF7/ARF19* (Fukaki *et al.*, 2002). En réponse à l'accumulation de l'auxine, la dégradation de *SLR/IAA14* permet la dérépression des facteurs de transcription ARF7 et ARF19 qui peuvent activer l'expression de leurs gènes cibles, en particulier les gènes appartenant à la famille des protéines LATERAL ORGAN BOUNDARIES DOMAIN (LBD).

Parmi les facteurs de transcription de la famille LBDs, *LBD16* est connu pour jouer un rôle central dans l'initiation des RLs (Liu *et al.*, 2018). Ce gène est exprimé dans les noyaux des paires de cellules fondatrices spécifiées pendant leur migration et durant la division asymétrique (Goh *et al.*, 2012). Ces évènements de la formation des RLs sont perturbés chez des plantes transgéniques *pLBD16:LBD16-SRDX* dans lesquelles *LBD16* a été converti en répresseur transcriptionnel. De plus, l'expression de *LBD16* dans les cellules du péricycle est suffisante pour supprimer le défaut de formation de RLs chez le mutant *arf7arf19*. De ce fait, l'expression de *LBD16* est spécifique à l'initiation et est nécessaire pour que l'initiation ait lieu.

L'expression d'autres gènes de la famille des LBDs, en particulier *LBD18* et *LBD33,* est également requise pendant la première division asymétrique (Berckmans *et al.*, 2011). Les protéines codées par ces deux gènes sont capables de former un dimère pour réguler la transcription de *E2Fa*, un gène activateur des gènes impliqués dans la progression du cycle cellulaire. Le cycle cellulaire apparait donc comme une cible directe de la signalisation auxinique.

La plupart des cellules qui quittent le méristème basal sont arrêtées en phases G1 et seules les cellules situées en face des pôles de protoxylème sont capables de progresser dans le cycle cellulaire (Beeckman *et al.*, 2001). Cette progression est essentielle pour la première division asymétrique et est finement contrôlée par des sérines/thréonines kinases. Ces kinases sont des hétérodimères formées par une unité catalytique, appelé kinase cycline-dépendante (*CDK),* et une sous-unité régulatrice, appelée cycline (CYC). Plusieurs de ces cyclines sont impliquées dans l'initiation des RLs et participent à la transition G1-S (*CYCDs)* et G2-M (*CYCA2s*, *CYCB1;1*) du cycle cellulaire (De Smet, 2012; Beeckman *et al.*, 2001). La cycline *CYCB1;1* qui contrôle la transition G2-M est fortement exprimée dans les cellules fondatrices lors de leur division (Beeckman *et al.*, 2001). Cependant, si l'activation du cycle cellulaire est nécessaire à la formation des RLs, elle n'est pas suffisante pour déclencher leur formation. En effet, la surexpression de la cycline *CYCD3 ;1*, impliquée dans la transition G1-S, entraine une prolifération cellulaire mais ne permet pas la développement d'une RL (De Smet *et al.*, 2010). Cette absence d'organogénèse peut être surmontée par un traitement auxinique indiquant une régulation complexe de l'initiation par la signalisation auxinique. De nombreux gènes induits par cette signalisation ou exprimés indépendamment de celle-ci sont requis pour la formation des RLs et ont récemment été décrits dans plusieurs revues (Du and Scheres, 2017a; Trinh *et al.*, 2018).

L'initiation commence avec le gonflement des cellules fondatrices et la diminution du volume des cellules de l'endoderme (Vermeer *et al.*, 2014) (Fig. II.5). En même temps que ce changement morphologique se produit, le noyau s'arrondit, ce qui marque l'activation des cellules fondatrices (Fig. II.5A). Suite à leur activation, les noyaux de deux cellules fondatrices du péricycle migrent vers la paroi cellulaire qui les séparent et la première division anticline et asymétrique a lieu (De Smet *et al.* 2007; De Rybel *et al.* 2010) (Fig. II.5B). Cette division produit

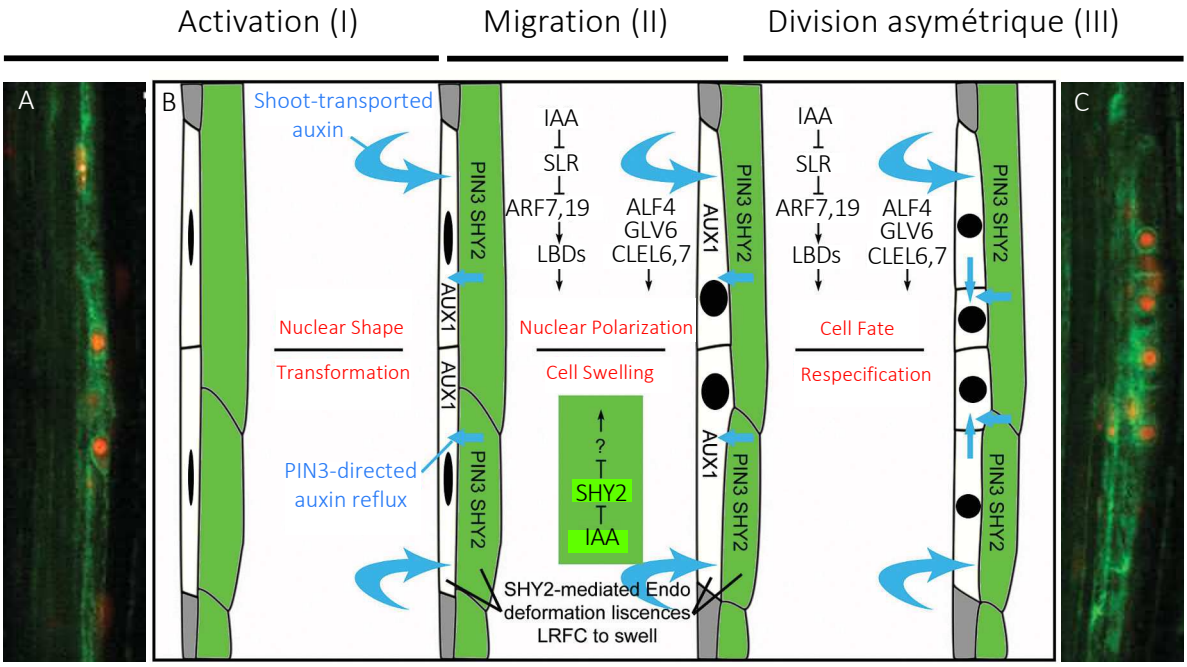

Fig. II.5. L'initiation des racines latérales se déroule en 3 étapes et est régulée par plusieurs modules de la signalisation auxinique. (I) L'initiation débute lorsque l'auxine s'accumule dans les cellules du péricycle spécifiées et active ces cellules (B). L'arrondissement des noyaux est considéré comme un marqueur de leur activation (A). (II) L'initiation se poursuit avec la migration des noyaux des cellules fondatrices du péricycle et dépend de l'induction de l'expression de *LBD16* par le module de réponse à l'auxine *SLR/IAA14-ARF7/ARF19*. En même temps que les noyaux migrent, l'endoderme subit une perte de son volume cellulaire, ce qui permet l'expansion radiale des cellules du péricycle. Ce processus est régulé par un deuxième module de signalisation de la réponse à l'auxine faisant intervenir *SHY2/IAA3*. (III) L'initiation se termine lorsque la première division asymétrique a eu lieu et que l'identité des quatre cellules filles est établie. La re-spécification du destin cellulaire de ces cellules ferait intervenir la signalisation auxinique médiée par *SLR/IAA14* (Du and Scheres. 2017; Goh *et al.,* 2012).

un primordium de RL au stade I, formé de 4 cellules de tailles inégales : deux petites cellules centrales flanquées par deux cellules plus larges (Casimiro, 2001; De Rybel *et al.*, 2010). Cette division est formative car elle produit des cellules filles avec des identités cellulaires différentes (Smolarkiewicz and Dhonukshe, 2013).

Ainsi, les cellules du péricycle sont sélectionnées par une série d'évènements qui leur permettent de devenir compétentes à former une RL puis sont activées afin d'initier des RLs. Cette succession d'évènements est régulée par un programme développemental complexe qui conduit à la première division asymétrique, laquelle initie la formation du primordium de RLs. Durant toutes les étapes précoces de la formation des RLs, l'auxine et la signalisation auxinique régulent l'expression de gènes impliqués dans le priming et la spécification des cellules du péricycle, puis l'activation et la division des cellules fondatrices. Après la première division asymétrique, ces cellules vont se diviser à plusieurs reprises et s'organiser pour former le primordium de la RL.

II.2. Organogénèse du primordium de racine latérale

Suite à l'initiation du primordium de RL, l'organogénèse et la croissance du primordium se poursuivent et un nouvel organe se forme puis émerge des tissus parentaux. Ce processus repose sur une série de divisions complexes et produit une structure très organisée dotée d'un méristème fonctionnel. Ce développement, originellement décrit par Malamy and Benfey (1997), peut être décomposé en 8 stades discrets. Le stade I du primordium, formé par une seule couche de cellules du péricycle de RL, est le point de départ de ce développement. A partir de ce primordium, une série de divisions ordonnées forme un primordium avec deux (stade II), puis trois (stade III) et, enfin, quatre couches cellulaires (stade IV). A partir du stade II, le primordium traverse l'endoderme et acquiert sa forme typique en dôme. Le primordium franchit ensuite le tissu du cortex (stade III) et atteint l'épiderme (stade VII). Cette nouvelle racine comprend un méristème fonctionnel identique à celui de la racine primaire, formé d'un centre quiescent entouré de cellules souches.

L'analyse de la séquence de divisions pendant la formation du primordium de RL a mis en évidence que la première division asymétrique est stéréotypique (Von Wangenheim *et al.*,

2016). Pendant le second tour de division, les cellules se divisent d'une façon anticline ou péricline et ce, d'une façon aléatoire. Ce patron non stéréotypique de division se poursuit après le deuxième tour de division. Entre deux divisions consécutives, les cellules changent l'orientation de leur plan de division de 90° et montrent une alternance entre des divisions anticlines et périclines. L'orientation de ces plans de division est importante pour produire des organes fonctionnels, et dépendrait de la capacité de cellules à répondre à l'auxine (Yoshida *et al.* 2014).

Un gradient d'auxine est formé dans le primordium de RL en développement et est nécessaire à la formation du méristème de RL (Benková *et al.*, 2003). Ce gradient est reflété par la réponse à l'auxine et peut être visualisé à l'aide du marqueur *DR5:GUS* (Fig. II.6A). Sa mise en place requiert l'action coordonnée de transporteurs d'influx et, surtout, de transporteurs d'efflux. Parmi ces transporteurs, la famille des transporteurs d'efflux *PIN-FORMED* (*PINs*) joue un rôle important dans la distribution de l'auxine dans les tissus du primordium (Fig. II.6B, C). Cette famille présente une forte redondance fonctionnelle et la mutation d'un gène *PIN* n'a que peu d'effet sur l'organogénèse du primordium (Blilou *et al.*, 2005; Benková *et al.*, 2003). Cependant, la mutation simultanée de plusieurs de ces gènes perturbe fortement l'établissement du gradient d'auxine puisque qu'elle induit la formation de primordia désorganisés (Benková *et al.*, 2003). La formation de ces massifs cellulaires chez le mutant *pin1pin3pin4* traité avec l'auxine montre que ces protéines ont un rôle important dès le stade II du développement du primordium de RL.

La localisation des protéines PINs est notamment régulée par les gènes *PLETHORAs* (*PLTs*). Les gènes *PLTs*, appartenant à la famille de facteurs de transcription *AINTEGUMENTA-like*, ont une fonction redondante dans la formation du primordium de RLs (Galinha *et al.*, 2007; Mähönen *et al.*, 2015; Aida *et al.*, 2004). L'expression des gènes *PLT3*, *PLT5* et *PLT7* dans les cellules du péricycle juste avant la première division asymétrique est requise pour l'expression de *PLT1*, *PLT2* et *PLT4* à des stades plus tardifs (Hofhuis *et al.*, 2013; Du and Scheres, 2017b). De ce fait, le mutant *plt3plt5plt7* forme des RLs anormales (Du and Scheres 2017b). Chez ce mutant, l'expression de *PIN1* et *PIN3* est réduite dans les stades tardifs de la formation du primordium, ce qui a pour conséquence d'empêcher la formation du gradient d'auxine.

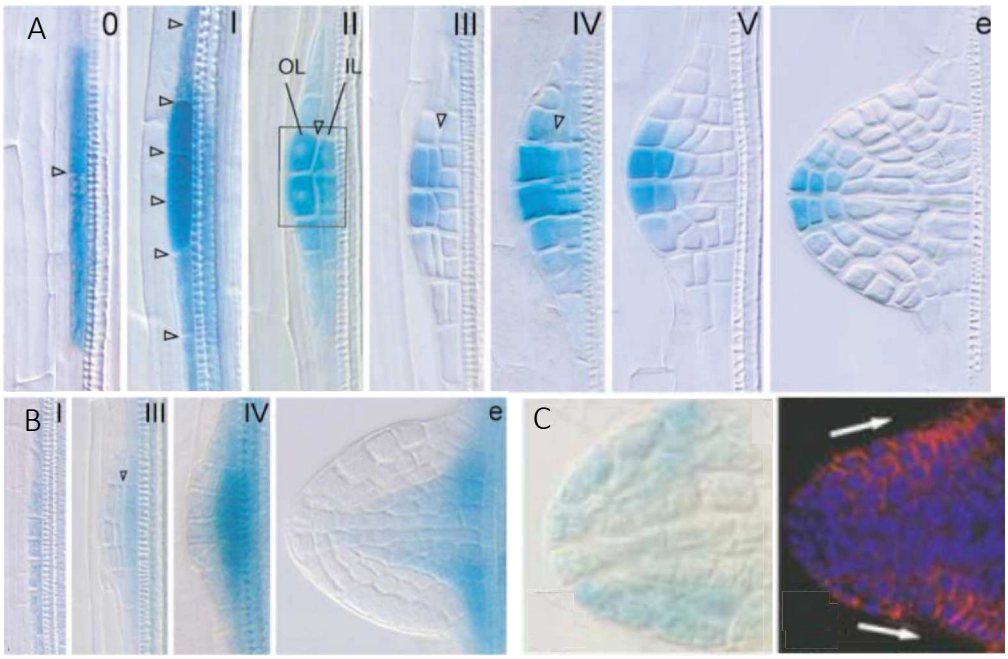

Fig. II.6. L'organogénèse du primordium de racine latérale dépend de l'établissement d'un gradient de l'auxine formé grâce à l'action des transporteurs d'efflux PINs. (A) La réponse à l'auxine observée avec le rapporteur *DR5:GUS* reflète la distribution de cette hormone dans le primordium. L'auxine s'accumule dans les cellules fondatrices de la racine latérale avant et pendant la première division cellulaire. Dans les stades suivants, le flux d'auxine est dirigé vers les cellules situées à l'apex du primordium, ce qui contribue à la formation d'un gradient d'auxine. (B-C) L'accumulation d'auxine dépend du patron d'expression et de la localisation des protéines PIN1 et PIN2 dans le primordium. PIN1 est présente dans les couches internes du primordium et dirige le flux vers l'apex du primordium (B) alors que PIN2 est localisée dans les couches externes et redirige le flux sur les flancs du primordium (C) (Benková *et al.,* 2003).

L'expression de *PLT3*, *PLT5* et *PLT7* à partir du stade II est donc requise pour la formation d'un maximum d'auxine et l'organogénèse du primordium de RL.

Chez le triple mutant, *plt3plt5plt7*, les gènes *SHORTROOT* (*SHR*) et *SCARECROW* (*SCR*) ne sont pas ou faiblement exprimés (Du and Scheres, 2017b). Comme les gènes *PLTs*, ces gènes sont connus pour leur rôle dans le développement racinaire. Ces deux gènes sont importants pour la différenciation des différentes couches dans le primordium de RL. En effet, ils sont exprimés à partir du stade II et leurs domaines d'expression délimitent les couches internes et externes du primordium, ce qui est important pour la formation du centre quiescent et l'organisation finale de cet organe (Goh *et al.*, 2016). De ce fait, la mutation des gènes *SHR* et *SCR* chez les mutants *shr-2* et *scr-3* perturbe les divisions périclines à partir du stade II et, par conséquent, affecte drastiquement l'organogenèse du primordium de RLs. Ce défaut d'organogénèse produit chez le mutant *shr* des racines anormales qui n'ont pas de structure interne et produisent des cellules non viables (Lucas *et al.*, 2011). Il apparait donc que la délimitation des domaines dans le primordium en développement soit cruciale pour l'organogénèse du primordium et la formation d'une RL fonctionnelle.

Simultanément à la formation du primordium, le domaine périphérique (ou flanquant) qui limite et contraint son développement est défini. Ce domaine forme un anneau de cellules autour du primordium et résulte de divisions radiales et tangentielles sur les flancs du primordium (Lucas *et al.* 2013). Plusieurs gènes régulant la formation du domaine périphérique ont été identifiés. *PUCHI* est un facteur de transcription de la famille *APETALA2/Ethylene Responsive Element Binding-like (AP2/*EREB-*like)* qui participe à définir les flancs des primordia de RLs. Son expression est observée au stade I puis se restreint au domaine périphérique au stade IV (Hirota *et al.*, 2007; Kang *et al.*, 2013). *PUCHI* semble nécessaire pour contrôler la prolifération et la différenciation des cellules flanquantes du primordium puisque la mutation de ce gène entraîne des divisions anticlinales supplémentaires et un élargissement anormal de ces cellules. De plus, l'expression de *PUCHI* est régulée par le module de signalisation de l'auxine *ARF7/ARF19* et co-agit avec *LBD16* et *LBD18* pendant la formation et l'émergence du primordium (Kang *et al.*, 2013).

Pendant son développement, le primordium s'organise pour donner naissance à un méristème fonctionnel. Ce nouvel organe doit émerger à travers l'endoderme, le cortex et l'épiderme pour pouvoir atteindre la rhizosphère.

II.3. Différenciation des tissus et émergence du primordium

Pendant les étapes tardives du développement, les tissus du primordium de la RL s'organisent et les cellules se différencient pour générer un primordium hautement organisé. L'utilisation de marqueurs de l'endoderme, du cortex et de l'épiderme a permis de visualiser le début de la différenciation de ces types cellulaires et a montré que le primordium sur le point d'émerger a une structure identique à celle de la racine primaire (Malamy and Benfey, 1997). En effet, le primordium est formé par un ensemble de couches cellulaires uniques et comprend un groupe de cellules méristèmatiques qui assurent le fonctionnement du méristème (Goh *et al.*, 2016).

Le méristème du primordium de RLs est fonctionnel et doit traverser l'épiderme pour émerger de la racine primaire et devenir actif. L'émergence de la RL est associée à une séparation des tissus cellulaires et à un allongement cellulaire qui permet la croissance radiale du primordium. L'émergence s'achève lorsque le primordium de RL arrive dans le milieu extérieur et s'accompagne d'une reprise de l'activité mitotique dans le méristème. Pendant l'émergence, la séparation des tissus, qui correspond à la perte d'adhérence des cellules le long de la lamelle moyenne, est assurée par des enzymes de remodelage de la paroi (Cell Wall Remodelling Enzymes, CWR), des polygalacturonases (PG) et des expansines (EXP) (Lee *et al.* 2009; Kumpf *et al.* 2013). L'induction de ces enzymes est dépendante d'une boucle rétroactive positive impliquant l'accumulation de l'auxine dans les cellules de l'épiderme et l'expression de *LAX3* dans ces cellules (Swarup *et al.*, 2008; Porco *et al.*, 2016). Ce processus est régulé par la signalisation auxinique et implique le module de signalisation *IAA14/SLR-ARF7-LBD29*.

L'auxine et la signalisation auxinique jouent ainsi un rôle central dans toutes les étapes de la formation des RLs (Du and Scheres, 2017a). L'auxine est nécessaire pour les étapes précoces de la formation des racines allant du priming à l'initiation des racines mais intervient

également pendant l'organisation du primordium et dans les étapes plus tardives pour permettre leur émergence.

III. Transduction du signal auxinique

Les auxines sont des molécules présentes à de faibles concentrations chez les plantes et contrôlent de nombreux aspects de leur croissance et de leur développement. Parmi ces processus développementaux, l'auxine régule: l'embryogénèse, l'initiation et le développement vasculaire des feuilles, la formation du fruit, et la formation des racines latérales (Fig. III.1) (Pattison *et al.* 2014; Scarpella *et al.* 2010; Jenikkand Barton, 2005; Du and Scheres, 2017a). Plusieurs molécules présentent une fonction auxinique mais la plus abondante chez les plantes est l'acide indole 3-acétique (AIA). L'AIA a été isolée il y a un siècle (Kögl *et al.* 1934) et s'est révélée être une hormone versatile contrôlant à la fois la division, l'élongation mais aussi la différenciation cellulaire. Puisque l'auxine régule de nombreuses fonctions cellulaires et contrôle la formation des organes chez les plantes, son homéostasie, son transport et sa perception sont finement régulés au niveau cellulaire et tissulaire.

III.1. Perception et signalisation

Au niveau cellulaire, la perception de l'auxine dans le noyau régule la transcription de gènes de réponse à l'auxine (Fig. III.2). Cette perception dépend de la formation d'un complexe comportant une multi-protéine SCF (SKP, CULLIN, F-BOX) (Gray *et al.*, 1999, 2002), une protéine de la famille TIR1/AFB (TRANSPORT INHIBITOR RESPONSE 1/AUXIN SIGNALING F-BOX PROTEINS) (Dharmasiri *et al.* 2005; Kepinski and Leyser 2005) et une protéine de la famille des Aux/IAA (Auxin/INDOLE ACETIC ACID) (Luo *et al.* 2018). Une quatrième famille de protéines, appelée AUXIN RESPONSE FACTORS (ARFs) régulent la transcription de gènes de réponse à l'auxine (voir revue de Li *et al.* 2016).

À une faible concentration d'auxine dans la cellule, les facteurs de transcriptions ARFs sont inhibés car ils forment des hétérodimères avec les protéines répressives AUX/IAA (Guilfoyle *et al.*, 1998; Guilfoyle and Hagen, 2007). Les protéines AUX/IAA répriment au moins

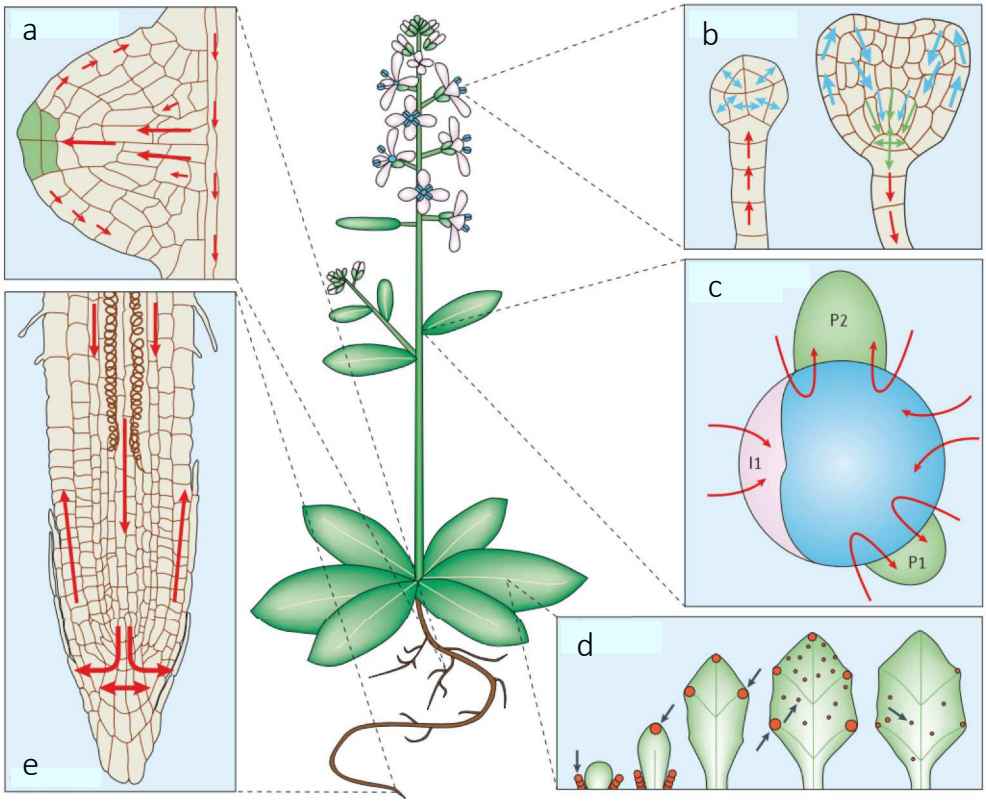

Fig. III.1. La distribution de l'auxine contrôle les processus développementaux. (a) *Racine latérale*. Le transport polarisé de l'auxine (flèche rouge) permet son accumulation à l'apex du primordium. (b) *Embryon*. Dans le jeune embryon (1 jour), l'auxine est apportée par *PIN7* puis redistribuée dans l'embryon. A un stade plus tardif (3 jours), le flux d'auxine s'inverse et l'auxine est exportée de l'embryon. (c) *Méristème apical caulinaire*. L'auxine est transportée de l'apex caulinaire (en bleu) vers les primordia de feuilles naissant (I1) et en développement (P1/P2). (d) *Feuilles.* L'auxine participe à la vascularisation des feuilles et régule leur développement. Dans la feuille, l'auxine est synthétisée (rond noir) et s'accumule localement (rond orange). (e) *Racine primaire*. Les protéines PINs dirigent le flux d'auxine vers le centre quiescent, puis le redirige vers l'épiderme (adapté de Teale *et al.,* 2006).

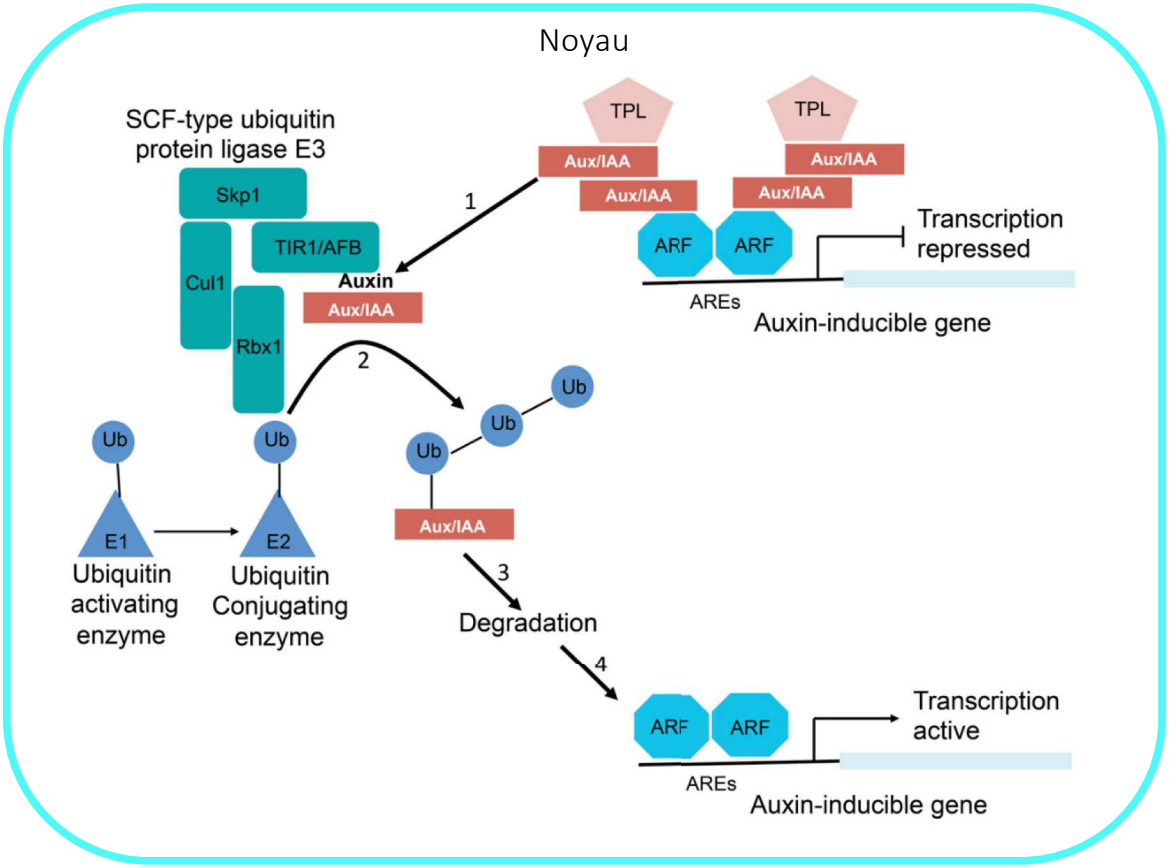

Fig. III.2. Régulation de la transcription par le complexe SCF$^{TIR1/AFB}$-Aux/IAA. Les gènes de réponse à l'auxine peuvent être activés par des dimères d'ARFs qui sont fixés dans le promoteur au niveau de séquences conservées appelées ARE ou AuxREs. Cependant les AUX/IAA interagissent avec les ARFs et participent au recrutement de protéines co-répressives, inhibant ainsi l'expression de ces gènes. Néanmoins, l'auxine agit comme une glue moléculaire qui rapproche les protéines TIR1/AFB et AUX/IAA (1), permettant ainsi la polyubiquitination des AUX/IAA par le complexe SCF de type ubiquitin ligase E3 (2) et leur dégradation par le protéasome (3). La destruction des AUX/IAA permet aux ARFs de se fixer dans les AuxRE des promoteurs et d'activer la transcription des gènes de réponse à l'auxine (4) (adapté de Leyser 2018).

en partie l'activité des ARFs en permettant le recrutement de protéines qui participent au remodelage de la chromatine (Szemenyei *et al.* 2008; Krogan *et al.* 2012). Parmi ces protéines, des histones désacétylases (HDACs) peuvent enlever des groupements acétyl au niveau de la queue des histones, ce qui modifie la conformation de la chromatine et favorise la répression transcriptionnelle (Bestor, 1998).

L'inhibition de la transcription peut être levée lorsque l'AIA s'accumule dans la cellule, favorisant ainsi la formation du complexe $SCF^{TIR1/AFB}$-Aux/IAA. À l'intérieur de ce complexe, l'AIA agit comme une glue moléculaire qui rapproche les protéines co-réceptrices TIR1/AFB et AUX/IAA (Villalobos *et al.*, 2012). Cette interaction permet l'ubiquitination des protéines AUX/IAA par le complexe $SCF^{TIR1/AFB}$ E3 ubiquitin ligase, induisant ainsi leur dégradation par le protéasome 26S (Gray *et al.*, 2001; Dos Santos Maraschin *et al.*, 2009). La dégradation de ces protéines permet l'activation des ARFs, qui se fixent au niveau des séquences de réponses à l'auxine (AuxRE) et induisent la transcription de leur cibles (Paponov *et al.*, 2008).

Les mécanismes de transduction du signal auxinique peuvent sembler relativement simples, mais la présence de plusieurs molécules auxiniques et de nombreux gènes codant pour les *TIR1/AFB* (5), *AUX/IAA* (29) et *ARFs* (23) permet une régulation dynamique de la réponse à l'auxine dans chaque tissu (Dharmasiri *et al.*, 2005; Overvoorde *et al.*, 2005; Chandler, 2016). Cette régulation dépend des interactions possibles entre les composants de cette voie de signalisation. Les 5 protéines TIR1/AFB peuvent hypothétiquement interagir avec 29 AUX/IAA, mais ont une affinité préférentielle pour certains de ces AUX/IAA (Villalobos *et al.* 2012; Shimizu-Mitao and Kakimoto 2014). D'autre part, une compilation de plusieurs interactomes a prédit que les AUX/IAA pourraient avoir près de 544 interactions différentes avec les ARFs (voir revue de Luo *et al.* 2018). En plus de ces interactions canoniques, il a été montré que les protéines AUX/IAA peuvent interagir entre-elles (Kim *et al.*, 1997) et que la répression transcriptionnelle pourrait impliquer la formation de multimères d'AUX/IAA et d'ARFs (Korasick *et al.*, 2014; Nanao *et al.*, 2014).

Ainsi, un grand nombre d'interactions sont possibles entre les protéines TIR1/AFB, AUX/IAA et ARFs. Cette multitude d'interactions explique comment l'auxine contribue à la

diversité de réponses transcriptionnelles qui régulent de nombreuses réponses développementales.

La transcription des gènes de réponse à l'auxine dépend de l'action d'ARFs. Chez *Arabidopsis*, parmi les 23 gènes de cette famille, 5 *ARFs* (5, 6, 7, 8 et 19) agissent comme des activateurs transcriptionnels alors que les autres *ARFs* seraient des répresseurs transcriptionnels. Les ARFs activateurs régulent la transcription via la dégradation des AUX/IAA et activent l'expression de nombreux gènes des familles *Aux/IAA* (*IAA1* and *IAA19*), *SAURs*, *GH3*, et *AS2/LOB* (voir revue de Guilfoyle and Hagen 2007). Parmi ces *ARFs*, *ARF5, 7* et *19* permettent la transcription de gènes qui régulent l'initiation des RLs (De Smet *et al.*, 2010; Okushima *et al.*, 2007). Par exemple, *ARF7* et *ARF19* activent directement l'expression de gènes de la famille *AS2/LOB*, qui contrôlent l'expression d'un gène activateur du cycle cellulaire (Berckmans *et al.*, 2011).

Bien que le rôle des *ARFs* activateurs a été bien décrit et certains des gènes cibles ont été identifiés, on ignore encore comment les répresseurs ARFs inhibent l'expression des gènes de réponse à l'auxine. Il a été précédemment proposé que les ARFs répresseurs pourraient interagir avec les AUX/IAA ou les ARFs activateurs pour réguler la transcription (Tiwari *et al.*, 2003; Hardtke *et al.*, 2004). Cependant, il est probable que les ARFs répresseurs et activateurs rivalisent pour se lier aux mêmes sites AuxREs (Vert *et al.*, 2008). Cette compétition entre les ARFs représente un autre niveau de complexité intervenant dans la régulation des gènes de la réponse à l'auxine.

La transduction du signal auxinique dépend en grande partie de la perception de l'auxine par le complexe $SCF^{TIR1/AFB}$-Aux/IAA et de la présence d'auxine dans les cellules. Le maintien de l'homéostasie intracellulaire de l'auxine est complexe et sa régulation fait intervenir un ensemble de voies métaboliques, pour lesquelles toutes les enzymes n'ont pas été identifiées, ainsi que des transporteurs d'auxines.

III.2. Homéostasie de l'auxine

L'homéostasie intracellulaire de l'auxine intègre à la fois la biosynthèse, la conjugaison et la dégradation de l'auxine, mais aussi le transport de l'auxine et sa compartimentation (Fig. III.3).

La biosynthèse de l'AIA a principalement lieu dans les jeunes feuilles et les cotylédons, mais peut également avoir lieu dans les feuilles en expansion et le système racinaire (Ljung *et al.*, 2001). Dans les racines, l'AIA est synthétisée localement au niveau des méristèmes de la racine primaire et des racines latérales (Ljung *et al.*, 2005).

Au niveau cellulaire, l'AIA serait synthétisée dans le cytoplasme via une voie métabolique dépendante du tryptophane (Zhao, 2012). La plupart des enzymes et intermédiaires intervenant dans cette biosynthèse ont été caractérisés (Ljung, 2013; Kasahara, 2016; Casanova-Sáez and Voß, 2019). Cependant, l'étude de mutants auxotrophes du maïs a montré que l'auxine pourrait également être synthétisée indépendamment du tryptophane (Wright *et al.*, 1991). Cette voie alternative existerait chez plusieurs espèces mais reste à ce jour peu décrite (Sitbon *et al.*, 2000; Epstein *et al.*, 2002).

Dans la cellule, l'auxine est retrouvée principalement sous forme conjuguée. La conjugaison de l'auxine permet son transport, son stockage et sa protection contre la dégradation (voir revue de Ljung 2013). Elle régule ainsi le niveau d'auxine dans la cellule et empêche sa toxicité. Ce processus permet la liaison de l'auxine à des sucres via une liaison ester et à des acides aminés, peptides ou protéines via une liaison amide (voir revue de Korasick *et al.* 2013). Les formes conjuguées via des liaisons amides sont majoritaires chez les plantes dicotylédones. En effet, certaines de ces molécules peuvent être hydrolysées et fournir de l'AIA à la cellule (Rampey *et al.*, 2004; LeClere, 2004).

Les différentes formes d'auxine, libres ou conjuguées, peuvent être dégradées pour réguler les différents pools d'auxine. Cette dégradation se fait essentiellement par décarboxylation non oxidative et entraine des modifications de la chaîne latérale et du noyau indole (voir revue de Ruiz Rosquete *et al.* 2012). Elle peut également être réalisée par

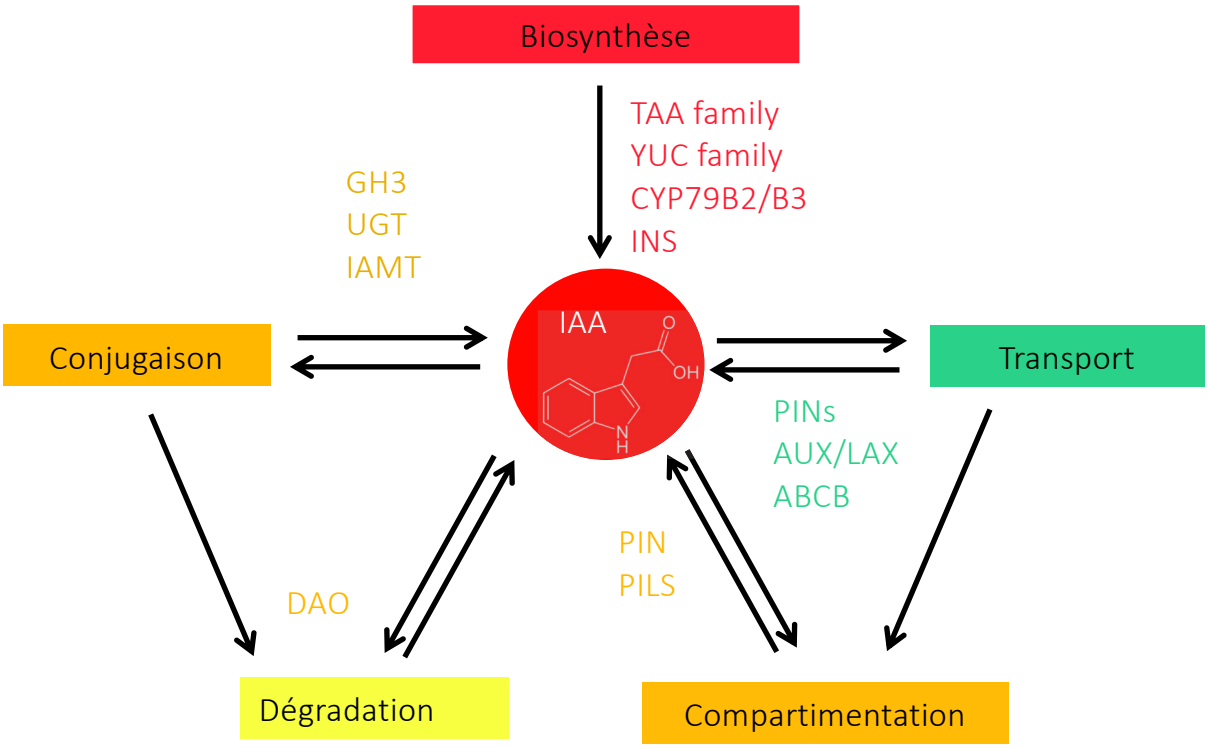

Fig. III.3. Métabolisme de l'auxine. La concentration en auxine dans la cellule dépend de sa biosynthèse, sa conjugaison, sa dégradation, sa compartimentation et son transport (adapté de Kasahara 2016). L'image de la molécule d'auxine provient de Wikimedia commons.

décarboxylation oxidative du noyau indole. Ces processus évitent une élévation du taux d'auxine dans la cellule et jouerait un rôle dans certains processus développementaux, ou pendant les réponses des plantes au stress oxidatif.

L'auxine peut également être transporté vers le réticulum endoplasmique par les protéines d'efflux de la famille PIN et PIN-likes (PILs), comme PIN5, PILS2 et PILS5 (voir revue de Barbez and Kleine-Vehn 2013). Cette compartimentation régulerait la quantité d'auxine dans le cytoplasme et pourrait permettre la conjugaison de l'auxine dans le réticulum endoplasmique. Les mécanismes exacts de cette compartimentation restent à découvrir.

Au niveau tissulaire, le transport de l'auxine par des transporteurs spécifiques est également important pour l'établissement de gradients, qui sont essentiels dans les processus développementaux, et représentent un niveau de contrôle supplémentaire de l'homéostasie de l'auxine.

III.3. Transport de l'auxine

Dans les plantes, l'auxine est distribuée par un transport à longue distance et par un transport polarisé de cellule à cellule (voir revue de Petrasek and Friml 2009; Grones *et al.* 2015; Abualia *et al.* 2018). Le transport à longue distance de l'AIA des organes sources aux racines assure un transport rapide de l'AIA via le phloème (Cambridge and Morris, 1996). Au contraire, le transport polarisé permet un transport plus lent de l'auxine de cellule à cellule et joue un rôle crucial dans la formation des gradients d'auxine à l'échelle de l'organe (Goldsmith, 1997). Ce transport nécessite l'action coordonnée de transporteurs membranaires d'influx et d'efflux, qui permettent respectivement l'entrée et la sortie de l'auxine dans la cellule. Il est assuré par 3 principales classes de transporteurs : (1) des protéines de la famille AUXIN RESISTANT1/LIKE AUX1 (AUX1/ LAX) (Swarup and Péret, 2012), (2) des protéines PIN-formed (PINs) (Adamowski and Friml, 2015), (3) des P-glycoproteins (PGP) de la famille à ATP binding cassette (ABCB) (Cho and Cho, 2013).

La caractérisation du mutant *auxin resistant 1* (*aux1*), qui présente un fort agravitropisme et un phénotype de résistance à l'auxine, a permis la découverte de la famille

AUX/LAX. Les protéines AUX/LAX sont des transporteurs d'influx qui assurent le transport de l'AIA de l'apoplasme aux cellules (Swarup and Péret, 2012). Chez *Arabidopsis*, la famille *AUX/LAX* est formée de 4 gènes fortement conservés nommés *AUX1*, *LAX1*, *LAX2* et *LAX3*. Cette famille de gènes forme une sous-classe spécifique aux plantes à l'intérieur de la superfamille des perméases à acides aminées et auxine. Elle contribuent à la distribution de l'auxine pendant certains processus développementaux y compris la vascularisation des cotylédons (*LAX2*) (Péret *et al.* 2012), l'initiation régulière des feuilles (*LAX1* et *LAX2*) (Bainbridge *et al.*, 2008) et la formation des RLs (*AUX1* et *LAX3*) (Swarup *et al.*, 2008; Marchant *et al.*, 2002).

Les gènes *PINs* codent pour des protéines transmembranaires qui assurent l'efflux de l'auxine. Chez *Arabidopsis*, 8 gènes ont été identifiés et sont généralement divisés en deux sous-groupes. Le premier sous-groupe de gènes (« short » *PINs*) comprend *PIN5/6/8* et codent pour des transporteurs adressés à la membrane du réticulum endoplasmique et participe donc au transport intracellulaire d'auxine (Křeček *et al.* 2009). Les gènes du deuxième groupe (« long » *PINs*), formé par *PIN1/2/3/4/7*, codent quant à eux pour des protéines qui sont localisées à la membrane plasmique et exportent l'AIA de la cellule (Zazímalová *et al.* 2010). Ces protéines sont localisées de façon asymétrique à la membrane plasmique et leur polarité est responsable de la direction des flux d'auxines (Blilou *et al.* 2005; Wisniewska 2006). De ce fait, la polarisation des protéines PINs est critique pour la formation des gradients et des maxima d'auxine qui sont nécessaires à de nombreux processus développementaux (Vieten *et al.*, 2007; Petrasek and Friml, 2009; Grunewald and Friml, 2010).

Certaines protéines PGP assurent également le transport d'influx et d'efflux de l'auxine (voir revue de Cho and Cho 2013). Ces protéines, localisées de façon uniforme à la membrane plasmique, transportent l'auxine de façon active contre son gradient de concentration (Park *et al.*, 2017). Contrairement aux PINs, ces protéines sont retenues à la membrane plasmique, indépendamment des signaux internes et externes, et assureraient potentiellement le transport basal de l'auxine de cellule à cellule (Grones and Friml, 2015).

III.4. Outils pour suivre l'auxine *in planta*

La capacité à visualiser la distribution de l'auxine est essentielle pour comprendre comment cette phytohormone régule de façon dynamique le développement et a grandement été améliorée par le développement récent de marqueurs histochimiques et fluorescents. La création du premier élément de réponse à l'auxine synthétique DR5 a initié le développement d'une série de biosenseurs pour l'auxine (Ulmasov *et al.*, 1997). Le rapporteur DR5 a été créé en réalisant une mutagenèse dirigée dans un élément AuxRE rencontré chez le promoteur du gène *GH3* du soja. Ce marqueur est formé de 7 à 9 répétitions en tandem de 11 paires de bases incluant le motif canonique TGTCTC et marque les sites de la réponse transcriptionnelle à l'auxine en activant des rapporteurs comme la β-glucuronidase, des protéines fluorescentes ou la luciférase. La fusion de 7 répétitions en tandem de 11 bp avec un promoteur minimal CaMV35S contrôlant l'expression du gène GUS a donné naissance au rapporteur DR5:GUS (Fig. III.4A) (Sabatini *et al.*, 1999).

Cette version du marqueur DR5 a d'abord été améliorée en fusionnant 9 répétitions inversées de 11 bp en tandem avec le même promoteur minimal et une séquence régulatrice du virus de la mosaïque du tabac pour créer la version DR5rev (Fig. III.4B) (Friml *et al.*, 2002). Cependant, la découverte de la séquence TGTCGG, qui a une meilleure affinité pour la liaison aux *ARFs* (Boer *et al.*, 2014), a conduit au développement d'un marqueur de réponse à l'auxine plus sensible, appelé DR5v2 (Fig. III.4C) (Liao *et al.*, 2015). Ce marqueur est exprimé dans des domaines additionnels comparé au marqueur DR5 et est un bon outil pour visualiser des réponses à l'auxine même faibles dans les tissus de l'embryon en formation ou dans la racine primaire. Cependant, l'expression de ces marqueurs ne reflète pas directement le niveau endogène d'auxine, mais plutôt sa réponse intégrative dans une voie de signalisation complexe (Chapman and Estelle, 2009).

Plus récemment, un autre type de marqueur, appelé DII-venus, a été créé pour suivre la distribution de l'auxine dans les tissus (Fig. III.4D) (Brunoud *et al.*, 2012). Le senseur DII-venus est formé par la fusion traductionnelle entre le domaine II (DII ou degron) de la protéine IAA28 et la protéine fluorescente à maturation rapide VENUS sous le contrôle d'un promoteur constitutif. D'une manière dose-dépendante à la présence d'auxine, le domaine DII est

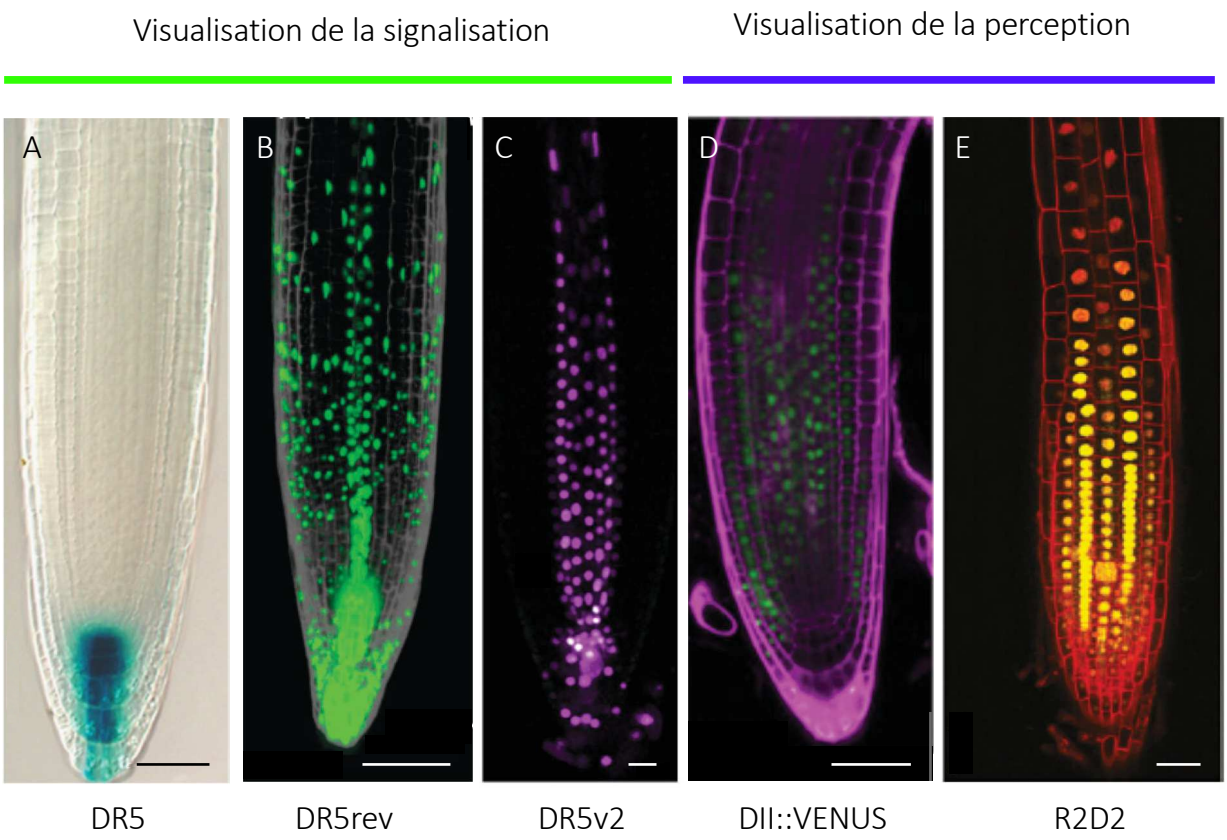

Fig. III.4. Marqueur de la perception et de la signalisation auxinique. (A) DR5::GUS. La première version de DR5 consistant en 7 répétitions de la séquence TGTCTC fusionnées à la β-glucuronidase marque les sites d'accumulation de l'auxine. (B) DR5rev::VENUS-N7 est une version améliorée du marqueur DR5, avec 9 répétitions de la même séquence de réponse à l'auxine. (C) p35S-DHFR::DR5v2-ntdTomato-DR5-n3GFP. Le rapporteur DR5v2, plus sensible que DR5 et DR5rev, révèle la signalisation auxinique dans des domaines additionnels comme le métaxylème et le péricycle. (D) p35S::DII:VENUS-N7. DII-VENUS à l'avantage d'être basé sur un mécanisme de la signalisation auxinique et permet une visualisation plus directe de la distribution de l'auxine. (E) p35S-DHFR::RPS5A-DII-ntTomato-RPS5A-DII-n3VENUS. R2D2 comprend un domaine DII et un domaine II muté, fusionnés chacun à une protéine fluorescente, et à été créé pour effectuer des mesures quantitatives des signaux de réponse à l'auxine (Yan *et al.,* 2013; Xuan *et al.,* 2015; Liao *et al.,* 2015; Rowe *et al.,* 2016; Barbez *et al.,* 2017).

ubiquitiné et la protéine dégradée par le système qui prend en charge les AUX/IAA, de sorte que l'absence de fluorescence dans une cellule reflète la présence d'auxine. Par rapport aux précédents marqueurs, ce nouveau senseur présente donc l'avantage de permettre la visualisation directe de la présence d'auxine, et apporte ainsi des informations spatio-temporelles sur la distribution de l'auxine dans les tissus. La nécessité de pouvoir quantifier ce signal entrant a conduit au développement d'un rapporteur ratiométrique appelé R2D2 (pour Ratiometric version of two DIIs).

Le gène rapporteur R2D2 combine sur un seul transgène la séquence DII-VENUS classique et une version mutée du domaine II (mDII) insensible à l'auxine, fusionné à une protéine fluorescente rouge (ntdTomato) (Fig. III.4E) (Liao *et al.*, 2015). R2D2 permet ainsi une mesure semi-quantitative de l'accumulation d'auxine, grâce au calcul de ratio entre les signaux émis par les deux protéines fluorescentes. De même que DII, ce marqueur permet une observation des changements de l'accumulation d'auxine au niveau cellulaire et en temps réel, mais avec l'avantage de pouvoir effectuer une quantification de ces changements.

Objectifs de la thèse

Ce travail de thèse s'inscrit dans un programme de recherche qui vise à étudier le développement et la plasticité du système racinaire. Il s'intéresse en particulier à comprendre comment se forment les rootlettes du lupin blanc et se focalise sur les évènements précoces de leur formation. L'étude qui suit a pour but (i) d'apporter une description précise de l'initiation des rootlettes et (ii) d'identifier des gènes régulant les premières étapes de leur formation. Ce travail de thèse se divise en trois chapitres :

Le chapitre 1 correspond à une étude histologique du développement de rootlettes qui a permis d'identifier des stades développementaux par analogie avec le développement de la racine latérale chez la plante modèle *Arabidopsis thaliana*. Afin de déterminer l'implication de l'auxine dans ce processus développemental, l'identification de gènes impliqués dans la voie de réponse à l'auxine (TIRs et AFBs) chez le lupin blanc a été initiée grâce aux premières ébauches de génome générées dans l'équipe en 2017. Le développement de la méthode de transformation par « hairy root » a permis d'utiliser le marqueur DR5 et de révéler l'établissement d'un gradient d'auxine dans les rootlettes. Ce chapitre correspond à un article publié dans le journal Physiologia Plantarum, à l'occasion d'un numéro spécial sur la thématique « Root Biology: Adventitious, lateral and primary roots – development, growth and adaptation to the environment ».

Le chapitre 2 correspond à une étude plus détaillée de la contribution respective des différents tissus (péricycle, endoderme et cortex) dans la formation du primordium de rootlettes. La maitrise en routine du protocole « hairy root » a permis d'utiliser plusieurs marqueurs identifiés par analogie avec des gènes marqueurs chez la plante modèle (spécifique de certains tissus ou marqueurs des divisions cellulaires). Ce chapitre est écrit sous la forme d'un article scientifique en préparation.

Finalement, le chapitre 3 correspond à une approche visant à identifier des régulateurs de la formation des rootlettes chez le lupin par génétique inverse. Pour cela, des données transcriptomiques couvrant les différents stades du développement des rootlettes ont été produites au laboratoire. Leur analyse a permis d'identifier des gènes candidats (facteurs de

transcription, FT) pour lesquels une étude fonctionnelle en « hairy root » a été réalisée. L'inhibition de ces FT par fusion avec le domaine répresseur SRDX a permis, dans certains cas, de bloquer la formation des racines protéoïdes, suggérant une implication de ces gènes dans ce mécanisme de développement. Ce chapitre est écrit sous la forme d'un article scientifique en préparation.

L'ensemble des approches présentées dans cette thèse a visé à mieux caractériser le développement des rootlettes, tant du point de vue anatomique que moléculaire dans le contexte de la création d'une nouvelle équipe au sein de l'unité B&PMP en Juillet 2015. Les données de séquence génomique du lupin blanc ont été obtenues par l'équipe fin 2017 et les données transcriptomiques courant 2018. Grâce à l'obtention progressive de ces données, ce projet a pu évoluer vers des approches plus moléculaires et finalement fonctionnelles.

CHAPITRE 1

Description anatomique et hormonale du développement du primordium de rootlette chez le lupin blanc

Avant-propos

Ce premier chapitre a pour but (1) d'apporter une description anatomique des premiers stades de développement des rootlettes et (2) de déterminer dans quelle mesure leur formation est similaire aux racines latérales des dicotylédones, en se focalisant sur la réponse à l'auxine. A cette fin, nous apportons une description des stades successifs dans la formation des rootlettes avec une approche histologique. Nous nous sommes ensuite concentrés sur le rôle de l'auxine pendant la formation de la rootlette et avons caractérisé le profil d'expression tissulaire du marqueur synthétique de réponse à l'auxine *DR5:GUS,* ainsi que l'expression de gènes en lien avec le transport, la perception ou la signalisation auxinique.

Cette étude, présentée sous la forme d'un article scientifique publié dans *Physiologia Plantarum*, apporte une référence histologique de la formation des rootlettes chez le lupin blanc à la communauté scientifique s'intéressant aux adaptations développementales du système racinaire. Cette approche élargit nos connaissances sur la formation des racines chez une espèce de légumineuse d'importance agronomique, comme le lupin blanc.

Article 1: Anatomical and hormonal description of rootlet primordium development along white lupin cluster root

Cécilia Gallardo[‡], Bárbara Hufnagel[‡], Célia Casset, Carine Alcon, Fanny Garcia, Fanchon Divol, Laurence Marquès, Patrick Doumas and Benjamin Péret[*]

BPMP, CNRS, INRA, Montpellier SupAgro, Univ Montpellier, Montpellier, France

Correspondence

[*]Corresponding author, e-mail : benjamin.peret@cnrs.fr

[‡]These authors contributed equally to this work.

Abstract

Cluster root (CR) is one of the most spectacular developmental adaptations, it can be found in a few species from a dozen botanical families, including white lupin (*Lupinus albus*) in the *Fabaceae* family. These spectacular structures are produced in phosphate-deprived conditions and are made of hundreds of short roots, the rootlets. White lupin is the only crop bearing CRs and is considered as the model species for CR studies. However, little information is available on their atypical development, including the molecular events that trigger their formation. To provide insights on CR formation, we performed an anatomical and cellular description of rootlet development in white lupin. Starting with a classic histological approach, we described rootlet primordium development and defined 8 developmental stages from rootlet initiation to their emergence. Due to the major role of hormones in the developmental program of root system, we next focussed on auxin-related mechanisms. We observed the establishment of an auxin maximum through rootlet development in transgenic roots bearing the *DR5:GUS* auxin reporter. Expression analysis of the main auxin related genes (TIR, ARF, AUX/IAA…) during a detailed time course revealed specific expression associated with the formation of the rootlet primordium. We showed that *LaTIR1b* expression progressively established a gradient during rootlet primordium formation and that *LaARF5* is expressed in the vasculature but absent in the primordium itself. Altogether, our results bring a description of the very early cellular events leading to CR formation and reveal some of the auxin-related mechanisms.

Abbreviations: CR, cluster root; GUS, ß-glucuronidase; LR, lateral root; PCR, polymerase chain reaction; Pi inorganic phosphate; *LaARF5*, *Lupinus albus* auxin response factor 5; *LaTIR1b*, *Lupinus albus* transport inhibitor response 1b.

Introduction

Cluster roots or proteoid roots are specific organs that are produced by the *Proteaceae* and a limited number of species belonging to several botanical families that are adapted to habitats with extremely low soil fertility (Shane and Lambers 2005, Lambers *et al.* 2015). Indeed, cluster roots correspond to bottlebrush-like clusters of rootlets with limited growth occurring along lateral roots (reviewed in Vance *et al.* 2003 ; Fig. 1A, B). These organs represent an evolutionary adaptation to phosphorus-impoverished soils. As a result, cluster roots exhibit four main characteristics regarding their development and physiology (Skene, 2000): i) a massive induction of rootlets (up to 20-100 per cm), ii) a determinate development leading to a limited growth and subsequent entry into senescence, iii) an exudative burst resulting in massive secretion of protons, organic acids, phenolics and phosphate remobilizing enzymes and iv) a high phosphate uptake capacity. The secretion of protons can be imaged with a pH indicator such as bromocresol purple (Fig. 1C). A high level of ferric reductase activity is also associated with cluster root physiology and can be revealed biochemically (Fig. 1D).

White lupin (*Lupinus albus*) is an annual legume traditionally cultivated around the Mediterranean and is also the only cultivated crop that can form cluster roots. It is a model of interest because of its quick life cycle compared to other species, mainly bushes and trees, sharing the ability to form these structures. Moreover, white lupin has the capacity to form nitrogen-fixing nodules as a result of the symbiotic interaction with *Bradyrhizobium sp.* but has lost the ability to form mycorrhizal associations (Lambers and Teste 2013). Interestingly, many cluster root forming species share this lack of ability for mycorrhization. The capacity to form cluster roots in lupin allows a reduction of phosphate fertilizer use in the field and results in a beneficial interaction in mixed cultures (Cu *et al.*, 2005), this represents an interesting example to lower our dependency on this source of agricultural input.

In this study, we used white lupin cluster root as a model to study a highly exacerbated mode of lateral root initiation and development. Indeed, production of numerous rootlets means that several sites of lateral root formation are activated in an almost synchronous manner (Hagström *et al.*, 2001). Regular lateral root development involves several fundamental mechanisms that have been largely described, including in the model plant *Arabidopsis thaliana*. Lateral root formation starts early in the primary root apex where pre-branching sites are defined (Moreno-Risueno *et al.* 2010, Xuan *et al.* 2015). Later on, founder cell specification

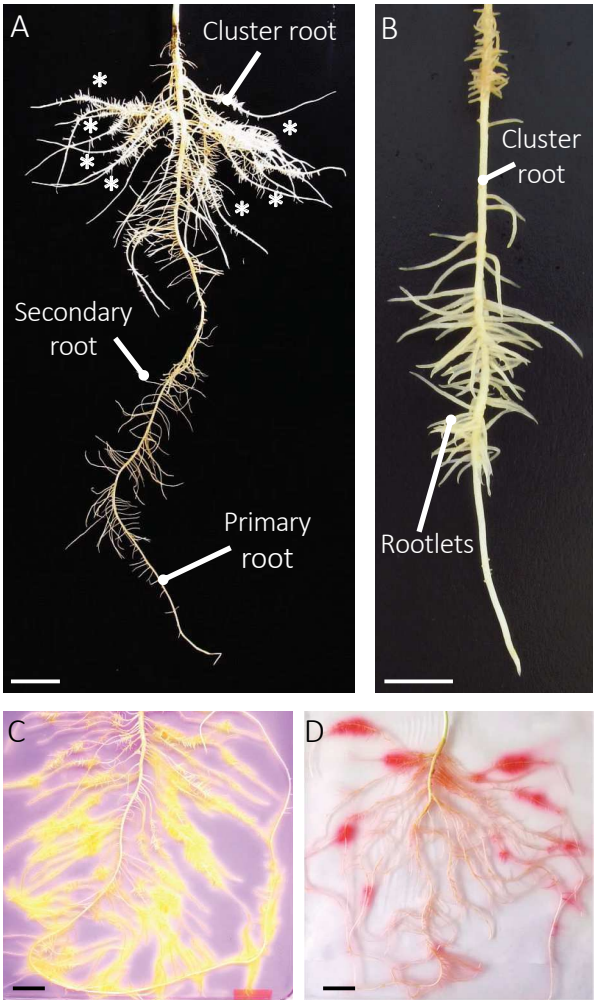

Fig. 1. White lupin architecture and physiology in low phosphate conditions. (A and B) Root architecture of a 21-day-old white lupin (*Lupinus albus*) comprising many CRs in the upper part of the root system (asterisks). CRs are secondary roots producing hundreds of short roots with determinate development, known as rootlets (B). (C and D) Physiological assays of 19-day-old lupin root systems placed on agar plates containing bromocresol purple (BCP) (C) or bathophenanthroline disulfonic acid disodium salt (BPDS) in the presence of Na-Fe EDTA (D). (C) BCP is a purple pH indicator that turns yellow when the roots are acidifying the medium with proton excretion (pH< 5). (D) BPDS allow visualisation of ferric reductase activity upon reduction of Fe_3^+ to Fe_2^+, with appearance of a pink coloration. Scale bars are 2.5 cm (A, C, D) and 0.5 cm (B).

occurs in the pericycle to trigger the initiation event (Dubrovsky *et al.* 2008, De Rybel *et al.* 2010). The lateral root primordium then undergoes a series of divisions following a defined pattern (Malamy and Benfey, 1997) and simultaneously emerges through the outer tissues to reach the rhizosphere (Laskowski *et al.*, 2006). This developmental process is thought to be iterative for higher order lateral roots but very few studies have focussed on this subsequent step. In lupin, we can imagine that these fundamental mechanisms are amplified to produce hundreds of rootlets. It is therefore possible to learn more about the regulatory mechanisms of lateral root development by studying lupin cluster root development.

It is well known that several hormones control lateral root formation (Fukaki and Tasaka, 2009), among which auxin acts as a positive regulator (Du and Sheres 2017a) whereas cytokinins have a negative impact (Laplaze *et al.*, 2007). Auxin transport is polar and achieved by various transporters including PIN efflux and AUX/LAX influx carriers (Benková *et al.* 2003, Billou *et al.* 2005). Auxin regulates the transcriptional activity of several genes through the action of the $SCF^{TIR/AFB}$ complex, which comprises TIR1 auxin receptor (F-box protein) (Dharmasiri *et al.* 2005, Kepinski and Leyser 2005) and a SCF (SKP-Cullin F-box) type ubiquitin E3 ligase. Together with the Aux/IAA repressor, they form the auxin receptor complex. In the presence of the ligand, the complex tags Aux/IAA for degradation, therefore releasing the ARF (Auxin Response Factor) proteins. ARF proteins are known to regulate (activate or repress) transcription by binding to specific Auxin Response Elements (AuxRE) in the target gene promoter (Ulmasov *et al.* 1997, Ulmasov *et al.* 1999). It was shown that auxin plays a major role during cluster root formation with auxin accumulation involved and expression of hormone-related genes such as YUCCA, AUX1 and PIN1 (Wang *et al.* 2014, Wang *et al.* 2015, Meng *et al.* 2013). In fact, the establishment of a meristem is always accompanied by the establishment of an auxin maximum (Benková *et al.*, 2003). Such auxin gradient has not yet been described in white lupin rootlets. But given the determinate nature of their meristems, the establishment of such a gradient may be transitory or not even happen.

In this study, we focussed on rootlet development because it represents an optimal model for lateral root development for two major reasons: i) rootlets are massively and synchronously induced in phosphate starvation conditions and ii) rootlets have a determinate development. We achieved a histological description of rootlet development during cluster root formation in white lupin to describe the early cellular division events. We demonstrated the establishment of an auxin gradient during rootlet primordia formation by studying the

DR5:GUS marker in white lupin. We set up a time course sampling approach to dissect auxin-related gene expression and focussed on two genes. Cloning *LaTIR1b* and *LaARF5* promoters allowed us to determine their expression pattern during rootlet development and to validate an important role of auxin during this process.

Results

Characterisation of rootlet primordium development in white lupin

If the cellular events leading to the formation of lateral roots have been well described (Malamy and Benfey 1997, Casimiro *et al.* 2003, Péret *et al.* 2009, Von Wangenheim *et al.* 2016), especially in the model plant *A. thaliana*, little information is available about the contribution of root tissues to cluster root development, especially in white lupin. To describe cluster root development, our aim was first to provide a tissular description of rootlet primordia development. To achieve this objective, we generated thin cross sections of 14-day-old cluster roots that were subsequently stained with toluidine blue to reveal the cell layers. Lupin roots comprise only one layer of pericycle, endodermis and epidermis; cortical cells displayed up to 5-6 layers (Fig. 2A and B). Observation of these thin sections by means of photonic microscopy allowed the observation of the early cellular events throughout the course of rootlet development. By analogy with lateral root development in the model plant Arabidopsis, we defined eight developmental stages from initiation (stage I) to emergence (stage VIII), as shown in Fig. 2 and described below.

On the cross sections, the earliest visible event of rootlet formation corresponded to a periclinal division in the pericycle close to a protoxylem pole (Stage Ia, Fig. 2C, black arrow). This division was followed by a second pericline division in the pericycle cells (Stage Ib, Fig. 2D, black arrows). At stage II, it seemed that pericycle cells continued to divide periclinally as more cell walls were observed in these cells. These divisions gave birth to two pericycle layers: P1 and P2. Approximately at the same moment, periclinal divisions were also observed in the endodermis tissue, overlaying the pericycle cells (Stage II, Fig. 2E, black arrow). As a consequence, we observed a rootlet primordium with 4 layers (P1, P2, E1, E2) that was about 10 cells in length (Stage II, Fig. 2E). A first radial division was also seen in the pericycle at the lateral primordium boundary (Stage II, Fig. 2E, purple arrow). The following stage was characterized by further periclinal divisions in the pericycle and endodermis tissues (Stage III,

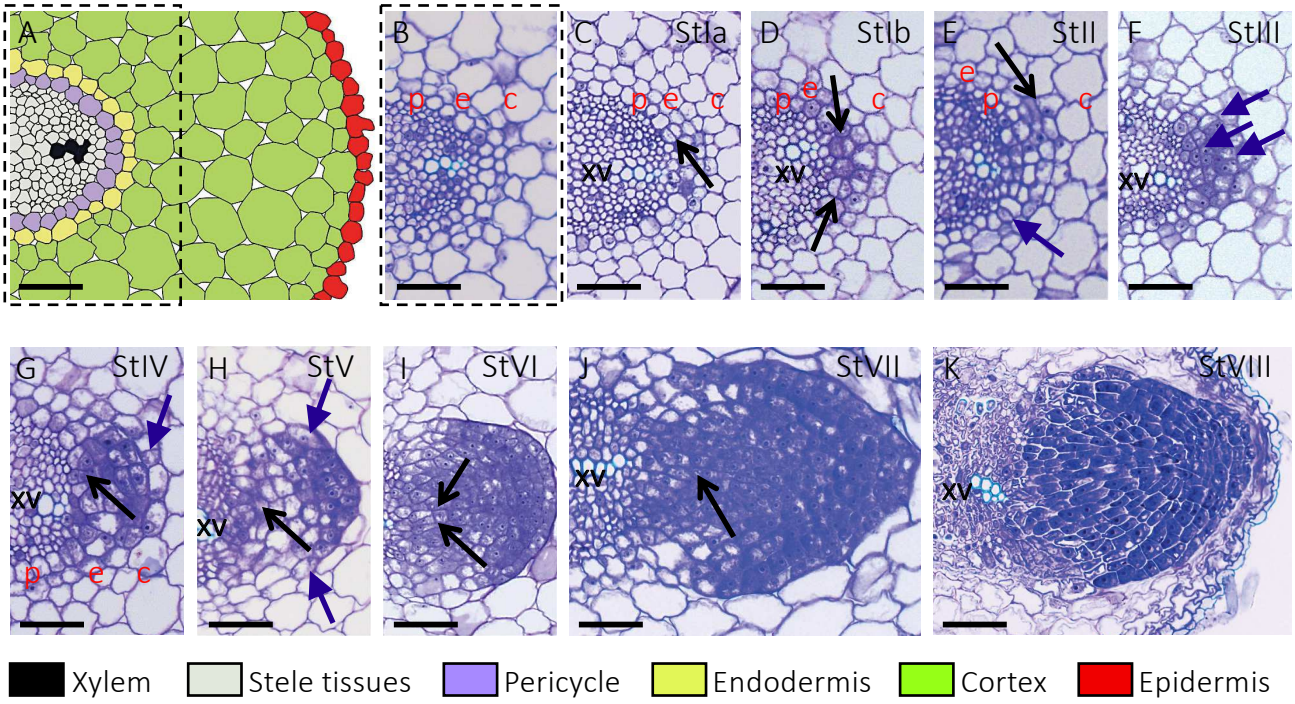

Fig. 2. Rootlet primordium development during CR formation in white lupin. Radial cellular organisation of white lupin CR (A) drawn from a thin cross section of CR from 24-day-old P-deficient plants (B). Xylem vessel elements are stained in blue and non-lignified cells walls are stained in purple by toluidine blue. (C) A first periclinal division is seen in the pericycle at stage Ia. (D) A second cell is dividing in the pericycle (stage Ib). (E) Periclinal divisions are occurring in the endodermis (stage II). (F) Numerous anticlinal divisions are seen in the pericycle and endodermis tissues (stage III).(G) More cell divisions in the pericycle and endodermis give rise to a dome-shaped rootlet primordium that is about to cross cortex and several cells are dividing at the base of the primordium between the pericycle and protoxylem pole (stage IV). (H) Cells are proliferating at the base and the apex of the primordium (stage V). (I) Primordium has crossed half of the cortex and some elongated cells are appearing in the centre of the primordium (stage VI). (J) The rootlet primordium is made of numerous cells and is about to reach the epidermis of the secondary root. Note the deformation of the cortex occurring when rootlet is about to emerge (stage VII). (K) The new primordium is crossing the epidermal layer and reaching the rhizosphere (stage VIII). p, pericycle; e, endodermis; c, cortex; xv, xylem vessels. Scale bars are 50 µm.

Fig. 2F, purple arrows). Cell divisions in the next following stages became more and more difficult to characterize as the primordium was increasing both in length and width. Numerous cells continued to divide, giving progressively birth to a typical dome shaped primordium. At stage IV, rootlet primordium development coincided with intensive cell divisions happening between the xylem pole and the P1 pericycle tissue in the procambial tissue (Stage IV, Fig. 2G, black arrow). A radial division was seen in the overlaying cortical tissue, suggesting a possible role of cortex tissue in rootlet primordium development (Stage IV, Fig. 2G, purple arrow). Stage V of rootlet primordium development coincided with further divisions in the procambial tissue and at the apex of rootlet primordium. (Stage V, Fig. 2H, black arrow). Lens shaped cells also appeared at the edges of rootlet primordium (Stage V, Fig. 2H, purple arrows). In the next stage of rootlet development, stage VI, rootlet primordium had crossed half of the main cluster root and was much larger. This progression through the outer tissues caused the surrounding cortical cells to be distorted and displaced (Stage VI, Fig. 2I). At this stage, elongated cells could be observed in the centre of the rootlet primordium, reminiscent of vascular elements (Stage VI, Fig. 2I, black arrows). A core of cells at the apex gave rise to a croissant shaped structure that looks like a typical root cap at the tip of the rootlet primordium (Stage VI, Fig. 2I). From this stage onward, new cell divisions were really difficult to characterize due to the high number of cells and their small volume. At stage VII, the primordium was crossing the last layers of cortical cells of the main cluster root and was about to emerge in the surrounding rhizosphere. At this stage, an important number of elongated cells were visible in the centre of the rootlet primordium and seemingly connected to the vasculature of the main cluster root (Stage VII, Fig. 2J, black arrow). Primordia grew from 70 µm in width and 115 µm in length at stage IV (Fig. 2G) to 180 µm in width and 220 µm in length at stage VIII (Fig. 2K). When the rootlet was about to emerge, the primordium was more than 4 times longer than Arabidopsis LR primordium, which is typically about 50 µm in length. In the last step, stage VIII, the new formed rootlet was crossing the epidermis and emerging (Stage VIII, Fig. 2K).

Establishment of an auxin gradient during rootlet morphogenesis

The major role of auxin during LR development has been described into great detail (Lavenus *et al.*, 2013), notably with the help of the synthetic auxin reporter DR5 (Ulmasov *et al.*, 1997). We generated white lupin composite transgenic "*hairy root*" plants expressing the

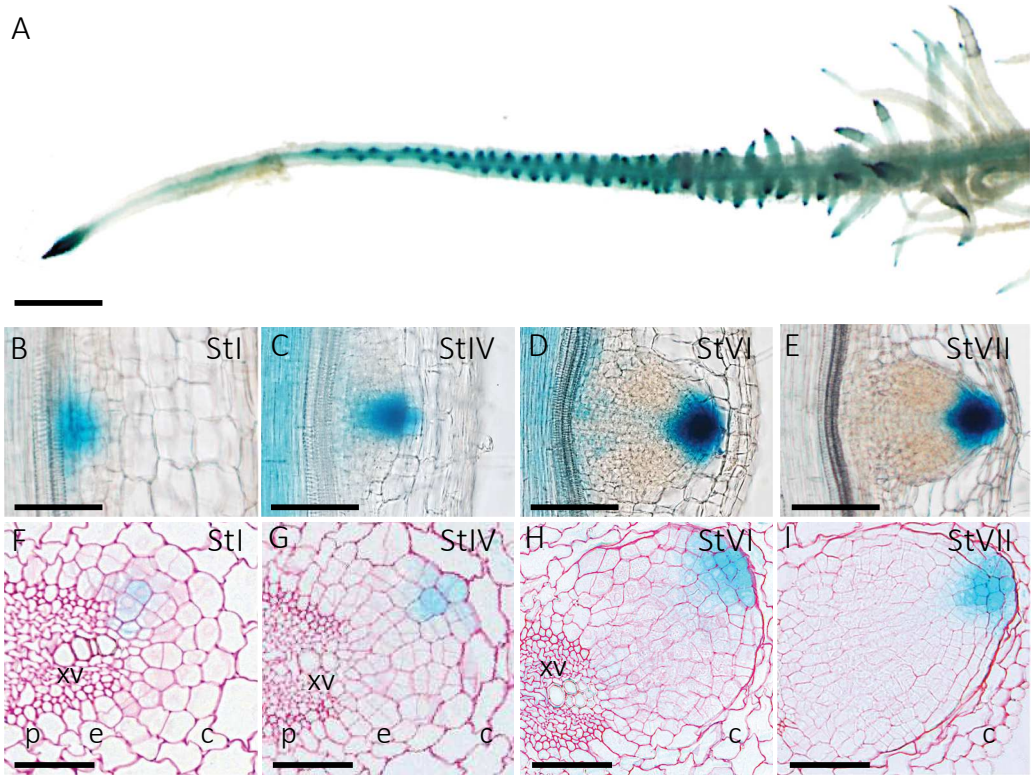

Fig. 3. Establishment of an auxin gradient during CR and rootlet development. (A–I) *DR5:GUS* pattern of expression in lupin 'hairy root' seedlings grown on low-phosphate medium. (A) Fully mature whole CR. (B–E) *DR5:GUS* expression was observed on thick longitudinal sections (80 µm) at stage I (B), stage IV (C), stage VI (D) and stage VII (E). (F–I) *DR5:GUS* expression was also observed on thin cross sections (6 µm) in the juvenile region of the CR counterstained with ruthenium red at corresponding stages: stage I (F), stage IV (G), stage VI (H) and stage VII (I). p, pericycle; e, endodermis; c, cortex; xv, xylem vessels. Scale bars are 100 µm

DR5 reporter fused to the ß-glucuronidase gene. Our first goal was to determine whether the "*hairy root*" system is suitable to observe auxin related developmental mechanisms and subsequently to determine whether an auxin gradient is established during rootlet organogenesis. In white lupin, the DR5 marker, an artificial promoter made of 7 tandem repeats of an auxin responsive element isolated from soybean (*Glycine max*), showed a strong conserved pattern compared to other species. Indeed, DR5 expression was seen in the cluster root tip and vasculature (Fig. 3A and S1A). In rootlet primordium, GUS activity was observed at stage I of development (Fig. 3B), in one of the first dividing cells, close to the protoxylem pole. At stage IV, when divisions give rise to a dome shaped primordium, GUS activity was observed in a few cells at its tip (Fig. 3C). From this stage onward, a strong DR5 response builds up in the primordium apex (Fig. 3C-E, G-I). After emergence, strong GUS activity was detected in the root cap whereas the zone above the rootlet tip was displaying a weak GUS activity (Fig. S1B-D). Expression in the vasculature was observed in mature rootlets (Fig. S1C, D). Our observations of the *DR5:GUS* reporter suggest that an auxin gradient is established during rootlet initiation up to their emergence and maintained during their later development.

Time course analysis of key auxin signalling genes during rootlet development

In order to identify key auxin signalling genes potentially involved in rootlet development, we performed *in silico* analysis of the available transcriptomic data in white lupin (Secco *et al.*, 2014). In that study, transcriptomic data were produced from 3 parts of cluster roots (tip of cluster root, physiologically immature cluster root and mature cluster root) as well as 2 parts of regular lateral roots (tip of the lateral root and mature lateral root). We identified several auxin related genes in this dataset encompassing *ARFs*, *Aux/IAAs*, *TIRs*, *PINs*, *AUX-LAXs* and we shortlisted 8 genes (Table S1) that showed consistent results with BLAST (*i.e.* for which the cDNA sequence matched the expected orthologous sequences from other species and showed a similar overall gene structure) and for which we managed to amplify fragments by qPCR.

The available transcriptomic dataset (Secco *et al.*, 2014) study represents an important tool for cDNA discovery but we wanted to study gene expression level with a higher resolution than the existing data. Therefore, we developed a sampling method to describe rootlet development along a time course. Our analysis of white lupin root system allowed us to locate

the first cluster of rootlets on the cluster root and perform a temporal sampling covering the different phases of rootlet emergence. We measured the distance to primary root that we defined as the distance between the primary root and the first cluster of rootlets (Fig. S2A). We sampled 1 cm of cluster root at a distance of 1 cm from the primary root from 7 days after germination every 12 hours for 5 days, therefore we were able to cover the entire rootlet developmental process. Indeed, 55% of cluster roots initiate at 1 or 1.5 cm from the primary root and the sampled zone therefore comprises 77 % of the produced rootlets (Fig. S3B). Samples were collected for total RNA extraction and subsequent qRT-PCR analysis (Fig. 4A-B) and imaging (Fig. 4C). We observed that rootlet initiation occurred at 12h after the first sampling (has) and that rootlet emergence occurred at 72 has (Fig. 4C).

Expression analysis of the 8 auxin-related genes showed various overall behaviours during rootlet development (Fig. 4 and Fig. S3). Some genes did not show a clear induction or repression response but varied along the time course such as *LaTIR1a* and *LaARF14b*. Others showed a general repression such as *LaARF5*, *LaIAA28* and *LaARF14a* (although for this gene one biological replicate strongly differs from the other 3). Two genes showed a peak of induction at around 72 has, such as *LaPIN1* or *LaLAX3,* but not all biological replicates showed matching patterns. Interestingly, *LaTIR1b* showed a general induction during the time course. We decided to focus our attention on two genes: La*TIR1b* and *LaARF5* as shown in Fig. 4A and Fig. 4B. *TIR1* codes for a protein that is part of the SCF/TIR complex, which promotes Aux/IAA protein degradation when auxin is present; and *ARF5* is known to play a role in the very early stages of LR development ensuring the identity of the founder cells (De Smet *et al.*, 2010). Interestingly, *LaTIR1b* is slightly induced during our time course with a peak of expression at 72 has (Fig. 4A). This coincides with the emergence stage. On the opposite, *LaARF5* is repressed during rootlet formation (Fig. 4B), which may suggest a negative control by auxin accumulation in the rootlet primordium.

LaTIR1b and *LaARF5* expressions are altered during rootlet development

We aligned the cDNA-deduced protein sequence of *LaTIR1b* and *LaARF5* with their orthologous genes from *A. thaliana* and generated phylogenetic trees (Fig. 5A and Fig. S4). *LaTIR1b* appeared to be the closest ortholog of *AtTIR1* with 77% identity at the entire protein level, suggesting that the automatic annotation was fairly accurate (Fig. 5A). However, *LaARF5*

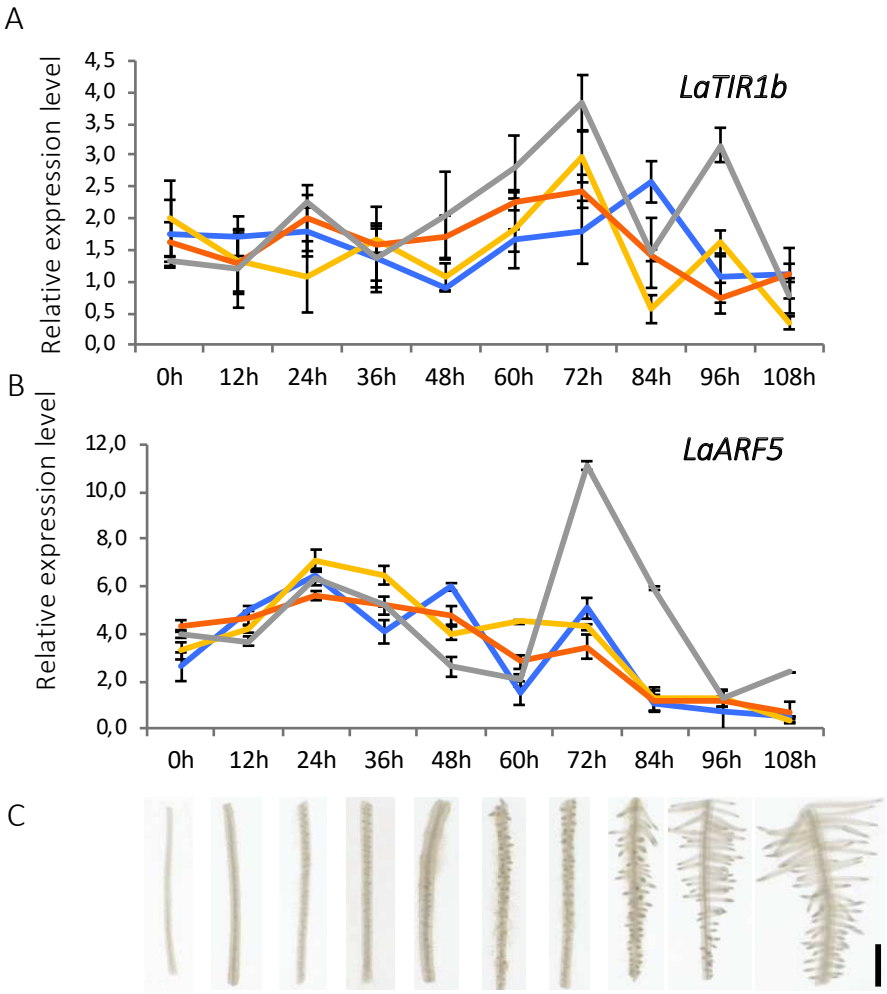

Fig. 4. Relative expression levels of *LaTIR1b* and *LaARF5* during rootlet development. Expression levels of *LaTIR1b* (A) and *LaARF5* (B) are relative to the first time point (0 h) and normalised to *LaUBQ*. Data are mean± SD of eight CRs coming from four lupin plants (n= 8) with four technical replicates each. Four biological replicates are shown in different colours. (C) 1 cm CR samples collected 1 cm away from the primary root every 12h were used to assess transcript level during CR development. Scale bar is 0.25 cm.

groups in a branch that contains 3 close orthologs: *AtARF11*, *AtARF18* and *AtARF9*. Its highest identity level is with *AtARF11* at 70% and its identity level to AtARF5 is only 50% suggesting that this gene annotation is not very accurate (Fig. S4) but that it is still an ARF protein. Furthermore, *LaARF5* is predicted to act as a repressor like *AtARF11* and not as an activator like *AtARF5*.

In order to characterize the expression pattern of these two genes, we used an *in silico* genome walking approach to identify the promoter regions of *LaTIR1b* and *LaARF5* (see Methods). These promoters were amplified from genomic DNA and subsequently cloned and sequenced to validate their nucleotide sequence. We then analysed the promoter region of the two genes using the SOGO database (Higo *et al.* 1999), which revealed numerous potential binding sites for various transcription factors amongst which some are hormone related (Table S2) and thus potentially important in the context of rootlet development. We highlighted these elements in the promoter of each gene (Fig. 5B and Fig. 6A). The promoters of *LaTIR1b* (Fig. 5B) and *LaARF5* (Fig. 6A) each contain a canonical auxin responsive element (AuxRE) that is known to be a target site for ARF transcription factors. They also contain several ARR sites (Arabidopsis Response Regulator) that are present in the promoter of cytokinin-induced genes (3 for *LaTIR1b* and 4 for *LaARF5*). The promoter of *LaARF5* contains a gibberellin-related binding site and 2 sites found in SAUR genes (Small Auxin Up-Regulated RNA), these sites were not found in the promoter of *LaTIR1b*.

In order to further characterize the expression pattern governed by these promoters, we fused them to the ß-glucuronidase coding region to create *pLaTIR1b:GUS* and *pLaARF5:GUS* expression vectors. These vectors were transfected into *Agrobacterium rhizogenes* and used to genetically transform white lupin plants by *hairy root* (Uhde-Stone *et al.*, 2005). We examined *pLaTIR1b:GUS* expression during the development of rootlets. In developing primordia, *pLaTIR1b* was first expressed at stage III (Fig. 5C) and a slight expression gradient was visible at the apex primordia in the following developmental stages (Fig. 5D-F). In the rootlet, a very strong gradient of expression was observed in young and middle-aged rootlets (Fig. 5G-J) and a maximum of expression remained in the rootlet tip, corresponding to the meristem and elongation zone (Fig. 5I-J). In the rootlet, *LaTIR1b* was expressed in the vasculature throughout their lifetime and expression at the rootlet tip faded away in older rootlets (Fig. 5K).

We also examined *pLaARF5:GUS* expression during rootlet development. Our analysis revealed that *pLaARF5* is expressed in the cluster root vasculature but its expression is absent from the rootlet primordium. No GUS coloration was found from early stage up to after

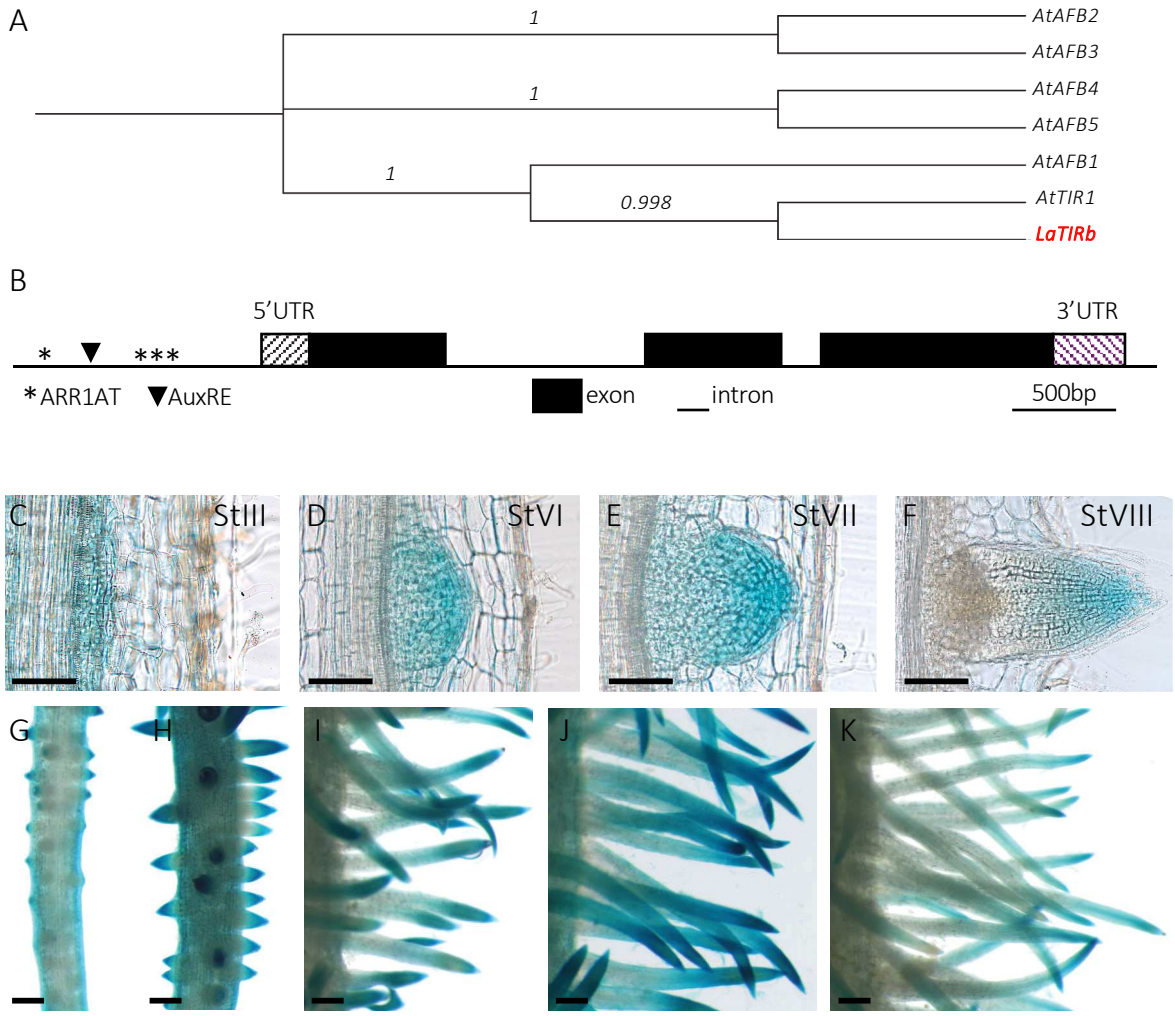

Fig. 5. Genetic study and expression pattern of *LaTIR1b*, a lupin orthologue of Arabidopsis *TIR1*. (A) Neighbour joining tree showing relationship of *LaTIR1b* with *AtTIR/AFB* from Arabidopsis thaliana. *LaTIR1b* gene structure seems to be closely related to *AtTIR1*. The bootstrap consensus tree was inferred from 500 replicates. Branches corresponding to partitions reproduced in less than 50% bootstrap replicates were collapsed. (B) Gene structure of *LaTIR1b*. Hormone-related cis-acting regulatory elements, exons, introns and position of 5'UTR and 3'UTR are shown (graph to scale). (C–K) Expression pattern of *pLaTIR1b:GUS* in 4-week-old plants grown in low phosphate conditions. GUS activity was found in developing primordia of rootlets at stage III (C), stage VI (D), stage VII (E), stage VIII (F) and appeared homogeneous along the cluster at early (G) and late stages (H) of rootlet formation. Later on, expression showed a clear gradient with stronger activity at the rootlet tip at three stages of rootlet development: young rootlets (I), middle-aged rootlets (J) and old rootlets (K). Scale bars are 100 µm (C–F) and 0.5 mm (G–K).

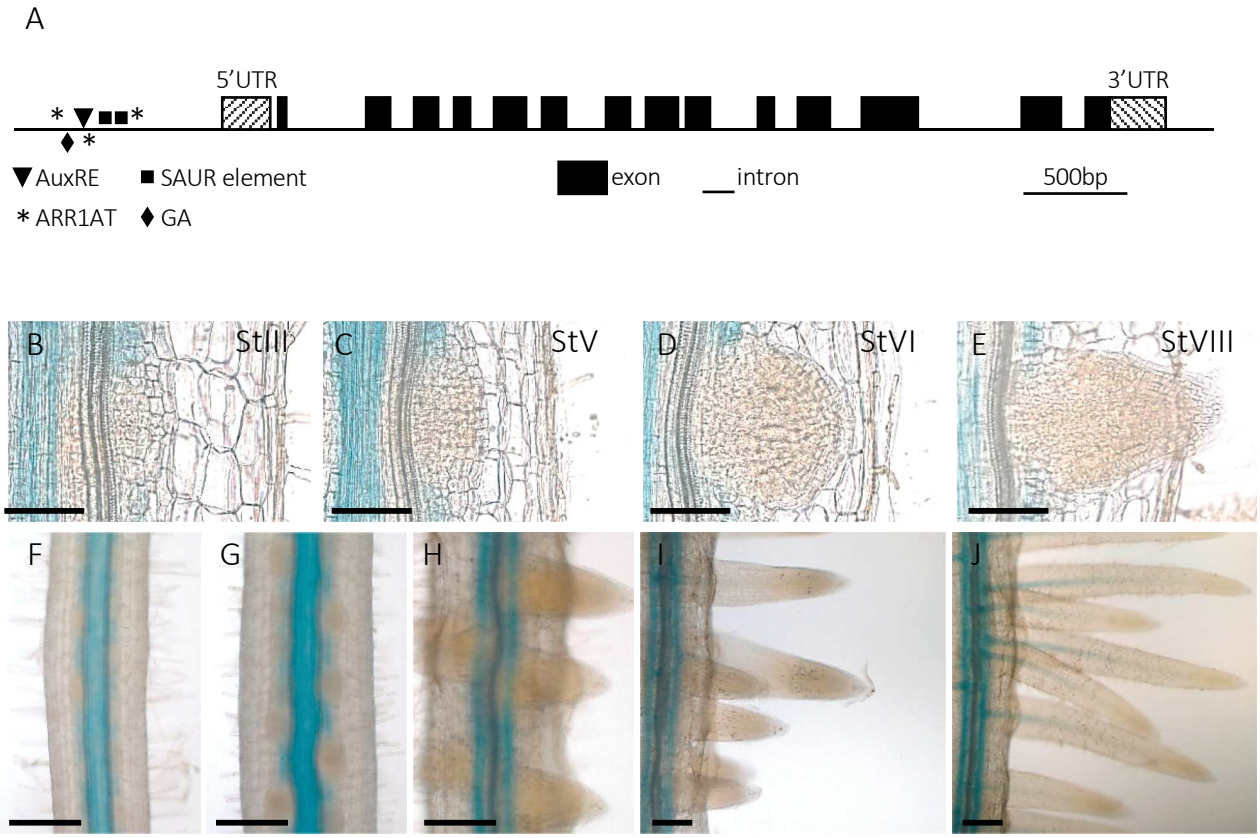

Fig. 6. Genetic study and expression pattern of *LaARF5*, a lupin orthologue of Arabidopsis thaliana *ARF11*. (A) Gene structure of *LaARF5*. Hormone-related cis-acting regulatory elements (as defined in Table S2), exons, introns and position of 5'UTR and 3'UTR are shown (graph to scale). (B–J) Expression pattern of *pLaARF5:GUS* in 4-week-old plants grown in low phosphate conditions. GUS activity was absent in developing primordia of rootlets at stage III (B), stage V (C), stage VI (D), stage VIII (E) and remained in the CR vasculature (F), absent from early (G) and late stages of rootlet emergence (H) and mature rootlet (I). Expression resumed in the vasculature in old rootlets (J). Scale bars are 100 µm (B–E) and 200 µm(F–J).

emergence (Fig. 6B-E). Growth of the rootlet primordium seemed to even lower the expression in the surrounding tissues (Fig. 6F-G), what is consistent with the global repression of this gene found in our qRT-PCR analysis (Fig. 4B). At later rootlet development, expression in the vasculature could be detected, mimicking the expression profile in the cluster root (Fig. 6J).

Discussion

Previous work on white lupin cluster root has been largely focussed on its physiology because it is a very active organ with high levels of exudation involved in the root phosphate acquisition (Neumann *et al.* 2000, Massonneau *et al.* 2001, Yan *et al.* 2002, Hocking and Jeffery 2004). In this study, we decided to focus on cluster root because of its atypical mode of development, corresponding to the production of numerous rootlets initiated in a synchronous manner and with a limited lifetime. Our approach has revealed that the early divisions of rootlets are very similar to what is observed in other species lateral root development, like the model plant *A. thaliana* or even in legumes. Indeed, lateral root development in these species is initiated by divisions in the pericycle cells in front of the xylem poles (Dubrovsky *et al.*, 2000), and this is the case for white lupin rootlets (Fig. 2). Cellular division in the endodermis and cortex are regularly observed in legume species – like *Medicago truncatula* (Herrbach *et al.*, 2014) – but not in *A. thaliana*, this may be linked with the presence of numerous cortical cell layers and with the comparatively important size of the primordia. We provide here a detailed anatomical description of the various stages of rootlet development along the cluster root that will prove useful in the future to characterize mutants or genetically altered plants but also to go deeper into the study of the molecular mechanisms of regulation of cluster root development.

In parallel, we have set up an original sampling procedure that covers the entire development process, from the rootlet initiation to the rootlet senescence, and, even if some discrepancies are observed, most probably due to plant to plant genetic variability, this system allows for the description of gene expression profiling during rootlet development. We focussed here on describing some auxin-related gene expressions and we identified two genes with contrasted expression profiles (Fig. 4). Further analysis of their expression pattern at the tissular level confirmed the induction and repression of *LaTIR1b* and *LaARF5,* respectively (Fig.

5 and 6), and validated our time course sampling method to study rootlet development. *LaARF5* was previously annotated based on RNAseq assembly in the absence of a reference genome for white lupin (Secco *et al.*, 2014). Phylogeny analysis revealed that it is the closest ortholog to *AtARF11*. In accordance, *LaARF5* and *AtARF11* are both predicted to be repressor ARFs whereas *AtARF5* is an activator. Furthermore, *AtARF5/MONOPTEROS* is expressed in lateral root primordium from as early as stage I and up to emergence (De Smet *et al.* 2010; Ckurshumova *et al.* 2014) whereas *LaARF5* is not expressed in cluster root primordia (Fig. 5). Further work will be needed to understand how these two genes are regulated, including by hormonal signals, and how they fit in larger gene regulatory networks. Whole-genome transcriptional studies are an essential step to finely identify new genes regulating lateral root development and the cluster root model seems to be perfectly adapted to this strategy.

Another key feature of rootlet development is that they all enter into senescence simultaneously. In fact, rootlet meristems are determinate, meaning that they stop dividing and undergo full differentiation up to their tip (Watt and Evans, 1999a). This mode of growth is directly related to the function of the cluster root and to the chemical nature of phosphate. Indeed, inorganic phosphate is poorly mobile in the soil, therefore cluster roots are able to remobilize as much phosphate as possible and subsequently uptake it for the plant nutrition (Hinsinger *et al.*, 2011). However, soil phosphate patches are quickly used up and new clusters are produced in a distant site to forage for more phosphate. As a result, cluster roots are ephemeral structures by nature due to rootlets determinacy. In laboratory conditions (hydroponic culture medium), we expose roots systems to a permanent and homogeneous lack of phosphate. In these conditions, rootlets are produced, grow to their mature length and then stop growing demonstrating that there is no need for a feedback from the medium to control their growth behaviour. This raises several important questions regarding the order of events leading to rootlet growth arrest: when does cell elongation and division stop? Is the determinacy of the meristem already established in the rootlet primordium? Does the primordium ever acquire a meristematic organisation? Does a maximum of auxin form in the rootlet meristem? Here, the use of the DR5 marker allowed us to confirm the establishment of such a maximum of auxin that seems to be maintained throughout the course of rootlet development up to its mature length (Fig. 3 and S1). More work will be needed to describe precisely how rootlet determinacy is genetically controlled and if a mechanism similar to what is known about *A. thaliana* primary root development can be described (Balzergue *et al.*, 2017).

In this regard, studying the establishment of a quiescent centre and its maintenance during rootlet growth could be of great interest.

With regards to root developmental adaptations, white lupin is a fantastic model to parallel with other models like *A. thaliana* or *M. truncatula* for a better understanding of the mechanisms regulating the development of lateral roots but many genomic tools are still missing to conduct further analysis. We believe that future work will produce these tools and help understand how cluster root development is tightly controlled to produce such amazing structures.

Materials and methods

Plant materials and growth conditions

Seeds of white lupin (*Lupinus albus* cultivar Amiga) were used in all experiments (obtained from Florimond-Desprez). Seeds were germinated on vermiculite substrate for 4 days. Seedlings were cultivated in growth chambers under controlled conditions (16h light / 8h dark, 25°C day / 20°C night, 65 % relative humidity, PAR intensity 200 µmol.m^{-2}.s^{-1}). After germination, 4 seedlings were transferred to 1.6 L pots. The hydroponic solution was modified from (Abdolzadeh *et al.*, 2010) without phosphate, according to the following composition: $MgSO_4$, 54 µM; $Ca(NO_3)_2$ 400 µM; K_2SO_4 200 µM; Na-Fe-EDTA 10 µM; H_3BO_3 2.4 µM; $MnSO_4$ 0.24 µM; $ZnSO_4$ 0.1 µM; $CuSO_4$ 0.018 µM; Na_2MoO_4 0.03 µM. The nutrient solution was continuously aerated and was renewed every 7 days.

Cluster root physiological assays

For all functional assays, the roots of 3-week-old plants were thoroughly washed in ultra pure water, and carefully pressed on agar sheets to avoid damaging the roots and covered with a transparent film. For visualisation of protons excretion, agar sheets contained: 0.8 % agar (w/v), 0.005 % bromocresol purple buffered with Tris HCl 1 mM pH=6, 2mM K_2SO_4 and 1 mM $CaSO_4$. For visualisation of ferric reductase activity, agar sheets were prepared as follows: 0.8 % agar (w/v), 100 µM Na-Fe-EDTA, 300 µM bathophenanthroline disulfonic acid, 1 mM K_2SO_4. Agar plates were allowed to set at room temperature for 6 hours in the dark.

Low coverage genome sequencing

In order to generate a genomic dataset of white lupin, DNA from leaf tissue was extracted using Qiagen Genomic-tip 100 according to the manufacturer's protocol. The integrity and quality of total DNA was checked using NanoDrop 1000 Spectrophotometer (ND1000) and formaldehyde agarose gel electrophoresis, and DNA was quantified using a Qubit fluorometer. Short-reads sequencing (150-bp) was performed using the Illumina Hiseq 3000 platform at GenoToul (Toulouse, France), generating 79,424,562 reads. Quality assessment and trimming of the reads were performed with FastQC (http://www.bioinformatics.babraham.ac.uk/projects/fastqc) and the FASTX-Toolkit (http://hannonlab.cshl.edu/fastx_toolkit/index.html), respectively.

In silico genome walking

In order to identify the promoter sequences of *LaTIR1b* (LAGI02_15246) and *LaARF5* (LAGI02_2355) whose cDNA were obtained from the white lupin gene index (LAGI02) previously published (Secco *et al.*, 2014), we set up a technique that we named *in silico* genome walking (ISGW). ISGW is achieved in 2 steps: first the Illumina reads are mapped against a cDNA sequence from the gene of interest (reference sequence) using BBmap v. 37.41 (https://sourceforge.net/projects/bbmap/) and second all mapping reads are assembled into a slightly larger contig using CAP3 (Huang and Madan, 2009). The process is repeated by using the larger contig as a reference for a next round of assembly, therefore initiating the genome walking process (both ways). ISGW was performed until we obtained contigs containing 1000 bp upstream of the ATG start codon. This sequence information was then used to clone the promoter by PCR amplification.

Molecular cloning

The primers for *pLaTIR1b* (F-5'-TCATTTCCAAACTTATAAGTGG-3'; R-5'-GGTCGTTGATTCACTGATGAAACG-3') and *pLaARF5* (F-5'-GATCCTTTTAGAGAGTTGG-3'; R-5'-GCAACACCATCAAATTCAATAAG-3') were designed using Primer3Plus (Untergasser *et al.* 2012). They were used to amplify a total of 986 bp and 898 bp upstream of the start codon of *LaTIR1b* and *LaARF5* respectively, from white lupin genomic DNA with the addition of the attb1 (5'-

GGGGCCAAGTTTGTACAAAAAAGCAGGCT-3') and attb2 (5'-CCCCCCACTTTGTACAAGAAAGCTGGGT-3') adapters. Amplified fragments were subsequently cloned into the pDONR221 by Gateway reaction. The promoters were then cloned into the binary plasmid pKGW-FS7 (Karimi *et al.*, 2002) containing a GFP-GUS fusion by Gateway cloning.

Bacterial strain

Agrobacterium rhizogenes strain *ARquaI* was used to perform *hairy root* transformation of white lupin. Bacteria were transformed with the binary plasmid by electroporation and confirmed by PCR and sequencing. LB agar plates (agar 0.8 %) added with acetosyringone 100 µM were inoculated with 200 µL of liquid bacteria culture and incubated at 28°C for 24 hours to get a bacterial lawn. Bacterial lawn was used for white lupin seedling transformation.

Hairy root transformation of white lupin

White lupin seedlings were transformed following protocol previously described (Uhde-Stone *et al.*, 2005). White lupin seeds were surface sterilised by 4 washes in osmosed water, 30 min sterilization in bleach (Halonet 20%) and washed 6 times in sterile water. Seeds were germinated in the dark in water. After germination, radicles of 1 cm were cut over 0.5 cm with a sterile scalpel. The radicles were inoculated with the *A. rhizogenes* culture. Fifteen inoculated seedlings were placed on square agar plates (0.7 % agar in 1X Hoagland solution) containing 15 $\mu g.mL^{-1}$ kanamycin. Plates were placed vertically in growth chambers (Fitotron, Weiss Technik) in controlled conditions: 18 h light / 6 h dark, at 25°C, 60 % relative humidity with a PAR intensity of about 130 $\mu mol.m^{-2}.s^{-1}$. Seedlings were transferred to fresh plates every 7 days for 3 weeks after germination. Timentin (150 $\mu g.mL^{-1}$) was added to the agar medium after 1 week on plates to limit bacterial growth. Plants growing *hairy root*s were transferred after 3 weeks in 1.6 L pot containing nutrient solution with 15 $\mu g.mL^{-1}$ timentin. Nutrient medium was renewed each week. After 7 days in hydroponic conditions, CRs were sampled on *hairy root* plants. Each root represents an independent transformation event and we observed n=89 roots from *DR5:GUS* plants, n=47 roots from *pTIR1b:GUS* plants and n=26 roots from *pARF5:GUS* plants.

Histochemical analysis

Histochemical staining of β-glucuronidase was performed on CRs from *hairy root* plants. Samples were incubated in a phosphate buffer containing 1 $mg.mL^{-1}$ X-Gluc as a substrate (X-Gluc 0.1 % ; phosphate buffer 50 mM, pH 7, potassium ferricyanide 2 mM, potassium ferrocyanide 2 mM, Triton X-100 0.05 %). Coloration was performed as follows: 2 hour incubations for *pDR5:GUS*, 30 min incubation for *pLaTIR1b:GFP-GUS*, or 2.5 hours for *pLaARF5:GFP-GUS*. Tissues were fixed in a 2% formaldehyde / 1% glutaraldehyde / 1% caffeine solution in a phosphate buffer at pH 7. Tissues were fixed for 2.5 hours under shaking at room temperature and then 1.5 hours at 4°C.

Microscopic analysis

For thin section, roots were dehydrated in successive ethanol solutions with increased concentrations: 50% (30 min), 70% (30 min), 90% (1 h), 95% (1 h), 100% (1 h), 100% (overnight). Samples were impregnated with 50% pure ethanol and 50% resin (v/v), then in 100 % resin. CRs were embedded in Technovit 7100 resin (Heraeus Kulze, Wehrheim, Germany) according to the manufacturer's recommendations. For thick sections of 80 µm, cluster roots were embedded in agarose 4% (m/v) and cut with a vibratome (Microcut H1200, Biorad). The whole mount root tissues were cleared with 0.1% ClearSee (Kurihara *et al.*, 2015) in PBS 1X solution and mounted on slides in water. Thin sections of 6 µm were produced using a microtome (RM2165, Leica Microsystems). They were counterstained for 5 min either with 0.05% toluidine blue or with 0.1% ruthenium red in a phosphate buffer (pH 7.4). All sections were observed with a colour camera on epifluorescence microscope (Olympus BX61 with Camera ProgRes®C5 Jenoptik and controlled by ProgRes Capture software).

Expression analysis

A total of 8 CRs coming from 4 independently grown plants were sampled 7 days after germination every twelve hours. Total RNA from these samples was extracted using the Direct-zol RNA MiniPrep kit (Zymo Research) according to the manufacturer's recommendations. RNA concentration was measured on a NanoDrop (ND1000) spectrophotometer. Poly(dT) cDNA were prepared from 1.5 µg total RNA using the revertaid First Strand cDNA Synthesis (Thermo Scientific). Gene expression was measured by qRT-PCR (LightCycler 480, Roche Diagnostics)

using the SYBR Premix Ex Taq (Tli RNaseH, Takara) in 384-well plates (Dutscher). Target quantifications were performed with specific primer pairs designed using Universal Probe Library software (Roche). The two primer pairs used in the parallel PCR reaction were: *LaTIR1b* F-5'-AACCTACTACGTTGGTGTCCTCA-3' and *LaTIR1b* R-5'-CTCTGTCGAGCAGACTCCTGT-3' ; *LaARF5* F-5'-GACGATGAAAATGACATGATGC-3' and *LaARF5* R-5'-AATAATACAGAATTCCGGCCATC-3'. Expression level was normalised to *LaUbiquitin*. The primer pairs used were *LaUbiquitin* F-5'-ATGTCAAAGCCAAGATCCAAG-3' and R-5'-GAACCTTCCCAGAATCATCAA-3' (Meng *et al.*, 2012). All qRT-PCR experiments were performed in technical quadruplicates and the values presented represent means ± s.d.. Relative gene expression levels were calculated according to the ΔΔCt method (Livak and Schmittgen, 2001). All experiments were performed as 4 biological replicates.

Acknowledgements

This project has received funding from the European Research Council (ERC) under the European Union's Horizon 2020 research and innovation programme (Starting Grant Lupin Roots - grant agreement No 637420 to B.P.). CG is the recipient of a fellowship from GAIA doctoral school of Montpellier University. We acknowledge the help of the PHIV imaging platform for technical assistance and access to microscopy equipment.

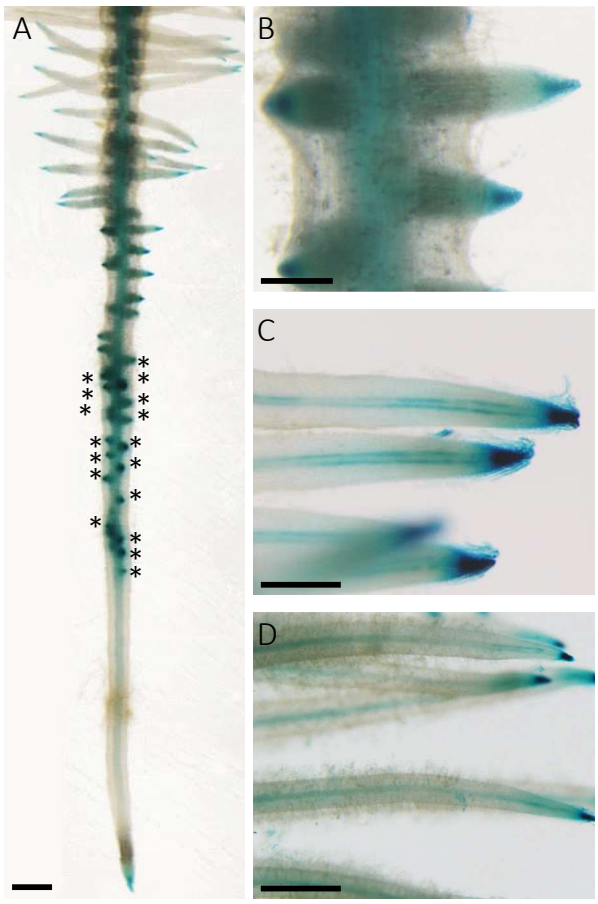

Fig. S1. *DR5:GUS* expression pattern in white lupin cluster root. Histochemical localization of GUS activity in transgenic cluster roots directed by synthetic auxin responsive DR5 promoter. *DR5:GUS* activity was observed in cluster root (A) and rootlet during (B) and after emergence (C,D). GUS activity was seen in P deficient cluster roots at different stages of development. Newly forming primordia of rootlets show strong GUS activity (asterisks) (A). During later stages of rootlet development, blue stain decreased and remained in the rootlet tip and is visible in the stele (C). In old rootlets exhibiting many root hairs, GUS activity was found in the rootlet tip and appear in the stele (D). Scale bars are 1 mm (A,C,D) and 0.5 mm (B).

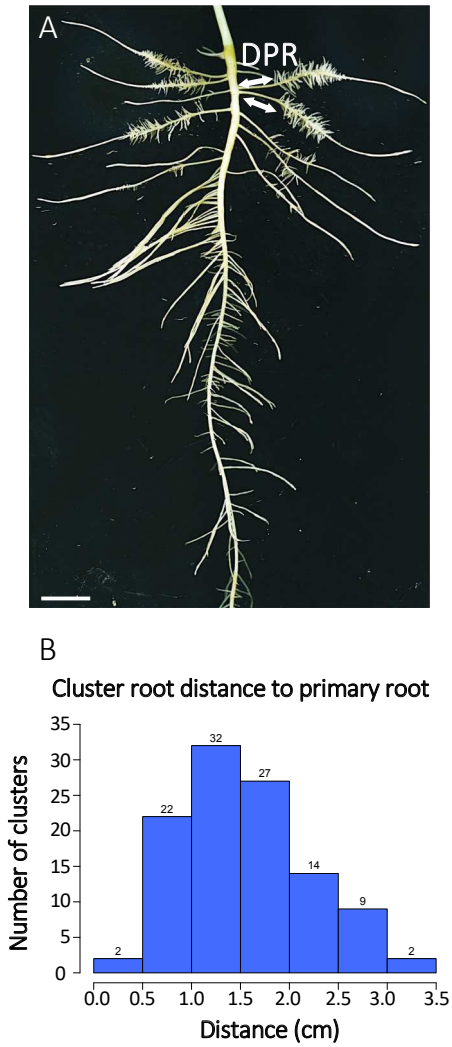

Fig. S2. Distance to primary root of the first cluster of rootlets is a robust trait. (A) Root system architecture of a 15-days-old white lupin grown in hydroponics showing the distance to primary root (DPR). (B) Number of cluster root in each class of DPR. Scale bar is 2.5 cm.

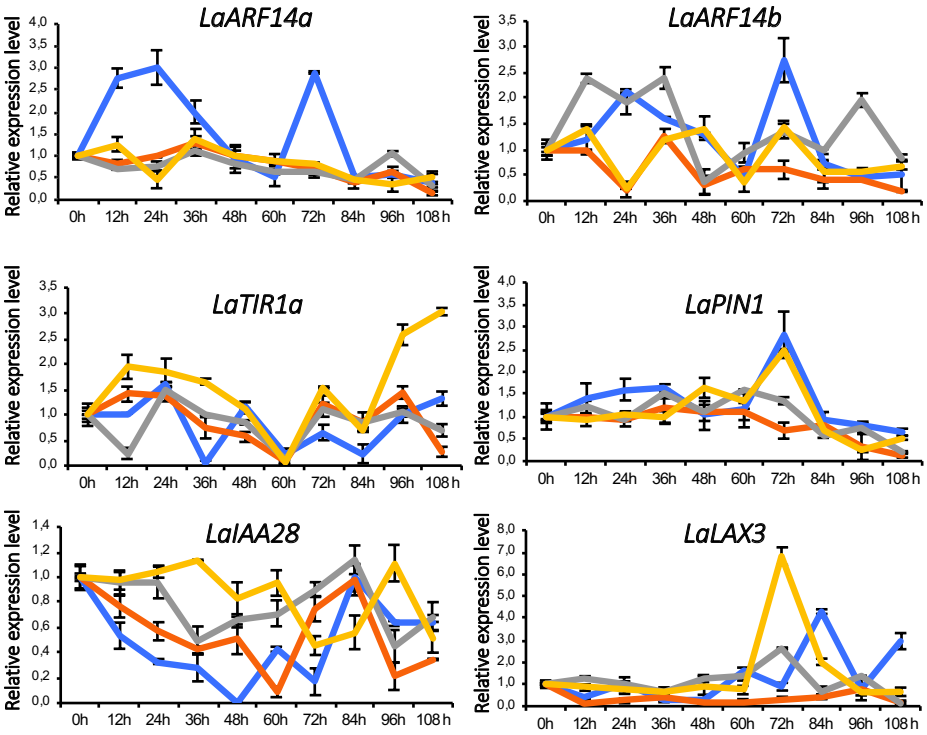

Fig. S3. Relative level of expression of 6 auxin-related genes during cluster root development. Expression levels are relative to the first time point (0h) and normalized to *LaUbiquitin*. Data are mean ± standard deviation of 8 cluster roots coming from 4 lupin plants (n=8) with 4 technical replicates each. Data presented for each plot are 4 biological replicates in different colours. Gene identifiers are given in Table S1.

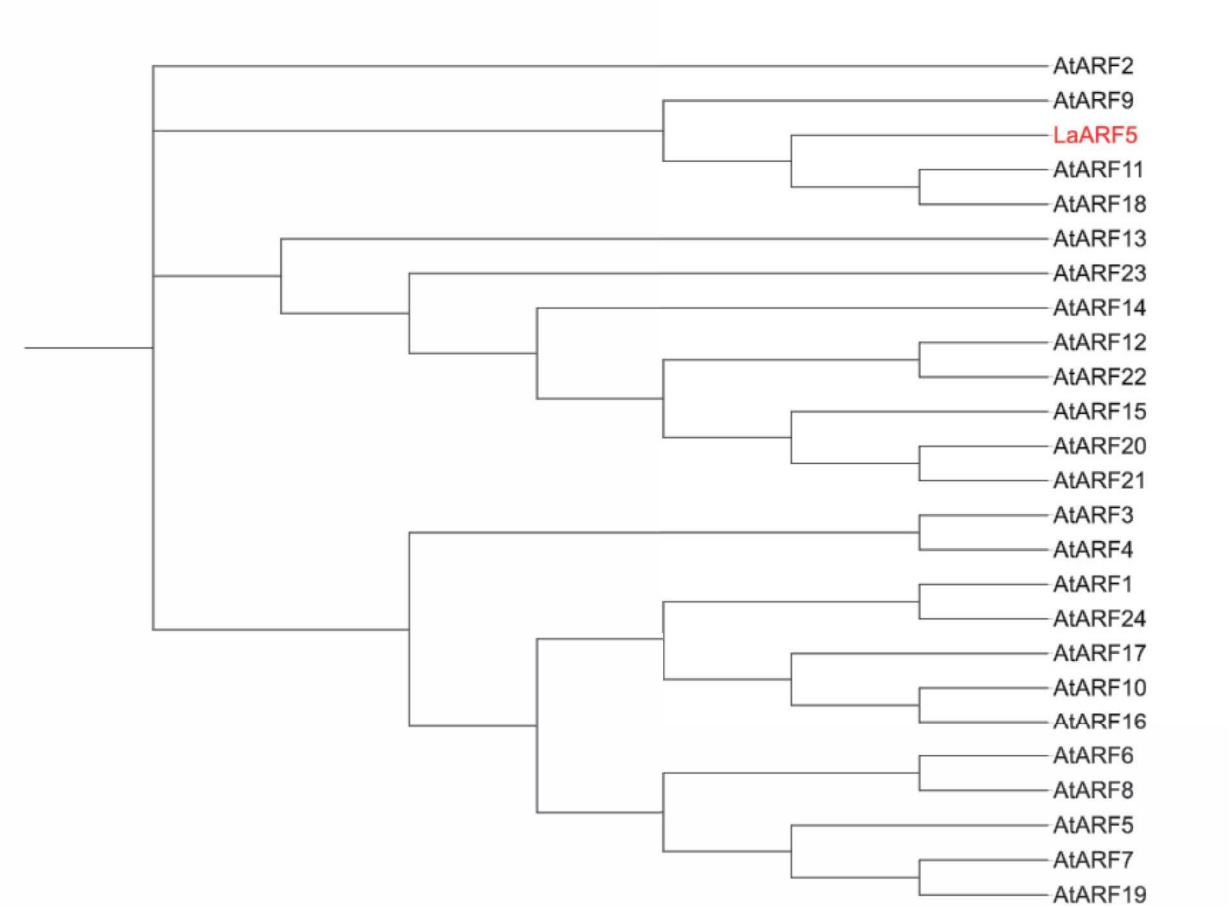

Fig. S4. Neighbour joining tree showing relationship of *LaARF5* with auxin response factors from *Arabidopsis thaliana*. Neighbour joining tree showing relationship of *LaARF5* with the 24 ARF proteins from *A. thaliana*. The bootstrap consensus tree was inferred from 500 replicates. Branches corresponding to partitions reproduced in less than 50°/o bootstrap replicates were collapsed. *LaARF5* protein is branching with 3 close orthologs from *A. thaliana* (*AtARF9, AtARF11, AtARF18*).

Gene	Seq id Secco	Expression Secco *et al.*, 2014						
		Expression FPKM					Ratio	
		TR	MR	TCR	ICR	MCR	TCR/MCR	TCR/ICR
LaTIR1a	LAGI02_23711	7,36	4,17	5,79	6,39	2,92	1,98	0,91
LaTIR1b	LAGI02_15246	15,73	8,42	13,10	12,55	7,10	1,85	1,04
LaARF14a	LAGI02_22919	41,47	65,89	58,65	60,71	49,46	1,19	0,97
LaARF14b	LAGI02_24689	23,56	31,98	31,73	28,81	24,24	1,31	1,10
LaARF5	LAGI02_2355	4,80	7,59	9,02	4,29	3,14	2,87	2,10
LaPIN1	LAGI02_14116	7,86	3,48	5,57	1,82	0,41	13,59	3,06
LaIAA28	LAGI02_13906	123,85	36,69	88,84	65,48	39,18	2,27	1,36
LaLAX3	LAGI02_15524	15,73	3,24	11,27	5,39	2,22	5,08	2,09

Table S1. Shortlist of auxin-related genes identified in white lupin. *LaTIR1a/b, Lupinus albus transport inhibitor response a/b; LaARF5/14a/14b, Lupinus albus auxin responsive factor 5/14a/14b; LaPIN1, Lupinus albus PIN-FORMED gene 1; LaIAA28, Lupinus albus auxin-responsive gene 28; LaLAX3, Lupinus albus Like AUX1 3*. For each auxin-related gene identified in the Secco *et al.,* (2014) database, is presented the identifier name of the cDNA, the mRNA level of transcripts (expression FPKM) in the different part of the lateral root (TR: tip of the root; MR: mature root) and in the different part of a cluster root from young to old (TCR: tip of the cluster root; ICR: immature cluster root; MCR: mature cluster root). Ratio of transcripts level between tip of the cluster root and mature cluster root, as well as ratio of transcripts level between tip of the cluster root and immature cluster root are also indicated.

A

LaTIR1b				
Site name	**Organism**	**Position**	**Sequence**	**Function**
AuxRE	*Arabidopsis thaliana / Glycine max / Oryza sativa*	135	TGTCTC	ARF binding site
ARR1AT	*Arabidopsis thaliana*	63 478 533	NGATT NGATT NGATT	ARR1 binding element

B

LaARF5				
Site name	**Organism**	**Position**	**Sequence**	**Function**
AuxRE	*Arabidopsis thaliana / Glycine max / Oryza sativa*	42	TGTCTC	ARF binding site
CATATG site	*Glycine max*	176 262	CATATG CATATG	Found in NDE element in SAUR gene ; involved in auxin responsiveness
ARR1AT	*Arabidopsis thaliana*	18 49 350 839	NGATT NGATT NGATT NGATT	ARR1 binding element
Pyrimidin-Box	*Oryza sativa / Hordeum vulgare*	4	CCTTTT	Related to gibberellin responsive gene
TATCCAC-Box	*Hordeum vulgare*	849	ATCCAC	Part of conserved cis acting response complex (GARC) necessary for full gibberellin response

Table S2. List of hormone-related cis-acting elements identified in *LaTIR1b* and *LaARF5* promoters. The region 1000 bp upstream the start codon was analysed in silica using the SOGO online tool. Only the hormone related elements were listed: site name, organism of origin, position from the beginning of the promoter sequence (5'), element sequence and functional annotation of the site.

CHAPITRE 2

Initiation et organogénèse du primordium de rootlette

Avant-propos

Une étude précédente a montré que les rootlettes initiées le long des racines protéoïdes, sont issues de divisions dans les tissus faisant face aux pôles de xylème (Johnson *et al.*, 1996), de façon très similaire à la formation des racines latérales chez les dicotydédones. Cependant, si le péricycle donne naissance à un pool de cellules qui se divisent activement, nos résultats précédents suggèrent que d'autres tissus, en particulier l'endoderme et le cortex, contribuent également à la formation des rootlettes (Gallardo *et al.*, 2018). Le développement de ces racines imite plus spécifiquement le développement des racines latérales chez les légumineuses, où ces tissus semblent également être impliqués (Herrbach *et al.*, 2014).

Dans ce deuxième chapitre, nous essayons d'apporter une description détaillée de la morphologie des racines protéoïdes, en nous focalisant sur le développement des rootlettes. Nous avons concentré notre analyse sur les premiers stades de leur développement jusqu'à leur émergence. Dans ce but, nous avons poussé plus loin les études anatomiques réalisées dans le chapitre 1, afin de définir plus finement la séquence de développement. Cette étude a été rendue possible par la disponibilité de la séquence du génome du lupin blanc, qui a permis l'identification de marqueurs moléculaires (Hufnagel *et al.*, 2019). En nous appuyant sur les données transcriptomiques générées dans l'équipe, nous avons identifié chez le lupin des orthologues de marqueurs spécifiques aux tissus chez *Arabidopsis*. L'initiation et l'organogenèse des rootlettes ont ensuite été étudiées avec l'aide de ces marqueurs, ce qui a conduit à définir un modèle de la formation de ces racines chez le lupin blanc. Ce travail élargit nos connaissances sur la formation post-embryonnaire des racines et sur l'acquisition des tissus chez une espèce de légumineuse. Ces expérimentations sont présentées sous la forme d'un article scientifique en préparation.

Article 2: Rootlet primordium initiation and organogenesis in white lupin

Cécilia Gallardo[‡], Bárbara Hufnagel[‡], Célia Casset, Alexandre Soriano, Laurence Marquès, Patrick Doumas and Benjamin Péret[*]

BPMP, CNRS, INRA, Montpellier SupAgro, Univ Montpellier, Montpellier, France

Correspondence

[*]Corresponding author, e-mail : benjamin.peret@cnrs.fr

[‡]These authors contributed equally to this work.

Abstract

In severely nutrient impoverished-soils, micronutrients especially inorganic phosphate (Pi) is poorly available to plants. To cope with such scarcity, plants have evolved to produce specialized root organs dedicated to improve phosphorus acquisition. White lupin (*Lupinus albus L.*) is a cultivated legume that is well adapted to grow on such degraded soils. When exposed to Pi-limitation, white lupin forms cluster roots, which are dense clusters of short tertiary roots that appear on lateral roots. How rootlets are initiated and how rootlet primordium patterning occurs are poorly described. In order to understand these processes, we investigated cluster root formation at early stages of rootlet development in white lupin. To follow cell organization over the course of rootlet primordium formation, we identified a set of tissue-specific markers based on the genome sequence of white lupin and on detailed transcriptomic data. With this approach, we have highlighted that rootlet primordium arise from divisions in pericycle, endodermis and cortex. Based on expression pattern of reporter lines, we propose a model for rootlet initiation and patterning in white lupin. This work provides a fine description of specialized rootlets and suggests that third-order root development, as lateral roots, is a fine-tuned process.

Key words: rootlets, cluster roots, white lupin, patterning, primordium organization, cell lineage.

Introduction

Cluster roots (CRs) are considered to be one of the major adaptations to improve plant nutrient acquisition, with nitrogen-fixing nodules and mycorrhizas (Neumann and Martinoia, 2002). However, CRs differ from nodules and mycorrhizas as they form without the presence of a symbiot and use root developmental program to form (Lamont 2003, Gallardo et al 2018). CR bearing species can be found in soils where nutrients are poorly available to plants including Western Australia and South Africa (Dinkelaker *et al.*, 1995; Lambers *et al.*, 2003). Plants forming CRs can absorb inorganic phosphate (Pi) at a faster rate than non-forming CRs plants (Poo and Cone, 1974; Vorster and Jooste, 1986). Because this developmental adaptation has a selective advantage, CR arose in a whole range of distant families from *Cyperaceae* in monocots to *Proteaceae*, *Fabaceae*, *Moraceae* and *Betulaceae* in dicots (Dinkelaker *et al.*, 1995; Lambers *et al.*, 2003). Thus, CR is an adaptive trait of plants to cope with P-depleted nutrient soils (Lambers *et al.*, 2015; Neumann and Martinoia, 2002). Because most of the phosphate is mostly concentrated in the top soil layer, CR are produced in the upper part of the root system (Lynch and Brown, 2001). The CR is an exacerbated developmental response, that results from regulation of rootlet initiation and rootlet determinacy (Skene, 2001, 2003). Therefore, CR is a good model to study these mechanisms as a high number of rootlets are successively produced in a short period of time and are available for experiments.

White lupin is the only annual crop that forms CRs under Pi deficiency. Among all CR forming species, white lupin is the species that focus the most attention for studies on CR morphology and CR physiology (Johnson *et al.*, 1996; Watt and Evans, 1999a; Hagström *et al.*, 2001; Neumann and Martinoia, 2002; Uhde-Stone *et al.*, 2003; Cheng *et al.*, 2011). *Lupinus albus* can form up to 35-45 rootlets per cm (Dinkelaker *et al.*, 1989) and secrete massive amount of organic acids and protons (Neumann and Martinoia, 2002; Massonneau *et al.*, 2001; Sas *et al.*, 2001). Such physiological modifications can increase the availability of complexed Pi which can be beneficial to other species in intercropped or mixed cultures (Li *et al.*, 2010; Braum and Helmke, 1995; Cu *et al.*, 2005). Mixed culture of wheat with white lupin was shown to increase shoot P uptake up to 45 % in wheat (Cu *et al.*, 2005). Altogether, white lupin is a crop of interest with specific developmental features and physiology.

In many angiosperms, secondary roots arise from pericycle as for the model plant *Arabidopsis thaliana* (Herrbach *et al.*, 2014; Malamy and Benfey, 1997; Orman-Ligeza *et al.*,

2013; Laskowski *et al.*, 1995). In this clade, some monocots lateral root show contribution of dividing endodermal cells including some *Poaceae* like *Oryza sativa* and *Zea mays* (Hochholdinger *et al.*, 2004). In dicots, some Legume species also show contribution of division in endodermis and cortex including *Glycine max, Lotus japonicus* and *Medicago truncatula* (Byrne *et al.*, 1977; Op den Camp *et al.*, 2011; Herrbach *et al.*, 2014). In *Arabidopsis*, it was proposed that lateral root primordium (LRP) development is a 8-stage process (Malamy and Benfey, 1997) that can be described as a two-step developmental model (Laskowski *et al.*, 1995). LRP formation starts with an early developmental phase (stage I-IV) during which initiation occurs and several rounds of divisions produce a four-layered primordium (Malamy and Benfey, 1997). Then, a second phase follows (stage V-VII) during which cells start to differentiate and organize to form an organ with tissue organization similar to the primary root meristem (Trinh *et al.*, 2018). Transition between these two developmental phases marks the onset of quiescent center establishment and formation of meristematic initials (Goh *et al.*, 2016). In regard to these processes, very little information is available for third order roots like white lupin rootlets. In white lupin, xylem pole pericycle cells are recruited to become founder cells and divide during initiation (Gallardo *et al.*, 2018). However, despite few anatomic studies, post-initiation developmental stages with the participation of other cells layers and tissue patterning has not been yet described (Watt and Evans, 1999a; Skene *et al.*, 1996).

In an effort to understand CR formation and rootlet patterning, we have initiated an anatomic study to define discrete developmental stages throughout early events of rootlet development. The root structure of rootlet is more complex than *Arabidopsis* lateral root with multiple cell layers. This complexity makes it difficult to follow establishment of the different tissues over the course of rootlet development. We therefore identified a set of tissue-specific marker genes by taking advantage of the white lupin genome sequence that we previously generated (Hufnagel *et al.*, 2019) together with detailed transcriptomics datasets. These markers allow to observe the switch from cell proliferation to cell differentiation in the rootlet primordium. Altogether, our results suggest that CR primordium is formed by an ordered series of divisions into pericycle, endodermis and cortex of rootlets. These divisions seem to be tightly regulated from an early stage during rootlet development and produce a highly organized structure with differentiated tissues. Key steps for rootlet primordium formation were described by analogy with *Arabidopsis* lateral root primordium development.

Results

Developmental stages of rootlet primordium

To provide a detailed description of cluster root development, thin cross sections of 7 to 9 day old lupin seedlings were stained with ruthenium red to observe all developmental stages along cluster root development. Observation of these sections confirmed that early events of cluster root development can be described in 8 discrete developmental stages.

Stage I. Initiation is the first visible event of CR formation. It consists of two asymmetrical anticlinal divisions in the pericycle (Fig. IB). Initiation continues with the appearance of divisions in parallel orientation compared to the root axis (Fig. 1C, black arrow). In the longitudinal plane, approximately 6 cells show these periclinal divisions. Peripheral cells are not dividing, creating the boundaries of the primordium. In the overlaying epidermis, an increased number of anticlinal divisions is clearly seen as compared to the surrounding epidermis cells. About 8 cells are formed from these divisions.

Stage II. All pericycle cells participating in the rootlet primordium seem to have divided (Fig. 1D). These divisions in the pericycle lead to the formation of two layers, named P1 (inner layer) and P2 (outer layer). Following these divisions, cells start to swell and expand in the radial direction. Simultaneously, periclinal divisions occur in the endodermis that divides this layer into E1 (inner layer) and E2 (outer layer) (Fig. 1D, black arrow).

Stage III. A dozen of cells continue to divide in the 4-layered primordium (Fig. 1E). Anticlinal divisions are seen in the most peripheral cells in the pericycle. Surprisingly, anticlinal divisions are also seen in the cortex (Fig. 1E, purple arrows).

Stage IV. A dome shaped rootlet primordium begins to form. The dividing cortex comprises 9 cells in length. 4 cells at the base of the primordium started to divide between the xylem pole and the P1 inner layer (Fig. 1F, black arrow). Numerous radial, anticlinal and periclinal divisions happen in the tissues derived from pericycle and endodermis.

Stage V. Primordium expands radially to give a typical dome-shaped primordium, pushing the overlaying cortical layers. Cells at the base of the primordium (Fig. 1G, black arrow) continue to divide. The number of cells in the overlaying cortex increases to 11 cells in length.

Stage VI. The rootlet primordium is at mid-way through the lateral root tissues, deforming the cortical layers around. The stage VI primordium begins to look like a mature root

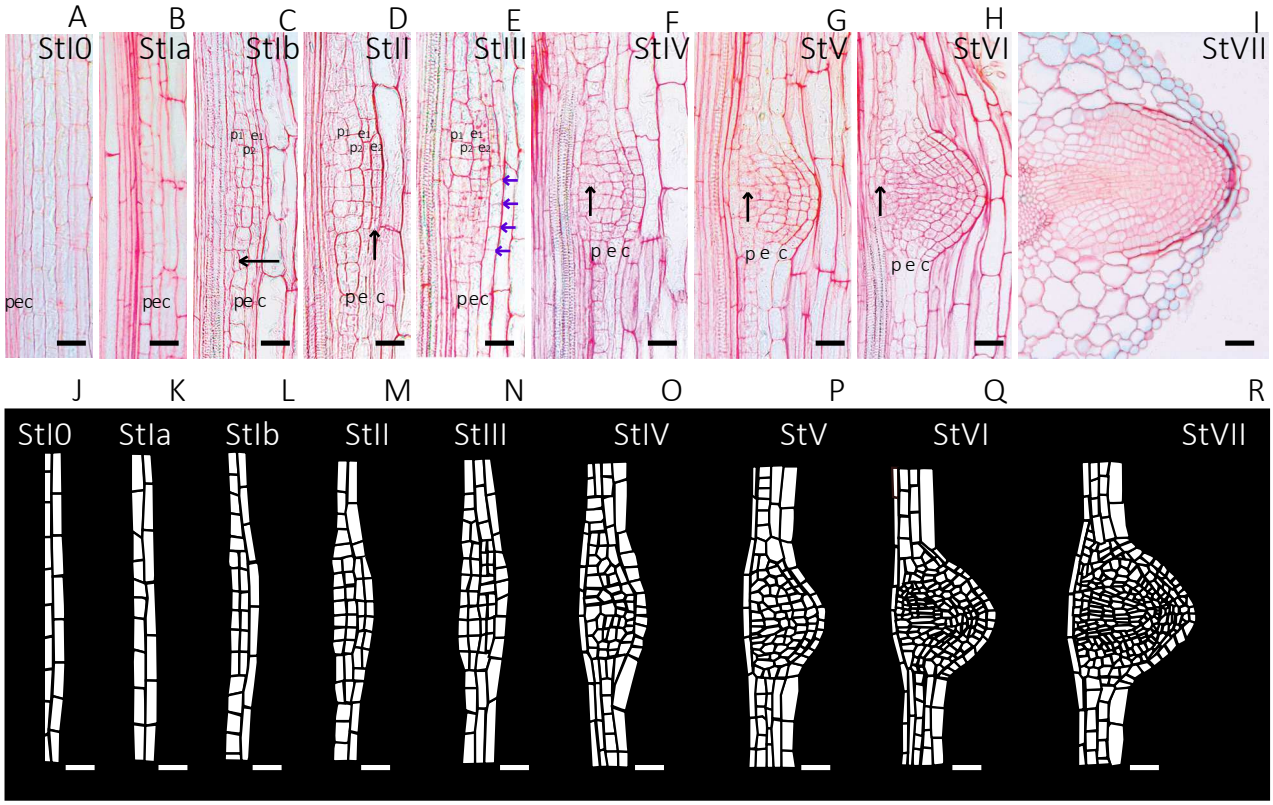

Fig. 1. Rootlet primordium developmental stages. (A-I) Longitudinal sections of a cluster root stained with ruthenium red depicting all developmental stages of rootlet development. (J-R) Schemes depicting images above. (A, J) Stage 0. Close look at pericycle and endodermis tissues before initiation. (B, K) Stage Ia. First asymmetric division in pericycle. (C,L) First periclinal divisions in the pericycle and first anticlinal divisions in the endodermis. (D,M) Stage II. A flatten four-layered primordium: while the pericycle tissue have already divided, the endodermis tissues is dividing as well. (E, N) Stage III. More cells divide in the two endodermal derived layers and several divisions are seen in the cortex. (F, O) Stage IV. Many anticlinal and radial divisions are shaping the rootlet primordium. (G, P) Stage V. The dome-shaped primordium begin to appear. Divisions at the core of the primordium seem to push mechanically the overlaying other tissue layers. (H, Q) Stage VI. The primordium is half-way through the cortical layers. An increasing number of cells are seen in all cell layers. (I, R) Stage VII. The rootlet is about to emerge from cluster root tissues. Scale bar: 50 *μm*.

with 6 layers (Fig. 1H), that could be the pericycle (surrounding the stele tissue), the endodermis, 3 cortical layers and a protective root cap at the tip of the rootlet primordium. An increasing number of cells can be counted in the pericycle and endodermal layers, as well as in the cortex. At this stage, there is a total of 16 cuboid cells in the cortex and four central cells at the tip are observed surrounded by 6 cells on each side. 3 cells seem to go through another round of division in E1 to give a pool of really tiny cells in the center of the primordium. In the most inner tissue, at the core of the primordium, cells that seem to be derived from P1 have a strong elongated shape reminiscent of the particular shape of vascular cells (Fig. 1H, black arrow).

Stage VII. The rootlet primordium is about to emerge and cross the last layer of the cluster root, the epidermis (Fig. 1I). The primordium enlarges and distinguishing the different tissues inside the growing rootlet becomes challenging. Many anticlinal divisions seem to continue in the different layers of the primordium. The vascular tissue seems to be established as many elongated cells are connecting the cluster root stele to the rootlet primordium.

Gene identification for tissue-specific marker lines

Classic histology allows to describe precisely early developmental stages of rootlet formation and to define discrete stages associated with particular anatomic features. However, cell types cannot be easily separated based solely on their shape during early developmental stages. To which extent pericycle, endodermis and cortex tissues are involved in rootlet initiation and rootlet outgrowth has yet to be determined. Another question is to decide when tissues are starting to differentiate. To address these questions, a limited number of markers (using the ß-glucuronidase gene as reporter) specifically expressed in different tissue types were tested. These lines were chosen (1) based on the protein sequence homology between known cellular markers in the model plant Arabidopsis and (2) based on their expression profile in the white lupin transcriptomic dataset. Due to genome triplication, gene families are often larger in white lupin than in *Arabidopsis* (https://www.whitelupin.fr/) and expression data help directing our choice. On top of these cellular markers, we also used the well-described cell division marker *AtCYCB1;1* by transferring directly the *Arabidopsis* promoter in white lupin.

First, we chose a list of markers based on their tissular expression in *Arabidopsis thaliana:* two pericycle and endodermis markers (*AtWOL*, *AtSCR1*), one cortical markers (*AtPEP*)

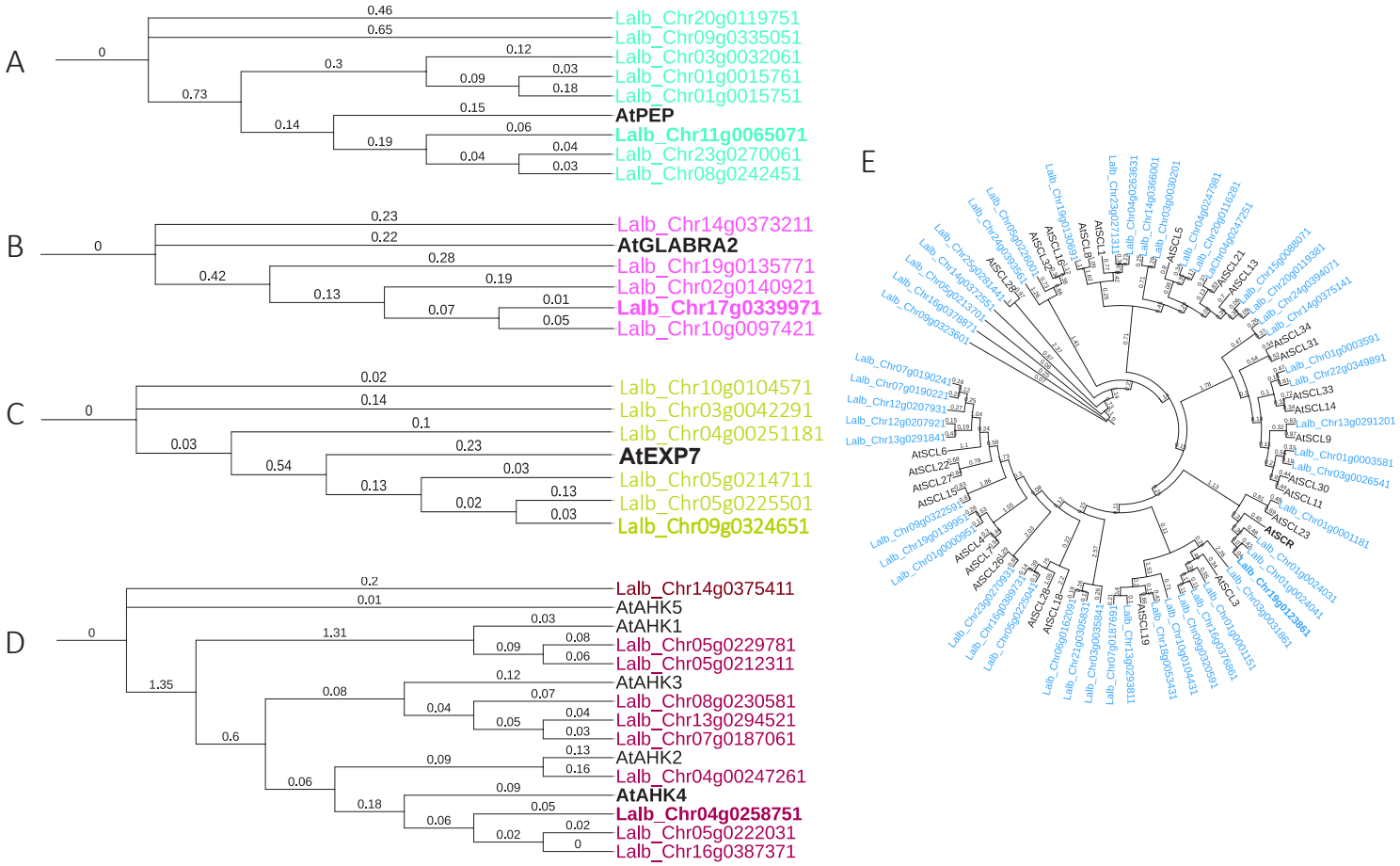

Fig. 2. Phylogenetic relationship of lupin and *Arabidopsis* protein sequences. The trees were constructed using the Neighbor-Joining method using the phylogeny tool from LIRMM (http://phylogeny.lirmm.fr/phylo_cgi/index.cgi). The bootstrap consensus tree was inferred from 500 replicates. Branches corresponding to partitions reproduced in less than 50% bootstrap replicates were collapsed. The analysis was performed using amino acid sequences extracted from white lupin genome (https://www.whitelupin.fr/) and from public database tair (https://www-Arabidopsis.org)

and two epidermal markers (*AtGL2*, *AtEXP7*) (Lie Sevin-Pujol *et al.*, 2017; Marquès-Bueno *et al.*, 2016) (Fig. S1). Orthologous lupin genes were found by comparing *Arabidopsis* protein sequences with all the cDNA-deduced protein sequences of lupin. Comparison was made by multiple comparison alignment by local BLAST on our custom lupin database and by generating phylogenetic trees (Fig. 2). We also took advantage of the NCBI database to identify the closest protein sequences in other legumes species: *Medicago truncatula, Cicer arietinum, Lupinus angustifolius* and *Glycine max* (Fig. S2). Phylogenetic trees that were generated were comparing either lupin protein sequences with *Arabidopsis* protein sequences (Fig. 2) or lupin protein sequences with other legumes protein sequences (Fig. S2). In parallel, expression level of the orthologous genes was checked in our RNAseq databases.

AtPEP was branching with 3 lupin protein sequences (Fig 2A). Both *Lalb_Chr23g0270061* and *Lalb_Chr011g0065071* were expressed over the course of primordium development and showed a matching pattern in temporal and spatial datasets (Fig. 3A, 3B). Lalb_Chr011g0065071 had a protein score identity (59.59%) higher than Lalb_Chr23g0270061 (44.39%).

AtGL2 protein sequence was similar to 4 lupin protein sequences (Fig. 2B, Fig. 3B). Among them, *Lalb_Chr19g0135771* had a different pattern from the other 3 genes in the temporal dataset (Fig. 4C) and was not expressed in the spatial dataset (Fig. 4D). *Lalb_Chr10g0097421* and *Lalb_Chr17g0339971* were the only highly expressed genes whose expression pattern matched between the two RNAseq datasets (Fig. 3C, 3D). Lalb_Chr17g0339971 has the higher percentage of identity (37.60%) with *AtGL2* at the whole protein level between those four genes.

AtEXP7 protein sequence was branching 3 lupin protein sequences (Fig. 2C). Expression patterns were very alike for *Lalb_Chr09g0324651* and *Lalb_Chr05g0225501* and were the most induced after rootlet emergence (Fig. 3E, 3F). Comparison of these sequences with *AtEXP7* revealed that Lalb_Chr09g0324651 had a better percentage identity at the whole protein level (63.50%) than Lalb_Chr05g0225501 (62.39%).

AtAHK4/AtWOL was branching with 3 lupin protein sequences (Fig. 2D). These 3 genes had a similar expression pattern with a strong induction at 48 h and a strong repression at 84 h (Fig. 3G). *Lalb_Chr04g0258751* was the strongest expressed gene (Fig. 3G, 3H) and appeared to be the closest ortholog with 67.58 % identity at the entire protein level. Phylogenetic tree revealed that is was also the closest ortholog to *Lupinus angustifolius HK4* gene (Fig. S2D).

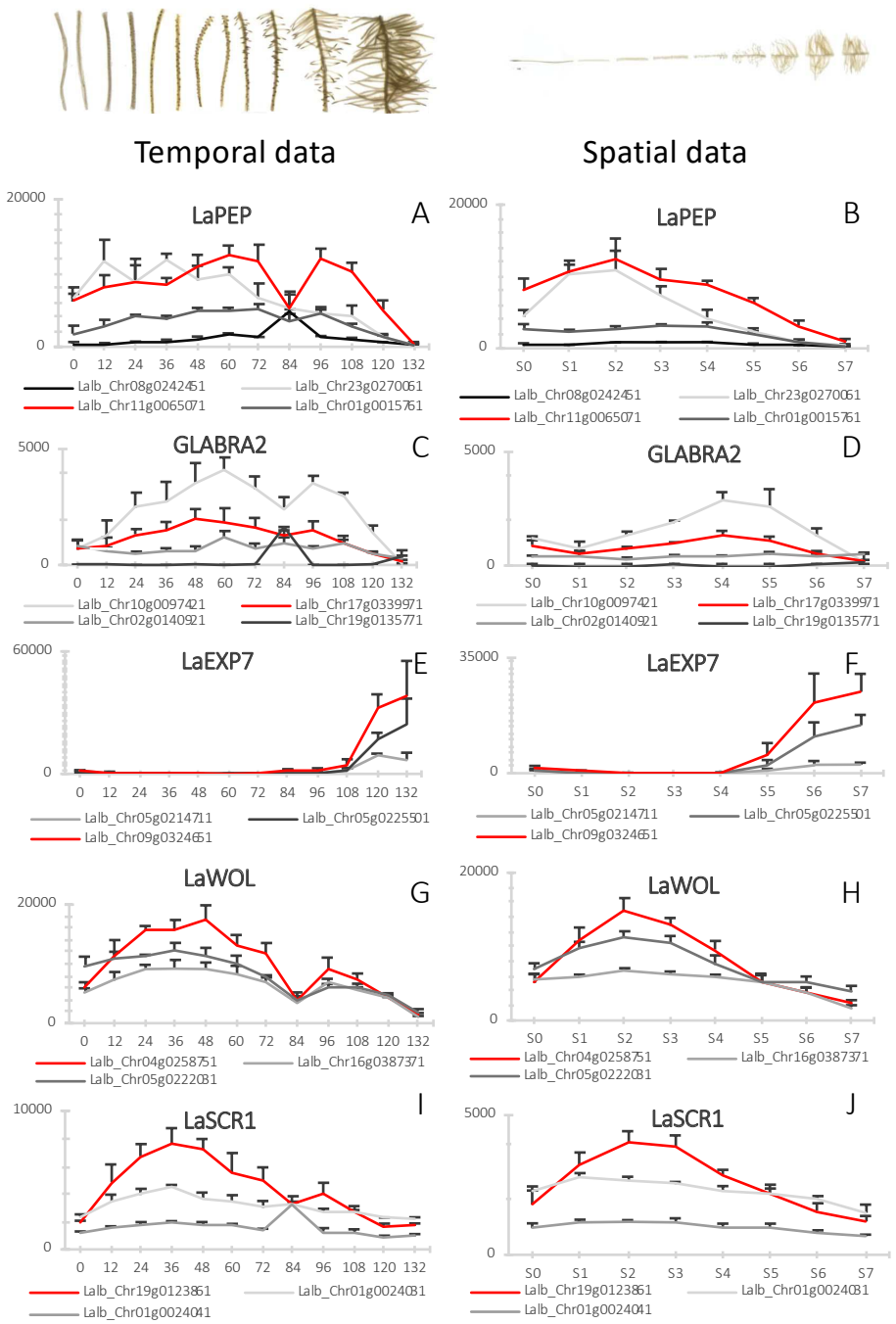

Fig. 3. Expression levels of lupin marker gene candidates during rootlet development in RNA-seq datasets. Data from temporal dataset are shown in graph A to I, while data from spatial dataset are shown in graphs B to J. Genes which promoters were cloned are colored in red. Data from temporal dataset correspond to mean ± SD of eight CRs from 4 lupin plants (n=8). Data from spatial dataset correspond to mean ± SD of ten CRs from 5 lupin plants (n=10). On the y-axis, values represent gene expression values (total number of reads) and each graduation corresponds to 2000 reads. On the x-axis, values represent the number of hours from the debut of cluster root formation, 0h, up to the end of their development, 132 hours (Temporal dataset); and CRs developmental stages from meristematic zone, S0, up to mature CRs, S7 (Spatial dataset).

AtSCR was branching with 3 lupin protein sequences (Fig. 2E). *Lalb_Chr19g0123861* was reported to have a strong expression at 36 h during rootlet emergence (Fig. 3I, 3J) and was reported to have the strongest percentage of identity at the protein level with *AtSCR* (59.35%). Protein sequence was revealed to be 100% identical to 776 amino acids of *LaSCR1* identified by Sbabou *et al.* (2010). Comparison of protein sequences between lupin and other legumes species showed that *LaSCR1* protein sequence is similar to *Cicer arietinum* protein SCARECROW (Fig. S2E).

Genes selected for further analysis were: *Lalb_Chr04g0258751* (*LaWOL*), *Lalb_Chr19g0123861* (*LaSCR1*), *Lalb_Chr17g0339971* (*LaGL2*), *Lalb_Chr11g0065071* (*LaPEP*), *Lalb_Chr09g0324651* (*LaEXP7*) (Fig. 3, red lines). Length of the promoter amplified for each gene was at least 1500 bp and is reported into table S1. *pLaSCR1* construct was not the one used by Sbabou *et al.* (2010) but was 1510 bp amplified upstream of the *Lalb_Chr19g0123861* ATG. The lupin promoters were cloned into a dual reporter system with GUS and GFP as visual markers and introduced into white lupin roots via *Agrobacterium rhizogenes*-mediated root transformation. Transformed tissue can be selected by using classical GUS staining and/or visualise by GFP fluorescence. Because of strong autofluorescence in hairy root plant, and difficulties to screen for GFP-expressing root, we ended up not using GFP. CR tissular expression pattern was compared among independent transformed roots. Number of individual plants and individual roots tested are summarized in table S2.

CR expression of tissue-specific marker lines

To characterize tissue specific expression, promoter:GUS expression pattern was first assessed into secondary-order roots *i.e.* apex of cluster roots. CRs stained for GUS for each marker are shown in Fig. 4, as well as cross sections produced in these lines. The markers were clearly expressed into specific cell/tissue types:

pAtCycB1;1:GUS allows to follow cell divisions in plant tissues. *AtCycB1;1* is expressed prior mitosis at the G2/M transition and selectively degraded by proteolysis, which requires a short peptide named “destruction box”. *pAtCycB1;1:GUS*, was cloned with this mitotic signal and reports accurately the *CycB1;1:GUS* accumulation pattern in G2/M transition (Colón-Carmona *et al.*, 1999). At the CR tip, *pAtCycB1;1:GUS* expression is seen in cell patches in the

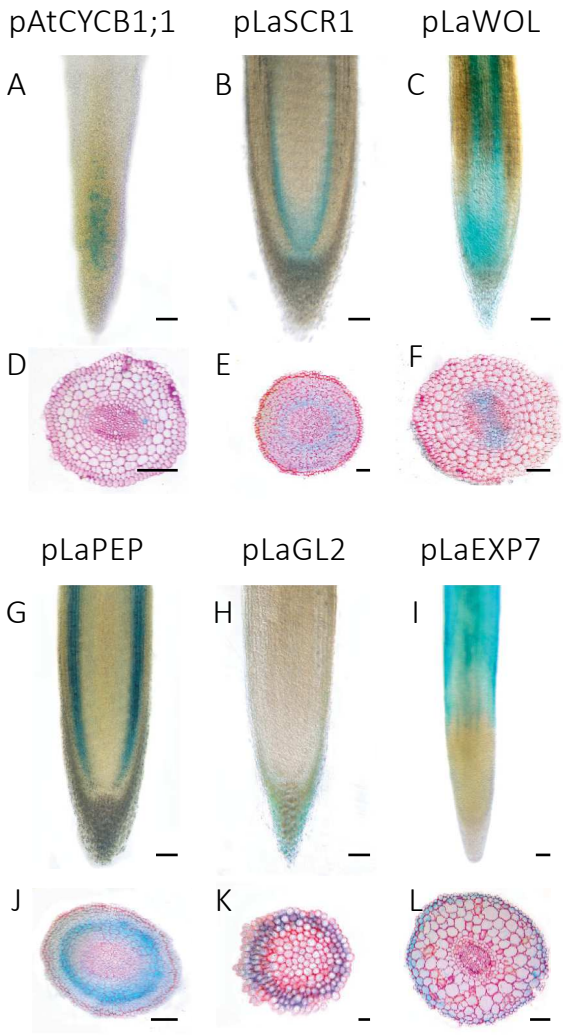

Fig. 4. Expression profiles of six promoters-GUS fusions in the cluster root tip. Promoters profiles shown are: (A, D) *pAtCYCB1;1,* (B, E) *pLaSCR1*, (C, F) *pLaWOL*, (G, J) *pLaPEP*, (H, K) *pLaGL2*, (I, L) *pLaEXP7*. (A, B, C, G, H, I) Images are longitudinal sections in the meristematic and elongation zones. (D, E, F, J, K ,L) Cross sections are images through different cluster root zones: the meristematic zone (E, K), the elongation zone (J), the differentiation zone (D, F, L). Scale bar: 100 *µm*.

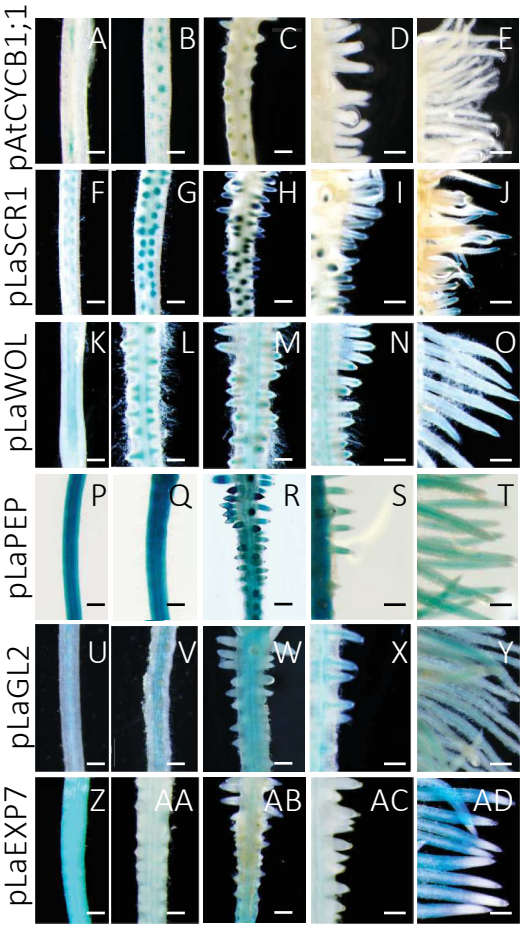

Fig. 5. Expression profiles of six promoters-GUS fusions in cluster roots. Promoters profiles shown are: (A-E) *pAtCYCB1;1*, (F-J) *pLaSCR1*, (K-O) *pLaWOL*, (P-T) *pLaPEP*, (U-Y) *pLaGL2*, (Z-AD) *pLaEXP7*. **(A-E) p*AtCYCB1;1*.** (A-C) Staining is seen in primordia of dividing cells. (D-E) Staining disappears after rootlet emergence. **(F-J) *pLaSCR1:GUS*.** (F-G) Staining is apparent only in primordia. (H-J) Expression is restricted to the rootlet tip after emergence and in mature rootlet. **(K-O) *pLaWOL:GUS*.** (K-L) Staining is seen in primordia and CR stele. (M-N) GUS is apparent in CR stele and at rootlet tips. (O) GUS is observed in rootlet stele when rootlet stele is connected to CR vasculature. **(P-T) *pLaPEP:GUS*.** (P-Q) Staining is seen in CR cortex. (R-T) Staining is also apparent in the cortex of rootlet but is not expressed in the rootlet meristem. **(U-Y) *pLaGL2:GUS*.** (U-V) Staining is observed in CR stele but is not seen in primordia. (W-X) Staining is observed in CR stele but not in emerged rootlet. (Y) Promotor is expressed in rootlet vasculature when rootlets are covered with root hairs. **(Z-AD) *pLaEXP7:GUS*.** (Z) Staining is seen in epidermis in CR differentiation zone. (AA-AC) Promotor is not expressed in the rootlet emergence zone. (AD) Staining is observed in rootlet differentiation zone but is not expressed in meristematic and elongation zones. Scale bar: 350 *µm* (column 1-3), 150 *µm* (column 4), 500 *µm* (column 5).

meristematic zone (Fig. 4A). Expression is also seen in pericycle cells in the differentiation zone of the CR. A transverse section in this zone is shown in Fig. 4D. Later on, *pAtCycB1;1:GUS* is expressed in dividing cells in tissue contributing to CR primordium formation (Fig. 5B, 5C). Soon after emergence *pAtCycB1;1:GUS* staining can no longer be seen (Fig. 5D) suggesting that cell division stops.

pLaSCR1:GUS expresses in the endodermis of CR tip (Fig. 4B). In the meristematic zone, staining seems to include the endodermis/cortex initial and may also include cells of the quiescent center. A transverse section near the meristematic zone is shown in Fig. 4E. It sometimes appears a light staining in the first cortical layer (Fig. 4E). Promoter expression is also observed in rootlet primordia and rootlet meristematic zone after rootlet emergence (Fig. 5G-H).

pLaWOL:GUS line was expressed in the stele of CR (Fig. 4C). Staining was not observed in the elongation zone but was seen in the differentiation zone in the stele (Fig. 5K). A transverse section through differentiation zone shows GUS staining in stellar tissue along xylem axis and pericycle cells facing the xylem poles (Fig. 4F). Staining in the stele disappears in the primordium patterning zone and became restricted only to pericycle cells and the stele of the primordium. (Fig. 5L, 5M). *pLaWOL:GUS* was observed in the stele of emerged rootlet with a stronger staining in the meristematic zone were QC is expected to locate (Fig. 5M, 5N).

pLaPEP:GUS is specific to cortical cells. Promoter is strongly expressed in the root meristematic zone, and is not expressed in endodermis/cortex initial (Fig. 4G). A transverse section in the beginning of elongation zone is shown in Fig. 4J. Expression tends to fade away in the elongation zone in the shootward direction. Similar pattern for *pLaPEP:GUS* is observed in primordium and emerged rootlet (Fig. 5S).

pLaGL2:GUS is expected to be expressed in the non-hair forming epidermal cells (Malamy and Benfey, 1997) but observed staining is not the one expected in lupin CR**.** In the CR tip, expression was seen in the lateral root cap (Fig. 4H). A cross-section through the root cap is shown in Fig. 4K. GUS staining is also strong in the pericycle in the differentiation zone in between the primordia (Fig. 5U, 5V). *pLaGL2:GUS* shows also expression in the vasculature in emerged and mature rootlet (Fig. 5X, 5Y).

pLaEXP7:GUS is expressed in the beginning of the differentiation zone but is not expressed in the meristem at CR tip (Fig. 4I). Therefore, this marker line is useful to observe transition between the elongation zone and the differentiation zone. Epidermis expression in

the differentiation zone is shown in Fig. 4L. Staining was excluded from primordium patterning zone (Fig. 5AA) but is observed later when root hairs start to appear on growing rootlets (Fig. 5AD).

Tissue specific marker expression through CR development

After assessing the expression pattern of the 6 markers in the secondary roots, we used them to generate a description of rootlet development (tertiary root primordium). We assessed the various stages of development to recreate a time course description of these rootlets.

Cell division

To identify which root cell types divide to contribute to the rootlet primordium formation, *pAtCycb1;1:GUS* was observed from stage 0 onward (Fig. 6A-D). GUS staining is first observed at stage 0 in one pericycle cell opposite the xylem pole, before apparition of a pericline cell wall (Fig. 6A). At stage II, some endodermal cells overlaying pericycle cells also show GUS staining (Fig. 6B) which support the observation made on CR sections (Fig. 1C). At stage IV, two cells that seem to belong to cortical tissue seem to divide as well (Fig. 6C). Cortical cells were also found to divide in Fig. 1 (Fig. 1D, Fig. 1E). These observations support the hypothesis that cortical cells contribute to rootlet primordium patterning.

Endodermis

pLaSCR1:GUS endodermal marker expression is first seen in 5 endodermal cells at stage II when these cells start to divide (Fig 6E). At stage III, staining is not only observed in E1 and E2 but also in the overlaying cortical cells (Fig. 7B). This expression pattern persists until stage V (Fig. 6F). At stage VI, *pLaSCR1:GUS* expression starts to be restricted to two inner layers that are surrounding the stele with a typical U-shaped profile (Fig. 6G). A group of cells abutting these two layers also show weak GUS staining at the tip of the rootlet primordium (Fig. 6G, Fig. 7D). This expression profile remains the same when the rootlet is about to emerge (Fig. 6H, Fig. 7E).

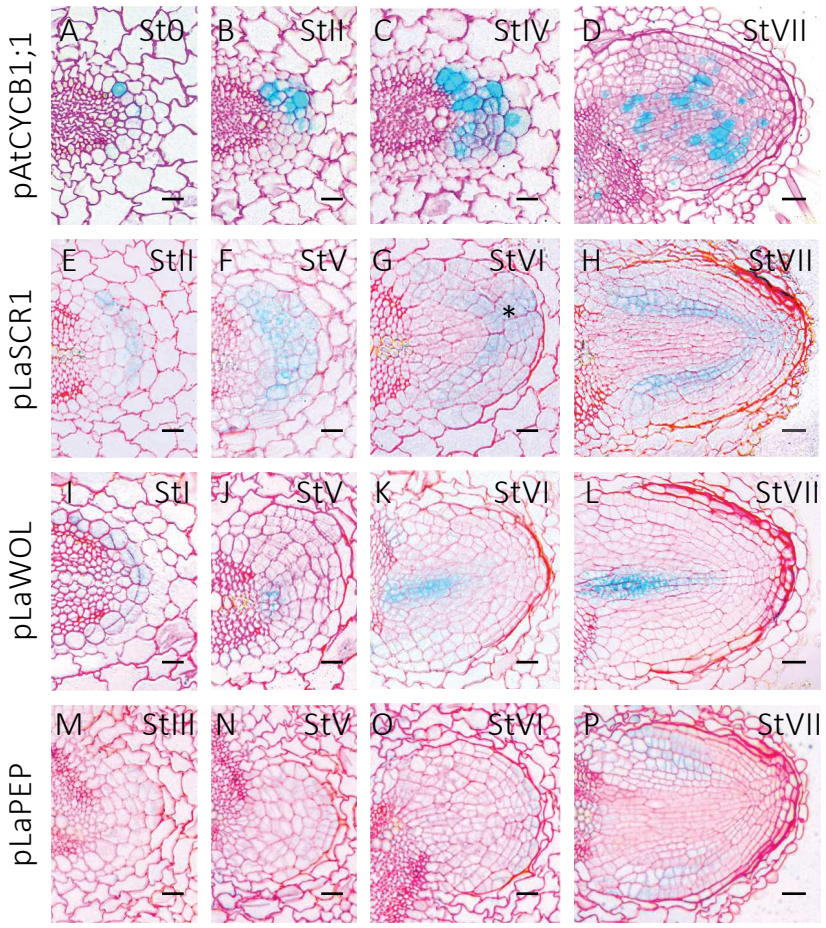

Fig. 6. Cell cycle and tissue-specific markers expression during rootlet development. Images are thin cross section showing GUS activity in 4 markers lines. **(A-D)** ***pAtCYCB1;1:GUS*****.** St0 (A), StII (B), StIV (C) Staining is seen in the pericycle (A), in the endodermis (B) and in the cortex (C). StVII (D) Numerous cells divide when the rootlet is about to emerge. **(E-H)** ***pLaSCR1:GUS*****.** StII (E) Staining appears specifically in 6 endodermal cells. StV (F). GUS staining appears in E1/E2 and cortical cells. StVI (G), StVII (H) Staining is restricted to two layers around central stele and a group of cells at the tip of the rootlet (asterisk). **(I-L)** ***pLaWOL:GUS*****.** StI (I) GUS staining is observed in pericycle cells opposite a xylem pole. StV (J) Staining is apparent in a few cells at the base of the primordium. StVI (K), StVIII (L) Staining is observed in elongated cells found at the core of the primordium. **(M, P)** ***pLaPEP:GUS*****.** StIII (M) GUS staining is hardly observed at this stage. StV (N), StVI (O) Weak staining is seen in CRs derived cortical cells at the rootlet tip. StVII (P) Stronger staining is observed in tissues in the presumptive cortical layers of the rootlet. Scale bar: 50 *µm.*

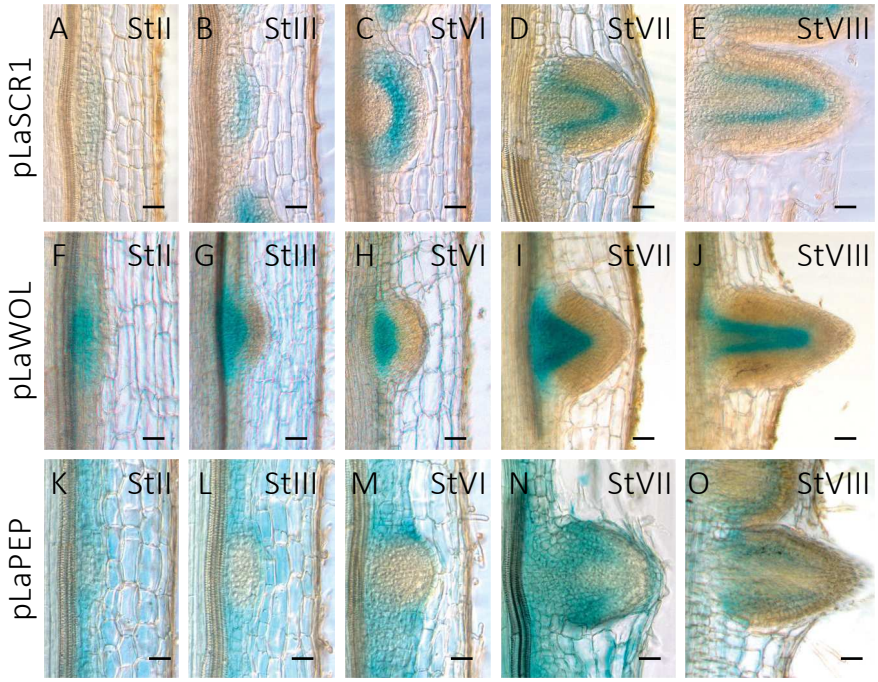

Fig. 7. Glucuronidase expression in rootlet primordia of three tissue-specific expressing lines. Images are longitudinal sections through CR. **(A-E)** ***pLaSCR1:GUS*****.** StII (A), StIII (B) Staining is observed only in the endodermis. StVI (C) to StVIII (E) Staining appears to be expressed in two adjacent cell layers surrounding the stele. **(F-J)** ***pLaWOL:GUS*****.** StII (F) Staining is seen in the pericycle. StIII (G), StVI (H) Staining is observed in the stele-derived tissues. StVII (I), StVIII (J) Staining is observed in central tissues at the core of PR. **(K-O)** ***pLaPEP:GUS***. StII (K), StIII (L) Staining is seen in the cortex of the CR but is not expressed in the primordium. StVI (M) Staining appears in the cortical cells overlaying PR. StVII (N), StVIII (O) Staining is observed in the presumptive cortical layers of the PR. Scale bar: 50 *μm.*

Stele/Vasculature

pLaWOL:GUS marker line stains 6 pericycle cells in P1/P2 at stage I after the first pericline division (Fig. 6I). At later stages, the staining pattern become limited to a group of cells at the base of the primordium that might be derived from P1 (Fig. 6J, Fig. 7H). At stage VI, staining is clearly observed in elongated shaped-cells at the center of the primordium (Fig. 6K). Before emergence, staining in those cells reveals that these cells continue to elongate (Fig. 6L). Expression territory might include as well the newborn rootlet pericycle tissue (Fig. 7I). Staining seem to be stronger expressed in this tissue than in elongated cell at the center of the primordium (Fig. 7J). This pattern is not seen on the cross section in Fig. 6L.

Cortex

Marker line *pLaPEP:GUS* is not expressed in the first stages of rootlet development (Fig. 6M). At stage V, a faded expression can be observed in the tip of the primordium when divisions are seen in the cortex (Fig. 6N). This expression profile persists at stage VI (Fig. 6O, Fig. 7M). Before emergence, staining is expressed in 3 to 4 cortical cell layers at the edges of the primordium but is not expressed in all cortical cell files nor in the initials of these files (Fig. 6P, Fig. 7N).

Endodermal, stellar and cortical marker lines show GUS staining in the expected rootlet layers. At stage VI, the primordia seem to be organized into distinct cell files that would be the stele, the endodermis and the cortex. The transition from stage V to stage VI seems to be crucial for establishment of the radial patterning of the rootlet.

Discussion

Rootlet primordium formation involves division in endodermis, cortex and vascular parenchyma

In angiosperms, despite the fact that pericycle cells facing xylem pole are the most important cells contributing to LR, other tissues including endodermis, cortex or vasculature have been reported to participate to LR patterning (Torres-Martínez *et al.*, 2019). White lupin can develop specialized post-embryonic root, named rootlets that are not found in *Arabidopsis*,

emphasizing the fact that studies on this type of roots cannot be directly compared to *Arabidopsis* lateral root.

Numerous dicots from *Fabaceae* (Mallory *et al.* 1970; Byrne *et al.* 1977; Op den Camp *et al.* 2011; Herrbach *et al.* 2014) and *Solanaceae* (Ivanchenko *et al.*, 2006) were reported to show endodermal divisions, as well as several species from monocots families like *Poaceae* (Bell and McCully 1970; Jansen *et al.* 2012; Orman-Ligeza *et al.* 2013) and *Amaryllidaceae* (Casero *et al.*, 1996). In the endodermis, like in the pericycle, the first divisions were anticlinal. Anatomical studies of maize and barley (Bell and McCully, 1970; Orman-Ligeza *et al.*, 2013), *Medicago truncatula* (Herrbach *et al.*, 2014) and *Solanum lycopersicum* (Ivanchenko *et al.*, 2006), showed that anticlinal division in the endodermis appears as early as stage III LRP. In white lupin endodermis, these divisions are also observed (Fig. 1C,D). Later on, the cells derived from the parental endodermis layer undergo periclinal divisions. Two or more layers from endodermal origin can results from these divisions (Demchenko and Demchenko, 2001; Bell and McCully, 1970; Ivanchenko *et al.*, 2006; Orman-Ligeza *et al.*, 2013). These endodermal derived cells can either contribute to the structure of LRP, or form a temporary structure that will be replaced by a permanent structure derived from pericycle tissue after emergence. In *Cucurbita maxima*, the endodermis participates to the cortex, the epidermis, the root cap and vascular tissues of the lateral root (Mallory *et al.*, 1970). In maize and tomato, two layers derived from the endodermis form a temporary structure with a cap-like structure, which is sloughed-off just before or after LR emergence (Ivanchenko *et al.*, 2006; Bell and McCully, 1970). This structure has been described as a “poche digestive” (french for digestive pocket) or “Tasche” (german for pocket) (Péret *et al.*, 2009a). It was suggested that this structure produce hydrolyzing enzymes that facilitate the passage of the primordium through the parental tissues (Karas and McCully, 1973). These enzymes were thought to help the progression by modification of the cell wall composition in the overlaying cells (Péret *et al.*, 2009a). Coupled with enzyme release, destruction of the integrity of endodermal cell files on the flanking borders, was observed just before emergence (Clowes 1978). In white lupin, the degradation of the endodermal cells at the base of LRP was observed at stage VI (Fig. 1G). This observation suggests that endodermis may facilitate rootlet crossing through cortical layers. Whether the endodermis derivates participate or not in the final structure of the rootlet primordium cannot be determined solely based on anatomical studies.

In more complex cases, cell divisions can also be observed in the overlaying cortex (Ilina *et al.*, 2018; Herrbach *et al.*, 2014; Demchenko and Demchenko, 2001). These intriguing divisions in cortex are observed on white lupin cluster root sections. Recruitment of the cortex to the LR formation is still unclear. Whether these divisions participate to the permanent body of the rootlet in white lupin or are unrelated to rootlet formation is a question that needs to be addressed. Division in the inner cortex is often observed in *Fabaceae* species (Herrbach *et al.*, 2014; Op den Camp *et al.*, 2011; Mallory *et al.*, 1970; Byrne *et al.*, 1977) while participation of several cortex layers is characteristic of *Cucurbitaceae* species (Ilina *et al.*, 2018; Mallory *et al.*, 1970). In certain species from these families, both endodermis and cortex can divide to form a root-cap like structure (Torres-Martínez *et al.*, 2019). This root cap structure was suggested to play a protective role for the core of pericycle derivatives that crosses the parent root by limiting mechanical damages (Karas and McCully, 1973). Another additional role for these divisions is to facilitate the primordium crossing and emergence (Péret *et al.* 2009; Orman-Ligeza *et al.* 2013). White lupin rootlet primordium has to cross at least 4 layers of cortex to emerge, which is particularly challenging for emergence process to happen. Divisions in the overlaying cortex produce small cells that might ease emergence of rootlet primordium. Besides, another potential role for these divisions is related to quiescent center establishment. Organization of a quiescent center within the developing primordium need proliferating cells (Malamy and Benfey, 1997; Torres-Martínez *et al.*, 2019). In lupin, numerous cells are dividing in the pericycle, endodermis and cortex and may meet this need for cell proliferation. This active proliferation as shown with *CycB1;1:GUS* (Fig. 6A-D) marker may lead to temporary establishment of quiescent center in rootlet primordium, before meristem exhaustion (Shishkova *et al.*, 2008).

Vascular parenchyma, a tissue of the vascular cylinder can participate in primordium organogenesis by connecting the newborn primordium to the parent vasculature. Contribution of vascular parenchyma is seen both in monocots (Bell and McCully, 1970; Clowes, 1978) and dicots (Byrne *et al.* 1977; Ilina *et al.* 2018). In particular, in dicots, periclinal divisions were observed in soybean as early as stage II LRP (Byrne *et al.*, 1977). Eventually, these divisions lead to the formation of several cell files that connect the LRP to the parent root. Also, mitotic figures were observed in *Cucurbita pepo* in parenchyma cells (Ilina *et al.* 2018). During zucchini LRP organogenesis, the parenchyma cells continue to divide and increased number of parenchyma cells, as well as enlargement of the primordium base is observed. In white lupin, first periclinal

divisions in cluster root vasculature were observed at stage IV rootlet primordium. Interestingly, vascular parenchyma contribution was also noticed in *Medicago truncatula* at stage IV LRP (Herrbach *et al.*, 2014). However, vascular parenchyma involvement during LRP development in *Arabidopsis* has not been reported and not described (Malamy and Benfey, 1997). Altogether, our results shows that several tissues of the cluster root may contribute to the development of rootlets or facilitate the crossing of tissues.

A model for rootlet patterning

We are trying to understand the complexity of rootlet primordium patterning. In the model plant *Arabidopsis*, primary and lateral root primordium share anatomic similarities (Tian *et al.*, 2014). Moreover, many genes governing root apical meristem formation are also involved in lateral root primordium formation (Du and Scheres, 2017b; Hofhuis *et al.*, 2013; Lucas *et al.*, 2011; Di Laurenzio *et al.*, 1996; Forzani *et al.*, 2014; Goh *et al.*, 2016). Despite the fact that root development seems to be an iterative process, very few studies focused on tertiary root. In particular, little is known about the processes that control tissue contribution during rootlet patterning.

A rootlet primordium develops through a highly ordered number of divisions. The first visible step of rootlet development is initiation, which is known to involve a series of molecular, cellular and anatomical events (Vermeer and Geldner, 2015; De Smet, 2012). Initiation starts with nuclei migration in two adjacent lateral root founder cells and continues with an asymmetric division. Although it is difficult to follow nuclei migration without the use of a dynamic approach, first asymmetric division in a founder cell is visible in white lupin (Fig. 1B). This first division is considered to be tightly regulated and is fundamental for the subsequent developmental stages (Von Wangenheim *et al.*, 2016). Rootlet initiation is pursued with the appearance of periclinal divisions in pericycle cells. These divisions are easily identifiable on root section with a uniseriate pericycle because the cells that divide are distinct from the rest of the flanking pericycle cells.

In the next steps of primordium development, cells proliferate to establish a self-organizing primordium that creates a structure comprising all root layers (Von Wangenheim *et al.*, 2016). If lateral root primordium has a layered structure similar to primary root meristem, it is expected that such structure would be conserved in third-order roots. In order to see

whether this hypothesis is right, each cell layer must be assigned an identity. It is possible to determine tissue identity with the use of marker lines. Over the past 20 years, many promoters with tissue-specific activity have been identified in *Arabidopsis* and other angiosperm species (Marquès-Bueno *et al.*, 2016). With the amount of genomic and transcriptomic data that is now available in white lupin, it is possible to identify lupin orthologous gene to one's favorite gene. This advances led us to identify endogenous lupin promoters to drive reporter gene and follow establishment of rootlet tissues. The use of these tissue-specific marker line make it possible identify tissue identity through rootlet development. Tracking promoter expression pattern allows to follow the fate of particular groups of cells in the primordium rof rootlet. Tissue layers present in stage VII primordium rootlet can be traced back to the tissue layers in young primordium rootlet. As was done for *Arabidopsis* LRP (Malamy and Benfey, 1997), we propose to deduce cell lineage in the rootlet primordium.

In the rootlet primordium, the tissues forming the stele may be derived from two different tissues of the lateral root. The vascular tissues seem to be derived from divisions in the pericycle and in the parenchyma tissues of the lateral root. Note the periclinal division in the parenchyma (Fig. 8F, StIV, black arrow) and the cells that elongate at the base of the primordium at stage V like typical vascular cells (Fig. 8G, StV, black arrow). In contrast, the pericycle of the rootlet might be derived from the P2 layer in the primordium, after the first periclinal division in pericycle at stage Ib. The cells belonging to the endodermis and inner cortex of the rootlet might be derivatives from the cluster root endodermis, and may separate at stage VI via a periclinal division in the E1 layer (white arrow, Fig. 8H). These two tissues connect with a single cell that might be the cortex/endodermal initial (Fig. 8H, StVI, red arrow). The outer layers of cortex may be defined after periclinal divisions in the cells derived from the E2 layer. The epidermis and root cap of the rootlet primordium are possibly derived from cells of the inner cortex of the lateral root (Fig. 8G, StV) and may separate after subsequent divisions in this layer. Quiescent center position may be inferred from *pLaSCR1:GUS* pattern expression. In *Arabidopsis*, *AtSCR* and quiescent center markers are simultaneously expressed in OL2 at stage V (Goh *et al.*, 2016). Indeed, *de novo* formation of the quiescent center in LRP depends on a SCR-mediated formative cell division. White lupin quiescent center is possibly positioned in the abutting cell of the endodermis and inner cortex located at the tip of the primordium at stage VII (Fig. 8I, StVII, red stars). Altogether, the model for rootlet development suggests that the core of rootlet primordium would be derived from the cluster root pericycle and

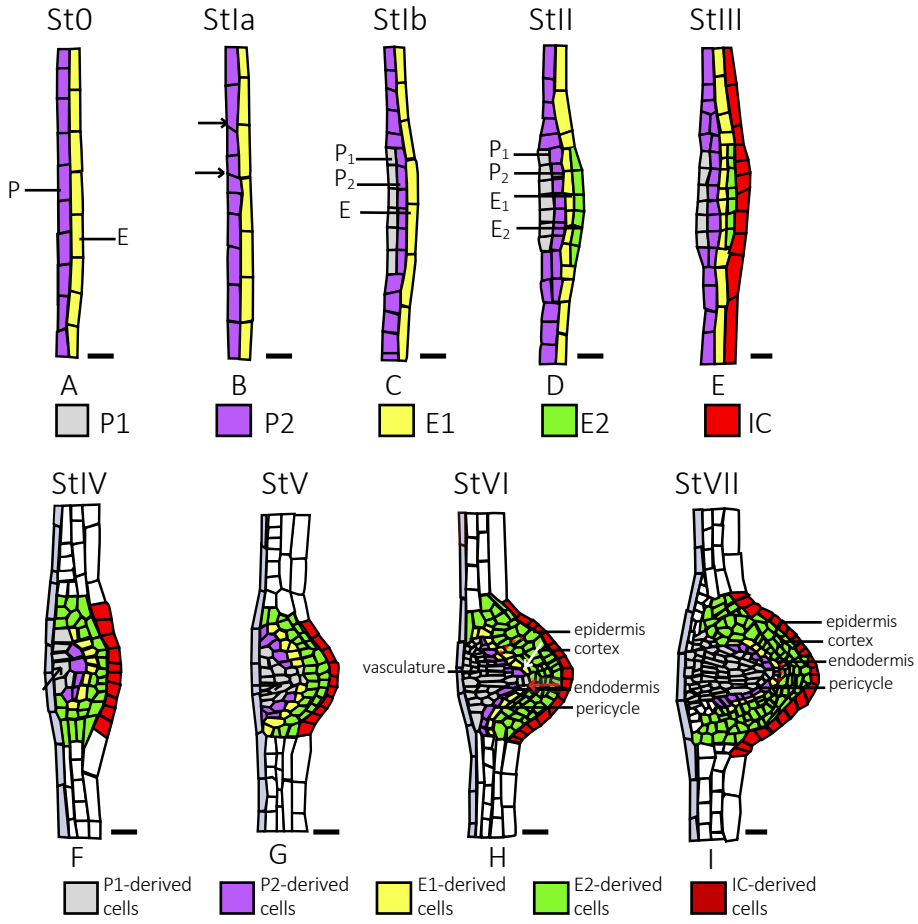

Fig. 8. Schematic representation of rootlet primordium development in white lupin. Scheme based on longitudinal sections of white lupin cluster root shown in Fig. 1. Drawings were made by tracing all cells present in the longitudinal sections. Images indicate divisions and appearance of cell layers at each developmental stage. Colors indicate putative cell lineage in the growing rootlet primordium from stage I to stage VII. **(A-E) Early stages of rootlet development**. St0 (A) Pericycle and endodermis before the first division. StIa (B) First two asymmetrical divisions are seen in the pericycle. StIb (C) A periclinal division in the pericycle gives rise to two layers, P_1 and P_2. StII (D) A periclinal division in the endodermis gives rise to two layers E_1 and E_2. StIII (E) Anticlinal divisions in the adjacent cortex. **(F-I). Rootlet patterning and tissue differentiation**. StIV(F), StV(G) Divisions are observed at the base of the primordium (black arrows). StVI (H) Differentiation of tissue layers inside the rootlet primordium. White arrow points out the presumptive division in the endodermis/cortex initial, while red stars indicate the position of cortical layers. StVIII (I) The organisation of the rootlet primordium is reminiscent of the primary root meristem. Scale bar: 50 *µm*.

endodermis, while the protective forming layers of the epidermis and the root cap arised from divisions in the inner cortex of the cluster root.

Materials and methods

Plant materials and growth conditions

Seeds of white lupin (*Lupinus albus L. cv. Amiga*) calibrated at 7 mm were used in all experiments. White lupin plants were cultivated in growth chambers under controlled conditions (16 h light / 8 h dark, 25°C day / 20°C night, 65 % relative humidity, and PAR intensity 200 µmol.m^{-2}.s^{-1}). The hydroponic solution was modified from (Abdolzadeh *et al.*, 2010) without phosphate, and was composed of: $MgSO_4$, 54 µM; $Ca(NO_3)_2$ 400 µM; K_2SO_4 200 µM; Na-Fe-EDTA 10 µM; H_3BO_3 2.4 µM; $MnSO_4$ 0.24 µM; $ZnSO_4$ 0.1 µM; $CuSO_4$ 0.018 µM; Na_2MoO_4 0.03 µM. Plants were grown either in 1,6 L pots or 200 L tanks. Solution was aerated continuously. For plants in pots, the nutrient solution was renewed every seven days.

Molecular cloning

The primers to amplify the promoter sequences of *LaSCR1*, *LaWOL*, *LaPEP*, *LaGL2, LaEXP7* were designed using Primer3plus (http://www.bioinformatics.nl/cgi-bin/primer3plus/primer3plus.cgi). All primers sequences used are summarised in table. S3. Primers were used to amplify at the minimum 1500 bp upstream of the start codon from white lupin genomic DNA. Sizes of all the promoters amplified are summarized in Table. S3. AttB1 (5'-GGGGCCAAGTTTGTACAAAAAAGCAGGCT-3') and attb2 (5'-CCCCCCACTTTGTACAAGAAAGCTGGGT-3') adapters were added in the primers. Amplified fragments were subsequently cloned into the pDONR221 by Gateway reaction. The promoters were then cloned into the binary plasmid pKGW-FS7 containing a GFP-GUS fusion by Gateway cloning.

Bacterial strain

Agrobacterium rhizogenes strain *ARqual* was used to perform *hairy root* transformation of white lupin. Bacteria were transformed with the binary plasmid by electroporation.

Transformation was confirmed by PCR and sequencing. LB agar plates added with sucrose 2%, acetosyringone 100 µM and appropriate antibiotics were inoculated with 200 µL of liquid bacteria culture, and incubated at 28°C for 24 hours to get a bacterial lawn. Bacterial lawn was used for white lupin seedling transformation.

Hairy root transformation of white lupin

White lupin seedlings were transformed with a protocol that was adapted from a protocol previously published (Uhde-Stone *et al.*, 2005). White lupin seeds calibre 8 mm were surface sterilised by 4 washes in osmosis water, 30 min sterilization in bleach (Halonet 20%) and washed 6 times in sterile water under sterile conditions. Seed were germinated on half Murashige and Skoog medium (pH was adjusted to 5.7). After germination, radicles of 1 cm were cut over 0.5 cm with a sterile scalpel. The radicles were inoculated with the *Agrobacterium rhizogenes* lawn. Fifteen inoculated seedlings were placed on square agar plates (0.7% agar in 1X Hoagland solution) containing 15 µg.mL^{-1} Kanamycin. Composition of Hoagland medium without phosphate was the following one: $MgSO_4$, 200 µM ; $Ca(NO_3)_2$ 400 µM ; KNO_3 325 µM ; NH_4Cl 100 µM ; Na-Fe- EDTA 10 µM ; H_3BO_3 9.3 µM ; $MnCl_2$ 1.8 µM ; $ZnSO_4$ 0.17 µM ; $CuSO_4$ 0.06 µM ; Na_2MoO_4 2.3 µM. Plates were placed vertically in controlled conditions: 16 h light / 8 h dark, 25°C day / 20°C night, 65 % relative humidity, and PAR intensity 200 µmol.m^{-2}.s^{-1}. After 7 days on plates, 60 seedlings were transferred to 12x16.5x5.5 cm trays (20 seedlings per tray) and watered with 500 mL osmosis water. After 12 days, plants presenting hairy roots were transferred to hydroponics in 1.6 L pots containing nutrient solution. Nutrient medium was renewed each week. After 7 days in hydroponic conditions, CRs were sampled on *hairy root* plants.

Histochemical analysis

Histochemical staining of β-glucuronidase was performed on CRs from *hairy root* plants. Samples were incubated in a phosphate buffer containing 1 mg.mL^{-1} X-gluc as a substrate (X-Gluc 0.1 %; phosphate buffer 50 mM, pH 7, potassium ferricyanide 2 mM, potassium ferrocyanide 2 mM, Triton X-100 0.05 %). Zone of CRs with non-emerged rootlets were cutted into 4 to 5 sections and fixed (formaldehyde 2%, glutaraldehyde 1%, caffeine solution 1%,

phosphate buffer at pH 7). Fixation was performed for 2.5 h under agitation at room temperature and then 1.5 h at 4°C.

Miscroscopic analysis

Prior to embedding, roots were progressively dehydrated in ethanol solutions with increased concentrations: 50% (30 min), 70% (30 min), 90% (1 h), 95% (1 h), 100% (1 h), 100% (overnight). Samples were impregnated with 50% pure ethanol and 50% resin (v/v) for 2 days, then in 100 % resin for 5 days. CRs were embedded in Technovit 7100 resin (Heraeus Kulze, Wehrheim, Germany) according to the manufacturer's recommendations. Thin sections of 10 µm were produced using a microtome (RM2165, Leica Microsystems) and counterstained for 30 min with 0.1% ruthenium red and rinsed two times with ultrapure water. All sections were observed with a colour camera on epifluorescence microscope (Olympus BX61 with Camera ProgRes®C5 Jenoptik and controlled by ProgRes Capture software). Macroscopic photographs of whole CRs were taken with stereomicroscope (SZX16, Olympus).

Phylogenetic trees

White lupin cDNA-deduced protein sequences were retrieved from our white lupin genome sequence tool (https://www.whitelupin.fr/). Arabidopsis protein sequences were extracted from TAIR database (https://www-arabidopsis-org.insb.bib.cnrs.fr/) and protein sequences from *Lupinus angustifolius, Medicago trunctula, Cicer arietinum, Glycine max* were downloaded from NCBI database (https://www.ncbi.nlm.nih.gov/protein).

Phylogenetic tree were generated with online phylogenetic tool designed by LIRMM (http://phylogeny.lirmm.fr/phylo_cgi/simple_phylogeny.cgi?workflow_id=342ed8d5040742480134127e81e1ed09&tab_index=1). The bootstrap consensus tree was inferred from 500 replicates. Branches corresponding to partitions reproduced in less than 50% bootstrap replicates were collapsed. Trees were customized using the iTOL interface (https://itol.embl.de/upload.cgi).

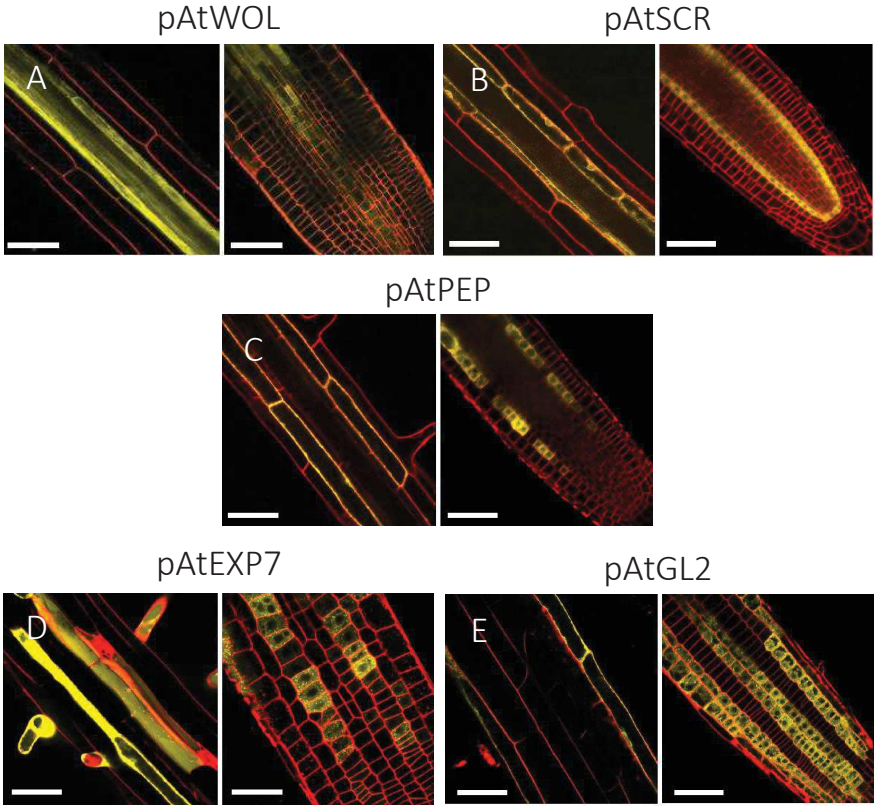

Fig. S1. Expression profile of 5 *Arabidopsis thaliana* tissue-specific genes in the primary root (Marquès-Bueno *et al.,* 2016). (A) WOODEN LEG (WOL) is expressed in the stele and mainly in pericycle cells. (B) SCARECROW (SCR) expression is observed in the endodermis and the quiescent center. (C) PEP expression is seen in the cortex in the transition and elongation zones. (D-E) EXPANSIN7 (EXP7) and GLABRA2 (GL2) are expressed in the root in the trichoblasts and atrichoblasts respectively. Scale bar is 50 *µm.*

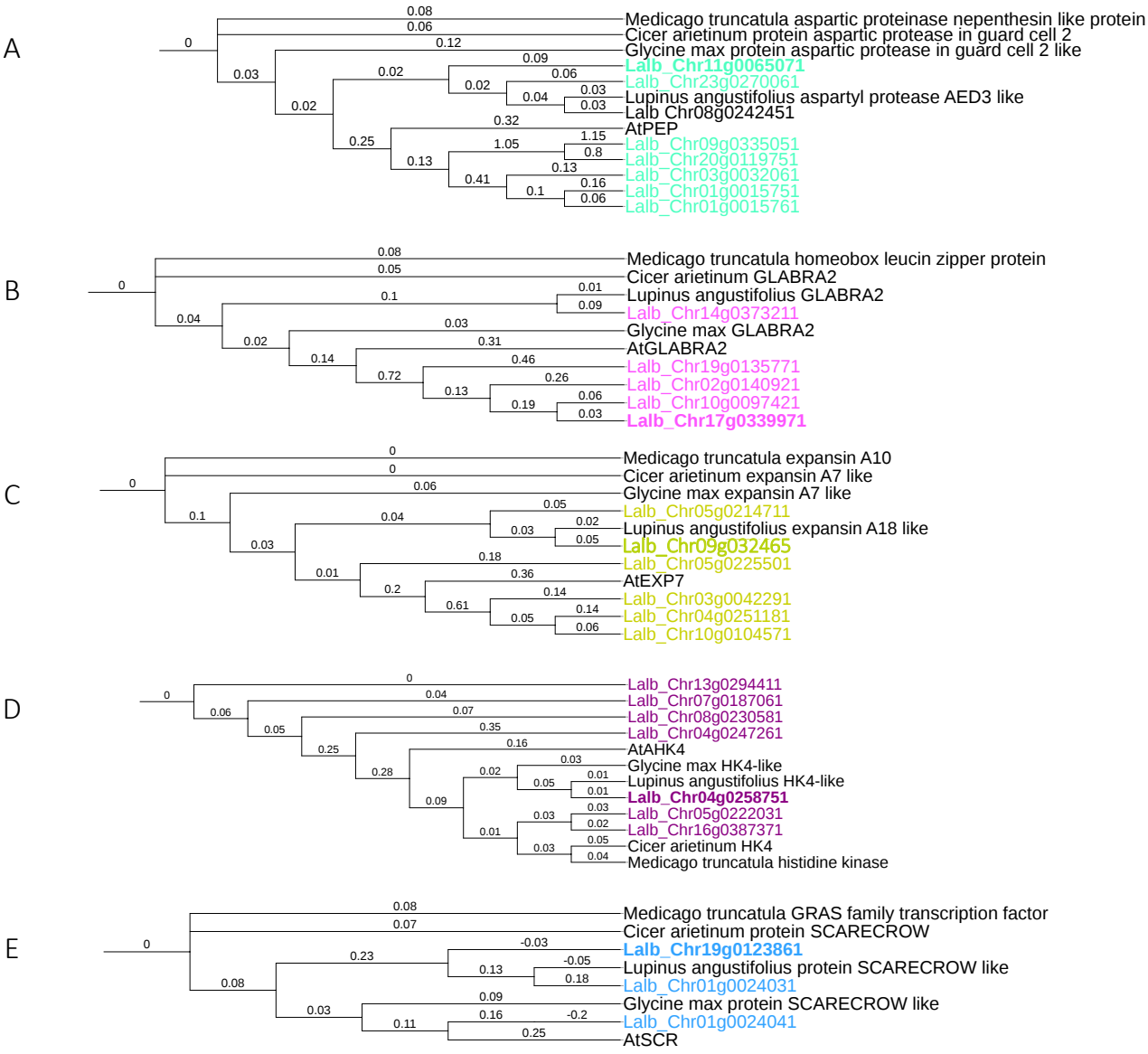

Fig. S2. Neighbour joining tree showing relationship of white lupin protein sequences and other legumes protein sequences. The trees were constructed using the Neighbor-Joining method using the phylogeny tool from LIRMM (http://phylogeny.lirmm.fr/phylo_cgi/index.cgi). The bootstrap consensus tree was inferred from 500 replicates. Branches corresponding to partitions reproduced in less than 50% bootstrap replicates were collapsed. The analysis was performed using amino acid sequences extracted from white lupin genome (https://www.whitelupin.fr/) and from NCBI (https://www.ncbi.nlm.nih.gov/) for other legume species.

Promoter name in *Arabidopsis*	Reference paper	Gene Atg number (or other source)	Lupin promotor name	Promotor size (bp)	Expected tissular expression in roots
AtCYCB1;1	Colón Carmona et al (1999)	At4g37490	-	1800	Dividing cells at G2/M phase
AtSCR1	Marquès-Bueno et al (2016)	At3g54220	LaSCR1	1510	Pericycle / endoderme
AtWOL	Marquès-Bueno et al (2016)	At2g01830	LaWOL	1570	Pericycle
AtPEP	Marquès-Bueno et al (2016)	At1g09750	LaPEP	1540	Cortex
AtGL2	Marquès-Bueno et al (2016)	AT1G79840	LaGL2	1499	Epidermis
AtEXP7	Marquès-Bueno et al (2016)	At1g12560	LaEXP7	1499	Epidermis

Table S1. Description of the marker genes in this study. White lupin genes name, promoter length and expected tissular expression of all promoter tested are described.

	Number of plants tested	% of positive plants (among tested plants)	Number of cluster roots tested for GUS staining	% CR with positive GUS staining	% CR with a specific GUS staining
AtCYCB1;1	55	25	28	75	98
LaSCR1	32	50	45	80	95
LaWOL	35	40	40	68	93
LaPEP	35	51	33	60	90
LaGL2	38	82	28	73	96
LaEXP7	37	54	25	84	93

Table S2. Hairy root transformation efficiency, GUS staining efficiency and pro:GUS tissue staining specificity.

Gene name	Gene name identifier (ID number)	Primer name	Primer sequence (5’ -> 3’)
Primers for promotor amplification			
LaSCR1	Lalb_Chr19g0123861	LaSCR1extF	AAATGTATTAATTGGAGCAACAAAAG
LaSCR1	Lalb_Chr19g0123861	LaSCR1extR	GCACTAGTCAAAGGACTACC
LaSCR1	Lalb_Chr19g0123861	LaSCR1AttB1F	**GGGGACAAGTTTGTACAAAAAAGCAGGC**AGGA GTTTGGCACAGCGATTTA
LaSCR1	Lalb_Chr19g0123861	LaSCR1AttB2R	**CCCCCCACTTTGTACAAGAAAGCTGGGT**CCCATC GAAGCCATGTTATGTG
LaWOL	Lalb_Chr05g0222031	LaWOLextF	TGGAAGGTACATGGGTTTTG
LaWOL	Lalb_Chr05g0222031	LaWOLextR	AAGCTCTCTGTGCCTGAATG
LaWOL	Lalb_Chr05g0222031	LaWOLAttB1F	**GGGGACAAGTTTGTACAAAAAAGCAGGC**TCACT GGTCCGGTCAAAAAG
LaWOL	Lalb_Chr05g0222031	LaWOLAttB2R	**CCCCCCACTTTGTACAAGAAAGCTGGGT**CAGCAA AAAATTATCTTTGCTTAGTTTC
LaPEP	Lalb_Chr11g0065071	LaPEPextF	TGAACCGTTAGATCTGTGACTG
LaPEP	Lalb_Chr11g0065071	LaPEPextR	AGGTCTGAGTCATCGGTTTG
LaPEP	Lalb_Chr11g0065071	LaPEPAttB1F	**GGGGACAAGTTTGTACAAAAAAGCAGGCT**CAAG AGTGCCATTATTTTTGTTGGAG
LaPEP	Lalb_Chr11g0065071	LaPEPAttB2R	**CCCCCCACTTTGTACAAGAAAGCTGGGT**GGTTGA TAGAATAGAAGGAAAAGAGG
LaGL2	Lalb_Chr17g0339971	LaGL2extF	ATGCACATTACTATACTACATCCTC
LaGL2	Lalb_Chr17g0339971	LaGL2extR	GAAGGGTAATGGGTCTTTTGG
LaGL2	Lalb_Chr17g0339971	LaGL2AttB1F	**GGGGACAAGTTTGTACAAAAAAGCAGGC**GTATC AAGATTTGATTTCCCTATTTTC
LaGL2	Lalb_Chr17g0339971	LaGL2AttB2R	**CCCCCCACTTTGTACAAGAAAGCTGGGT**ACTTCT AGTTCTGGGTTTCTCTC
LaEXP7	Lalb_Chr05g0214711	LaEXP7extF	AGGGCTGACAATGAAAATGGG
LaEXP7	Lalb_Chr05g0214711	LaEXP7extR	CGCAGAAGCAGTCTCATCAC
LaEXP7	Lalb_Chr05g0214711	LaEXP7AttB1F	**GGGGACAAGTTTGTACAAAAAAGCAGGCT**GGAT GCTGATGCGAAATTGCTTGTTTACGA
LaEXP7	Lalb_Chr05g0214711	LaEXP7AttB2R	**CCCCCCACTTTGTACAAGAAAGCTGGGT**GGCTAA GCTTGGATATGTGCT
Primers for sequencing			
-	-	M13F	TGTAAAACGACGGCCAGT
-	-	M13R	CAGGAAACAGCTATGACCATG
-	-	FS7-F-V2	ACGTGACTCCCTTAATTCTC
-	-	eGFP-R-out	TAGGTCAGGGTGGTCACGAG

Table. S3. List of primers used for molecular cloning

CHAPITRE 3

Identification de gènes impliqués dans la formation des racines protéoïdes

Avant-propos

Dans ce troisième chapitre, nous avons cherché à comprendre les mécanismes moléculaires qui régulent les étapes précoces de la formation des rootlettes chez le lupin blanc. Afin d'identifier des gènes susceptibles d'être impliqués dans ces stades, l'équipe a généré un transcriptome détaillé couvrant les différentes étapes développementales de la formation des rootlettes (Post-Doctorante Bárbara Hufnagel). Les données de séquençage ont été assemblées par notre bioinformaticien (Alexandre Soriano). J'ai par la suite analysé les niveaux d'expression issus de ce transcriptome en me focalisant sur les premiers stades de développement. L'analyse des niveaux d'expression a permis d'établir des listes de gènes qui sont induits avant et pendant l'initiation des rootlettes. Ces gènes ont montré un patron d'expression spécifique et étaient plus exprimés au cours des premières étapes de la formation de ces racines. Ces listes comprenaient des facteurs de transcription et des kinases, qui sont connus pour jouer un rôle important dans les processus développementaux. Une dizaine de ces gènes ont ainsi été sélectionnés pour la réalisation d'un crible fonctionnel. La fonction putative des gènes candidats a été étudiée grâce à la technologie CRES-T (Chimeric Repressor Gene Silencing Technology) ou l'ARN interférent chez le lupin blanc. Des analyses phénotypiques et moléculaires ont montré que plusieurs de ces gènes pourraient participer aux réseaux de gènes qui contrôlent la formation des rootlettes.

Le chapitre suivant est présenté sous la forme d'un article scientifique. Cet article met l'accent sur les mécanismes moléculaires du développement précoce des rootlettes et souligne l'importance de certains facteurs de transcription pendant leur formation.

Article 3: Identification of gene involved in early steps of cluster root formation

Cécilia Gallardo[1], Bárbara Hufnagel[1], Alexandre Soriano[1], Quentin Rigal[1], Fanchon Divol[1], Laurence Marquès[1], Patrick Doumas[1], Benjamin Péret[1*]

[1]BPMP, CNRS, INRA, Montpellier SupAgro, Univ Montpellier, Montpellier, France

Correspondence

[*]Corresponding author, e-mail: benjamin.peret@cnrs.fr

Abstract

One of the main strategies used by plants for the effective acquisition of phosphate is the formation of cluster roots (CR). Cluster roots are lateral roots forming one or several cluster(s) of small roots with determinate growth called rootlets. Understanding these mechanisms is important to understand how root plasticity is shaped by the environment. In this study, the molecular events involved in early steps of CR development were investigated. We used RNA-seq technology to describe the changes in gene expression during the course of CR development in white lupin. Transcriptome analysis revealed the existence of a dynamic network across the early stages of cluster formation. We identified a total of 111 and 216 genes whose expression is induced in cluster roots prior and during initiation respectively. Several transcription factors and a kinase with a previously known function in lateral root formation display increased level of their expression compared to regular lateral roots (without rootlets). To investigate the function of these genes, we produced a dominant repressor version of the transcription factors (Chimeric Repressor Silencing Technology) and used RNA silencing to down-regulate the expression of a white lupin kinase candidate. Our results indicate that 3 lupin genes may participate to the control of rootlet initiation or early patterning. Overall, this study provides new insights into the molecular events that control the exacerbated development of white lupin cluster roots. White lupin can serve as a model-species to discover the molecular mechanisms that trigger CR development.

Key words: rootlet, cluster roots, white lupin, root development, transcription factor, SRDX.

Introduction

Plants are sessile organisms that deal continuously with the heterogeneity of nutrients available in the soil. To overcome this heterogeneity, plants have acquired the ability to modulate the development of their root system. The geometry of the root system, or root system architecture (RSA) is therefore highly plastic (Hodge, 2004) and is determined mainly by primary root growth and *de novo* organogenesis of lateral roots (LR) (Tian *et al.*, 2014; Banda *et al.*, 2019). Developmental plasticity is strongly beneficial to plants, especially in soil where nutrients are poorly available or became scarce due to overexploitation. Indeed, plastic responses of the root system can enhance physiological ion-uptake in nutrient-rich patches (Neumann and Martinoia, 2002). These responses are important adaptive strategy to P-depleted soil, and include the formation of specialized organs such as cluster roots (Lambers *et al.*, 2006).

Cluster roots are secondary root organs and are considered to be one the three main adaptations of plants to nutrient acquisition, along with nodules that allow N_2 fixation and mycorrhiza that provide hosts plants access to organic P and N forms (Neumann and Martinoia, 2002). Cluster roots correspond to secondary roots or lateral roots, that can form numerous short roots with limited growth called rootlets (Skene, 2003). One main recognizable feature of these organs is the presence of numerous rootlets at successive developmental stages in the cluster zone (Sbabou *et al.*, 2010). These short roots are formed when phosphate (Pi) starvation is maintained and results from a massive and quick initiation of new roots from cluster roots tissues (Neumann *et al.*, 2000). Rootlets initiate at every protoxylem poles in the cluster root zone while lateral roots are known to be initiated randomly from pericycle cells of primary roots (Johnson *et al.*, 1996; Hagström *et al.*, 2001). Therefore, cluster roots may be regarded not as typical lateral roots but as specific lateral roots with an exacerbated development

Of the species that form cluster roots, white lupin (*Lupinus albus L.*) has been extensively studied and used as a model to understand the physiological changes associated with their formation (Watt and Evans, 1999b). Indeed, the large secretion of organic chelators such as citrate and malate, as well as enzymes (phosphohydrolases) and protons from mature rootlets is known to mobilize Pi adsorbed on soil particles making it available for white lupin (Lambers *et al.*, 2013). In the past twenty years, many progresses have been made to understand the metabolic changes linked to this “exudative burst”, using physiological assays

(Watt and Evans, 1999a; Massonneau *et al.*, 2001) and the molecular characterization of the genes involved in these changes (Peñaloza *et al.*, 2002). Recently, genome wide transcriptomic studies has provided new insights into the molecular mechanisms controlling these metabolic modifications (O'Rourke *et al.*, 2013a; Wang *et al.*, 2015a; Zanin *et al.*, 2019). These studies highlighted the effect of the environment on cluster root function and have revealed a key implication of hormones in their development. However, the molecular mechanisms controlling the effect of the environment on cluster root formation are still unknown.

In the present study, we investigated the molecular mechanisms of white lupin cluster root development to understand how environmental cues can induce strong initiation of lateral roots. The fundamental molecular players of lateral root development have been originally discovered in *Arabidopsis thaliana* (Péret *et al.*, 2009b; De Smet *et al.*, 2006). The early events determining the ability of cells to form LR occur in the primary root tips. This succession of events start with priming which involves a massive oscillatory expression of thousands of genes, and leads to the formation of LR pre-branch sites and subsequent specification of LR founder cells (Moreno-Risueno *et al.*, 2010). Molecular evidences suggest that *LATERAL ORGAN BOUNDARIES DOMAIN16* (*LBD16*) is required for LR priming during the oscillation (Moreno-Risueno *et al.*, 2010), while *MEMBRANE-ASSOCIATED KINASE REGULATOR4* (*MAKR4*) may convert LR pre-branch sites into competent sites to form LR after the oscillation (Xuan *et al.*, 2015). Later on, specified LR founder cells perceive auxin and are triggered to divide (Casimiro *et al.*, 2001). This first asymmetric division is critical for LR formation and requires the progression of pericycle cells into the cell cycle (Feng *et al.*, 2012) and the activation of the nuclear migration (Goh *et al.*, 2012), as mediated by LBD29 and LBD16 proteins respectively. Following this division, the LBD16-dependant induction of *PUCHI*, contribute to LR primordium morphogenesis by controlling the pattern of division during early stages (Hirota *et al.*, 2007; Goh *et al.*, 2019). This organogenesis is largely dependent on auxin flux direction, canalized by PIN proteins (Benková *et al.*, 2003), and the transduction of the auxin signal (Du and Scheres, 2017a).

Here, in order to understand the molecular regulation of Pi-induced cluster root formation, we generated a detailed transcriptomic dataset of white lupin cluster root development. Our RNA-seq was produced to cover 12 successive stages of their development, from organ initiation to post-emergence growth. Based on this data, 9 candidate genes, mostly transcription factors that are strongly expressed during early stages of rootlet development,

were selected. Interestingly, this shortlist of genes included known regulators of lateral root formation but also genes for which a function in lateral root patterning has not been yet described. To investigate the function of these transcription factors, we took advantage of the Chimeric Repressor Silencing Technology (CRES-T) (Ohta *et al.*, 2001; Hiratsu *et al.*, 2004), that allows the silencing of multiple targets of transcription factors and has been used to resolve experimental issue related to functional redundancy of transcriptional families (Eklund *et al.*, 2010; T. Goh *et al.*, 2012). RNA interference, which has been successfully employed to silence white lupin genes (Uhde-Stone *et al.*, 2005), was complementary used to down-regulate the expression of the white lupin gene *LaMAKR4*. The constructs were used to transform white lupin roots and were delivered via *Agrobacterium rhizogenes*. Our results suggest that some of the genes that were selected may have a function related to rootlet development during early stages.

Results

Differential gene expression due to rootlet formation

The remarkable ability of white lupin to initiate numerous rootlets led us to question about the molecular events controlling their formation. With the aim to identify genes regulating early steps of rootlet development, a detailed transcriptomic dataset of 12 successive developmental stages of cluster roots was generated. We took advantage of the fact that cluster roots are consistently produced at a precise location in the root system. Phenotypic analysis showed that the highest number of clusters appears on cluster roots at a location situated between 1 cm and 1.5 cm away from the primary root. (Gallardo *et al.*, 2018). To determine the developmental stages associated to each sample, we observed cluster root anatomy at each harvested stage (Fig. 1A). Rootlets seem to be initiated 24 hours after the beginning of sampling, after which primordium became organized and emerged (48h). Following the emergence process, rootlets grow until their meristem differentiate, and became fully covered with root hairs (120 h).

To confirm the developmental stages associated to the early steps of cluster root formation, we produced root sections of the developmental zones used for the RNA-seq survey up to 36 hours (Fig. 1B). No developmental events associated to rootlet formation was

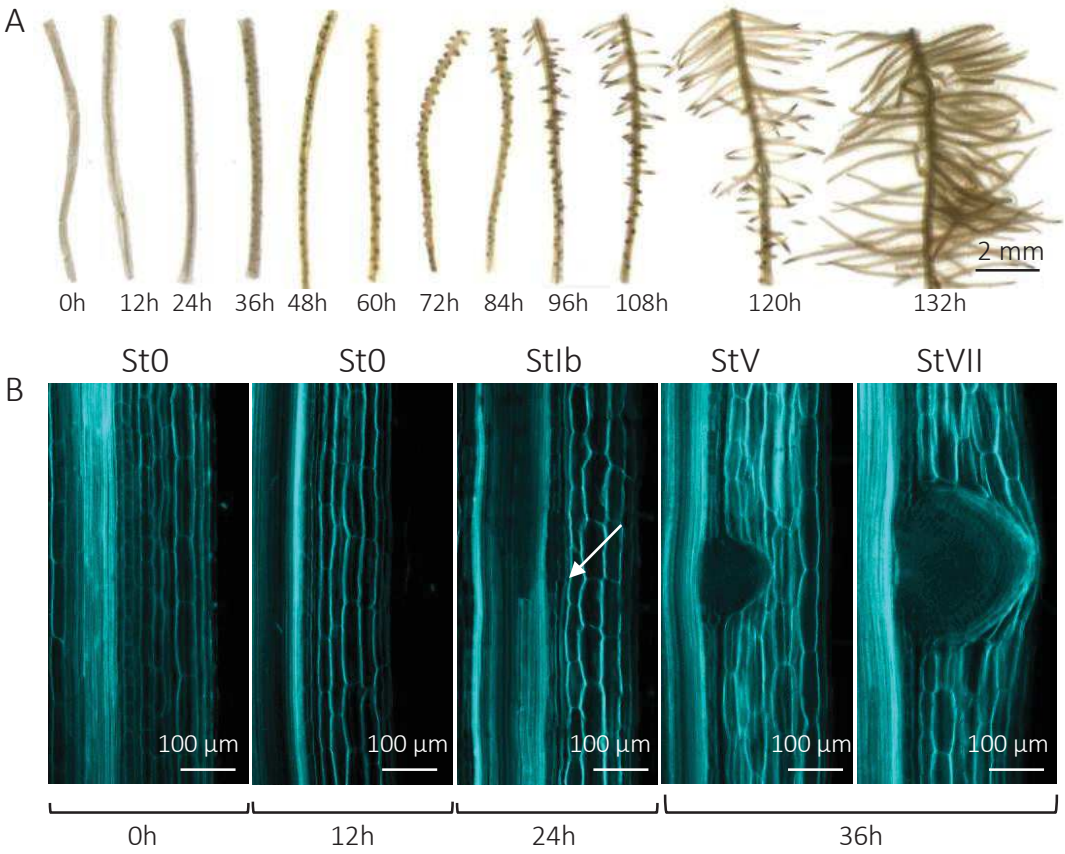

Fig. 1. Developmental stages of cluster root formation. (A) Anatomy of the cluster root zone used for transcriptomic studies, showing the initiation and growth of numerous rootlets. (B) Formation of a primordium of rootlet takes place over a period of 36 hours. Rootlets are initiated 24h after the start of the developmental kinetic. Images are representative of n=20 roots (A) and n=8 roots (B).

observed in the T0 and T12 CR parts, suggesting that only molecular events are taking place at these stages. The presence of stage Ib primordia in T24 CR sections confirmed that rootlets are initiated 24 hours after the beginning of sampling (Fig. 1B, StIb). After initiation, cells actively divide to form a dome-shaped primordium. (Fig. 1B, StV). This organ eventually develops into a well-organized meristem (Fig. 1B, StVII).

We then performed a differential expression analysis by comparing transcripts found in early steps of rootlet development (T0 to T36) to lateral roots (defined as second order lateral roots bearing no rootlet). To visualize the genes differentially expressed in early steps of the cluster root development, we generated two matrixes showing the number of genes up-regulated (Fig. 2A) or down-regulated (Fig. 2B) in the intersections of cluster root parts. In total, our analyses identified 287 genes expressed by more than 3 fold in at least one pair-wise comparison between early developmental stages and LR, and 555 genes expressed by less than 3 fold (File S1, Table S1 and S2). A gene ontology (GO) term enrichment analysis of these two sets revealed that up-regulated genes were associated to developmental processes, while down-regulated genes were mostly related to metabolic processes (Fig. S1). This observation suggests a tight regulation of metabolic pathways during developmental processes such as cell fate commitment and cell differentiation.

In addition, 29 transcription factor (TFs) families display differential expression in the four cluster root parts compared to LR. The AP2-EREB family is the largest family up-regulated in forming cluster roots (Fig. 2C). We identified 11 members of the AP2-EREB family showing higher expression in CR section compared to LR. Interestingly, genes belonging to this family are known to be involved in developmental processes including the specification of floral organ identity or the formation of LR primordium (Riechmann and Meyerowitz, 1998). In contrast, the NAC and MYB TF families show decreased expression compared to lateral roots. These two TF families are large and display diverse functions in plants. NAC TFs were found to be related to the response to environmental stresses or development processes (cotyledons, shoot apical meristem and LR formation) (Olsen *et al.*, 2005), while plant MYB proteins are involved in the regulation of primary and secondary metabolism, cell fate and identity or developmental processes (Dubos *et al.*, 2010).

We performed hierarchical clustering on 287 genes up-regulated in forming CR compared to LR, and found 5 five main clusters, with cluster 4 and 5 containing the majority of genes (Fig. 3). Clusters 1 and 2 include genes with the highest expression at T0 and decreased

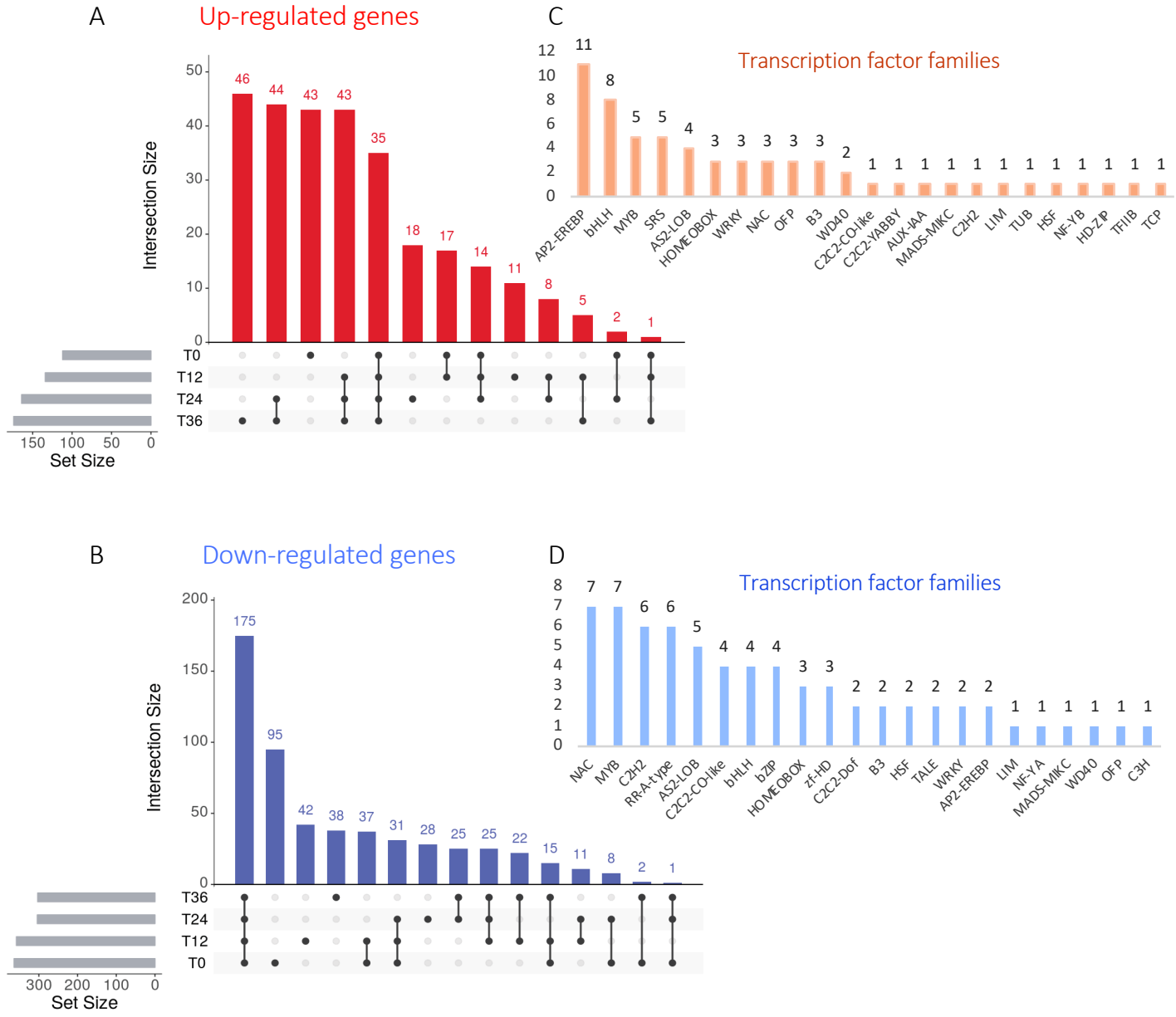

Fig. 2. Matrix layout for all intersections of differentially expressed gene in T0, T12, T24 and T36 CR parts compared to lateral roots. (A-B) Gene up-regulated (A) and down-regulated (B) in the different set comparisons. Each set is indicated by the dots or connected dots below its respective bar. For each comparison, the number on top of each bar represents the number of differentially expressed genes. (C-D) Graphs show the different transcription factors families present in the datasets of up-regulated genes shown in A (C) and down-regulated genes shown in B (D). The number on the top of each bar represents the number of genes present in each family.

expression in T24 and T36 CR parts. In contrast, genes in cluster 4 have low expression at T0 and increased expression in T12, T24 and T36 CR sections. Clusters 4 and 5 have the same expression profile but genes in cluster 4 show continuous increased expression between T24 and T36, whereas it is not the case for genes in cluster 5. Cluster 3 displays the smallest number of genes among all clusters. These genes showed an atypical expression profile with a strong expression between T0 and T24 and a decreased expression between T24 and T36.

We then performed GO term enrichment analysis in each cluster independently (Fig. S2). Cluster I showed enrichment of GO term related to the phenylpropanoid pathway and lignin biosynthesis (*TRA2, OMT1*), iron ion homeostasis (*FRO2, ORG2, APTase9*), root development and meristem maintenance (*LBD16, PUCHI, WOX5*) (Fig. 3B, Fig. S2A, Table S3). Up-regulation of genes involved in developmental processes correlates with the fact that rootlet morphogenesis has started in T0 to T36 CR parts. This results are also in agreement with data showing that genes involved in Fe-acquisition are highly expressed in P-deficient roots (Venuti *et al.*, 2019). For cluster 2, we identified enrichment of GO term related to cell-to cell junction assembly (*CASP1,3,5*) and lignin metabolism (*DIR9, 16, 18, 25, PER64*) (Fig. 3B, Fig. S2B, Table S4). The genes coding for CASPs proteins exhibit rapid decrease of their expression from T0 to T36 CR parts, indicating differential regulation of casparian strip membrane domain during early stages of rootlet formation. Similarly, expression patterns of *DIR* genes, which code for proteins involved in lignin synthesis, suggest changes in the lignin biosynthesis pathway between T0 and T36 CR parts. In cluster 3, we identified a restricted number of GO term enriched, associated to genes involved in carboxylic acid metabolism (Fig. S3C, Table S5). More interestingly, we found genes that may be related to rootlet development including *PUCHI*, a gene involved in the definition of LR primordium boundaries, a gene coding for a protein of the LOB-domain family (*LBD1*) and an auxin signalling component (*IAA30*).

For cluster 4, including 84 genes, we identified enrichment of GO term related to developmental processes (shoot and root organ development), regulation of transcription and response to auxin (Fig. S3D, Table S6). Most of genes associated to the regulation of developmental processes were either linked to the control of shoot organ development like leaves, flowers and gynoecium (*NGA1, LBD12, TCP2, CRF2*) or root formation. Among these genes, several transcription factors are known to be involved in the activity and the maintenance of the lateral root meristem (*PLT1, PLT4, WOX5*), as well as the formation of the root cap (*SMB, FEZ*). In addition, genes regulating auxin homeostasis (*SRS5, SHI, WRKY23,*

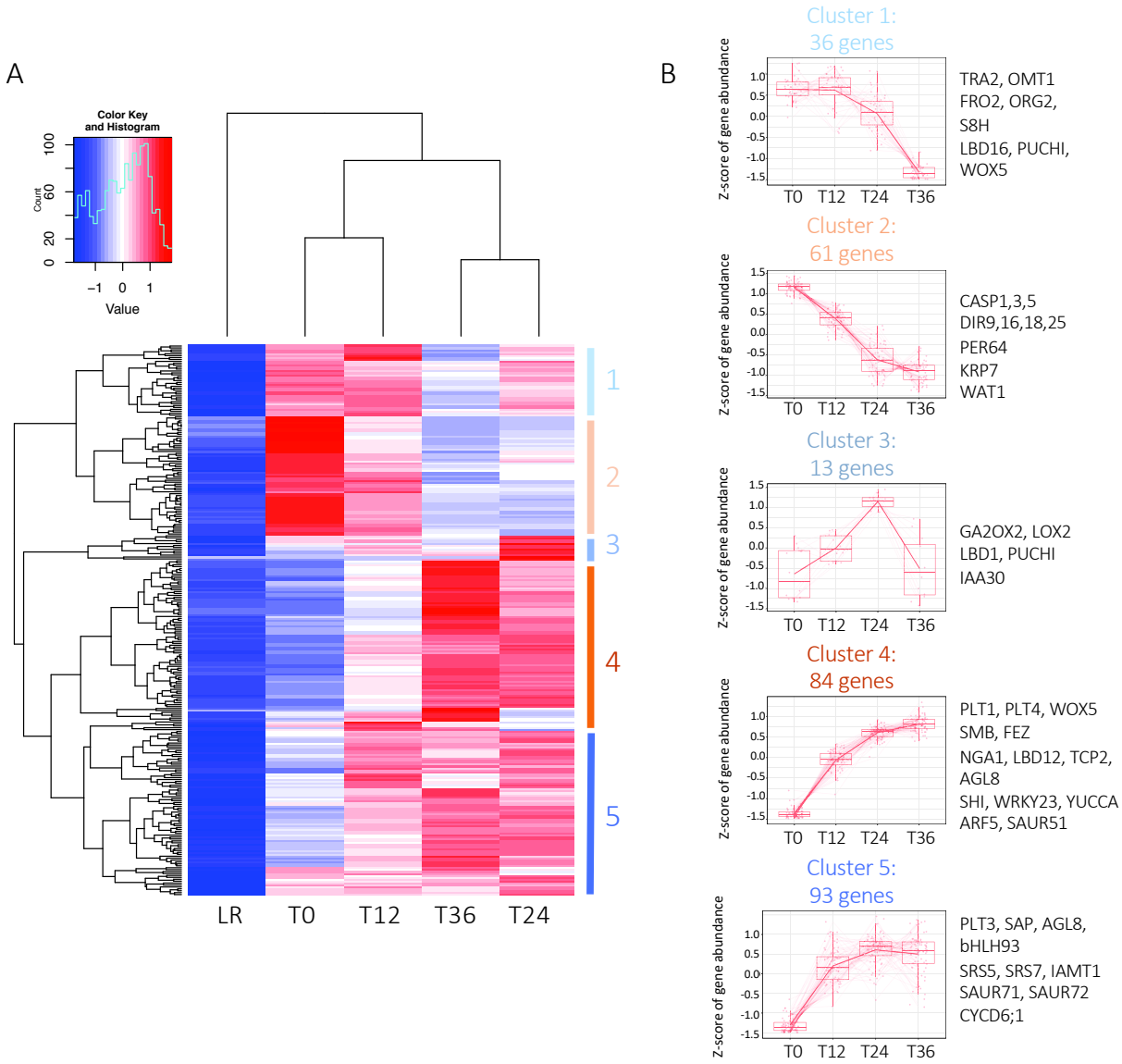

Fig. 3. Hierarchical clustering of genes differentially expressed during early developmental stages. (A) Hierarchical clustering analysis identified 5 main clusters among the 287 up-regulated genes compared to LR. (B) Visualisation of average expression pattern of the genes contained in each cluster. Cluster 1 contains genes involved in the phenylpropanoid pathway, iron homeostasis, root development and maintenance of the meristem. Cluster 2 include genes related to cell-to-cell junction establishment and lignin metabolism. Cluster 3 is linked with carboxylic acid metabolism. Cluster 4 and 5 comprise genes related to developmental processes, the regulation of transcription and response to auxin.

YUCCA9) and auxin-signalling mediated pathway (*ARF5, SAUR51*) were up regulated compared to LR in CR parts (T0 to T36).

In cluster 5, main GO terms enriched were also associated to the regulation of developmental processes (*LEP, SAP, AGL8, bHLH93*), auxin homeostasis (*SRS5, SRS7, IAMT1)* and response to auxin (SAUR71, SAUR72) (Fig. S3E, Table S5). Interestingly, the enriched GO term "single organism process" was including a cell-cycle gene (*CYCD6;1*) having a function in the cortex/endodermis stem cell division and a gene belonging to the PLETHORA family (*PLT3*) (Table S7). Altogether, these results support a strong link between auxin and developmental processes during rootlet morphogenesis.

Selection of genes involved in early steps of rootlet development

The global analysis of the transcriptomic data led to the identification of genes involved in late stages of rootlet development, in particular genes associated to the formation and maintenance of the meristem. In order to identify genes regulating early stages of rootlet development, we performed a second analysis on the assumption that these genes are specifically induced during early stages of cluster root development. For this purpose, we looked for genes (1) induced at early steps of CR formation and (2) exhibiting decreased or no expression at more advanced developmental stages.

First, we searched for genes induced in the earlier steps of cluster root formation in order to find genes that might be involved in pre-initiation events. To this end, we selected genes for which 20% of transcripts were found in T0 and T12 CR parts (gene exhibiting less than 500 reads in total were not selected). On the basis of this criterion, we identified a list of 111 genes induced in T0 and T12 CR parts (File 1, Table S8). The expression profile of these genes is shown in Fig. 4A and B. GO term enrichment analysis on this genes list showed that genes highly expressed in T0 and T12 CR parts were involved in ion transport, aromatic compound biosynthetic process and the regulation of transcription (Fig. S2A, Table S9). Given the important role of transcriptional regulators in developmental processes, we focussed our attention on the subset of genes annotated as TFs. We identified 20 TFs belonging to 11 families in this dataset (Fig. 4C). Among, all families, the MYB and bHLH TFs were the most abundant genes. To assign a putative name and function to these genes, we relied on white lupin gene annotation and compared the cDNA deduced white lupin protein sequences to *Arabidospsis*

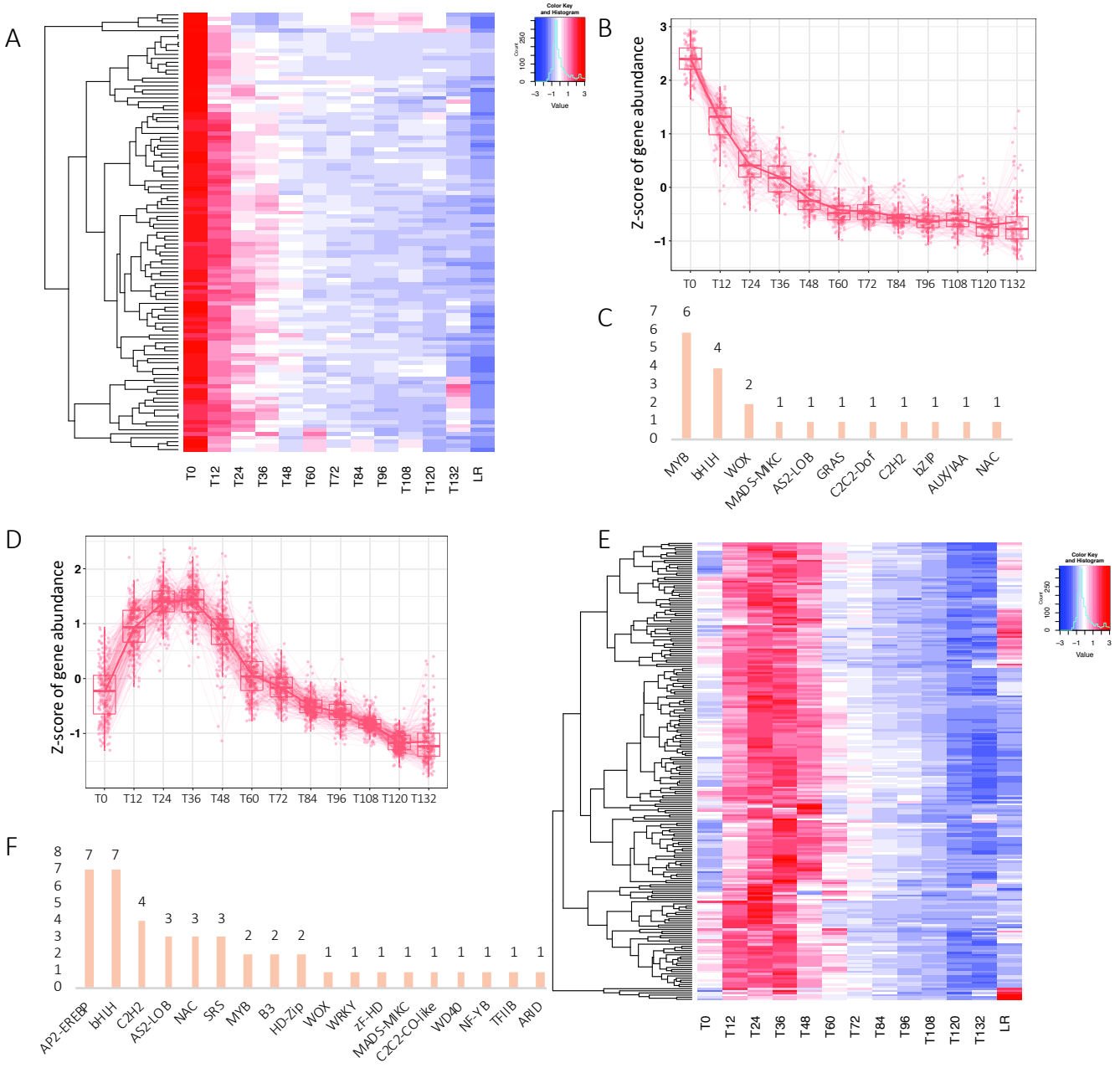

Fig. 4. Expression pattern of genes highly induced during early steps of cluster root formation. (A-B) Heatmap (A) and gene expression pattern (B) of the 111 genes induced in T0 and T12 CR parts. (C) Graph showing the families of transcription factors induced in T0 and T12 samples. (D-E) Expression pattern (D) and heatmap (E) of the 216 genes induced in the samples T12, T24, T36, T48. (F) Graph showing the families of transcription factors induced in T12, T24, T36, T48 CR parts.

protein sequences. This analysis led to the identification of *Lalb_Chr10g0098091*, a gene homologous to *AtMYB124*, which regulates *PIN3* expression in the endodermis during LR initiation (Chen *et al.*, 2015). Interestingly, comparison of protein sequences between white lupin and *Arabidopsis* also identified *Lalb_Chr21g0307221* as an orthologous gene to *AtMAKR4*. This gene, firstly identified by transcriptome profiling, is required for the conversion of pre-branch sites into LR (Xuan *et al.*, 2015). Protein sequences of *Lalb_Chr10g0098091* and *Lalb_Chr21g0307221* were found to be 47.82 % and 55.32 % similar to AtMAKR4 and AtMYB124 respectively. These two genes were selected for further study (Table S10).

In parallel, we looked for genes involved in rootlet initiation and/or patterning. For this purpose, we selected genes that were induced in T12 to T36 CR parts. Therefore, we filtered genes for which 40% of transcripts were represented in T12 to T36 CR parts (gene exhibiting less than 500 reads in total were not selected). This analysis led to the identification of 216 genes (File S1, Table S11), exhibiting similar expression pattern (Fig. 4D, E). This list was enriched with GO terms associated to developmental processes, regulation of biosynthesis of secondary metabolites and lignin, and response to auxin (Fig. S3B, Table S12). In this list, we identified 42 genes belonging to 18 TF families. Amongst them, a shortlist of 8 TFs was selected for further analysis. These genes were selected because of their particular expression profile (Fig. 5). A subset of candidates was chosen for their homology with genes involved in LR formation and they were named *LaLBD16*, *LaLBD29*, *LaPUCHI* (Table S13 and S14). Some other genes did not display any root-related function but were chosen based on other criteria (Table S13 and S14). These genes were named *LaERF12*, *LaSTY1*, *LaNFY-B5* and *LaNAC044*. The function of the previous genes was further studied by generating white lupin transgenic roots.

Generation of white lupin transgenic lines

To address the physiological significance of the 9 selected candidate genes and their potential role in mediating rootlet formation, we conducted two approaches to either silence gene or block the function of the candidate *in planta*.

In order to study the function of the 8 TFs, and avoid the limitations due to the functional redundancy, we generated transgenic hairy roots of white lupin expressing a dominant repressor version of these genes with the Chimeric Repressor Silencing Technology (CRES-T). The coding sequence of the 8 genes lacking the stop codon was fused to the SRDX

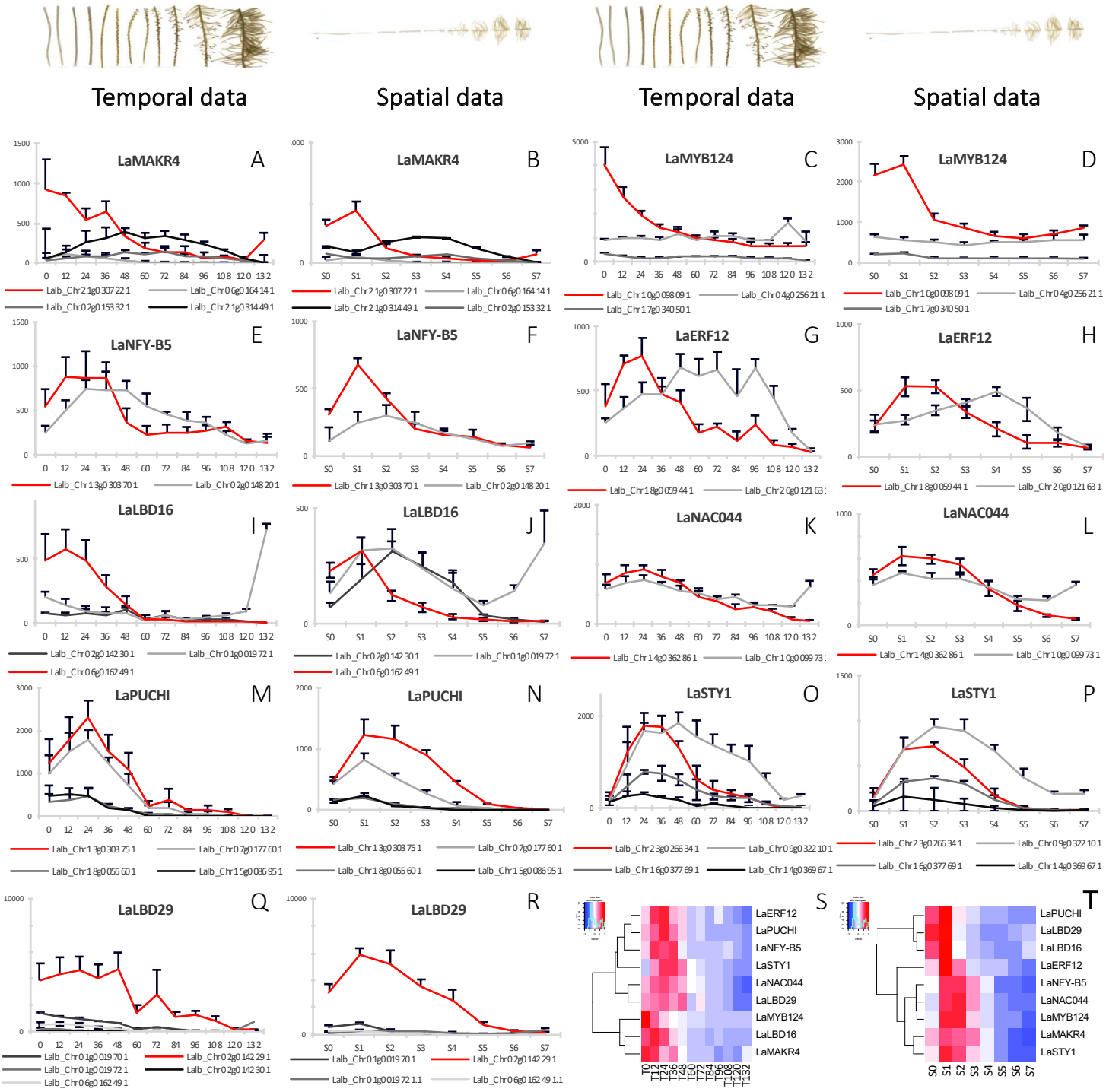

Fig. 5. Expression levels of lupin genes during rootlet development in RNA-seq datasets. (A-R) Data coming from temporal dataset are shown in graphs A to R in alternated columns. Y axis display gene expression in normalized count. X axis represent either hours after the beginning of sampling (temporal data) or a sample section number from 1 to 7 (spatial dataset). Genes for which coding sequences were cloned are colored in red. For temporal data, data are mean ± SD of eight CRs coming from 4 lupin plants (n=8). For spatial dataset, data are mean ± SD of ten CRs coming from 5 lupin plants (n=10). (S-T) Heatmap of the expression profile of 9 selected candidate genes in temporal (S) and spatial (T) datasets.

repression domain, also known as EAR motif (LDLDLELRLGFA), and placed under the Cauliflower Mosaic Virus 35S promoter. These converted TFs are expected to compete with the native TFs to bind and regulate the expression of their target gene. Thus, expressing the dominant repressor version of the TFs under a strong promoter ensure that the expression of their target gene is suppressed dominantly over the activity of the native transcription factors.

To investigate the role of *LaMAKR4* candidate, we produced white lupin hairy roots expressing a long hairpin (hp) RNA to reduce the expression of *LaMAKR4* by RNA interference (RNAi). A 523 bp-fragment (245 to 739 bp) of the *LaMAKR4* coding sequence (990 bp) was amplified and cloned into the Gateway RNAi vector pK7-GWIWG2 (II), a vector that has been shown to result in efficient RNAi silencing in lupin (Cheng *et al.*, 2011). Lupin roots were transformed with the MAKR4-RNAi construct. In parallel, roots transformed with a RNAi construct targeting the white lupin *RuBisCO* gene, which is not expressed in lupin roots, and a *p35S::GUS* vector were used as positive controls of the transformation.

Phenotypic analysis of transgenic lines

To see whether our candidate genes are functionally involved or not in rootlet development, we investigated the effect of each construct on rootlet formation. For this purpose, white lupin composite plants were produced and the phenotype of 24 plants for each construct and controls was analysed. After 12 days in hydroponics, the number of cluster roots formed was assessed as well as the weight of the shoots and roots. Among the 9 transgenic lines (Fig. 6 and 7), we showed that CR formation was strongly reduced in 3 transgenic lines expressing the *LaERF12*, *LaBD16*, and *LaSTY1* genes fused to the SRDX sequence (Fig. 6). This reduction could be observed on the transformed root system of these lines, which did not display the specific hairy root phenotype (Fig. 7). We also observed a reduction of CR number in *LaNFY*-B5 plants. However, in this case, the observed phenotype was not reproducible between biological replicates and we obtained fewer plants than for other construct (n=17). Phenotypic comparison showed that *p35S::LaERF12-SRDX*, *p35S::LaLBD16-SRDX* and *p35S::LaSTY1-SRDX* transgenic lines had a similar vigour than control plants transformed with *p35S::GUS* vector. Indeed, average shoot (Fig. 6B) and root dry weight (Fig. 6C) was not different between transgenic and control plants, resulting in a similar root to shoot ratio between lines.

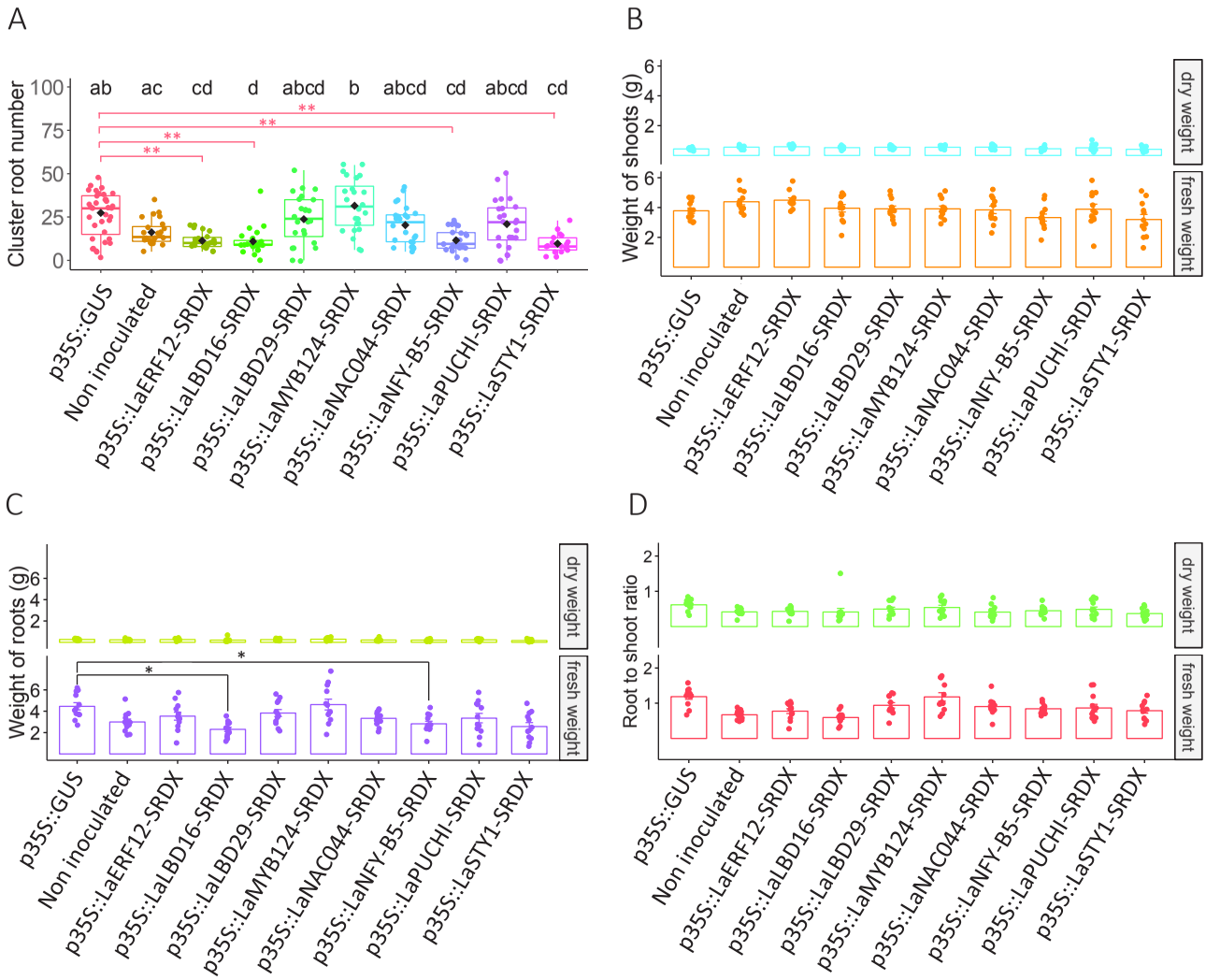

Fig. 6. Transgenic lines over expressing lupin TFs fused to the SRDX repressor domain. (A) Cluster root number in eight dominant repressor transgenic lines (n=24): *p35S::LaERF12-SRDX*, *p35S::LaLBD16-SRDX*, *p35S::LaLBD29-SRDX*, *p35S::LaMYB124-SRDX*, *p35S::LaNAC044-SRDX*, *p35S::LaNFY-B5-SRDX*, *p35S::LaPUCHI-SRDX*, *p35S::LaSTY1-SRDX*. 3 dominant repressor lines exhibit a reduction of the number of cluster roots on the whole root system compared to the control line *p35S::GUS*. (B-C) Fresh and dry weight of shoots (B) or roots (C) of the eight transgenic lines. (D) Ratio between the root weight and the shoot weight in the eight transgenic lines.

Fig. 7. Phenotype of white lupin composite plants compared to p35S::GUS control plants. The 3 dominant repressor lines *p35S::LaLBD16-SRDX, p35S::LaERF12-SRDX and p35S::LaSTY1-SRDX* display a strong reduction of the number of cluster roots formed. Images presented are representative of n=24 plants.

Discussion

Transcription factors involved in rootlet development

Cluster roots represent an important adaptation of the root system of plants coping with poor availability of Pi. Investigating the molecular mechanisms underlying this developmental process is important to understand how such organs are formed. Recently, several studies have used RNA-seq technology to study global changes in gene expression in white lupin cluster roots exposed to low Pi medium (Wang *et al.*, 2014; Secco *et al.*, 2014; O'Rourke *et al.*, 2013a). In our team, the recent sequencing of the white lupin genome and the generation of a developmental transcriptomic dataset provided useful resources to analyse cluster root development. In the present study, we investigated the early molecular mechanisms involved in the formation of rootlet. For this purpose, we focussed our analysis on transcriptomic changes occurring prior to and during rootlet initiation and organogenesis.

We performed differential expression analysis between genes expressed in early CR parts (T0 to T36) compared to lateral root, and identified a set of 287 up-regulated genes during early stages of rootlet development. This set of genes comprises transcription factors, which are known to be central regulators of lateral root formation in species with simpler root architecture like *Arabidopsis*. In young CR parts, the increased expression of the *LOB-DOMAIN BOUNDARIES 16* gene (*LBD16*), a gene playing a crucial role in promoting the first asymmetric division, and *PUCHI*, a gene involved in LR patterning and expressed in LR initiation sites after the first division (Goh *et al.*, 2012; Goh *et al.*, 2019), reflects the strong activation of rootlet initiation in cluster roots. The occurrence of these divisions implies the re-entry of xylem pole pericycle cells into the cell cycle (Himanen *et al.*, 2002), and the auxin-dependent activation of cell-cycle genes, such as the G1-to-S *CYCD5;1* and the G2-to-M *CYCB2;3* cyclins, which are strongly induced in cluster roots.

Several genes of the PLETHORA (PLT) family, which are also activated in response to auxin and regulate cell proliferation and differentiation in LR primordium were identified. More specifically, the up-regulation of genes orthologous to *AtPLT1*, *AtPLT2* and *AtPLT4*, which contribute to stem cell niche establishment and maintenance (Du and Scheres, 2017b), suggests that *de novo* formation of rootlet meristem has started in young CR parts (T0-T36). The expression of the *WUS-RELATED HOMEOBOX 5* (*WOX5*) and the *PHAVULOTA* (*PHV*) stem

cell niche functioning regulators further supports this hypothesis. In addition, the identification of several genes regulating cell division in the stem cell niche is in agreement with activation of the rootlet meristem. In the model plant *Arabidopsis*, the expression of the *CYCD6;1* is required for the periclinal division in the cortex-endodermis initial, giving rise to the cortex and endodermis tissues (Sozzani *et al.*, 2010). Similarly, the *FEZ* transcription factor and its regulator, *SOMBRERO* (*SMB*), regulate the cell division plane of the columella and root cap/epidermis initials (Willemsen *et al.*, 2008). Thus, differential expression of TFs in our transcriptomic data shows that rootlet initiate and establish a meristem in less than 36 hours (T0 to T36).

A tight regulation of auxin homeostasis and signalling

Because cluster roots form a dense packing of short lateral roots, it is expected that auxin acts as a central regulator of their development. A role for auxin has long been proposed by experiments using exogenously applied auxin, showing that this hormone was sufficient to induce CR in high-Pi conditions that normally repress their formation (Gilbert *et al.*, 2000). The regulation of auxin transport and auxin homeostasis is essential for the local accumulation of auxin that acts as a positional signal for *de novo* LR branching (Dubrovsky *et al.*, 2008). In *Arabidopsis*, auxin has been shown to be transported from shoots to roots to induce LR development (Bhalerao *et al.*, 2002). In contrast, in white lupin, auxin synthetized in roots is regarded as the major source of auxin inducing rootlet formation (Meng *et al.*, 2013). Consistent with these findings, the up-regulation of *YUCCA9*, a gene coding for an enzyme involved in tryptophan-dependant IAA biosynthesis, strongly supports the local synthesis of auxin in the rootlet cluster zone.

Beside its biosynthesis, the distribution of auxin in the CR root zone also depends on its transport and the regulation of its intracellular concentration. Unlike previous reports which showed high expression of *AUXIN TRANSPORTER 1* (*AUX1*) and *PIN-FORMED 1* (*PIN1*) during early steps of rootlet formation (Wang *et al.*, 2014), we did not found a strong up-regulation of these genes compared to LR. However, the high induction of the auxin efflux transporter *PIN7* in T12 to T36 CR parts, suggests a potent role for this gene in the canalization of auxin fluxes in forming CR roots. This auxin fluxes result in strong accumulation of auxin in rootlet founder cells and later at the tip of the rootlet primordium, as evidenced by the DR5 reporter (Gallardo

et al., 2018). The establishment of the auxin gradient requires dynamic repolarization of PIN polarity, which might be assisted by the induction of the WRKY23 transcription factor, which was recently shown to regulate PIN polarization in *Arabidopsis* primary root (Prát *et al.*, 2018).

As auxin gradients are crucial for organ patterning and morphogenesis, the concentration of auxin is also tightly regulated. To avoid toxic concentration, auxin levels are regulated both by auxin conjugation and compartmentation. We identified *WALLS ARE THIN1* (*WAT1*), a tonoplast-localized efflux transporter that exports auxin from the vacuole to the cytoplasm, as an actor of IAA compartmentation in CR parts. In addition, IAA *CARBOXYLMETHYLTRANSFERASE 1* (*IAMT1*), an enzyme inactivating IAA by converting it to its IAA-methyl ester form, and amido-synthetases of the GRETCHEN HAGEN 3 protein family, such as *GH3.1*, are probable regulator of auxin homeostasis in forming CR roots.

In response to auxin accumulation, many genes display rapid and specific responses. Amongst them, the genes belonging to three major families, AUX/IAA, SAUR, and GH3, have been the most thoroughly studied. These genes are known to be primary auxin responses genes and their expression is induced within minutes in response to an auxin treatment (Hagen and Guilfoyle, 2002). Here, the induction of a Small Auxin-Upregulated RNA (*SAUR51* and the auxin responsive gene *IAA30*, which are respectively expressed in LR primordia) (Van Mourik et al., 2017) or accumulate in the quiescent center cells (Sato and Yamamoto, 2008), showed that auxin signal is transduced to pattern the rootlet primordium. The auxin response in cluster root involved as well the expression of *MONOPTEROS/AUXIN RESPONSE FACTOR 5 (MP/ARF5)*. Up-regulation of *MP/ARF5*, that regulates LR initiation, suggests that rootlet initiation may be at least in part mediated by the signalling cascade controlling LR development. Altogether, these results indicate that auxin homeostasis and signalling have a key role in the developmental processes associated to rootlet formation.

Functional screen identifies 3 putative candidates

In white lupin, the simultaneous expression of hundreds of genes coordinates the sequential development of numerous rootlets. This massive initiation of organs is a complex process that integrates the perception of Pi limitation and the subsequent activation of gene controlling developmental processes (Secco *et al.*, 2014; Wang *et al.*, 2014). In order to identify genes regulating these processes, we have selected two sets of candidates, which are

specifically induced prior to and during LR initiation. Amongst them, we have found several transcription factors known to be involved in LR formation or having a yet unknown function. These genes belong to the transcription factor families that are differentially expressed over the course of rootlet formation: the AP2/EREB family (*PUCHI*, *ERF12*), the MYB family (*MYB124*), the SRS family (*STY1*), the AS2/LOB family (*LBD16, LBD129*), the NAC family (*NAC044*) and the NFY family (*NFY-B5*).

In order to test the involvement of these transcription factors during rootlet formation, we have generated 9 independent lupin transgenic lines expressing the coding sequence of these genes fused to the SRDX sequence. The SRDX sequence is a repressor domain, which has been effectively used to convert transcription factors into dominant repressors, which could suppressed the expression of specific target genes, even in the presence of redundant transcriptions factors (Hiratsu *et al.*, 2003). It has been recently shown that white lupin has experienced a massive triplication event, resulting in the presence of large gene families in its genome (Hufnagel *et al.*, 2019). This feature was observed for several of our candidate genes (Fig. 5) and the generation of chimeric repressor of transcription factors was used to bypass the possible functional redundancy of lupin transcription factors. To check whether our chimeric constructs have an effect on rootlet formation, we have used the white lupin hairy root system as a quick way to generate transgenic plants. Interestingly, three transgenic lines over-expressing the p35S::LaLBD16-SRDX, p35S::LaSTY1-SRDX and p35S::LaERF12-SRDX transgenes, display significant reduction of the total number of CR formed in their hairy root system. Therefore, we propose a role for these genes in rootlet development.

Our transcriptomic analyses suggest a central role for auxin during rootlet development. Interestingly, out of three candidate genes that display a function associated to developmental processes, two are orthologous with *Arabidopsis* genes related to the control of auxin homeostasis or are part of an auxin-dependent signalling pathway. *AtLBD16* was showed to be required for the first asymmetric division initiating LR development (Goh *et al.*, 2012), while *AtSTY1* was proposed to act upstream of local *maxima* establishment via the regulation of auxin biosynthesis rate (Eklund *et al.*, 2010). The pivotal role of *AtLBD16* in LR formation is established and the AtLBD16-SRDX expression driven by the 35S promoter was previously shown to inhibit LR formation (Goh *et al.*, 2012). Thus, it is very likely that the white lupin *LaLBD16* gene has a conserved function during rootlet initiation. However, the expression of the LBD29-SRDX chimeric repressor had no effect on rootlet formation. Because this gene regulates LR initiation

as well, it suggests that the different white lupin LBD fused with the SRDX cannot inactivate the redundant function of all LBDs and pinpoint the existence of specificities amongst the gene family.

The *STY1* gene also belongs to a TF family (SHI/STY), with overlapping functions. In *Arabidopsis*, out of the 10 genes of the SHI family, several SHI/STY-related genes contribute to the apical-basal patterning required for the development of organs such as the gynoecium, the stamen, the leaves and flowers (Kuusk *et al.*, 2002; Ståldal *et al.*, 2012; Baylis *et al.*, 2013). The regulatory function of the SHI/STY genes is related to the auxin biosynthesic pathway. Among these genes, the function of *AtSTY1* has been the most thoroughly characterized. *AtSTY1* was shown to modulate the expression of genes regulating auxin biosynthesis (Eklund *et al.*, 2010), as well as genes coding for enzymes controlling the remodelling of plant cell walls (Ståldal *et al.*, 2012). Interestingly, because the expression of the AtSTY1-SRDX construct in *Arabidopsis* prevented the formation of a functional shoot apical meristem, it is possible that *AtSTY1* regulates formation or maintenance of meristem (Eklund *et al.*, 2010). Therefore, *AtSTY1* can be regarded as a regulator of organ formation process, such as rootlet development. In this regard, it will be interesting to see whether rootlet primordium development is arrested in LaSTY1-SRDX plants.

In contrast to *AtLBD16* and *AtSTY1*, the biological function of *AtERF12* has not been reported. *AtERF12* belongs to the subfamily VIII (or B1) of the ethylene response factor family (ERF) that includes several genes participating to developmental processes. Amongst them, *DORNROSCHEN* (*DRN*) (Banno *et al.*, 2001) and *FRIZZY PANICLE* (*FZP*) (Komatsu *et al.*, 2003) were respectively shown to participate in the regulation of organ and floral meristem identities. Interestingly, ethylene biosynthesis and signalling participate in the regulation of rootlet development, as exogenous application of ethylene precursor or ethylene synthesis inhibitor alter CR formation (Wang *et al.*, 2014). The positive regulation of *AtERF12* by *AtEIN3*, a TF with a crucial role in ethylene signal transduction, indicates that *AtERF12* may act downstream of *AtEIN3* (Quan *et al.*, 2017). Whether *LaERF12* acts downstream of ethylene and participates in the ethylene mediated response regulating rootlet formation is an open question. Even though *AtERF12* function is still elusive, the expression of *Medicago truncatula* orthologous *MtERF12*, in the stele and inner cortical layers of the root, as well as nodule during its development (Larrainzar *et al.*, 2015), strongly suggests that *ERF12* is in certain species, an actor of developmental processes such as nodule organogenesis. Our results provide valuable insights into the early molecular mechanisms controlling CR formation

and a key resource to unravel the developmental program used by white lupin to form these organs.

Materials and methods

Plant materials and growth conditions

Seeds of white lupin (*Lupinus albus L. cv. Amiga* from Florimond Desprez, France) calibrated at 7 mm were used in all experiments. White lupin plants were cultivated in growth chambers under controlled conditions (16 h light / 8 h dark, 25°C day / 20°C night, 65% relative humidity, and PAR intensity 200 µmol.m^{-2}.s^{-1}). The hydroponic solution was modified from (Abdolzadeh *et al.*, 2010) without phosphate, and was composed of: $MgSO_4$, 54 µM; $Ca(NO_3)_2$ 400 µM; K_2SO_4 200 µM; Na-Fe-EDTA 10 µM; H_3BO_3 2.4 µM; $MnSO_4$ 0.24 µM; $ZnSO_4$ 0.1 µM; $CuSO_4$ 0.018 µM; Na_2MoO_4 0.03 µM. White lupin plants were grown either in 1.6 L pots or 200 L tank in hydroponic media continuously aerated. For plants in pots, the nutrient solution was renewed every seven days.

Transcriptome sequencing

The transcriptome sequencing project was carried out in the team and led by Bárbara Hufnagel. In order to generate a temporal transcriptome of white lupin cluster root development, a total of eight CRs were sampled on four independently grown plants, after 4 days of culture in hydroponics. One centimeter of CR was sampled at a distance of 1 cm from the primary root on the top part of the root system, on the second lateral root, every 12 h for 5 days. As a control, 1-cm of lateral roots 1-cm away from the primary root was sampled. For each experiment, four biological replication were produced. Total RNA was extracted from all frozen samples using the Direct-zol RNA MiniPrep kit (Zymo Research, Irvine, CA) according to the manufacturer's recommendations. The samples were sequenced using illumina Novaseq instrument. A spatial transcriptome dataset was also generated (see methods in Hufnagel *et al.* 2019).

Molecular cloning to generate gene fusion with SRDX

All construct were made using Gateway cloning technology (Invitrogen) according to manufacturer's instructions. The coding sequence of the 9 genes was amplified with a high fidelity polymerase (Phusion, ThermoFisher) on a pool of root cDNA by PCR using specific primers summarized in table. S15. The final size of the PCR amplified cds is sum up in table S16. The resultant coding sequence were amplified by PCR to add Gateway attB sites and SRDX sequences, and recombined into the pDONR221 Gateway entry vector (Invitrogen). These sequences were then recombined in a tripartite Gateway reaction with pENTR-35S-L4 (Invitrogen) containing the cauliflower mosaic virus 35S promoter (CAMV35S) into the pK7m24GW, containing a 35S terminator, to create the plasmid pK7m24GW-35S-cds-SRDX. All constructs were checked by DNA sequencing (Eurofins) with primers listed in table S17. p35S::GUS (with intron) was kindly provided by Isabelle Chérel (INRA, Laboratory of Biochemistry and Plant Molecular Physiology, Montpellier).

Molecular cloning for RNAi

A 523 pb fragment of the coding region of the *Lalb_Chr21g0307221* (LaMAKR4) was amplified using the primers LaMAKRint-F and LaMAKR4int-R and a 628 bp fragment of *Lalb_Chr25g0281541* fragment was amplified with primers LaRBC-F and LaRBC-R (table. S18). attBs flanking sites were then added by PCR with primers on LaMAKR4 fragment with LaMAKR-attB1-F and LaMAKR4-attB2 or with LaRBC-attB1-F and LaRBC-attB2-R to LaRBC fragments (Table. S14). The PCR products flanked with attBs sites were cloned into the pDONR221 Gateway entry vector (Invitrogen). This fragment was then introduced in the pK7GWIWG2(II) vector by LR recombination (Invitrogen) under the control of the constitutive promoter 35S. The sequence of the constructs was verified by sequencing (table S17).

Bacterial strain

All binary vectors were introduced into *Agrobacterium rhizogenes* by electroporation and into *Agrobacterium tumefaciens* by thermal chock. Transformation of bacteria with plasmids was confirmed by PCR with the primers used for the sequencing of binary plasmids. A bacterial lawn of *Agrobacterium rhizogenes* was used to transform white lupin roots by hairy root

transformation. To produce a bacterial lawn, LB agar plates containing 2% sucrose, 100 µM acetosyringone and appropriate antibiotics were inoculated with 200 µL of liquid bacteria culture, and then incubated at 28°C for 24 hours.

Hairy root transformation of white lupin

White lupin seedlings were transformed with a protocol that was adapted from a protocol previously published (Uhde-Stone *et al.*, 2005). White lupin seeds calibre 8 mm were surface sterilised by 4 washes in osmosis water, 30 min sterilization in bleach (Halonet 20%) and washed 6 times in sterile water under sterile conditions. Seeds were germinated on half Murashige and Skoog medium containing 1 % sucrose (pH was adjusted to 5.7). After germination, radicles of 1 cm were cut over 0.5 cm with a sterile scalpel. The radicles were inoculated with the *Agrobacterium rhizogenes* lawn. Fifteen inoculated seedlings were placed on square agar plates (0.7 % agar in 1X Hoagland solution) containing 15 µg.mL^{-1} Kanamycin. Composition of Hoagland medium without phosphate was the following one: $MgSO_4$, 200 µM ; $Ca(NO_3)_2$ 400 µM ; KNO_3 325 µM ; NH_4Cl 100 µM ; Na-Fe- EDTA 10 µM ; H_3BO_3 9,3 µM ; $MnCl_2$ 1,8 µM ; $ZnSO_4$ 0,17 µM ; $CuSO_4$ 0,06 µM ; Na_2MoO_4 2,3 µM. Plates were placed vertically in controlled conditions: 16h light / 8h dark, 25°C day / 20°C night, 65 % relative humidity, and PAR intensity 200 µmolm^{-2} s^{-1}. After 7 days on plates, 60 seedlings were transferred to 12x16,5x5,5 cm trays (20 seedlings per tray) and watered with 500 mL osmosis water. After 12 days, plants with hairy roots were transferred to hydroponics in 1.6 L pots containing nutrient solution. Nutrient medium was renewed each week. After 7 days in hydroponic conditions, CRs were sampled on *hairy root* plants.

Histology and microscopy

After 4 days in hydroponics, cluster roots were sampled using the method used for the generation of the temporal transcriptomic dataset. A total of 8 roots samples were collected on four individual plants every 12 hours for 36 hours. Root tissues were fixed under vacuum for 2 hours (4% formaldehyde in PBS1X) and cleared with Clearsee solution (Xylitol 10 %, Sodium deoxycholate 15 %, Urea 25 %) for 48 hours. During this 48 hours, Clearsee solution was renewed two times. For root staining with calcofluor, roots were bathed into calcofluor-cleersee solution (0,001 % calcofluor) for 1h30 under vacuum and rinsed for 5 min two times

in Clearsee to eliminate calcofluor excess. To produce thick section of 80 µm, cluster roots were embedded in agarose 4% (m/v) and cut with a vibratome (Microcut H1200, Biorad). Cluster root images were taken with confocal microscope Leica SP8 coupled with LASX software. Calcofluor was excited at 405 nm using an argon laser and emission was collected between 440 and 460 nm.

Phylogenetic tree

Phylogenetic trees comparing protein sequences of white lupin and *Arabidopsis* of LBD class Ia subtype C family, SRS family, and ERF family subfamily VIII/B1 were constructed with the pipeline proposed by NGPhylogeny.fr (https://ngphylogeny.fr/workspace/history/70cd372fcce217d8). Sequences were aligned with MAFFT (v.7407_1) (Katoh and Standley, 2013)and cleaned with BMGE (v1.12_1) (Criscuolo and Gribaldo, 2010) when needed. The phylogenetic tree was generated using the maximum likelihood method implemented in FastME and inferred from 1000 replicates (v.2.6.6.1_1) (Lefort *et al.*, 2015). The LG substitution model was used assuming an estimated equilibrium frequencies and a low rate heterogeneity across sites (gamma distribution of 1.0). Tree visualization was realized with the iTOL platform (v4.2.3 platform) (https://itol.embl.de/upload.cgi).

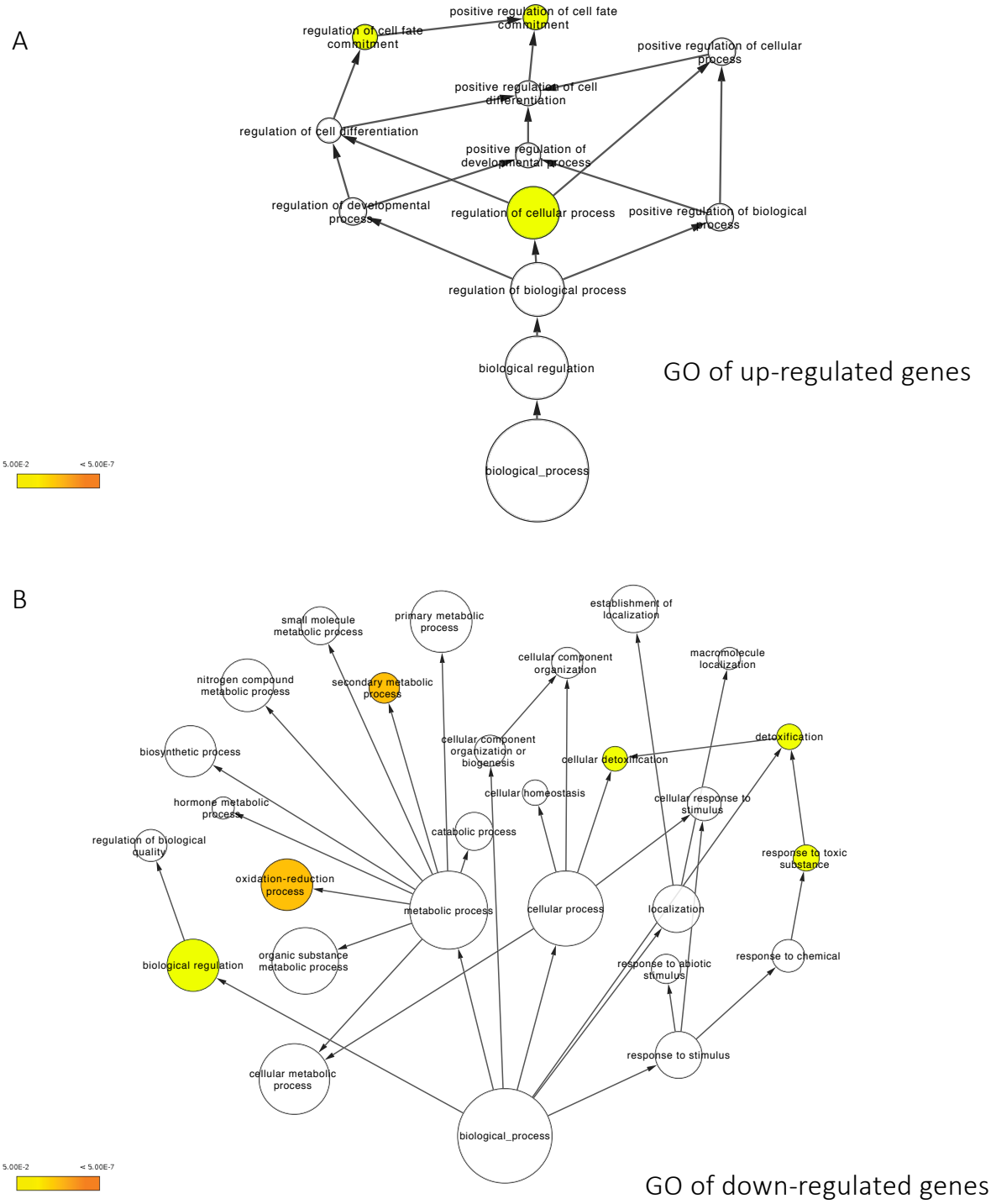

Fig. S1. Networks of GO term enrichment for the genes up-regulated in T0, T12, T24 and T36 CR parts compared to LR. (A) Network of the GOs of the up-regulated genes in Fig. 2A (B) Network of the GOs of the down-regulated genes in Fig. 2B.

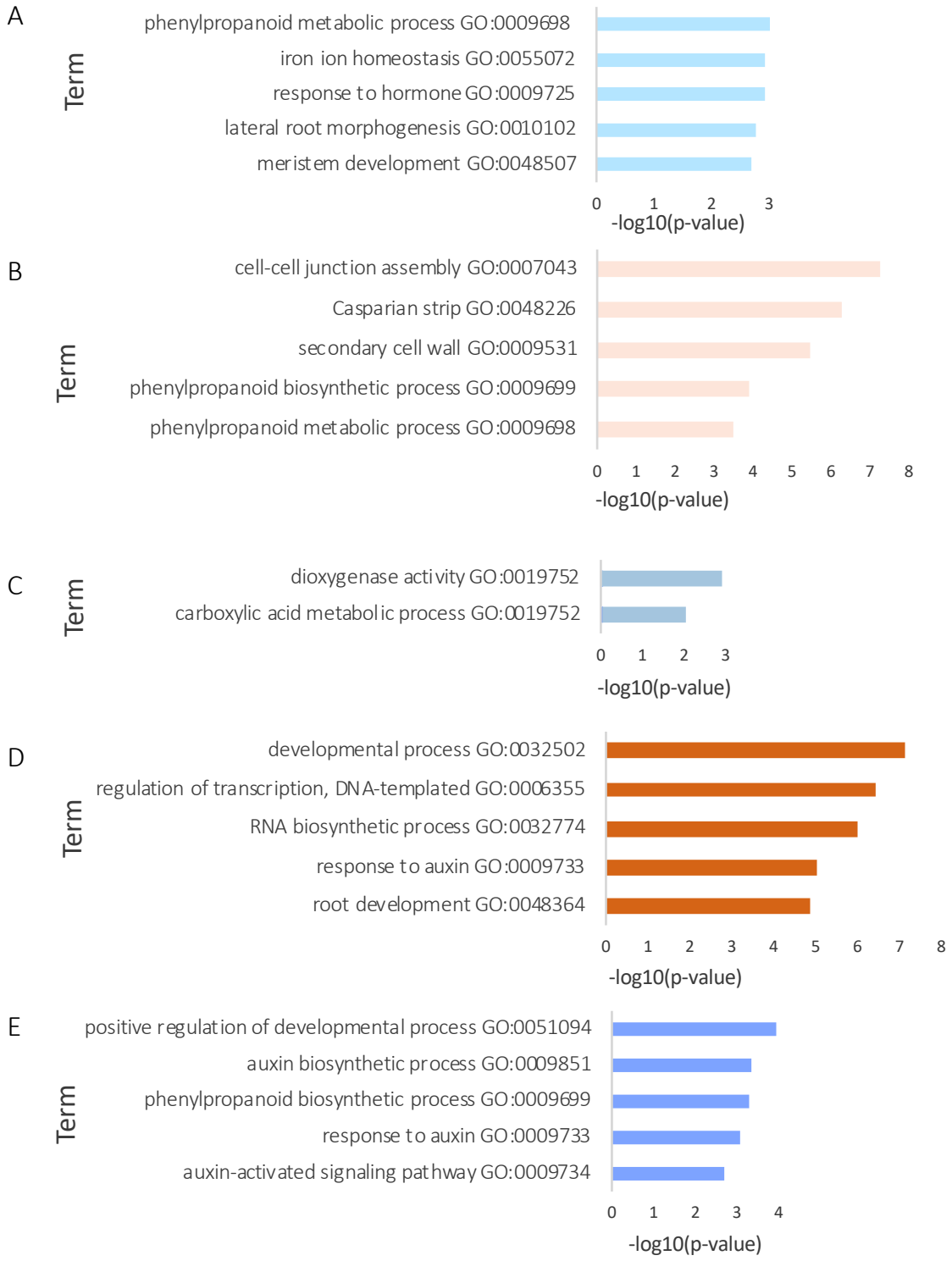

Fig. S2. Enriched GO terms associated to the genes up-regulated during CR development shown in Fig.3. Graphs showing significantly enriched GO terms (y-axis) and their p-values for the genes clusters shown in Fig. 3: cluster 1 (A), cluster 2 (B), cluster 3 (C), cluster 4 (D), cluster 5 (E).

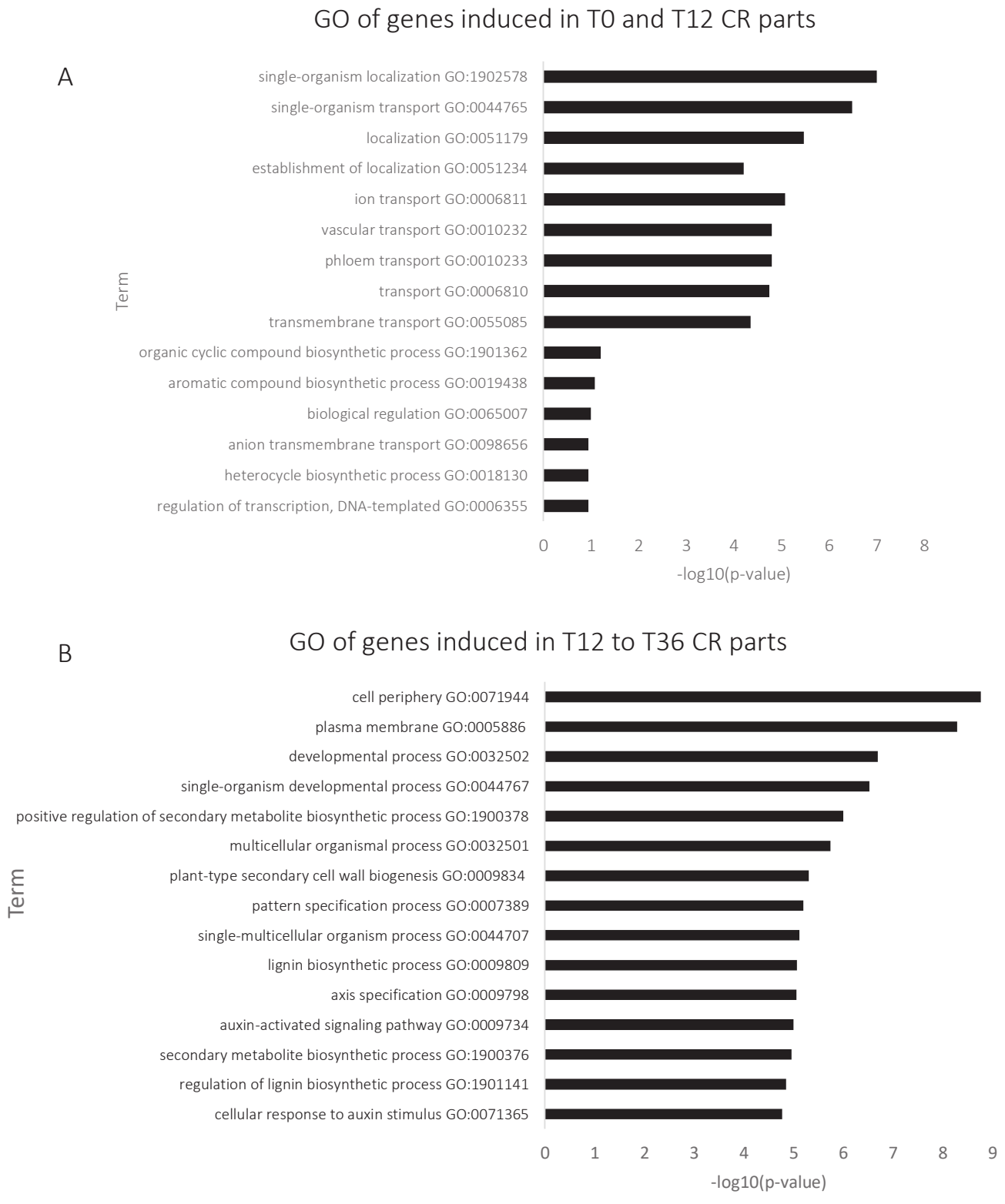

Fig. S3. Top 15 enriched GO terms for the genes highly induced during early steps of cluster root formation shown in Fig. 4. Graphs showing the top significantly enriched GO terms (y-axis) and their p-values, associated to the genes induced in (A) T0 and T12 CR parts and (B) T12 to T36 CR parts.

GO.ID	Term	Annotated	Count	Expected	p-value	q-value	Genes
GO:0010035	response to inorganic substance	899	6	0.93	0.00027	4.782e-01	AT2G46680, AT3G12900, AT3G13610, AT3G29320, AT5G13420, AT5G59310
GO:0009699	phenylpropanoid biosynthetic process	145	3	0.15	0.00045	4.782e-01	AT3G13610, AT5G13420, AT5G54160
GO:0009698	phenylpropanoid metabolic process	185	3	0.19	0.00091	4.782e-01	AT3G13610, AT5G13420, AT5G54160
GO:0044699	single-organism process	11098	20	11.52	0.00094	4.782e-01	AT1G01580, AT1G08440, AT1G19530, AT1G80660, AT2G32830, AT2G39050, AT2G42430, AT2G46225, AT2G46680, AT3G11260, AT3G12830, AT3G12900, AT3G13610, AT3G29320, AT3G49180, AT3G56970, AT5G13420, AT5G18560, AT5G54160, AT5G59310
GO:0055072	iron ion homeostasis	48	2	0.05	0.00114	4.782e-01	AT1G01580, AT3G56970
GO:0009725	response to hormone	1655	7	1.72	0.00119	4.782e-01	AT2G46680, AT3G11260, AT3G12830, AT3G12900, AT3G29320, AT5G18560, AT5G59310
GO:0070887	cellular response to chemical stimulus	1197	6	1.24	0.00121	4.782e-01	AT2G46680, AT3G12830, AT3G12900, AT3G13610, AT3G29320, AT5G18560
GO:0034614	cellular response to reactive oxygen species	52	2	0.05	0.00133	4.782e-01	AT3G12900, AT3G13610
GO:0042221	response to chemical	2847	9	2.95	0.00165	4.782e-01	AT2G46680, AT3G11260, AT3G12830, AT3G12900, AT3G13610, AT3G29320, AT5G13420, AT5G18560, AT5G59310
GO:0010102	lateral root morphogenesis	58	2	0.06	0.00165	4.782e-01	AT2G42430, AT5G18560
GO:0010101	post-embryonic root morphogenesis	59	2	0.06	0.00171	4.782e-01	AT2G42430, AT5G18560
GO:0009719	response to endogenous stimulus	1767	7	1.83	0.00175	4.782e-01	AT2G46680, AT3G11260, AT3G12830, AT3G12900, AT3G29320, AT5G18560, AT5G59310
GO:0010015	root morphogenesis	238	3	0.25	0.00188	4.782e-01	AT2G42430, AT3G11260, AT5G18560
GO:0032870	cellular response to hormone stimulus	880	5	0.91	0.0019	4.782e-01	AT2G46680, AT3G12830, AT3G12900, AT3G29320, AT5G18560
GO:0050896	response to stimulus	6373	14	6.61	0.00198	4.782e-01	AT1G01580, AT2G16660, AT2G39050, AT2G46680, AT3G11260, AT3G12830, AT3G12900, AT3G13610, AT3G29320, AT3G56970, AT5G13420, AT5G18560, AT5G59310, AT5G63810
GO:0048507	meristem development	243	3	0.25	0.00199	4.782e-01	AT3G11260, AT3G49180, AT5G18560
GO:0071495	cellular response to endogenous stimulus	899	5	0.93	0.00209	4.782e-01	AT2G46680, AT3G12830, AT3G12900, AT3G29320, AT5G18560
GO:0009809	lignin biosynthetic process	75	2	0.08	0.00275	6.050e-01	AT5G13420, AT5G54160
GO:0055080	cation homeostasis	276	3	0.29	0.00286	6.059e-01	AT1G01580, AT1G80660, AT3G56970
GO:0009888	tissue development	603	4	0.63	0.00328	6.232e-01	AT2G46225, AT3G11260, AT3G49180, AT5G18560
GO:0098771	inorganic ion homeostasis	294	3	0.31	0.00342	6.232e-01	AT1G01580, AT1G80660, AT3G56970
GO:1901701	cellular response to oxygen-containing compound	617	4	0.64	0.00356	6.232e-01	AT2G46680, AT3G12900, AT3G13610, AT3G29320
GO:0071310	cellular response to organic substance	1028	5	1.07	0.00373	6.232e-01	AT2G46680, AT3G12830, AT3G12900, AT3G29320, AT5G18560
GO:0010033	response to organic substance	2026	7	2.1	0.0038	6.232e-01	AT2G46680, AT3G11260, AT3G12830, AT3G12900, AT3G29320, AT5G18560, AT5G59310
GO:0050801	ion homeostasis	318	3	0.33	0.00426	6.248e-01	AT1G01580, AT1G80660, AT3G56970
GO:0009808	lignin metabolic process	96	2	0.1	0.00445	6.363e-01	AT5G13420, AT5G54160
GO:0009414	response to water deprivation	333	3	0.35	0.00484	6.734e-01	AT2G46680, AT3G29320, AT5G59310
GO:0009415	response to water	339	3	0.35	0.00509	6.734e-01	AT2G46680, AT3G29320, AT5G59310
GO:0044550	secondary metabolite biosynthetic process	347	3	0.36	0.00543	6.839e-01	AT3G13610, AT5G13420, AT5G54160
GO:0048527	lateral root development	107	2	0.11	0.0055	6.839e-01	AT2G42430, AT5G18560

Table S3. TOP 30 GO enriched terms of the 36 genes up-regulated in cluster 1 of Fig .3

GO.ID	Term	Annotated	Count	Expected	p-value	q-value	Genes
GO:0007043	cell-cell junction assembly	5	3	0.01	5.2e-08	2.860e-04	AT2G27370, AT2G36100, AT5G15290
GO:0042349	guiding stereospecific synthesis activity	26	4	0.04	9.9e-08	2.905e-04	AT1G07730, AT2G39430, AT3G24020, AT4G13580
GO:0034329	cell junction assembly	6	3	0.01	1,00E-07	2.860e-04	AT2G27370, AT2G36100, AT5G15290
GO:0034330	cell junction organization	9	3	0.02	4.3e-07	6.149e-04	AT2G27370, AT2G36100, AT5G15290
GO:0048226	Casparian strip	8	3	0.02	5.1e-07	4.915e-04	AT2G27370, AT2G36100, AT5G15290
GO:0044426	cell wall part	10	3	0.02	1.1e-06	4.915e-04	AT2G27370, AT2G36100, AT5G15290
GO:0044462	external encapsulating structure part	11	3	0.02	1.5e-06	4.915e-04	AT2G27370, AT2G36100, AT5G15290
GO:0009531	secondary cell wall	14	3	0.03	3.3e-06	8.110e-04	AT2G27370, AT2G36100, AT5G15290
GO:0045216	cell-cell junction organization	9	3	0.02	4.3e-07	6.149e-04	AT2G27370, AT2G36100, AT5G15290
GO:0044763	single-organism cellular process	8410	28	14.87	6.4e-05	7.322e-02	AT1G05100, AT1G07730, AT1G14520, AT1G17170, AT1G21460, AT1G22360, AT1G49620, AT1G55020, AT1G69850, AT2G19770, AT2G26640, AT2G27370, AT2G36100, AT2G38530, AT2G39430, AT2G43330, AT3G03910, AT3G12120, AT3G24020, AT3G30340, AT3G56970, AT4G11150, AT4G13580, AT4G21440, AT4G27450, AT5G15290, AT5G38710, AT5G42180
GO:0009699	phenylpropanoid biosynthetic process	145	4	0.26	0.00013	1.239e-01	AT1G07730, AT2G39430, AT3G24020, AT4G13580
GO:0044699	single-organism process	11098	32	19.62	2,00E-04	1.634e-01	AT1G05100, AT1G07730, AT1G13245, AT1G14520, AT1G17170, AT1G21460, AT1G22360, AT1G26320, AT1G49620, AT1G55020, AT1G69850, AT2G19770, AT2G26640, AT2G27370, AT2G36100, AT2G38180, AT2G38530, AT2G39430, AT2G43330, AT2G44060, AT3G03910, AT3G12120, AT3G24020, AT3G30340, AT3G56970, AT4G11150, AT4G13580, AT4G21440, AT4G27450, AT5G15290, AT5G38710, AT5G42180
GO:0050790	regulation of catalytic activity	517	6	0.91	0.00029	2.034e-01	AT1G07730, AT1G17860, AT1G49620, AT2G39430, AT3G24020, AT4G13580
GO:0009698	phenylpropanoid metabolic process	185	4	0.33	0.00032	2.034e-01	AT1G07730, AT2G39430, AT3G24020, AT4G13580
GO:0065009	regulation of molecular function	553	6	0.98	0.00041	2.193e-01	AT1G07730, AT1G17860, AT1G49620, AT2G39430, AT3G24020, AT4G13580
GO:0043436	oxoacid metabolic process	1326	9	2.34	0.00045	2.193e-01	AT1G14520, AT1G22360, AT1G55020, AT1G69850, AT2G26640, AT3G03910, AT3G12120, AT4G27450, AT5G38710
GO:0006082	organic acid metabolic process	1330	9	2.35	0.00046	2.193e-01	AT1G14520, AT1G22360, AT1G55020, AT1G69850, AT2G26640, AT3G03910, AT3G12120, AT4G27450, AT5G38710
GO:0044710	single-organism metabolic process	5206	19	9.2	0.00078	3.432e-01	AT1G05100, AT1G07730, AT1G14520, AT1G17170, AT1G22360, AT1G26320, AT1G55020, AT1G69850, AT2G26640, AT2G38180, AT2G39430, AT3G03910, AT3G12120, AT3G24020, AT4G11150, AT4G13580, AT4G27450, AT5G38710, AT5G42180
GO:0019752	carboxylic acid metabolic process	1209	8	2.14	0.00115	4.699e-01	AT1G14520, AT1G22360, AT1G55020, AT2G26640, AT3G03910, AT3G12120, AT4G27450, AT5G38710
GO:0044281	small molecule metabolic process	1964	10	3.47	0.00193	5.939e-01	AT1G14520, AT1G22360, AT1G55020, AT1G69850, AT2G26640, AT3G03910, AT3G12120, AT4G11150, AT4G27450, AT5G38710
GO:0019748	secondary metabolic process	511	5	0.9	0.00202	5.939e-01	AT1G07730, AT1G17170, AT2G39430, AT3G24020, AT4G13580
GO:0044711	single-organism biosynthetic process	1986	10	3.51	0.0021	5.939e-01	AT1G07730, AT1G14520, AT1G55020, AT2G26640, AT2G39430, AT3G12120, AT3G24020, AT4G11150, AT4G13580, AT5G38710
GO:0042545	cell wall modification	157	3	0.28	0.00271	5.939e-01	AT2G27370, AT2G36100, AT5G15290
GO:0016053	organic acid biosynthetic process	567	5	1	0.00317	5.939e-01	AT1G14520, AT1G55020, AT2G26640, AT3G12120, AT5G38710
GO:0046394	carboxylic acid biosynthetic process	567	5	1	0.00317	5.939e-01	AT1G14520, AT1G55020, AT2G26640, AT3G12120, AT5G38710
GO:0044550	secondary metabolite biosynthetic process	347	4	0.61	0.00326	5.939e-01	AT1G07730, AT2G39430, AT3G24020, AT4G13580
GO:0015850	organic hydroxy compound transport	49	2	0.09	0.00341	5.939e-01	AT1G69850, AT2G43330
GO:0006633	fatty acid biosynthetic process	177	3	0.31	0.00379	6.194e-01	AT1G55020, AT2G26640, AT3G12120
GO:0009628	response to abiotic stimulus	1987	9	3.51	0.00723	9.516e-01	AT2G16660, AT2G26640, AT2G38530, AT2G44060, AT3G04720, AT4G11150, AT4G21440, AT5G12020, AT5G38710
GO:0006950	response to stress	3567	13	6.31	0.00732	9.516e-01	AT1G26320, AT1G55020, AT1G80130, AT2G26640, AT2G38530, AT2G44060, AT3G04720, AT3G56970, AT4G11150, AT4G21440, AT5G12020, AT5G38710, AT5G42180

Table S4. Top 30 GO enriched terms of the 62 genes up-regulated in cluster 2 of Fig .3

GO.ID	Term	Annotated	Count	Expected	p-value	q-value	Genes
GO:0019752	carboxylic acid metabolic process	1209	3	0.46	0.00939	1,00E+00	AT1G22340, AT1G30040, AT3G45140
GO:0051213	dioxygenase activity	163	2	0.06	0.0013	1,00E+00	AT1G30040, AT3G45140

Table S5. GO enriched terms of the 13 genes up-regulated in cluster 3 of Fig .3

GO.ID	Term	Annotated	Count	Expected	p-value	q-value	Genes
GO:0032502	developmental process	3324	25	8.05	7.5e-08	2.669e-04	AT1G02800, AT1G19850, AT1G26870, AT1G30950, AT1G34110, AT1G75520, AT1G79580, AT2G28250, AT2G30130, AT2G30370, AT2G46870, AT3G11260, AT3G20840, AT3G28857, AT3G58850, AT3G60650, AT4G18390, AT4G23750, AT5G13910, AT5G17430, AT5G35770, AT5G55250, AT5G60910, AT5G65640, AT5G66350
GO:0065007	biological regulation	6714	36	16.26	1.3e-07	2.669e-04	AT1G02810, AT1G04180, AT1G15460, AT1G19250, AT1G19850, AT1G26870, AT1G30950, AT1G34110, AT1G68780, AT1G75520, AT1G79580, AT2G30370, AT2G46870, AT2G47260, AT3G11260, AT3G19500, AT3G20840, AT3G28857, AT3G58850, AT4G03270, AT4G18290, AT4G18390, AT4G23750, AT4G31800, AT4G33800, AT4G37630, AT5G04820, AT5G13910, AT5G17430, AT5G27690, AT5G35770, AT5G55250, AT5G56220, AT5G60910, AT5G65640, AT5G66350
GO:0051094	positive regulation of developmental process	98	6	0.24	1.4e-07	2.669e-04	AT1G79580, AT3G11260, AT4G18390, AT5G13910, AT5G35770, AT5G60910
GO:0007275	multicellular organismal development	2794	22	6.77	2.9e-07	3.003e-04	AT1G02800, AT1G19850, AT1G26870, AT1G30950, AT1G34110, AT1G75520, AT1G79580, AT2G30130, AT2G30370, AT2G46870, AT3G11260, AT3G20840, AT3G60650, AT4G18390, AT4G23750, AT5G13910, AT5G17430, AT5G35770, AT5G55250, AT5G60910, AT5G65640, AT5G66350
GO:0006355	regulation of transcription, DNA-templated	2599	21	6.29	3.9e-07	3.003e-04	AT1G19850, AT1G26870, AT1G30950, AT1G79580, AT2G46870, AT2G47260, AT3G11260, AT3G19500, AT3G20840, AT3G28857, AT3G58850, AT4G18390, AT4G23750, AT4G31800, AT5G04820, AT5G13910, AT5G17430, AT5G35770, AT5G60910, AT5G65640, AT5G66350
GO:0044707	single-multicellular organism process	2847	22	6.89	4,00E-07	3.003e-04	AT1G02800, AT1G19850, AT1G26870, AT1G30950, AT1G34110, AT1G75520, AT1G79580, AT2G30130, AT2G30370, AT2G46870, AT3G11260, AT3G20840, AT3G60650, AT4G18390, AT4G23750, AT5G13910, AT5G17430, AT5G35770, AT5G55250, AT5G60910, AT5G65640, AT5G66350
GO:1903506	regulation of nucleic acid-templated transcription	2611	21	6.32	4.2e-07	3.003e-04	AT1G19850, AT1G26870, AT1G30950, AT1G79580, AT2G46870, AT2G47260, AT3G11260, AT3G19500, AT3G20840, AT3G28857, AT3G58850, AT4G18390, AT4G23750, AT4G31800, AT5G04820, AT5G13910, AT5G17430, AT5G35770, AT5G60910, AT5G65640, AT5G66350
GO:2001141	regulation of RNA biosynthetic process	2611	21	6.32	4.2e-07	3.003e-04	AT1G19850, AT1G26870, AT1G30950, AT1G79580, AT2G46870, AT2G47260, AT3G11260, AT3G19500, AT3G20840, AT3G28857, AT3G58850, AT4G18390, AT4G23750, AT4G31800, AT5G04820, AT5G13910, AT5G17430, AT5G35770, AT5G60910, AT5G65640, AT5G66350
GO:0051252	regulation of RNA metabolic process	2650	21	6.42	5.4e-07	3.432e-04	AT1G19850, AT1G26870, AT1G30950, AT1G79580, AT2G46870, AT2G47260, AT3G11260, AT3G19500, AT3G20840, AT3G28857, AT3G58850, AT4G18390, AT4G23750, AT4G31800, AT5G04820, AT5G13910, AT5G17430, AT5G35770, AT5G60910, AT5G65640, AT5G66350
GO:0019219	regulation of nucleobase-containing compound metabolic process	2706	21	6.55	7.7e-07	3.813e-04	AT1G19850, AT1G26870, AT1G30950, AT1G79580, AT2G46870, AT2G47260, AT3G11260, AT3G19500, AT3G20840, AT3G28857, AT3G58850, AT4G18390, AT4G23750, AT4G31800, AT5G04820, AT5G13910, AT5G17430, AT5G35770, AT5G60910, AT5G65640, AT5G66350
GO:0006351	transcription, DNA-templated	2722	21	6.59	8.4e-07	3.813e-04	AT1G19850, AT1G26870, AT1G30950, AT1G79580, AT2G46870, AT2G47260, AT3G11260, AT3G19500, AT3G20840, AT3G28857, AT3G58850, AT4G18390, AT4G23750, AT4G31800, AT5G04820, AT5G13910, AT5G17430, AT5G35770, AT5G60910, AT5G65640, AT5G66350
GO:0097659	nucleic acid-templated transcription	2735	21	6.62	9.1e-07	3.813e-04	AT1G19850, AT1G26870, AT1G30950, AT1G79580, AT2G46870, AT2G47260, AT3G11260, AT3G19500, AT3G20840, AT3G28857, AT3G58850, AT4G18390, AT4G23750, AT4G31800, AT5G04820, AT5G13910, AT5G17430, AT5G35770, AT5G60910, AT5G65640, AT5G66350
GO:0032774	RNA biosynthetic process	2744	21	6.64	9.6e-07	3.813e-04	AT1G19850, AT1G26870, AT1G30950, AT1G79580, AT2G46870, AT2G47260, AT3G11260, AT3G19500, AT3G20840, AT3G28857, AT3G58850, AT4G18390, AT4G23750, AT4G31800, AT5G04820, AT5G13910, AT5G17430, AT5G35770, AT5G60910, AT5G65640, AT5G66350
GO:0044767	single-organism developmental process	3255	23	7.88	9.7e-07	3.813e-04	AT1G02800, AT1G19850, AT1G26870, AT1G30950, AT1G34110, AT1G75520, AT1G79580, AT2G30130, AT2G30370, AT2G46870, AT3G11260, AT3G20840, AT3G28857, AT3G60650, AT4G18390, AT4G23750, AT5G13910, AT5G17430, AT5G35770, AT5G55250, AT5G60910, AT5G65640, AT5G66350
GO:0034654	nucleobase-containing compound biosynthetic process	3009	22	7.29	1,00E-06	3.813e-04	AT1G19850, AT1G26870, AT1G30950, AT1G79580, AT2G46870, AT2G47260, AT3G11260, AT3G19500, AT3G20840, AT3G25570, AT3G28857, AT3G58850, AT4G18390, AT4G23750, AT4G31800, AT5G04820, AT5G13910, AT5G17430, AT5G35770, AT5G60910, AT5G65640, AT5G66350
GO:0032501	multicellular organismal process	3011	22	7.29	1.1e-06	3.933e-04	AT1G02800, AT1G19850, AT1G26870, AT1G30950, AT1G34110, AT1G75520, AT1G79580, AT2G30130, AT2G30370, AT2G46870, AT3G11260, AT3G20840, AT3G60650, AT4G18390, AT4G23750, AT5G13910, AT5G17430, AT5G35770, AT5G55250, AT5G60910, AT5G65640, AT5G66350
GO:2000112	regulation of cellular macromolecule biosynthetic process	2781	21	6.73	1.2e-06	4.038e-04	AT1G19850, AT1G26870, AT1G30950, AT1G79580, AT2G46870, AT2G47260, AT3G11260, AT3G19500, AT3G20840, AT3G28857, AT3G58850, AT4G18390, AT4G23750, AT4G31800, AT5G04820, AT5G13910, AT5G17430, AT5G35770, AT5G60910, AT5G65640, AT5G66350
GO:0010556	regulation of macromolecule biosynthetic process	2800	21	6.78	1.3e-06	4.131e-04	AT1G19850, AT1G26870, AT1G30950, AT1G79580, AT2G46870, AT2G47260, AT3G11260, AT3G19500, AT3G20840, AT3G28857, AT3G58850, AT4G18390, AT4G23750, AT4G31800, AT5G04820, AT5G13910, AT5G17430, AT5G35770, AT5G60910, AT5G65640, AT5G66350
GO:0031326	regulation of cellular biosynthetic process	2863	21	6.93	1.9e-06	5.720e-04	AT1G19850, AT1G26870, AT1G30950, AT1G79580, AT2G46870, AT2G47260, AT3G11260, AT3G19500, AT3G20840, AT3G28857, AT3G58850, AT4G18390, AT4G23750, AT4G31800, AT5G04820, AT5G13910, AT5G17430, AT5G35770, AT5G60910, AT5G65640, AT5G66350
GO:0009889	regulation of biosynthetic process	2881	21	6.98	2.1e-06	5.720e-04	AT1G19850, AT1G26870, AT1G30950, AT1G79580, AT2G46870, AT2G47260, AT3G11260, AT3G19500, AT3G20840, AT3G28857, AT3G58850, AT4G18390, AT4G23750, AT4G31800, AT5G04820, AT5G13910, AT5G17430, AT5G35770, AT5G60910, AT5G65640, AT5G66350

Table S6. TOP 30 GO enriched terms of the 84 genes up-regulated in cluster 4 of Fig .3 (part 1)

GO.ID	Term	Annotated	Count	Expected	p-value	q-value	Genes
GO:0051171	regulation of nitrogen compound metabolic process	2881	21	6.98	**2.1e-06**	5.720e-04	AT1G19850, AT1G26870, AT1G30950, AT1G79580, AT2G46870, AT2G47260, AT3G11260, AT3G19500, AT3G20840, AT3G28857, AT3G58850, AT4G18390, AT4G23750, AT4G31800, AT5G04820, AT5G13910, AT5G17430, AT5G35770, AT5G60910, AT5G65640, AT5G66350
GO:0051240	positive regulation of multicellular organismal process	90	5	0.22	**2.7e-06**	7.020e-04	AT3G11260, AT4G18390, AT5G13910, AT5G35770, AT5G60910
GO:0050794	regulation of cellular process	5237	29	12.68	**3.2e-06**	7.958e-04	AT1G19250, AT1G19850, AT1G26870, AT1G30950, AT1G34110, AT1G68780, AT1G75520, AT1G79580, AT2G46870, AT2G47260, AT3G11260, AT3G19500, AT3G20840, AT3G28857, AT3G58850, AT4G03270, AT4G18290, AT4G18390, AT4G23750, AT4G31800, AT4G37630, AT5G04820, AT5G13910, AT5G17430, AT5G35770, AT5G56220, AT5G60910, AT5G65640, AT5G66350
GO:0010468	regulation of gene expression	2970	21	7.19	**3.5e-06**	8.342e-04	AT1G19850, AT1G26870, AT1G30950, AT1G79580, AT2G46870, AT2G47260, AT3G11260, AT3G19500, AT3G20840, AT3G28857, AT3G58850, AT4G18390, AT4G23750, AT4G31800, AT5G04820, AT5G13910, AT5G17430, AT5G35770, AT5G60910, AT5G65640, AT5G66350
GO:0018130	heterocycle biosynthetic process	3243	22	7.85	**3.7e-06**	8.360e-04	AT1G19850, AT1G26870, AT1G30950, AT1G79580, AT2G46870, AT2G47260, AT3G11260, AT3G19500, AT3G20840, AT3G25570, AT3G28857, AT3G58850, AT4G18390, AT4G23750, AT4G31800, AT5G04820, AT5G13910, AT5G17430, AT5G35770, AT5G60910, AT5G65640, AT5G66350
GO:0050789	regulation of biological process	5923	31	14.34	**3.8e-06**	8.360e-04	AT1G02810, AT1G19250, AT1G19850, AT1G26870, AT1G30950, AT1G34110, AT1G68780, AT1G75520, AT1G79580, AT2G30370, AT2G46870, AT2G47260, AT3G11260, AT3G19500, AT3G20840, AT3G28857, AT3G58850, AT4G03270, AT4G18290, AT4G18390, AT4G23750, AT4G31800, AT4G37630, AT5G04820, AT5G13910, AT5G17430, AT5G35770, AT5G56220, AT5G60910, AT5G65640, AT5G66350
GO:0019438	aromatic compound biosynthetic process	3353	22	8.12	**6.4e-06**	1.356e-03	AT1G19850, AT1G26870, AT1G30950, AT1G79580, AT2G46870, AT2G47260, AT3G11260, AT3G19500, AT3G20840, AT3G25570, AT3G28857, AT3G58850, AT4G18390, AT4G23750, AT4G31800, AT5G04820, AT5G13910, AT5G17430, AT5G35770, AT5G60910, AT5G65640, AT5G66350
GO:0080090	regulation of primary metabolic process	3172	21	7.68	**9.9e-06**	1.953e-03	AT1G19850, AT1G26870, AT1G30950, AT1G79580, AT2G46870, AT2G47260, AT3G11260, AT3G19500, AT3G20840, AT3G28857, AT3G58850, AT4G18390, AT4G23750, AT4G31800, AT5G04820, AT5G13910, AT5G17430, AT5G35770, AT5G60910, AT5G65640, AT5G66350
GO:0009733	response to auxin	435	8	1.05	**9.9e-06**	1.953e-03	AT1G19850, AT1G26870, AT1G75520, AT1G75580, AT2G47260, AT3G11260, AT3G20840, AT5G66350
GO:1901362	organic cyclic compound biosynthetic process	3495	22	8.46	**1.3e-05**	2.399e-03	AT1G19850, AT1G26870, AT1G30950, AT1G79580, AT2G46870, AT2G47260, AT3G11260, AT3G19500, AT3G20840, AT3G25570, AT3G28857, AT3G58850, AT4G18390, AT4G23750, AT4G31800, AT5G04820, AT5G13910, AT5G17430, AT5G35770, AT5G60910, AT5G65640, AT5G66350

Table S6. TOP 30 GO enriched terms of the 84 genes up-regulated in cluster 4 of Fig. 3 (part 2)

GO.ID	Term	Annotated	Count	Expected	p-value	q-value	Genes
GO:0044699	single-organism process	11098	46	28.15	8.1e-06	4.633e-02	AT1G01580, AT1G07730, AT1G13245, AT1G14520, AT1G19530, AT1G19790, AT1G21460, AT1G22340, AT1G26870, AT1G30950, AT1G49620, AT1G68780, AT1G69850, AT1G75520, AT2G23790, AT2G26640, AT2G27370, AT2G30070, AT2G30370, AT2G38180, AT2G38530, AT2G39900, AT3G11260, AT3G12830, AT3G12900, AT3G15990, AT3G24020, AT3G29320, AT3G30340, AT3G60650, AT4G03270, AT4G11150, AT4G18160, AT5G04530, AT5G09550, AT5G13420, AT5G13910, AT5G26170, AT5G35770, AT5G54160, AT5G55250, AT5G59310, AT5G59990, AT5G60910, AT5G65640, AT5G66350
GO:0044763	single-organism cellular process	8410	37	21.33	5.8e-05	1.563e-01	AT1G07730, AT1G14520, AT1G19530, AT1G19790, AT1G21460, AT1G22340, AT1G26870, AT1G30950, AT1G49620, AT1G68780, AT1G69850, AT1G75520, AT2G23790, AT2G26640, AT2G27370, AT2G30070, AT2G30370, AT2G38530, AT2G39900, AT3G11260, AT3G12830, AT3G15990, AT3G24020, AT3G29320, AT3G30340, AT4G03270, AT4G11150, AT4G18160, AT5G04530, AT5G09550, AT5G13420, AT5G13910, AT5G26170, AT5G35770, AT5G54160, AT5G60910, AT5G66350
GO:0051240	positive regulation of multicellular organismal process	90	4	0.23	8.2e-05	1.563e-01	AT3G11260, AT5G13910, AT5G35770, AT5G60910
GO:0051094	positive regulation of developmental process	98	4	0.25	0.00011	1.573e-01	AT3G11260, AT5G13910, AT5G35770, AT5G60910
GO:0009851	auxin biosynthetic process	58	3	0.15	0.00044	4.147e-01	AT1G19790, AT1G75520, AT5G66350
GO:0007275	multicellular organismal development	2794	17	7.09	0.00046	4.147e-01	AT1G13245, AT1G19790, AT1G26870, AT1G30950, AT1G75520, AT2G30370, AT3G11260, AT3G12830, AT3G60650, AT4G11150, AT5G13910, AT5G35770, AT5G55250, AT5G59990, AT5G60910, AT5G65640, AT5G66350
GO:0009699	phenylpropanoid biosynthetic process	145	4	0.37	0.00051	4.147e-01	AT1G07730, AT3G24020, AT5G13420, AT5G54160
GO:0044707	single-multicellular organism process	2847	17	7.22	0.00058	4.147e-01	AT1G13245, AT1G19790, AT1G26870, AT1G30950, AT1G75520, AT2G30370, AT3G11260, AT3G12830, AT3G60650, AT4G11150, AT5G13910, AT5G35770, AT5G55250, AT5G59990, AT5G60910, AT5G65640, AT5G66350
GO:1901362	organic cyclic compound biosynthetic process	3495	19	8.87	0.00081	4.368e-01	AT1G07730, AT1G19790, AT1G26870, AT1G30950, AT1G72210, AT3G04030, AT3G11260, AT3G24020, AT3G29320, AT4G11150, AT5G04820, AT5G13420, AT5G13910, AT5G26170, AT5G35770, AT5G54160, AT5G60910, AT5G65640, AT5G66350
GO:0009733	response to auxin	435	6	1.1	0.00082	4.368e-01	AT1G19790, AT1G26870, AT1G75520, AT3G11260, AT3G12830, AT5G66350
GO:0009725	response to hormone	1655	12	4.2	0.00084	4.368e-01	AT1G19790, AT1G26870, AT1G75520, AT3G11260, AT3G12830, AT3G12900, AT3G29320, AT4G11150, AT5G13910, AT5G26170, AT5G59310, AT5G66350
GO:0044767	single-organism developmental process	3255	18	8.26	0.00095	4.453e-01	AT1G13245, AT1G14520, AT1G19790, AT1G26870, AT1G30950, AT1G75520, AT2G30370, AT3G11260, AT3G12830, AT3G60650, AT4G11150, AT5G13910, AT5G35770, AT5G55250, AT5G59990, AT5G60910, AT5G65640, AT5G66350
GO:0009850	auxin metabolic process	79	3	0.2	0.00107	4.453e-01	AT1G19790, AT1G75520, AT5G66350
GO:0032501	multicellular organismal process	3011	17	7.64	0.00109	4.453e-01	AT1G13245, AT1G19790, AT1G26870, AT1G30950, AT1G75520, AT2G30370, AT3G11260, AT3G12830, AT3G60650, AT4G11150, AT5G13910, AT5G35770, AT5G55250, AT5G59990, AT5G60910, AT5G65640, AT5G66350
GO:0032502	developmental process	3324	18	8.43	0.00122	4.505e-01	AT1G13245, AT1G14520, AT1G19790, AT1G26870, AT1G30950, AT1G75520, AT2G30370, AT3G11260, AT3G12830, AT3G60650, AT4G11150, AT5G13910, AT5G35770, AT5G55250, AT5G59990, AT5G60910, AT5G65640, AT5G66350
GO:0009698	phenylpropanoid metabolic process	185	4	0.47	0.00126	4.505e-01	AT1G07730, AT3G24020, AT5G13420, AT5G54160
GO:0019438	aromatic compound biosynthetic process	3353	18	8.51	0.00135	4.542e-01	AT1G07730, AT1G19790, AT1G26870, AT1G30950, AT1G72210, AT3G04030, AT3G11260, AT3G24020, AT4G11150, AT5G04820, AT5G13420, AT5G13910, AT5G26170, AT5G35770, AT5G54160, AT5G60910, AT5G65640, AT5G66350
GO:0009719	response to endogenous stimulus	1767	12	4.48	0.00148	4.703e-01	AT1G19790, AT1G26870, AT1G75520, AT3G11260, AT3G12830, AT3G12900, AT3G29320, AT4G11150, AT5G13910, AT5G26170, AT5G59310, AT5G66350
GO:0032870	cellular response to hormone stimulus	880	8	2.23	0.00168	5.058e-01	AT1G19790, AT1G75520, AT3G12830, AT3G12900, AT3G29320, AT5G13910, AT5G26170, AT5G66350
GO:0071495	cellular response to endogenous stimulus	899	8	2.28	0.00192	5.491e-01	AT1G19790, AT1G75520, AT3G12830, AT3G12900, AT3G29320, AT5G13910, AT5G26170, AT5G66350
GO:0009734	auxin-activated signaling pathway	214	4	0.54	0.00215	5.812e-01	AT1G19790, AT1G75520, AT3G12830, AT5G66350
GO:0051239	regulation of multicellular organismal process	531	6	1.35	0.00227	5.812e-01	AT2G30370, AT3G11260, AT5G13910, AT5G35770, AT5G59990, AT5G60910

Table S7. TOP 30 GO enriched terms of the 93 genes up-regulated in cluster 5 of Fig .3 (part 1)

GO.ID	Term	Annotated	Count	Expected	p-value	q-value	Genes
GO:0071365	cellular response to auxin stimulus	229	4	0.58	0.00275	6.050e-01	AT1G19790, AT1G75520, AT3G12830, AT5G66350
GO:0006811	ion transport	964	8	2.45	0.00296	6.271e-01	AT1G01580, AT1G69850, AT2G23790, AT2G30070, AT2G38530, AT3G15990, AT4G11150, AT4G18160
GO:0042446	hormone biosynthetic process	118	3	0.3	0.00338	6.905e-01	AT1G19790, AT1G75520, AT5G66350
GO:0050789	regulation of biological process	5923	25	15.02	0.00401	7.422e-01	AT1G07730, AT1G19790, AT1G26870, AT1G30950, AT1G49620, AT1G68780, AT1G69850, AT1G72210, AT1G75520, AT2G30370, AT3G04030, AT3G11260, AT3G12830, AT3G24020, AT3G29320, AT4G03270, AT5G04820, AT5G09550, AT5G13910, AT5G26170, AT5G35770, AT5G59990, AT5G60910, AT5G65640, AT5G66350
GO:0071310	cellular response to organic substance	1028	8	2.61	0.00436	7.422e-01	AT1G19790, AT1G75520, AT3G12830, AT3G12900, AT3G29320, AT5G13910, AT5G26170, AT5G66350
GO:0010033	response to organic substance	2026	12	5.14	0.00458	7.422e-01	AT1G19790, AT1G26870, AT1G75520, AT3G11260, AT3G12830, AT3G12900, AT3G29320, AT4G11150, AT5G13910, AT5G26170, AT5G59310, AT5G66350
GO:0009755	hormone-mediated signaling pathway	821	7	2.08	0.0047	7.422e-01	AT1G19790, AT1G75520, AT3G12830, AT3G29320, AT5G13910, AT5G26170, AT5G66350
GO:0050793	regulation of developmental process	617	6	1.57	0.00473	7.422e-01	AT2G30370, AT3G11260, AT5G13910, AT5G35770, AT5G59990, AT5G60910

Table S7. TOP 30 GO enriched terms of the 93 genes up-regulated in cluster 5 of Fig .3 (part 2)

GO.ID	Term	Annotated	Count	Expected	p-value	q-value	Genes
GO:1902578	single-organism localization	2160	23	6.72	1,00E-07	5.720e-04	AT1G01580, AT1G09240, AT1G14920, AT1G22710, AT1G25270, AT1G27940, AT1G62262, AT1G75500, AT1G80760, AT2G18196, AT2G19770, AT2G36590, AT2G38530, AT2G44290, AT3G05030, AT3G10600, AT3G24450, AT3G25620, AT3G30340, AT3G51895, AT4G27500, AT5G02940, AT5G50740
GO:0044765	single-organism transport	2119	22	6.6	3.3e-07	9.438e-04	AT1G01580, AT1G09240, AT1G14920, AT1G22710, AT1G25270, AT1G27940, AT1G62262, AT1G75500, AT1G80760, AT2G18196, AT2G36590, AT2G38530, AT2G44290, AT3G05030, AT3G10600, AT3G24450, AT3G25620, AT3G30340, AT3G51895, AT4G27500, AT5G02940, AT5G50740
GO:0051179	localization	2837	24	8.83	3.4e-06	6.483e-03	AT1G01580, AT1G09240, AT1G12150, AT1G14920, AT1G22710, AT1G25270, AT1G27940, AT1G62262, AT1G75500, AT1G80760, AT2G18196, AT2G19770, AT2G36590, AT2G38530, AT2G44290, AT3G05030, AT3G10600, AT3G24450, AT3G25620, AT3G30340, AT3G51895, AT4G27500, AT5G02940, AT5G50740
GO:0051234	establishment of localization	2730	23	8.5	6.2e-06	8.866e-03	AT1G01580, AT1G09240, AT1G12150, AT1G14920, AT1G22710, AT1G25270, AT1G27940, AT1G62262, AT1G75500, AT1G80760, AT2G18196, AT2G36590, AT2G38530, AT2G44290, AT3G05030, AT3G10600, AT3G24450, AT3G25620, AT3G30340, AT3G51895, AT4G27500, AT5G02940, AT5G50740
GO:0006811	ion transport	964	13	3	8.3e-06	9.495e-03	AT1G01580, AT1G62262, AT1G80760, AT2G18196, AT2G36590, AT2G38530, AT3G05030, AT3G10600, AT3G24450, AT3G51895, AT4G27500, AT5G02940, AT5G50740
GO:0010232	vascular transport	16	3	0.05	1.6e-05	1.287e-02	AT1G09240, AT1G14920, AT1G22710
GO:0010233	phloem transport	16	3	0.05	1.6e-05	1.287e-02	AT1G09240, AT1G14920, AT1G22710
GO:0006810	transport	2699	22	8.4	1.8e-05	1.287e-02	AT1G01580, AT1G09240, AT1G14920, AT1G22710, AT1G25270, AT1G27940, AT1G62262, AT1G75500, AT1G80760, AT2G18196, AT2G36590, AT2G38530, AT2G44290, AT3G05030, AT3G10600, AT3G24450, AT3G25620, AT3G30340, AT3G51895, AT4G27500, AT5G02940, AT5G50740
GO:0055085	transmembrane transport	1130	13	3.52	4.4e-05	2.796e-02	AT1G22710, AT1G25270, AT1G27940, AT1G62262, AT1G75500, AT1G80760, AT2G36590, AT3G05030, AT3G10600, AT3G25620, AT3G30340, AT3G51895, AT5G02940
GO:1901362	organic cyclic compound biosynthetic process	3495	24	10.88	0.00011	6.292e-02	AT1G09240, AT1G14350, AT1G14920, AT1G18400, AT1G19510, AT1G22490, AT1G22900, AT1G24625, AT1G29160, AT1G52890, AT1G68920, AT1G71692, AT1G75250, AT1G75500, AT2G01430, AT2G07050, AT2G22670, AT2G38090, AT3G11260, AT4G21440, AT4G35160, AT4G35900, AT4G37850, AT5G11590
GO:0019438	aromatic compound biosynthetic process	3353	23	10.44	0.00016	8.320e-02	AT1G14350, AT1G14920, AT1G18400, AT1G19510, AT1G22490, AT1G22900, AT1G24625, AT1G29160, AT1G52890, AT1G68920, AT1G71692, AT1G75250, AT1G75500, AT2G01430, AT2G22670, AT2G38090, AT3G11260, AT3G53140, AT4G21440, AT4G35160, AT4G35900, AT4G37850, AT5G11590
GO:0065007	biological regulation	6714	36	20.9	0.00021	1.001e-01	AT1G01580, AT1G14350, AT1G14920, AT1G18400, AT1G19510, AT1G22490, AT1G22900, AT1G24625, AT1G27940, AT1G29160, AT1G52890, AT1G62262, AT1G68920, AT1G71692, AT1G75250, AT1G75500, AT1G80760, AT2G01430, AT2G18196, AT2G19770, AT2G22670, AT2G38090, AT2G39370, AT2G39730, AT3G04720, AT3G05030, AT3G11260, AT3G47090, AT4G13260, AT4G21440, AT4G27500, AT4G35160, AT4G35900, AT4G37850, AT5G11590, AT5G50740
GO:0098656	anion transmembrane transport	183	5	0.57	0.00027	1.144e-01	AT1G62262, AT1G80760, AT2G36590, AT3G10600, AT3G51895
GO:0018130	heterocycle biosynthetic process	3243	22	10.1	0.00028	1.144e-01	AT1G09240, AT1G14350, AT1G14920, AT1G18400, AT1G19510, AT1G22490, AT1G24625, AT1G29160, AT1G52890, AT1G68920, AT1G71692, AT1G75250, AT1G75500, AT2G01430, AT2G22670, AT2G38090, AT3G11260, AT4G21440, AT4G35160, AT4G35900, AT4G37850, AT5G11590
GO:0006355	regulation of transcription, DNA-templated	2599	19	8.09	0.00032	1.144e-01	AT1G14350, AT1G14920, AT1G18400, AT1G19510, AT1G22490, AT1G24625, AT1G29160, AT1G52890, AT1G68920, AT1G71692, AT1G75250, AT2G01430, AT2G22670, AT2G38090, AT3G11260, AT4G21440, AT4G35900, AT4G37850, AT5G11590
GO:1903506	regulation of nucleic acid-templated transcription	2611	19	8.13	0.00034	1.144e-01	AT1G14350, AT1G14920, AT1G18400, AT1G19510, AT1G22490, AT1G24625, AT1G29160, AT1G52890, AT1G68920, AT1G71692, AT1G75250, AT2G01430, AT2G22670, AT2G38090, AT3G11260, AT4G21440, AT4G35900, AT4G37850, AT5G11590
GO:2001141	regulation of RNA biosynthetic process	2611	19	8.13	0.00034	1.144e-01	AT1G14350, AT1G14920, AT1G18400, AT1G19510, AT1G22490, AT1G24625, AT1G29160, AT1G52890, AT1G68920, AT1G71692, AT1G75250, AT2G01430, AT2G22670, AT2G38090, AT3G11260, AT4G21440, AT4G35900, AT4G37850, AT5G11590
GO:0051252	regulation of RNA metabolic process	2650	19	8.25	0.00041	1.264e-01	AT1G14350, AT1G14920, AT1G18400, AT1G19510, AT1G22490, AT1G24625, AT1G29160, AT1G52890, AT1G68920, AT1G71692, AT1G75250, AT2G01430, AT2G22670, AT2G38090, AT3G11260, AT4G21440, AT4G35900, AT4G37850, AT5G11590
GO:0051171	regulation of nitrogen compound metabolic process	2881	20	8.97	0.00042	1.264e-01	AT1G14350, AT1G14920, AT1G18400, AT1G19510, AT1G22490, AT1G24625, AT1G29160, AT1G52890, AT1G68920, AT1G71692, AT1G75250, AT1G75500, AT2G01430, AT2G22670, AT2G38090, AT3G11260, AT4G21440, AT4G35900, AT4G37850, AT5G11590
GO:0019219	regulation of nucleobase-containing compound metabolic process	2706	19	8.42	0.00053	1.482e-01	AT1G14350, AT1G14920, AT1G18400, AT1G19510, AT1G22490, AT1G24625, AT1G29160, AT1G52890, AT1G68920, AT1G71692, AT1G75250, AT2G01430, AT2G22670, AT2G38090, AT3G11260, AT4G21440, AT4G35900, AT4G37850, AT5G11590

Table S9. TOP 30 GO enriched terms of the 111 genes induced in T0 and T12 CR parts (part 1)

GO.ID	Term	Annotated	Count	Expected	p-value	q-value	Genes
GO:0080090	regulation of primary metabolic process	3172	21	9.87	0.00055	1.482e-01	AT1G14350, AT1G14920, AT1G18400, AT1G19510, AT1G22490, AT1G24625, AT1G29160, AT1G52890, AT1G68920, AT1G71692, AT1G75250, AT1G75500, AT2G01430, AT2G22670, AT2G38090, AT2G39370, AT3G11260, AT4G21440, AT4G35900, AT4G37850, AT5G11590
GO:0006351	transcription, DNA-templated	2722	19	8.47	0.00057	1.482e-01	AT1G14350, AT1G14920, AT1G18400, AT1G19510, AT1G22490, AT1G24625, AT1G29160, AT1G52890, AT1G68920, AT1G71692, AT1G75250, AT2G01430, AT2G22670, AT2G38090, AT3G11260, AT4G21440, AT4G35900, AT4G37850, AT5G11590
GO:0097659	nucleic acid-templated transcription	2735	19	8.51	6,00E-04	1.492e-01	AT1G14350, AT1G14920, AT1G18400, AT1G19510, AT1G22490, AT1G24625, AT1G29160, AT1G52890, AT1G68920, AT1G71692, AT1G75250, AT2G01430, AT2G22670, AT2G38090, AT3G11260, AT4G21440, AT4G35900, AT4G37850, AT5G11590
GO:0032774	RNA biosynthetic process	2744	19	8.54	0.00063	1.502e-01	AT1G14350, AT1G14920, AT1G18400, AT1G19510, AT1G22490, AT1G24625, AT1G29160, AT1G52890, AT1G68920, AT1G71692, AT1G75250, AT2G01430, AT2G22670, AT2G38090, AT3G11260, AT4G21440, AT4G35900, AT4G37850, AT5G11590
GO:0031323	regulation of cellular metabolic process	3229	21	10.05	7,00E-04	1.602e-01	AT1G14350, AT1G14920, AT1G18400, AT1G19510, AT1G22490, AT1G24625, AT1G29160, AT1G52890, AT1G68920, AT1G71692, AT1G75250, AT1G75500, AT2G01430, AT2G22670, AT2G38090, AT2G39370, AT3G11260, AT4G21440, AT4G35900, AT4G37850, AT5G11590
GO:2000112	regulation of cellular macromolecule biosynthetic process	2781	19	8.66	0.00074	1.628e-01	AT1G14350, AT1G14920, AT1G18400, AT1G19510, AT1G22490, AT1G24625, AT1G29160, AT1G52890, AT1G68920, AT1G71692, AT1G75250, AT2G01430, AT2G22670, AT2G38090, AT3G11260, AT4G21440, AT4G35900, AT4G37850, AT5G11590
GO:0010556	regulation of macromolecule biosynthetic process	2800	19	8.72	0.00081	1.716e-01	AT1G14350, AT1G14920, AT1G18400, AT1G19510, AT1G22490, AT1G24625, AT1G29160, AT1G52890, AT1G68920, AT1G71692, AT1G75250, AT2G01430, AT2G22670, AT2G38090, AT3G11260, AT4G21440, AT4G35900, AT4G37850, AT5G11590
GO:0006820	anion transport	354	6	1.1	0.00084	1.716e-01	AT1G62262, AT1G80760, AT2G36590, AT2G38530, AT3G10600, AT3G51895
GO:0019222	regulation of metabolic process	3768	23	11.73	0.00089	1.755e-01	AT1G14350, AT1G14920, AT1G18400, AT1G19510, AT1G22490, AT1G22900, AT1G24625, AT1G29160, AT1G52890, AT1G68920, AT1G71692, AT1G75250, AT1G75500, AT2G01430, AT2G22670, AT2G38090, AT2G39370, AT2G39730, AT3G11260, AT4G21440, AT4G35900, AT4G37850, AT5G11590

Table S9. TOP 30 GO enriched terms of the 111 genes induced in T0 and T12 CR parts (part 2)

Pros	Cons
LaMAKR4, MEMBRANE-ASSOCIATED KINASE REGULATOR 4	
• acts downstream of gene oscillations ; convert pre-branch sites into LRs (Xuan *et al.,* 2015) • one main obvious candidate induced at early stages: *Lalb_Chr21g0307221* • *makr4-1* mutants loss-of-function have unaltered pre-branch sites but fewer LRs (same for amiRNAi plants) (Xuan *et al.,* 2015)	• 4 lupin protein sequences are similar to the one of *AtMAKR4* but only *Lalb_Chr21g0307221* is strongly induced • phenotype of *makr4-1* mutant treated with auxin is not reported (is auxin modifying the phenotype of the mutant?)
LaMYB124, MYB DOMAIN PROTEIN 124 (or FLP for FOUR LIPS)	
• regulates LR initiation: expressed in the nucleus at stage I ; regulates PIN3 expression in the endodermis (Chen *et al.,* 2015) • one main obvious candidate highly induced at T0 and T12: *Lalb_Chr10g0098091* • *flp-1* and *flp-7* loss-of-function mutants have reduced LR number compared to WT Col at 6 DAG (Chen *et al.,* 2015)	• protein sequences of *Lalb_Chr10g0098091* and *Lalb_Chr04g0256211* are really similar (duplicated gene?) • *flp-1* and *flp-7* loss of function mutants have clusters of stomata on leaves. Plants have more water loss and are more sensitive to drought stress (Yang *et al.,* 1995)
LaLBD16, LATERAL ORGAN BOUNDARIES-DOMAIN 16	
• pivotal role in LR initiation (Goh *et al.,* 2012) • one main candidate with peak of expression in T12: *Lalb_Chr06g0162491* • up-regulated at T12 compared to LR • *lbd16-1* loss-of-function mutant shows a slight decrease number of LRs (Goh *et al.,* 2012) • LBD16-SRDX plants have no LR or fewer and primary development is normal (Goh *et al.,* 2012)	• *Lalb_Chr06g0162491* protein sequence is really similar to the one of genes *Lalb_Chr01g0019721* and *Lalb_Chr02g0142301* • when auxin is applied on *lbd16-1* mutant, there are more LRs (auxin can suppress the phenotype of the mutant)

Table S10. Pros and cons for selecting lupin candidate genes

GO.ID	Term	Annotated	Count	Expected	p-value	q-value	Genes
GO:0071944	cell periphery	3568	52	22.93	1.7e-09	1.671e-06	AT1G02860, AT1G05590, AT1G06490, AT1G08050, AT1G09380, AT1G09750, AT1G14040, AT1G15460, AT1G17140, AT1G18650, AT1G18670, AT1G20160, AT1G21980, AT1G23080, AT1G30320, AT1G32190, AT1G34300, AT1G47670, AT1G48870, AT1G64080, AT1G66250, AT1G69870, AT1G74720, AT1G75500, AT2G01950, AT2G03810, AT2G25070, AT2G25630, AT2G26570, AT2G28950, AT3G08870, AT3G24240, AT3G51370, AT3G51670, AT3G55430, AT4G13600, AT4G16370, AT4G16563, AT4G26540, AT4G28950, AT4G29360, AT4G31140, AT5G05340, AT5G07280, AT5G13170, AT5G17420, AT5G20230, AT5G46700, AT5G51550, AT5G54160, AT5G54590, AT5G60210
GO:0005886	plasma membrane	2894	45	18.6	5.1e-09	2.507e-06	AT1G02860, AT1G05590, AT1G06490, AT1G08050, AT1G09380, AT1G14040, AT1G15460, AT1G17140, AT1G18650, AT1G18670, AT1G21980, AT1G23080, AT1G30320, AT1G32190, AT1G34300, AT1G47670, AT1G48870, AT1G64080, AT1G66250, AT1G69870, AT1G74720, AT1G75500, AT2G01950, AT2G03810, AT2G25070, AT2G26570, AT3G08870, AT3G24240, AT3G51370, AT3G51670, AT3G55430, AT4G13600, AT4G16370, AT4G26540, AT4G28950, AT4G29360, AT4G31140, AT5G07280, AT5G13170, AT5G17420, AT5G20230, AT5G46700, AT5G54160, AT5G54590, AT5G60210
GO:0032502	developmental process	3324	46	21.21	2,00E-07	8.580e-04	AT1G02800, AT1G04820, AT1G05010, AT1G06490, AT1G19790, AT1G19850, AT1G20160, AT1G23080, AT1G28470, AT1G30490, AT1G32540, AT1G34110, AT1G53310, AT1G56150, AT1G63260, AT1G63820, AT1G63910, AT1G74720, AT1G75500, AT1G75520, AT2G01950, AT2G16500, AT2G22630, AT2G25630, AT2G28950, AT3G04070, AT3G12090, AT3G24240, AT3G28857, AT3G50070, AT3G52770, AT3G57670, AT4G16370, AT4G18640, AT4G23750, AT4G26540, AT4G29720, AT4G35550, AT4G37750, AT5G05340, AT5G07280, AT5G13170, AT5G13910, AT5G46700, AT5G55250, AT5G57390
GO:0044767	single-organism developmental process	3255	45	20.77	3,00E-07	8.580e-04	AT1G02800, AT1G04820, AT1G05010, AT1G06490, AT1G19790, AT1G19850, AT1G20160, AT1G23080, AT1G28470, AT1G30490, AT1G32540, AT1G34110, AT1G53310, AT1G56150, AT1G63260, AT1G63820, AT1G63910, AT1G74720, AT1G75500, AT1G75520, AT2G01950, AT2G16500, AT2G22630, AT2G25630, AT2G28950, AT3G04070, AT3G12090, AT3G24240, AT3G28857, AT3G50070, AT3G52770, AT3G57670, AT4G16370, AT4G18640, AT4G23750, AT4G26540, AT4G29720, AT4G35550, AT4G37750, AT5G07280, AT5G13170, AT5G13910, AT5G46700, AT5G55250, AT5G57390
GO:1900378	positive regulation of secondary metabolite biosynthetic process	4	3	0.03	1,00E-06	1.907e-03	AT1G63910, AT4G27260, AT5G05340
GO:0032501	multicellular organismal process	3011	41	19.21	1.8e-06	2.574e-03	AT1G02800, AT1G04820, AT1G05010, AT1G06490, AT1G19790, AT1G19850, AT1G20160, AT1G23080, AT1G28470, AT1G30490, AT1G34110, AT1G34300, AT1G53310, AT1G56150, AT1G63820, AT1G74720, AT1G75520, AT2G01950, AT2G16500, AT2G22630, AT2G25630, AT3G04070, AT3G12090, AT3G24240, AT3G50070, AT3G52770, AT3G57670, AT4G03230, AT4G16370, AT4G18640, AT4G23750, AT4G26540, AT4G29720, AT4G35550, AT4G37750, AT5G07280, AT5G13170, AT5G13910, AT5G46700, AT5G55250, AT5G57390
GO:0009834	plant-type secondary cell wall biogenesis	68	6	0.43	4.9e-06	5.593e-03	AT1G28470, AT1G63910, AT1G75500, AT2G38080, AT3G50220, AT5G17420
GO:0007389	pattern specification process	202	9	1.29	6.3e-06	5.593e-03	AT1G02800, AT1G19850, AT1G23080, AT1G30490, AT2G01950, AT3G52770, AT5G46700, AT5G55250, AT5G57390
GO:0044707	single-multicellular organism process	2847	38	18.16	7.6e-06	5.593e-03	AT1G02800, AT1G04820, AT1G05010, AT1G06490, AT1G19790, AT1G19850, AT1G20160, AT1G23080, AT1G28470, AT1G30490, AT1G34110, AT1G53310, AT1G56150, AT1G63820, AT1G74720, AT1G75520, AT2G01950, AT2G16500, AT2G22630, AT3G04070, AT3G12090, AT3G24240, AT3G50070, AT3G52770, AT3G57670, AT4G16370, AT4G18640, AT4G23750, AT4G26540, AT4G29720, AT4G35550, AT4G37750, AT5G07280, AT5G13170, AT5G13910, AT5G46700, AT5G55250, AT5G57390
GO:0009809	lignin biosynthetic process	75	6	0.48	8.6e-06	5.593e-03	AT1G63910, AT2G38080, AT4G36220, AT5G05340, AT5G20230, AT5G54160
GO:0009798	axis specification	44	5	0.28	8.8e-06	5.593e-03	AT1G19850, AT1G23080, AT1G30490, AT3G52770, AT5G55250
GO:0009734	auxin-activated signaling pathway	214	9	1.37	1,00E-05	5.720e-03	AT1G19790, AT1G19850, AT1G23080, AT1G56150, AT1G75500, AT1G75520, AT2G01950, AT5G46700, AT5G57390
GO:1900376	regulation of secondary metabolite biosynthetic process	22	4	0.14	1.1e-05	5.720e-03	AT1G63910, AT4G27260, AT5G05340, AT5G20230
GO:1901141	regulation of lignin biosynthetic process	8	3	0.05	1.4e-05	6.673e-03	AT1G63910, AT5G05340, AT5G20230
GO:0071365	cellular response to auxin stimulus	229	9	1.46	1.7e-05	7.480e-03	AT1G19790, AT1G19850, AT1G23080, AT1G56150, AT1G75500, AT1G75520, AT2G01950, AT5G46700, AT5G57390
GO:0009733	response to auxin	435	12	2.78	2.5e-05	9.948e-03	AT1G19790, AT1G19850, AT1G23080, AT1G56150, AT1G75500, AT1G75520, AT1G75580, AT2G01950, AT2G47260, AT4G27260, AT5G46700, AT5G57390
GO:0048507	meristem development	243	9	1.55	2.8e-05	9.948e-03	AT1G19850, AT1G30490, AT1G34110, AT3G24240, AT3G52770, AT4G26540, AT4G29720, AT4G37750, AT5G46700
GO:0010305	leaf vascular tissue pattern formation	28	4	0.18	2.9e-05	9.948e-03	AT1G19850, AT2G01950, AT3G52770, AT5G46700

Table S12. TOP 30 GO enriched terms of the 216 genes induced in T12 to T36 CR parts (part 1)

GO.ID	Term	Annotated	Count	Expected	p-value	q-value	Genes
GO:0007275	multicellular organismal development	2794	36	17.83	3,00E-05	9.948e-03	AT1G02800, AT1G04820, AT1G05010, AT1G19790, AT1G19850, AT1G20160, AT1G23080, AT1G28470, AT1G30490, AT1G34110, AT1G53310, AT1G56150, AT1G63820, AT1G74720, AT1G75520, AT2G01950, AT2G16500, AT2G22630, AT3G04070, AT3G24240, AT3G50070, AT3G52770, AT3G57670, AT4G16370, AT4G18640, AT4G23750, AT4G26540, AT4G29720, AT4G35550, AT4G37750, AT5G07280, AT5G13170, AT5G13910, AT5G46700, AT5G55250, AT5G57390
GO:0009888	tissue development	603	14	3.85	3.5e-05	9.948e-03	AT1G04820, AT1G19850, AT1G20160, AT1G30490, AT1G34110, AT1G53310, AT3G24240, AT3G52770, AT4G18640, AT4G26540, AT4G29720, AT4G37750, AT5G05340, AT5G46700
GO:0009808	lignin metabolic process	96	6	0.61	3.6e-05	9.948e-03	AT1G63910, AT2G38080, AT4G36220, AT5G05340, AT5G20230, AT5G54160
GO:1901064	syringal lignin metabolic process	2	2	0.01	4,00E-05	9.948e-03	AT1G63910, AT5G05340
GO:1901066	syringal lignin biosynthetic process	2	2	0.01	4,00E-05	9.948e-03	AT1G63910, AT5G05340
GO:1901428	regulation of syringal lignin biosynthetic process	2	2	0.01	4,00E-05	9.948e-03	AT1G63910, AT5G05340
GO:1901430	positive regulation of syringal lignin biosynthetic process	2	2	0.01	4,00E-05	9.948e-03	AT1G63910, AT5G05340
GO:0048589	developmental growth	472	12	3.01	5.4e-05	1.287e-02	AT1G04820, AT1G34110, AT1G53310, AT1G75500, AT2G25630, AT2G28950, AT3G12090, AT3G24240, AT3G28857, AT3G52770, AT3G57670, AT4G26540
GO:0065007	biological regulation	6714	65	42.84	0.00011	2.399e-02	AT1G02860, AT1G04880, AT1G06490, AT1G14040, AT1G15460, AT1G17140, AT1G19250, AT1G19790, AT1G19850, AT1G20160, AT1G22490, AT1G23080, AT1G28360, AT1G28470, AT1G30490, AT1G32540, AT1G34110, AT1G48870, AT1G56150, AT1G56210, AT1G63820, AT1G63910, AT1G75450, AT1G75500, AT1G75520, AT2G01950, AT2G16485, AT2G22630, AT2G24230, AT2G26710, AT2G33620, AT2G40200, AT2G41130, AT2G41180, AT2G47260, AT3G02550, AT3G04070, AT3G09360, AT3G19500, AT3G22810, AT3G24240, AT3G28857, AT3G47380, AT3G50070, AT3G52770, AT3G57670, AT4G16370, AT4G17350, AT4G18640, AT4G23750, AT4G26540, AT4G27260, AT4G28950, AT4G29720, AT4G35550, AT4G37750, AT5G05340, AT5G07280, AT5G13910, AT5G20230, AT5G46700, AT5G50740, AT5G55250, AT5G57390, AT5G64980
GO:0048509	regulation of meristem development	118	6	0.75	0.00011	2.399e-02	AT1G34110, AT3G24240, AT3G52770, AT4G26540, AT4G29720, AT5G46700
GO:0040007	growth	678	14	4.33	0.00012	2.399e-02	AT1G04820, AT1G34110, AT1G53310, AT1G56150, AT1G75500, AT2G25630, AT2G26710, AT2G28950, AT3G12090, AT3G24240, AT3G28857, AT3G52770, AT3G57670, AT4G26540
GO:0043455	regulation of secondary metabolic process	40	4	0.26	0.00012	2.399e-02	AT1G63910, AT4G27260, AT5G05340, AT5G20230

Table S12. TOP 30 GO enriched terms of the 216 genes induced in T12 to T36 CR parts (part 2)

Pros	Cons
LaLBD29, LATERAL ORGAN BOUNDARIES-DOMAIN 29	
• regulates LR initiation: maintain the capacity of pericycle cells to divide (Feng *et al.,* 2012) • one main obvious candidate: *Lalb_Chr02g0142290* • *lbd29* loss-of-function mutant shows a decrease in LR density compared to WT Col at 7 DAG and 14 DAG (Feng *et al.,* 2012)	• Protein sequences of *Lalb_Chr02g0142291* and *Lalb_Chr01g0019701* are really similar (duplicated gene?) • the phenotype of *lbd29* mutant treated with auxin is not reported (is auxin modifying the phenotype of the mutant?)
LaPUCHI	
• is important for cell division involved in LRP development ; is expressed from stage I LRP (Hirota *et al.,* 2007) • 2 genes strongly induced at T24: *Lalb_Chr13g0303751* and *Lalb_Chr07g0177601* • *puchi-1* loss-of-function mutant have shorter emerged LR than WT at 9 DAG • density of emerged LR is slightly reduced in *puchi-1* mutant compared to WT plants	• protein sequences of *Lalb_Chr13g0303751* and *Lalb_Chr07g0177601* are similar. These genes also have similar expression profiles. • *puchi-1* loss-of-function mutant phenotype is indistinguishable from WT Col at 20 DAG (Hirota *et al.,* 2007)
LaERF12, ETHYLENE RESPONSIVE TRANSCRIPTION FACTOR 12	
• encodes a member of the ERF (ethylene response factor) subfamily B-1 of ERF/AP2 transcription factor family (ERF12). • one main obvious candidate: *Lalb_Chr18g0059441* • induced by NAA treatment after 6 hours in Col0 and J0121 (source: tair, Arabidopsis Lateral root Initiation eFP browser) • in the LRP zone, slightly expressed in procambium and XPP cells (source: tair, Root eFP browser) • is responsive to phosphate deficiency. Gene expression increase after 6 hours of exposition to Pi starvation (source: tair, RootII eFP browser)	• no functional studies on *AtERF12* so far • protein sequence between lupin gene *Lalb_Chr18g0059441* and *AtERF12* is only 50% identical • *Lalb_Chr18g0059441* is only x3 more expressed in T12 compared to LR

Table S13. Pros and cons for selecting lupin candidate genes

Pros	Cons
LaSTY1, STYLISH 1	
• *LaSTY1* protein sequence is similar to *AtLRP1* (lateral root primordium 1) protein sequence. *AtLRP1* is a gene expressed before LRI and during LRP patterning (Smith *et al.,* 1995) • *AtSTY1* can act as a transcriptional activator regulating auxin biosynthesis (Eklund *et al.,* 2010) • two genes highly induced between T12 and T48: *Lalb_Chr23g0266341* and *Lalb_Chr09g0320901* • is expressed in the primordium of several organs (cotyledon, gynoecium) and during leaf vein development (Kuusk *et al.,* 2002; Baylis *et al.,* 2013) • *Lalb_Chr23g0266341* is 39 times more expressed at T12 compared to LR	• *sty1-1* and *sty2-1* mutants showed defective style, stigma as well as serrated leaves. No phenotype related to the root system is reported. • at least 6 SHI-related genes in white lupin • similarity at the protein level betwen *Lalb_Chr23g0266341* and *AtSTY1* is only 47%
LaNFY-B5, NUCLEAR FACTOR Y, SUBUNIT B5	
• some members of NFY transcription factors family are involved in developmental processes including nodule development (Petroni *et al.,* 2012) • strongly expressed in the procambium and endodermis in the differentiation zone and LRP zone (source: tair, Root eFP browser) • *Lalb_Chr13g0303701* is 11,5 times more expressed at T12 compared to LR	• not induced by auxin or Pi starvation • *AtNFY-B5* might participate in the HRS1/HHO1 response that represses primary root growth in response to Pi deprivation and NO_3^- availability (Medici *et al.,* 2015)
LaNAC044, NAC DOMAIN CONTAINING PROTEIN 44	
• some members of the NAC transcription factors family are involved in embryonic, floral, vegetative and lateral root development (Olsen *et al.,* 2015) • two genes are highly induced between T12 and T36: *Lalb_Chr14g0362861* and *Lalb_Chr10g099731* • *Lalb_Chr14g0362861* is 6,5 times more expressed at T12 compared to LR	• *Lalb_Chr14g0362861* and *Lalb_Chr10g099731* have similar expression profiles • *AtNAC044* was recently described to play a crucial role in causing G2 arrest in response to DNA damage (Takahashi *et al.,* 2019) • *Lalb_Chr14g0362861* protein sequence is only 48% similar at the protein level to *AtNAC044*

Table S14. Pros and cons for selecting lupin candidate genes

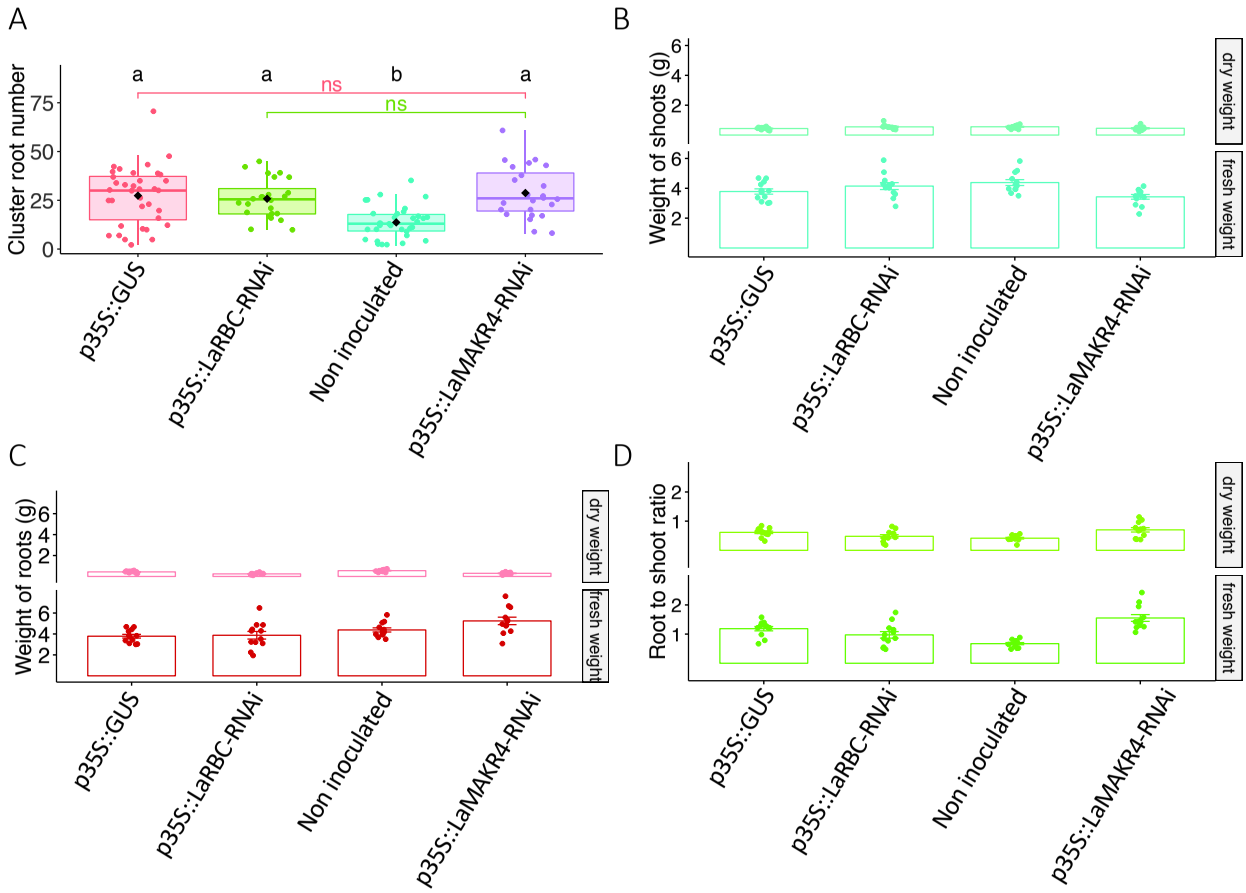

Fig. S4. Silencing of *LaMAKR4* kinase expression in white lupin. (A) Number of cluster roots formed on lupin root system as compared with hairy roots plants transformed with *p35S::GUS* and *p35S::LaRBC-RNAi*. (B-C) Fresh and dry weight of shoots (B) or roots (C) of the 3 transgenic lines.(D) Ratio between the root weight and the shoot weight in the 3 transgenic lines.

Fig. S5. Phenotype of white lupin transgenic root systems compared to untransformed plants and p35S::GUS control plants. Untransformed plants form cluster of rootlets close to the tip of the principal roots while all transgenic lines display continuous rootlet initiation on the roots formed from the cut. Images presented are representative of n=24 plants, except for LaNFY-B5-SRDX (n=17).

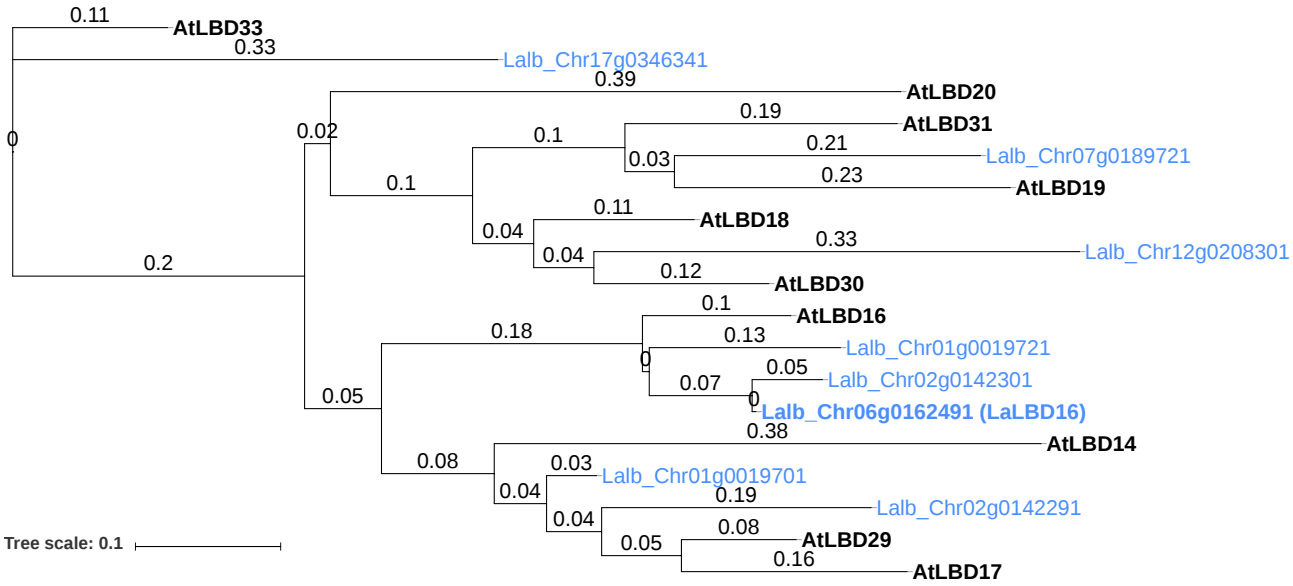

Fig. S6. Partial phylogenetic tree of LBDs class Ia subtype C of *Arabidopsis* and white lupin orthologs. The bootstrap consensus tree was inferred from 1000 replicates . The numbers on the branches indicate the length of the branches, which represents the evolutionary time between two nodes (unit: substitution per site).

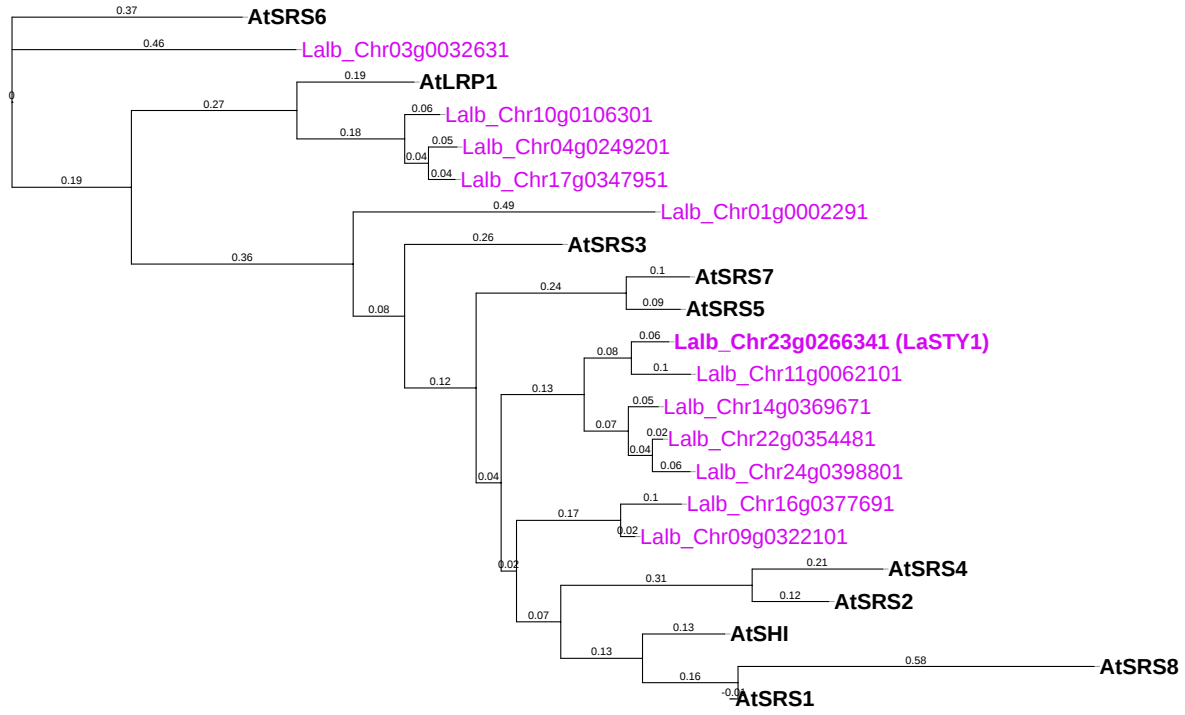

Fig. S7. Phylogenetic tree of SHI-RELATED SEQUENCE (SRS) family of *Arabidopsis* and white lupin orthologs. The bootstrap consensus tree was inferred from 1000 replicates. The numbers on the branches indicate the length of the branches, which represents the evolutionary time between two nodes (unit: substitution per site).

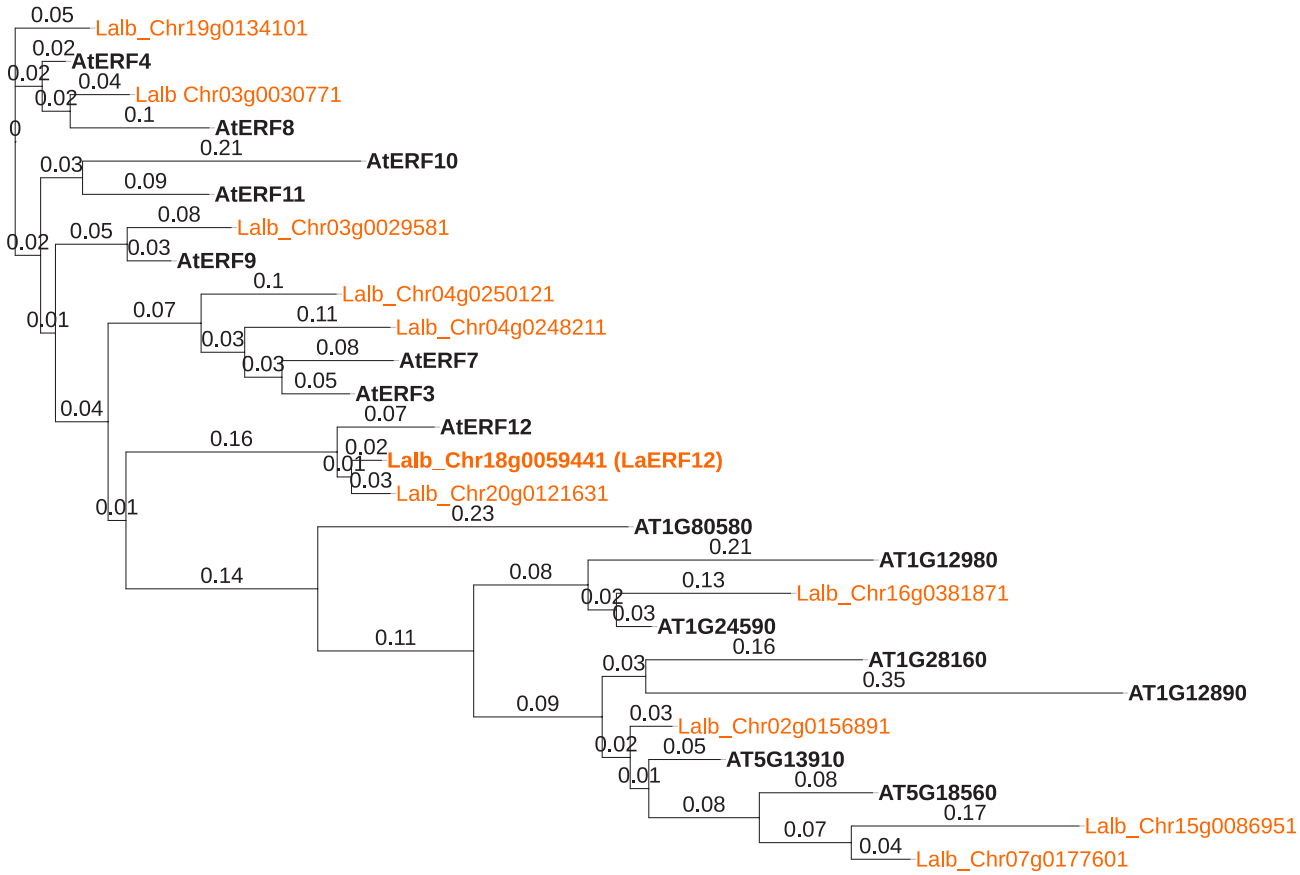

Fig. S8. Phylogenetic tree of the AP2/EREB subfamily VIII/B1 of *Arabidopsis* and white lupin orthologs. The bootstrap consensus tree was inferred from 1000 replicates. The numbers on the branches indicate the length of the branches, which represents the evolutionary time between two nodes (unit: substitution per site).

Gene name	Gene name identifier (ID number)	Primer name	Primer sequence (5’ -> 3’)
LaLBD16	Lalb_Chr06g0162491	LaLBD16-F	TTCTAGATCCAGATCGAGGTTATAGTTCCTCTGCATC
LaLBD16	Lalb_Chr06g0162491	LaLBD16-R	TTCTAGATCCAGATCGAGGTTATAGTTCCTCTGCATC
LaLBD29	Lalb_Chr02g0142291	LaLBD29-F	TACAAAAAAGCAGGCTATGATTCACACAAACCTGAAGAG
LaLBD29	Lalb_Chr02g0142291	LaLBD29-R	TTCTAGATCCAGATCGAGATATGATTGATTGTAACCAAAAG
LaMYB124	Lalb_Chr10g0098091	LaMYB124-F	TACAAAAAAGCAGGCTATGCAAGATATGAAGAAAAATCAGCAG
LaMYB124	Lalb_Chr10g0098091	LaMYB124-R	TTCTAGATCCAGATCGAGTAAGCTATGTAGTAGGGTTC
LaPUCHI	Lalb_Chr13g0303751	LaPUCHI-F	TACAAAAAAGCAGGCTATGTCATCCACTTCAGGTGCAT
LaPUCHI	Lalb_Chr13g0303751	LaPUCHI-R	TTCTAGATCCAGATCGAGGAAGAGTGGATGGTATC
LaSTY1	Lalb_Chr23g0266341	LaSTY1-F	TACAAAAAAGCAGGCTATGGCTGGGTTATTCTCTTTAG
LaSTY1	Lalb_Chr23g0266341	LaSTY1-R	TTCTAGATCCAGATCGAGGGATCTTGGGGGTAGG
LaNFY-B5	Lalb_Chr13g0303701	LaNFYB5-F	TACAAAAAAGCAGGCTATGGTGGACAACGTTGTTGGGAGTTG
LaNFY-B5	Lalb_Chr13g0303701	LaNFYB5-R	TTCTAGATCCAGATCGAGGCCTTGTCTTTCAGGGC
LaNAC044	Lalb_Chr14g0362861	LaNAC044-F	TACAAAAAAGCAGGCTATGTTCTACAGGAGCTGGATTATTG
LaNAC044	Lalb_Chr14g0362861	LaNAC044-R	TTCTAGATCCAGATCGAGTAGCCTGTCCATCCAATC
LaERF12	Lalb_Chr18g0059441	LaERF12-F	TACAAAAAAGCAGGCTATGTTCACGGCTTCATCTTCCTC
LaERF12	Lalb_Chr18g0059441	LaERF12-R	TTCTAGATCCAGATCGAGTAGCCACAATGGTGGAGG
-	-	attB1F	GGGGACAAGTTTGTACAAAAAAGCAGGCT
-	-	attB2R	GGGGACCACTTTGTACAAGAAAGCTGGGTTTAAGCGAAACCC
-	-	srdx-R	TGGGTTTAAGCGAAACCCAAACGGAGTTCTAGATCCAGATC

Table S15. List of primers used to create fusion between coding sequence and SRDX sequence

Gene identifier	Gene name	Amplicon length (bp)
Lalb_Chr06g0162491	LaLBD16	646
Lalb_Chr02g0142291	LaLBD29	802
Lalb_Chr10g0098091	LaMYB124	1414
Lalb_Chr13g0303751	LaPUCHI	1072
Lalb_Chr23g0266341	LaSTY1	895
Lalb_Chr13g0303701	LaNFY-B5	415
Lalb_Chr14g0362861	LaNAC044	1207
Lalb_Chr18g0059441	LaERF12	529
Lalb_Chr21g0307221	LaMAKR4	523

Table S16. Size of the coding sequences of the 9 white lupin amplified from cDNA.

Primer name	Primer sequence (5’ -> 3’)
pEN-L1-L2	
M13F	TGTAAAACGACGGCCAGT
M13R	CAGGAAACAGCTATGACCATG
pEX-35S::cds-SRDX	
pK7F	AGAAGACGGCTGCACTGAAC
T-35-Rout	GATTTGTAGAGAGAGACTGG
pEX-35S::MAKR4-RNAi	
p35S-F	TATCCTTCGCAAGACCCTTC
p35-F-out	GATTTGTAGAGAGAGACTGGTG
p35-R-out	TGGAGAGGACTGCAGGAC
Intron-F-out	ACAGTGAAGACACAGAAAGCC
Intron2-R-out	ATTCATATACCAGTTAACGTGTCTC

Table S17. List of primers used for sequencing

Gene name	Gene name identifier (ID number)	Primer name	Primer sequence (5’ -> 3’)
LaRBC	Lalb_Chr25g0281541	LaRBC-F	ATCGCTACAAAGGACGATGC
LaRBC	Lalb_Chr25g0281541	La-RBC-R	TTATCCCGGCAATAATGAGC
LaRBC	Lalb_Chr25g0281541	LaRBC-attB1-F	GGGGCAAGTTTGTACAAAAAAGCAGGCTATCGC TACAAAGGACGATGC
LaRBC	Lalb_Chr25g0281541	LaRBC-attB2-R	CCCCCCACTTTGTACAAGAAAGCTGGGTTTATCC CGGCAATAATGAGC
LaMAKR4	Lalb_Chr21g0307221	LaMAKR4-F	TACAAAAAAGCAGGCTCTTGCAAAACTCCACGAA CACTCC
LaMAKR4	Lalb_Chr21g0307221	LaMAKR4-R	TACAAGAAAGCTGGGTTCATGACAGAATTTGAG GGC
LaMAKR4	Lalb_Chr21g0307221	LaMAKR4-attB1-F	GGGGACAAGTTTGTACAAAAAAGCAGGCT
LaMAKR4	Lalb_Chr21g0307221	LaMAKR4-attB2-R	GGGGACCACTTTGTACAAGAAAGCTGGGT

Table S18. List of primers used to generate the long hairpin for RNAi

DISCUSSION GÉNÉRALE ET PERSPECTIVES

Ce travail de thèse a porté sur les premiers stades de la formation des rootlettes du lupin blanc. Chez cette légumineuse, nous avons fourni une description du développement du primordium de rootlette. Par analogie avec *Arabidopsis*, 8 stades discrets ont été définis au cours de sa formation. L'étude anatomique des RPd a montré que les rootlettes sont initiées en face des pôles de xylème à partir de divisions asymétriques dans plusieurs cellules adjacentes du péricycle. L'analyse détaillée des stades de développement a révélé la présence de divisions additionnelles dans l'endoderme et le cortex de la RPd. La visualisation du patron d'expression spatiotemporel du gène marqueur de la transition G2/M du cycle cellulaire *AtCYCB1;1* et du gène marqueur de l'endoderme *LaSCR1* a confirmé la contribution de ces tissus. L'expression de marqueurs spécifiques de l'endoderme, du cortex et du système vasculaire a montré que les tissus sont différenciés dans le primordium dès le stade VI, soulignant l'importance de la transition entre le stade V et VI pour l'établissement du patron radial de la rootlette.

Afin de montrer la contribution de l'auxine dans la formation de la rootlette, nous avons étudié l'expression tissulaire du rapporteur synthétique DR5. L'expression précoce de ce marqueur au stade I et la mise en place d'un gradient de son expression dans le primordium de rootlette en formation montre que l'auxine est nécessaire pour induire et contrôler l'organogénèse de ces racines, et ce malgré leur croissance déterminée. De plus, la visualisation d'un gradient très clair a permis de montrer que les racines transformées « hairy root » conservent une réponse hormonale proche des racines latérales d'*Arabidopsis*. Dans le but d'étudier les gènes en lien avec l'auxine, nous avons développé une méthode d'échantillonnage originale et avons focalisé notre attention sur deux gènes. Deux homologues des gènes *AtTIR1 (LaTIR1b)* et *AtARF11 (LaARF5)*, impliqués respectivement dans la perception et la signalisation auxinique ont été identifiés chez le lupin blanc. Ces gènes ont été annotés à partir de données RNAseq publiées (Secco *et al.*, 2014) et en l'absence, à ce moment, du génome du lupin blanc. La conservation du profil d'expression entre les gènes *LaTIR1b* et *AtTIR1*, le récepteur de l'AIA chez *Arabidopsis*, a confirmé la mise en place d'un gradient auxinique et la capacité des cellules du primordium de rootlette à percevoir l'auxine. En revanche, l'étude de la séquence protéique de *LaARF5* et de son profil d'expression suggère que ce gène a un rôle répresseur, au cours de la formation des rootlettes.

Dans le but d'identifier des gènes régulateurs de l'initiation et de l'organogénèse du primordium de rootlette, nous avons généré un transcriptome du développement des RPd et

analysé l'expression des gènes associés aux premiers stades de formation des rootlettes. Ces études ont permis d'identifier deux listes de gènes différentiellement exprimés dans la racine protéoïde, en comparaison avec une racine latérale ne formant pas de rootlette. Leur analyse a montré que les gènes surexprimés dans la racine protéoïde et en lien avec les processus développementaux sont majoritairement des gènes impliqués dans la formation et la maintenance du méristème. Une deuxième analyse se focalisant sur les gènes induits précocement a permis l'identification de 9 gènes candidats. L'implication de ces candidats dans la formation des rootlettes a été vérifiée par la fusion de la séquence codante de ces gènes avec le domaine répresseur SRDX et la production de plantes composites exprimant ces transgènes. L'analyse phénotypique du système racinaire de ces plantes a montré que les transgènes *p35S::LaLBD16-SRDX*, *p35S::LaERF12-SRDX*, et *p35S::LaSTY1-SRDX* réduisent significativement le nombre de racines protéoïdes formées. Cela implique que ces gènes pourraient réguler le développement des rootlettes.

I. Le lupin blanc, un modèle pour étudier le développement racinaire

Le système racinaire des plantes se forme de manière continue et présente un haut niveau de plasticité. Cette plasticité permet aux plantes d'explorer efficacement le sol et d'adapter leur architecture en réponse aux changements de l'environnement. Au cours de l'évolution, certaines plantes adaptées aux sols pauvres ont développé la capacité de former des racines protéoïdes. Ces racines, apparues dans une dizaine de familles botaniques, représentent une des adaptations développementales les plus avancées à la carence en phosphate (Dinkelaker *et al.*, 1995; Skene, 2000). Parmi les espèces capables de former les racines protéoïdes, le lupin blanc est l'espèce qui a servi de modèle pour l'étude de leur physiologie et de leur développement (Johnson *et al.*, 1996; Hagström *et al.*, 2001). Contrairement aux autres espèces qui sont majoritairement des plantes pérennes, le lupin blanc est une plante annuelle et constitue une plante d'intérêt agronomique. Des variétés modernes de lupin blanc, comme la variété AMIGA, ont été sélectionnées (Florimond DESPREZ, France, 1985) et montrent plusieurs traits d'intérêts. Parmi ces traits, la rapidité du cycle de vie (6-8 mois), l'homogénéité génétique et la facilité de l'utilisation des graines (absence de

vernalisation, homogénéité de germination) font de cette espèce une plante idéale pour étudier le développement des racines protéoïdes.

Sur le système racinaire du lupin blanc, les racines protéoïdes ont l'avantage de se former 12 jours après le transfert des plantes en hydroponie. La formation des RPd est inductible par l'absence de Pi dans le milieu (Gilbert *et al.*, 2000; P J Hocking and Jeffery, 2004). Ces racines sont initiées en grand nombre (20 à 30 rootlettes par cm) et leur développement peut être prédit. Nous avons ainsi montré que les rootlettes se forment sur la racine secondaire à une distance conservée de 1 à 1.5 cm de la racine primaire (Gallardo *et al.*, 2018). Cette prédictibilité, associée au développement séquentiel des rootlettes, font du lupin une espèce idéale pour étudier les stades précoces de la formation de ces racines. De plus, l'initiation continue des rootlettes, produit des structures formées par un gradient de stades développementaux (Sbabou *et al.*, 2010). Cette caractéristique offre la possibilité de suivre le développement d'une rootlette de son initiation jusqu'à l'arrêt de sa croissance et représente un avantage considérable pour des approches descriptives, comme des études plus moléculaires. Somme toute, le développement des racines protéoïdes du lupin blanc constitue un modèle de choix pour étudier le développement des racines latérales et révéler les mécanismes moléculaires qui régulent leur formation.

La technologie de séquençage des ADNc est un outil puissant pour étudier l'expression globlale des gènes dans les tissus et a permis de révéler l'expression différentielle de milliers de gènes pendant la formation des racines protéoïdes. Plusieurs études RNA-seq réalisées sur des racines protéoïdes entières (O'Rourke *et al.*, 2013a) ou sur des sections (Wang *et al.*, 2014; Secco *et al.*, 2014; Venuti *et al.*, 2019) ont permis d'étudier les bases moléculaires du développement et de la fonction des racines protéoïdes sur des plantes carencées en phosphate ou en fer. Afin d'identifier les mécanismes moléculaires associés aux étapes successives du développement des racines protéoïdes, notre équipe a généré un nouveau transcriptome (2018) en séquençant les transcripts présents dans la zone de l'amas de rootlettes pendant leur formation. Nos résultats montrent que de nombreux facteurs de transcription sont induits pendant les étapes précoces de la formation des rootlettes. Ce jeu de données est une ressource importante pour comprendre quels sont les mécanismes qui régulent le développement des rootlettes, ou pour révéler les régulations plus tardives qui interviennent dans l'arrêt de la croissance des rootlettes et de leur activité méristématique. Le

séquençage du génome du lupin blanc dans notre équipe (2018) a été indispensable à l'étude de ces données en permettant l'annotation des gènes différentiellement exprimés.

Des outils de génétique inverse sont nécessaires pour déterminer le fonctionnement des gènes identifiés par les approches de transcriptomiques. Des études précédentes ont montré que l'expression d'un gène d'intérêt peut être efficacement diminuée par ARN interférent, délivrée via *Agrobacterium rhizogenes*. Cette méthode a notamment été employée pour valider la fonction des gènes *LaMATE* (Uhde-Stone *et al.*, 2005), *LaSCR1* (Sbabou *et al.*, 2010), et *LaGPX-PDE* (Cheng *et al.*, 2011). Cependant, nos résultats montrent que les plantes composites transformées avec *LaMAKR4-RNAi* forment autant de racines protéoïdes que les plantes témoins, suggérant que ce gène ne régule pas le développement des rootlettes. Néanmoins, nous avons pu montrer que la technologie CRES-T peut être employée pour confirmer ou infirmer l'implication des gènes en lien avec la formation des racines protéoïdes. L'utilisation de cet outil a permis d'identifier 3 régulateurs potentiels de l'initiation et/ou du développement du primordium de rootlette. En parallèle de ces approches de génétique inverse, mon équipe d'accueil a produit et criblé une population EMS de lupin blanc pour identifier des mutants chez lesquels la formation des racines protéoïdes serait altérée. Plusieurs mutants produisant de façon constitutive des rootlettes ont déjà été identifiés et des analyses sont en cours pour identifier la/les mutations à l'origine de ces phénotypes via une approche de mapping par sequencing. Cette population pourra également être criblée par TILLING afin d'identifier des mutants pour les gènes d'intérêts mis en évidence dans ce travail de thèse, comme *LaLBD16*, *LaERF12* ou *LaSTY1*. Enfin, parce que des outils comme l'édition du gène via CRISPR/Cas permettent efficacement d'éteindre complétement l'expression des gènes, notre équipe essaye d'établir un protocole de transformation stable et héritable du lupin blanc.

II. Le développement des rootlettes est similaire à celui des racines latérales d'autres légumineuses

Avec l'étude anatomique de la formation des racines protéoïdes, nous avons pu décrire le développement des rootlettes comme une succession de 8 étapes, allant de l'initiation (stade I) à l'émergence (stade VIII). Nos observations ont montré une forte ressemblance entre l'initiation des rootlettes et celle des racines latérales *d'Arabidopsis,* qui ont lieu dans le péricycle. Cependant, dès le stade II, des différences marquantes sont vi-

isibles entre le lupin blanc et la plante modèle. En effet, des divisions sont observées dans l'endoderme (stade II) puis dans le cortex interne de la racine protéoïde (III) suggérant une contribution de ces tissus dans la formation du primordium de rootlette. Ces caractéristiques ont également été rencontrées pendant la formation des racines latérales chez plusieurs légumineuses, ce qui implique une régulation différente de l'organogénèse chez *Arabidopsis* et d'autres dicotylédones.

Chez les plantes à fleurs, les racines latérales sont initiées à partir d'une couche de cellules spécialisées formant le péricycle. Cette couche comprend deux populations de cellules distinctes, en fonction de la proximité des faisceaux vasculaires du phloème ou du xylème (Beeckman and De Smet, 2014). Chez les plantes monocotylédones, en particulier chez certaines espèces de céréales, les racines latérales sont initiées en face des pôles de phloème (Hochholdinger and Zimmermann, 2008). Cependant, chez la plupart des plantes, les sites de formation des primordia de racines latérales apparaissent uniquement dans les cellules du péricycle situées en face des pôles de xylèmes (Nibau *et al.*, 2008). Chez le lupin, comme chez *Arabidopsis* (Dubrovsky *et al.*, 2000), les primordia de racines sont initiés par des divisions dans les cellules fondatrices du péricycle. En effet, nous avons pu observer des primordia de rootlette au stade Ia qui sont formés de 4 cellules centrales flanquées de deux cellules plus larges, indiquant que la première division anticlinale formative est bien conservée entre ces deux espèces.

L'endoderme semble également jouer un rôle important dans la formation des primordia de rootlettes chez le lupin blanc. Nos résultats ont montré que les cellules de l'endoderme de la racine protéoïde se divisent de manière anticline (stade Ib) puis péricline (stade II). Des divisions dans l'endoderme ne constituent pas une exception chez les angiospermes car ces divisions ont été décrites chez plusieurs espèces de monocotylédones y compris l'ail (*Allium cepa*) (Casero *et al.*, 1996) ou l'orge (*Hordeum vulgare*) (Demchenko and Demchenko, 1996) mais également chez plusieurs autres légumineuses comme le pois (*Pisum sativum*) (Lloret *et al.*, 1989), le soja (*Glycine max*) (Byrne *et al.*, 1977) ou la luzerne (*Medicago truncatula*) (Herrbach *et al.*, 2014). Parmi les fougères aquatiques, on trouve également des plantes qui forment des racines latérales uniquement à partir de l'endoderme (De Smet *et al.*, 2006). La contribution de l'endoderme à la formation des primordia de racines latérales serait ainsi plus répandue que le suggère le paradigme formé chez la plante modèle *Arabidopsis*.

Cependant, le rôle exact de ces divisions reste à déterminer. Une des questions les plus importantes est de savoir si ces cellules endodermiques conservent leur identité ou bien deviennent indifférenciées. De façon intéressante, le marqueur SCR, considéré comme un marqueur de l'endoderme, est exprimé chez le lupin du stade II au stade V pendant le développement du primordium de rootlette. Ces résultats montrent que contrairement aux cellules du péricycle (Malamy and Benfey, 1997), ces cellules conservent leur identité et ne se dé-différencient pas pendant les étapes précoces de la formation des rootlettes.

Des divisions anticlines dans le cortex interne sont également visibles dès le stade III de la formation des rootlettes. La contribution du cortex est également retrouvée chez plusieurs espèces de *Fabaceae*, indiquant que cette caractéristique semble plutôt répandue chez cette famille botanique. En effet, il a été observé chez *Medicago* (Herrbach *et al.*, 2014) que le cortex interne se divise alors que, chez le lotier, on retrouve à la fois des divisions dans la couche interne et les couches externes du cortex (Op den Camp *et al.*, 2011). Néanmoins, ces évènements de division ne sont pas uniques aux légumineuses car on les retrouve chez des espèces de *Cucurbitaceae* comme le concombre (*Cucumus sativus*) (Torres-Martínez *et al.*, 2019). La présence de ces divisions pourrait être liée au fait que le primordia de racine doit traverser plusieurs couches de cortex pour émerger de la racine principale. De façon intéressante, ces divisions ne sont pas présentes chez *Arabidopsis* qui présente une structure racinaire très simple. Afin de vérifier cette hypothèse, il serait intéressant de voir comment le primordium de racine latérale se comporte chez des lignées transgéniques surexprimant le gène SHR et formant des couches surnuméraires de cortex (Henry *et al.*, 2017; Nakajima *et al.*, 2001).

La contribution du cortex à la formation du primordium de racine latérale est réminiscente des divisions que l'on peut observer pendant la formation des nodules. Chez les légumineuses, la prolifération du cortex interne contribue de façon significative à la formation des nodules indéterminés, comme chez *Medicago* (Xiao *et al.*, 2014) alors que les divisions qui ont lieu dans le cortex externe sont importantes pour le développement des nodules déterminés (Op den Camp *et al.*, 2011). De façon intéressante, la capacité à noduler a été observé chez une vingtaine d'espèces capables de former des racines protéoïdes (Skene, 1998), suggérant que le programme développemental racinaire peut être détourné pour les symbioses. En effet, chez les lupins, l'infection par des rhizobia comme *Bradyrhizobium sp* se traduit par la formation de nodules indéterminés, d'un type particulier, appelés nodules

lupinoïdes, qui forment des amas nodulaires entourant la racine primaire ou les racines latérales. Cependant, contrairement aux rootlettes, les nodules du lupin blanc se forment uniquement à partir des couches externes de cortex et possèdent un méristème actif comme dans le cas d'une racine latérale (González-Sama *et al.*, 2004). Le développement et le fonctionnement de ces deux organes sont donc globalement différents. Pourtant, chez les nodules lupinoïdes, qui forment généralement plusieurs méristèmes latéraux, l'activité mitotique peut cesser dans les méristèmes situés trop proches d'autres méristèmes (Łotocka *et al.*, 2012). Ces observations indiquent que des programmes génétiques régulent l'arrêt du fonctionnement du méristème, dans le nodule ainsi que dans la rootlette. En effet, ces deux organes peuvent former des méristèmes, lesquels peuvent devenir inactifs.

Une autre caractéristique des rootlettes est leur capacité à former un méristème de racine fonctionnel qui devient rapidement inactif après l'émergence. Pendant l'organogénèse du primordium de rootlette, il est évident que les tissus s'organisent, et les cellules acquièrent une nouvelle identité indiquant la mise en place d'un méristème. En effet, à partir du stade VI, les divisions dans la rootlette deviennent complexes et le patron d'expression du marqueur *LaSCR1* suggère que la division périclinale dans l'initiale du cortex et de l'endoderme a eu lieu. Ainsi, comme chez *Arabidopsis*, la transition entre les stades V et VI semble cruciale pour l'établissement d'un méristème (Goh *et al.*, 2012). Pour confirmer cette hypothèse, il serait intéressant d'utiliser un marqueur du centre quiescent, comme *WOX5* ou *QC25*, pour suivre sa mise en place. Dans le cadre de la thèse de Tamara Le Thanh (2ème année, Directeurs de thèse Patrick Doumas et Laurence Marquès), des analyses sont en cours dans notre équipe pour étudier le profil de différents marqueurs de l'activité méristématique (notamment des homologues d'*AtWOX5*) lors de la formation de la rootlette et devraient permettre de visualiser la formation puis l'extinction de ce méristème.

La comparaison du primordium de rootlette avec le primordium de racine latérale formé chez d'autres légumineuses montre que l'organogénèse de ces racines est très similaire. Chez le lupin, comme chez *Medicago*, la racine se forme en face des pôles de xylème et implique des divisions successives dans les tissus du péricycle, de l'endoderme et du cortex pour donner naissance à un nouvel organe. A cet égard, il apparait important d'étudier la formation des primordia de racines latérales chez le lupin blanc pour déterminer si ces processus développementaux sont conservés entre ces racines et les rootlettes. Cependant, contrairement aux rootlettes, les racines latérales ne forment pas des amas denses sur la racine

primaire. L'utilisation du « lateral root inducible system » (LRIS) consistant à traiter la plante successivement avec un inhibiteur du transport de l'auxine , comme le NPA, puis une auxine synthétique de type NAA, pourra permettre de contrôler l'initiation des racines latérales et de générer le matériel nécessaire à une telle étude (Himanen *et al.*, 2002). Cette approche a déjà fait ses preuves chez le maïs en permettant de déclencher l'initiation quasi-synchrone de RLs et a permis d'identifier des homologues des gènes impliqués dans l'initiation de la racine latérale (Crombez *et al.*, 2016).

III. L'auxine : un acteur central de la formation des rootlettes

Les racines protéoïdes sont formées par un ensemble très dense de rootlettes, proches des ensembles de méristèmes racinaires formés chez le mutant superproducteur d'auxine, *superroot* (Boerjan *et al.*, 1995). Parce que le développement de ces amas implique l'initiation massive et la formation d'un grand nombre de rootlettes, il n'est pas surprenant que la balance auxinique joue un rôle central dans ces processus développementaux (Wang *et al.*, 2015a). Chez la plante modèle, il a été montré que le priming, l'initiation et l'organogénèse du primordium de racine latérale sont des processus dépendant de l'auxine, nécessitant un transport intercellulaire de celle-ci médié par les protéines PINs, la formation d'un gradient et l'activation d'une signalisation auxinique régulant l'activité transcriptionnelle de gènes de réponse à l'auxine (Du and Scheres, 2017a). Il a été confirmé que l'auxine joue un rôle similaire chez le lupin blanc puisque l'application exogène d'auxine aux parties aériennes suffit à promouvoir la formation des racines protéoïdes, en présence d'une forte concentration en Pi qui supprime normalement leur initiation (Gilbert *et al.*, 2000; Skene and James, 2000). Afin d'expliquer l'initiation séquentielle des rootlettes, il a été proposé que les cellules du péricycle primées répondent localement à facteur longitudinal, comme l'augmentation de la concentration en auxine, déclenchant ainsi leur formation (Skene, 2000). En accord avec cette hypothèse, deux études récentes ont suggéré que la synthèse locale d'auxine et sa redistribution le long de la racine protéoïde ont un rôle critique pour leur développement (Meng *et al.*, 2013; Wang *et al.*, 2015a). En effet, la concentration élevée en auxine, ainsi que l'augmentation de l'expression de gènes de biosynthèse, du transport et de la réponse à l'auxine indiquent que l'action locale de l'aux-

ine induit la formation des rootlettes en aval de la signalisation induite par la carence en Pi.

Chez *Arabidopsis*, il a été montré que l'accumulation locale de l'auxine dans les cellules du péricycle est nécessaire et suffisante pour induire la spécification des cellules du péricycle de la racine latérale (Dubrovsky *et al.*, 2000). Dans cette étude, nous avons pu montrer que la perception de l'auxine et l'activation de la réponse à l'auxine corrèlent avec l'initiation et le développement du primordium de rootlette. En effet, nos observations suggèrent l'établissement progressif d'un gradient d'auxine de l'initiation de la rootlette jusqu'à son émergence. De façon surprenante, il semblerait que pendant la formation du primordium, l'auxine s'accumule dans les tissus adjacents du primordium de rootlette, en particulier dans les couches externes de cortex. Chez *Arabidopsis*, l'auxine diffuse de la pointe du primordium aux tissus adjacents (cortex/épiderme) pour réguler l'expression de gènes de remodelage de la paroi via une voie de signalisation impliquant le transporteur d'efflux d'auxine LAX, permettant *in fine* la perte d'adhérence des cellules entourant le primordium (Swarup *et al.*, 2008). On peut émettre l'hypothèse que, de même, chez le lupin, la diffusion progressive de l'auxine du primordium de rootlette aux tissus adjacents permet de faciliter le passage de ce nouvel organe au travers des couches successives de cortex qui le séparent du milieu extérieur. Afin de confirmer cette hypothèse, il sera intéressant de voir si l'auxine a une influence sur la plasticité de la paroi cellulaire. Le suivi de l'expression de gènes de remodelage de la paroi et l'observation du patron d'expression tissulaire de ces gènes pendant l'émergence des rootlettes sont réalisés par François Jobert (post-doc) dans le cadre d'un projet en collaboration avec la Suède (Collaboration avec Stéphanie Robert, UPSC, Umeå, Suède, Projet Kempe INUPRAG 2019-20).

IV. Des gènes maitres du développement?

Les racines protéoïdes sont des racines en forme de goupillons formées par un amas dense de racines tertiaires, et représentent avec les mycorhizes et les nodules, une des adaptations racinaires majeures des plantes pour l'acquisition efficace des nutriments (Skene, 1998). Ces organes sont formés par des espèces de plantes exposées à une faible disponibilité du Pi, et s'installent dans des environnements degradés, où elle sont considérées comme des espèces pionnières (Skene, 2000). Plusieurs espèces qui développent des racines protéoïdes

sont capables de former des symbioses fixatrices d'azote via l'association avec *Frankia* ou des *Rhizobia*. Cependant, la majorité des espèces qui peuvent former ces racines ont perdu la capacité à former des mycorhizes (Barbara *et al.*, 1995). Il semblerait que les plantes qui ne mycorhizent pas aient perdu la capacité à s'associer à des champignons pour des raisons environnementales ayant par la suite entrainé une perte des gènes de mycorhization, cette perte est estimée à 12-14 millions d'années pour le lupin blanc. Par la suite, l'absence de mycorhization aurait renforcé la nécessité de développer un nouveau mécanisme efficace pour améliorer la nutrition minérale, notamment phosphatée. En effet, la rapidité du développement des racines protéoïdes pourrait être un avantage dans les climats arides, où de courtes périodes de précipitation empêche l'établissement de mycorhizes fonctionnelles (Neumann and Martinoia, 2002). Cela explique pourquoi de nombreuses espèces produisant des racines protéoïdes sont principalement distribuées dans les régions de l'hémisphère sud, comme l'Afrique du Sud ou l'Australie.

Les racines protéoïdes sont produites par toutes les espèces de la famille des *Proteaceae* mais ont également été retrouvées dans un large éventail de famille botaniques (*Fabaceae*, *Betulaceae*, *Myricaceae*, *Elagnaceae*, *Casuarinaceae*, *Moraceae*) (Skene, 2000). Puisque les racines protéoïdes sont formées par de nombreuses espèces de plantes, une des questions les plus intéressantes est de savoir si des régulateurs uniques existent ou non chez ces espèces. En effet, la présence des racines protéoïdes chez des familles botaniques éloignées indique la possibilité que les racines protéoïdes aient pu être formées indépendamment chez ces espèces, et requiert l'expression finement régulée d'un nombre limité de gènes. Au contraire, le fait que les racines protéoïdes soient formées par ces espèces en réponse à des stimuli environnementaux précis, comme une carence en nutriment (Pi ou Fe), ou l'application exogène d'auxine suggère qu'une combinaison favorable de l'expression de gènes importants pour la formation des racines et la signalisation hormonale pourraient être le déterminant central de leur développement.

Afin de révéler les mécanismes moléculaires qui contrôlent la formation des racines protéoïdes, nous nous sommes intéressés aux gènes différentiellement exprimés au cours des stades précoces de leur développement. Pour ce faire, nous avons identifié l'ensemble des gènes surexprimés ou sous-exprimés dans la racine protéoïde par rapport à une racine latérale, ainsi que deux groupes de gènes exprimés spécifiquement au cours des étapes précoces de leur formation. Parce que les facteurs de transcriptions sont capables de réguler

simultanément l'expression de nombreux gènes et sont des régulateurs clés de nombreuses fonctions, nous avons focalisé notre attention sur cette catégorie de protéines. Cette approche a permis l'identification de 62 facteurs de transcription fortement exprimés dans la racine protéoïde par rapport à la racine latérale et 62 FTs spécifiquement exprimés dans les stades précoces de la formation des rootlettes. De façon intéressante, un certain nombre de ces FTs sont connus pour réguler l'initiation, le développement et le fonctionnement du méristème de racines latérales, indiquant qu'au moins une partie du programme développemental de racine latérale est recrutée pendant le développement des rootlettes. En effet, le développement des rootlettes semble impliquer au moins un des deux modules de la signalisation auxinique déclenchant l'initiation via *ARF5* et requiert l'expression de plusieurs cibles en aval de cette signalisation (LBD16, PUCHI). Plus tardivement, l'activation de *WOX5* et plusieurs protéines *PLETHORA* (PLT1, PLT2 et PLT4) qui contribuent à la formation de méristèmes *de novo* et au maintien de l'identité des cellules souches, suggère qu'un méristème est bien formé dans le primordium de rootlette, malgré l'arrêt rapide de son activité après l'émergence. En plus de ces gènes, de nombreux FTs pour lequel aucun lien n'a été établi avec la formation d'une racine sont exprimés. Il ne peut pas être exclu que ces gènes puissent jouer un rôle dans le développement des rootlettes.

Afin de déterminer si plusieurs de ces FTs sont des régulateurs participant au développement des rootlettes, nous avons initié une approche de génétique inverse. Chez les plantes, la redondance structurelle et fonctionnelle constitue un frein à l'identification de la fonction des facteurs de transcription, et plus particulièrement chez le lupin qui a subi une triplication de son génome (Hufnagel *et al.*, 2019). Pour surmonter ces difficultés, nous avons converti ces facteurs de transcription en répresseurs en les fusionnant avec le domaine répresseur SRDX. L'expression ectopique de ces protéines chimériques répressives a été utilisée pour induire un phénotype dominant négatif. Trois des lignées transgéniques produites montrent une réduction de la formation des racines protéoïdes, indiquant que ces gènes pourraient agir comme des régulateurs du développement de ces racines. En particulier, le phénotype des plantes transgéniques *p35S::LaLBD16-SRDX*, qui expriment un gène majeur contrôlant la première division, suggère que le transgène a effectivement altéré la formation de racines protéoïdes. En parallèle, l'obtention de phénotypes similaires chez les lignées transgéniques *p35S::LaSTY1-SRDX* et *p35S::LaERF12-SRDX*, indique que la formation des rootlettes serait positivement régulée par l'auxine et l'éthylène.

Afin de confirmer la fonction de ces 3 candidats, il est important d'identifier des lignées mutantes et voir si ces mutants sont affectés dans la formation des rootlettes. Ceci peut être réalisé par la production d'une population de TILLING et la mise en place d'un crible pour l'identification de mutants. Cette stratégie est actuellement mise en œuvre par l'équipe avec la création d'une petite population de 600 familles M2 (collaboration Adnane Boualem/Marion Dalmais, Plateforme EPITRANS, IPS2, Saclay). Dans le cadre du projet MicroLUP (ANR 2020-2024), cette population de TILLING sera étendue à environ 2500 familles pour augmenter les chances d'obtenir des mutants. Une étude fonctionelle plus fine pourra être envisagée grâce à ce matériel végétal et pourra alors initier un programme de recherche visant à décortiquer le rôle de ces gènes, en lien étroit avec la caractérisation des mutants EMS surproduisant constitutivement des racines protéoïdes (Projet ERC LUPIN ROOTS 2015-2020). L'identification des gènes régulant la formation des rootlettes permettra de tester le transfert horizontal de programmes développementaux potentiellement impliqués dans la formation des racines protéoïdes, ce qui permet d'envisager que ces structures puissent être transférées dans le futur à d'autres espèces cultivées.

ANNEXES : PUBLICATIONS, COMMUNICATIONS ET FORMATIONS

LISTE DE PUBLICATIONS

Anatomical and hormonal description of rootlet primordium development along white lupin cluster root. C. Gallardo, B. Hufnagel, C. Casset, C. Alcon, F. Garcia, F. Divol, L. Marquès, P. Doumas and B. Péret. Physiologia plantarum, 2018. doi: 10.1111/ppl.12714

COMMUNICATIONS ORALES

Histological and transcriptomic analysis of cluster root development in white lupin. C. Gallardo, B. Hufnagel, C. Casset, C. Alcon, F. Garcia, F. Divol, L. Marquès, P. Doumas and B. Péret. Lateral root workshop, Montpellier, France, 2017.

White lupin cluster root, a model to understand lateral root developmental adaptations. C. Gallardo, B. Hufnagel, Q. Rigal, A. Soriano, C. Alcon, B. Péret. IX International Conference on Legume Genetics and Genomics (ICLGG), Dijon, France, 2019

POSTER

The hidden legume roots: cluster root development in white lupin. C. Gallardo, B. Hufnagel, Q. Rigal, A. Soriano, B. Péret. IX International Conference on Legume Genetics and Genomics (ICLGG), Dijon, France, 2019

FORMATIONS

- Catégorie : Enseignement

Service d'enseignement du contrat doctoral. Enseignement de la Physiologie végétale et de la biologie cellulaire. Octobre à Décembre 2016. Université de Montpellier, France.

Nombre d'heures enregistrées: 64 h

- Catégorie: Communication.

International conference on legume genetics and genomics. Du 13 au 17 mai 2019. Dijon, France.

Nombre d'heures enregistrées: 12 h

- Catégorie: Communication.

Lateral root workshop. Du 13 au 17 mai 2019. Dijon, France.

Nombre d'heures enregistrées: 12 h

- Catégorie : Ouverture à l'interdisciplinarité

Winter School, Biology at different scales, an interplay between physics and biology. Du 13 au 24 mars 2017. Les Houches, France.

Nombre d'heures enregistrées: 25 h

- Catégorie : Éthique et intégrité scientifique

Formation à l'éthique de la recherche et à l'intégrité scientifique. Le 6 novembre 2017. Montpellier, France.

Nombre d'heures enregistrées: 7 h

- Catégorie : interdisciplinarité

MOOC Biodiversité et changement globaux. Du 04 au 23 octobre 2017. Université Virtuelle Environnement & Développement Durable (UVED).

Nombre d'heures enregistrées: 25 h

- Catégorie : Journée Doctorale

Présentation de l'école doctorale GAIA pour les premières années. Le 12 janvier 2017, Montpellier, France.

Nombre d'heures enregistrées: 2 h

Total d'heures enregistrées : 147 h / 7 formations

RÉFÉRENCES

A

Abdolzadeh, A., Wang, X., Veneklaas, E.J., and Lambers, H. (2010). Effects of phosphorus supply on growth, phosphate concentration and cluster-root formation in three Lupinus species. *Ann. Bot*. 105: 365–374.

Abualia, R., Benkova, E., and Lacombe, B. (2018). Transporters and Mechanisms of Hormone Transport in Arabidopsis. Adv. Bot. Res. 87: 115–138.

Adamowski, M. and Friml, J. (2015). PIN-Dependent Auxin Transport: Action, Regulation, and Evolution. Plant Cell Online 27: 20–32.

Aida, M., Beis, D., Heidstra, R., Willemsen, V., Blilou, I., Galinha, C., Nussaume, L., Noh, Y.S., Amasino, R., and Scheres, B. (2004). The PLETHORA genes mediate patterning of the Arabidopsis root stem cell niche. Cell 119: 119–120.

B

Bainbridge, K., Guyomarc'h, S., Bayer, E., Swarup, R., Bennett, M., Mandel, T., and Kuhlemeier, C. (2008). Auxin influx carriers stabilize phyllotactic patterning. Genes Dev. 22: 810–823.

Balzergue, C. et al. (2017). Low phosphate activates STOP1-ALMT1 to rapidly inhibit root cell elongation. Nat. Commun. 8: 15300.

Banda, J., Bellande, K., von Wangenheim, D., Goh, T., Guyomarc'h, S., Laplaze, L., and Bennett, M.J. (2019). Lateral Root Formation in Arabidopsis: A Well-Ordered LRexit. Trends Plant Sci.: 1–14.

Banno, H., Ikeda, Y., Niu, Q.W., and Chua, N.H. (2001). Overexpression of Arabidopsis ESR1 induces initiation of Shoot Regeneration. Plant Cell 13: 2609–2618.

Barbara, D., Christine, H., and H., M. (1995). Distribution and Function of Proteoid Roots and other Root Clusters. Bot. Acta 108: 183–200.

Barbez, E. and Kleine-Vehn, J. (2013). Divide Et Impera-cellular auxin compartmentalization. Curr. Opin. Plant Biol. 16: 78–84.

Baylis, T., Cierlik, I., Sundberg, E., and Mattsson, J. (2013). SHORT INTERNODES/STYLISH genes, regulators of auxin biosynthesis, are involved in leaf vein development in Arabidopsis thaliana. New Phytol. 197: 737–750.

Beeckman, T., Burssens, S., Inze, D., Moleculaire, V., Plantengenetica, D., and Interuniversitair, V. (2001). Peri-Cell Cycle. J. Exp. Bot. 52: 403–411.

Beeckman, T. and De Smet, I. (2014). Pericycle. Curr. Biol. 24: R378–R379.

Bell, J.K. and McCully, M.E. (1970). A histological study of lateral root initiation and development in Zea mays. Protoplasma 70: 179–205.

Benková, E., Michniewicz, M., Sauer, M., Teichmann, T., Seifertová, D., Jürgens, G., and Friml, J. (2003). Local, Efflux-Dependent Auxin Gradients as a Common Module for Plant Organ Formation. Cell 115: 591–602.

Berckmans, B. et al. (2011). Auxin-Dependent Cell Cycle Reactivation through Transcriptional Regulation of Arabidopsis E2Fa by Lateral Organ Boundary Proteins. Plant Cell 23: 3671–3683.

Bestor, T.H. (1998). Gene silencing: Methylation meets acetylation. Nature 393: 311.

Bhalerao, R.P., Eklöf, J., Ljung, K., Marchant, A., Bennett, M., and Sandberg, G. (2002). Shoot-derived auxin is essential for early lateral root emergence in Arabidopsis seedlings. Plant J. 29: 325–332.

Blilou, I., Xu, J., Wildwater, M., Willemsen, V., Paponov, I., Friml, J., Heldstra, R., Aida, M., Palme, K., and Scheres, B. (2005). The PIN auxin efflux facilitator network controls growth and patterning in Arabidopsis roots. Nature 433: 39–44.

Boer, D.R., Freire-Rios, A., Van Den Berg, W.A.M., Saaki, T., Manfield, I.W., Kepinski, S., López-Vidrieo, I., Franco-Zorrilla, J.M., De Vries, S.C., Solano, R., Weijers, D., and Coll, M. (2014). Structural basis for DNA binding specificity by the auxin-dependent ARF transcription factors. Cell **156**: 577–589.

Boerjan, W., Cervera, M.T., Delarue, M., Beeckman, T., Dewitte, W., Bellini, C., Caboche, M., Van Onckelen, H., Van Montagu, M., and Inzé, D. (1995). Superroot, a recessive mutation in Arabidopsis, confers auxin overproduction. Plant Cell **7**: 1405–1419.

Bournier, M., Tissot, N., Mari, S., Boucherez, J., Lacombe, E., Briat, J.F., and Gaymard, F. (2013). Arabidopsis ferritin 1 (AtFer1) gene regulation by the phosphate starvation response 1 (AtPHR1) transcription factor reveals a direct molecular link between iron and phosphate homeostasis. J. Biol. Chem. **288**: 22670–22680.

Braum, S.M. and Helmke, P.A. (1995). White lupin utilizes soil phosphorus that is unavailable to soybean. Plant Soil **176**: 95–100.

Brunoud, G., Wells, D.M., Oliva, M., Larrieu, A., Mirabet, V., Burrow, A.H., Beeckman, T., Kepinski, S., Traas, J., Bennett, M.J., and Vernoux, T. (2012). A novel sensor to map auxin response and distribution at high spatio-temporal resolution. Nature **482**: 103–106.

Byrne, J.M., Pesacreta, T.C., and Fox, J.A. (1977). Development and Structure of the Vascular Connection between the Primary and Secondary Root of Glycine max (L.) Merr. Am. J. Bot. **64**: 946–959.

C

Cambridge, A.P. and Morris, D.A. (1996). Transfer of exogenous auxin from the phloem to the polar auxin transport pathway in pea (Pisum sativum L.). Planta **199**: 583–588.

Casanova-Sáez, R. and Voß, U. (2019). Auxin Metabolism Controls Developmental Decisions in Land Plants. Trends Plant Sci. **24**: 741–754.

Casero, P.J., Casimiro, I., and Lloret, P.G. (1996). Pericycle proliferation pattern during the lateral root initiation in adventitious roots of Allium cepa. Protoplasma **191**: 136–147.

Casimiro, I., Beeckman, T., Graham, N., Bhalerao, R., Zhang, H., Casero, P., Sandberg, G., and Bennett, M.J. (2003). Dissecting Arabidopsis lateral root development. Trends Plant Sci. **8**: 165–171.

Casimiro, I., Marchant, A., Bhalerao, R.P., Beeckman, T., Dhooge, S., Swarup, R., Graham, N., Inzé, D., Sandberg, G., Casero, P.J., and Bennett, M. (2001). Auxin transport promotes Arabidopsis lateral root initiation. Plant Cell **13**: 843–52.

Chandler, J.W. (2016). Auxin response factors. Plant Cell Environ. **39**: 1014–1028.

Chandler, J.W. (2011). Founder cell specification. Trends Plant Sci. **16**: 607–613.

Chapman, E.J. and Estelle, M. (2009). Mechanism of Auxin-Regulated Gene Expression in Plants. Annu. Rev. Genet. **43**: 265–285.

Chen, Q. et al. (2015). A coherent transcriptional feed-forward motif model for mediating auxin-sensitive PIN3 expression during lateral root development. Nat. Commun. **6**.

Cheng, L., Bucciarelli, B., Liu, J., Zinn, K., Miller, S., Patton-Vogt, J., Allan, D., Shen, J., and Vance, C.P. (2011). White Lupin Cluster Root Acclimation to Phosphorus Deficiency and Root Hair Development Involve Unique Glycerophosphodiester Phosphodiesterases. Plant Physiol. **156**: 1131–1148.

Cho, M. and Cho, H.T. (2013). The function of ABCB transporters in auxin transport. Plant Signal. Behav. **8**: 6–9.

Chou, S.T., Khandros, E., Bailey, L.C., Nichols, K.E., Vakoc, C.R., Yao, Y., Huang, Z., Crispino, J.D., Hardison, R.C., Blobel, G.A., and Weiss, M.J. (2009). Graded repression of PU.1/Sfpi1 gene transcription by GATAfactors regulates hematopoietic cell fate. Blood **114**: 983–994.

Clowes, F.A.L. (1978). Chimeras and the Origin of Lateral Root Primordia in Zea mays. Ann. Bot. **42**: 801–807.

Colón-Carmona, A., You, R., Haimovitch-Gal, T., and Doerner, P. (1999). Spatio-temporal analysis of mitotic activity with a labile cyclin-GUS fusion protein. Plant J. **20**: 503–508.

Cripps, R.M. and Olson, E.N. (2002). Control of cardiac development by an evolutionarily conserved transcriptional network. Dev. Biol. **246**: 14–28.

Criscuolo, A. and Gribaldo, S. (2010). BMGE (Block Mapping and Gathering with Entropy): A new software for selection of phylogenetic informative regions from multiple sequence alignments. BMC Evol. Biol. **10**: 210.

Crombez, H., Roberts, I., Vangheluwe, N., Motte, H., Jansen, L., Beeckman, T., and Parizot, B. (2016). Lateral root inducible system in arabidopsis and maize. JoVE (Journal Vis. Exp.: e53481.

Cu, S.T.., Hutson, J., and Schuller, K.A. (2005a). Mixed culture of wheat (Triticum aestivum L.) with white lupin (Lupinus albus L.) improves the growth and phosphorus nutrition of the wheat. Plant Soil **272**: 143–151.

D

Demchenko, K.N. and Demchenko, N.P. (2001). Changes of root structure in connection with the development of lateral root primordia in wheat and pumpkins. In Recent Advances of Plant Root Structure and Function (springer: Dordrecht), pp. 39–47.

Demchenko, K.N. and Demchenko, N.P. (1996). Early stages of lateral root development in Triticum aestivum L. Acta Phytogeogr. Suec. **81**: 71–75.

Dharmasiri, N., Dharmasiri, S., and Estelle, M. (2005). The F-box protein TIR1 is an auxin receptor. Nature **435**: 441–445.

Diem, H.G., Duhoux, E., Zaid, H., and Arahou, M. (2000). Cluster Roots in Casuarinaceae: Role and Relationship to Soil Nutrient Factors. Ann. Bot. **85**: 929–936.

Dinkelaker, B., Hengeler, C., and Marschner, H. (1995). Distribution and function of proteoid roots and other root clusters. Acta Bot. **108**: 169–276.

Dinkelaker, B., Römheld, V., and Marschner, H. (1989). Citric acid excretion and precipitation of calcium citrate in the rhizosphere of white lupin (Lupinus albus L.). Plant, Cell Environ. **12**: 285–292.

Dolan, L., Janmaat, K., Willemsen, V., Linstead, P., Poethig, S., Roberts, K., and Scheres, B. (1993). Cellular organisation of the Arabidopsis thaliana root. Development **119**: 71–84.

Du, Y. and Scheres, B. (2017a). Lateral root formation and the multiple roles of auxin. J. Exp. Bot. **69**: 155–167.

Du, Y. and Scheres, B. (2017b). PLETHORA transcription factors orchestrate de novo organ patterning during *Arabidopsis* lateral root outgrowth. Proc. Natl. Acad. Sci. **114**: 201714410.

Dubos, C., Stracke, R., Grotewold, E., Weisshaar, B., Martin, C., and Lepiniec, L. (2010). MYB transcription factors in Arabidopsis. Trends Plant Sci. **15**: 573–581.

Dubrovsky, J.G., Doerner, P.W., Colón-Carmona, A., and Rost, T.L. (2000). Pericycle cell proliferation and lateral root initiation in Arabidopsis. Plant Physiol. **124**: 1648–1657.

Dubrovsky, J.G., Sauer, M., Napsucialy-Mendivil, S., Ivanchenko, M.G., Friml, J., Shishkova, S., Celenza, J., and Benkova, E. (2008). Auxin acts as a local morphogenetic trigger to specify lateral root founder cells. Proc. Natl. Acad. Sci. **105**: 8790–8794.

E

Eklund, D.M., Ståldal, V., Valsecchi, I., Cierlik, I., Eriksson, C., Hiratsu, K., Ohme-Takagi, M.,

Sundström, J.F., Thelander, M., Ezcurra, I., and Sundberg, E. (2010a). The Arabidopsis thaliana STYLISH1 protein acts as a transcriptional activator regulating auxin biosynthesis. Plant Cell **22**: 349–363.

Epstein, E., Cohen, J.D., and Slovin, J.P. (2002). The biosynthetic pathway for indole-3-acetic acid changes during tomato fruit development. Plant Growth Regul. **38**: 15–20.

F

Feng, Z., Sun, X., Wang, G., Liu, H., and Zhu, J. (2012). LBD29 regulates the cell cycle progression in response to auxin during lateral root formation in Arabidopsis thaliana. Ann. Bot. **110**: 1–10.

Forzani, C., Aichinger, E., Sornay, E., Willemsen, V., Laux, T., Dewitte, W., and Murray, J.A.H. (2014). WOX5 suppresses CYCLIN D activity to establish quiescence at the Center of the root stem cell niche. Curr. Biol. **24**: 1939–1944.

Franco-Zorrilla, J.M., Martin, A.C., Solano, R., Rubio, V., Leyva, A., and Paz-Ares, J. (2002). Mutations at CRE1 impair cytokinin-induced repression of phosphate starvation responses in Arabidopsis. Plant J. **32**: 353–360.

Friml, J., Benková, E., Blilou, I., Wisniewska, J., Hamann, T., Ljung, K., Woody, S., Sandberg, G., Scheres, B., Jürgens, G., and Palme, K. (2002). AtPIN4 mediates sink-driven auxin gradients and root patterning in Arabidopsis. Cell **108**: 661–673.

Fukaki, H., Tameda, S., Masuda, H., and Tasaka, M. (2002). Lateral root formation is blocked by a gain-of-function mutation in the solitary-root/IAA14 gene of Arabidopsis. Plant J. **29**: 153–168.

Fukaki, H. and Tasaka, M. (2009). Hormone interactions during lateral root formation. Plant Mol. Biol. **69**: 437–449.

G

Galinha, C., Hofhuis, H., Luijten, M., Willemsen, V., Blilou, I., Heidstra, R., and Scheres, B. (2007). PLETHORA proteins as dose-dependent master regulators of Arabidopsis root development. Nature **449**: 1053–1057.

Gallardo, C., Hufnagel, B., Casset, C., Alcon, C., Garcia, F., Divol, F., Marquès, L., Doumas, P., and Péret, B. (2018). Anatomical and hormonal description of rootlet primordium development along white lupin cluster root. Physiol. Plant.

Gilbert, G., Knight, J.D., Vance, C.P., and Allan, D.L. (2000). Proteoid Root Development of Phosphorus Deficient Lupin is Mimicked by Auxin and Phosphonate. Ann. Bot. **85**: 921–928.

Goh, T. et al. (2019). Lateral root initiation requires the sequential induction of transcription factors LBD16 and PUCHI in Arabidopsis thaliana. New Phytol.

Goh, T., Joi, S., Mimura, T., and Fukaki, H. (2012). The establishment of asymmetry in Arabidopsis lateral root founder cells is regulated by LBD16/ASL18 and related LBD/ASL proteins. Development **139**: 883–893.

Goh, T., Toyokura, K., Wells, D.M., Swarup, K., Yamamoto, M., Mimura, T., Weijers, D., Fukaki, H., Laplaze, L., Bennett, M.J., and Guyomarc'h, S. (2016). Quiescent center initiation in the Arabidopsis lateral root primordia is dependent on the SCARECROW transcription factor. Development **143**: 3363–3371.

Goldsmith, M.H.M. (1997). The Polar Transport of Auxin. Annu. Rev. Plant Physiol. **28**: 439–478.

Gonzalez-Rizzo, S., Crespi, M., and Frugier, F. (2006). The Medicago truncatula CRE1 Cytokinin Receptor Regulates Lateral Root Development and Early Symbiotic Interaction with Sinorhizobium meliloti. The Plant Cell. **18**: 2680–2693.

González-Sama, A., Lucas, M.M., De Felipe, M.R., and Pueyo, J.J. (2004). An unusual infection mechanism and nodule morphogenesis in white lupin (Lupinus albus). New Phytol. **163**: 371–380.

Gray, W.M., Hellmann, H., Dharmasiri, S., and Estelle, M. (2002). Role of the Arabidopsis RING-H2 protein RBX1 in RUB modification and SCF function. Plant Cell **14**: 2137–44.

Gray, W.M., Kepinski, S., Rouse, D., Leyser, O., and Estelle, M. (2001). Auxin regulates SCFTIR1-dependent degradation of AUX/IAA proteins. Nature **414**: 271–276.

Gray, W.M., Walker, L., Hobbie, L., Risseeuw, E., Banks, T., Crosby, W.L., Yang, M., and Estelle, M. (1999). Identification of an SCF ubiquitin–ligase complex required for auxin response in Arabidopsis thaliana. Genes Dev. **13**: 1678–1691.

Grones, P., Chen, X., Simon, S., Kaufmann, W.A., De Rycke, R., Nodzyński, T., Zažímalová, E., and Friml, J. (2015). Auxin-binding pocket of ABP1 is crucial for its gain-of-function cellular and developmental roles. J. Exp. Bot. **66**: 5055–5065.

Grones, P. and Friml, J. (2015). Auxin transporters and binding proteins at a glance. J. Cell Sci. **128**: 1–7.

Grunewald, W. and Friml, J. (2010). The march of the PINs: Developmental plasticity by dynamic polar targeting in plant cells. EMBO J. **29**: 2700–2714.

Guilfoyle, T.J. and Hagen, G. (2007). Auxin response factors. Curr. Opin. Plant Biol. **10**: 453–460.

Guilfoyle, T.J., Ulmasov, T., and Hagen, G. (1998). The ARF family of transcription factors and their role in plant hormone-responsive transcription. Cell. Mol. Life Sci. **54**: 619–627.

H

Hagen, G. and Guilfoyle, T. (2002). Auxin-responsive gene expression: Genes, promoters and regulatory factors. Plant Mol. Biol. **49**: 373–385.

Hagström, J., James, W.M., and Skene, K.R. (2001). A comparison of structure, development and function in cluster roots of Lupinus albus L. under phosphate and iron stress. Plant Soil **232**: 81–90.

Hammond, J.P. and White, P.J. (2008). Sucrose transport in the phloem: Integrating root responses to phosphorus starvation. J. Exp. Bot. **59**: 93–109.

Hammond, J.P. and White, P.J. (2011). Sugar Signaling in Root Responses to Low Phosphorus Availability. Plant Physiol. **156**: 1033–1040.

Hardtke, C.S., Ckurshumova, W., Vidaurre, D.P., Singh, S.A., Stamatiou, G., Tiwari, S.B., Hagen, G., Guilfoyle, T.J., and Berleth, T. (2004). Overlapping and non-redundant functions of the Arabidopsis auxin response factors MONOPTEROS and NONPHOTOTROPIC HYPOCOTYL 4. Development **131**: 1089–1100.

Henry, S., Dievart, A., Divol, F., Pauluzzi, G., Meynard, D., Swarup, R., Wu, S., Gallagher, K.L., and Périn, C. (2017). SHR overexpression induces the formation of supernumerary cell layers with cortex cell identity in rice. Dev. Biol. **425**: 1–7.

Hermans, C., Hammond, J.P., White, P.J., and Verbruggen, N. (2006). How do plants respond to nutrient shortage by biomass allocation? Trends Plant Sci. **11**: 610–617.

Herrbach, V., Remblière, C., Gough, C., and Bensmihen, S. (2014). Lateral root formation and patterning in Medicago truncatula. J. Plant Physiol. **171**: 301–310.

Himanen, K., Boucheron, E., Vanneste, S., Engler, J. de A., Inzé, D., and Beeckman, T. (2002). Auxin-Mediated Cell Cycle Activation during Early Lateral Root Initiation. Plant Cell **14**: 2339–2351.

Hinsinger, P., Brauman, A., Devau, N., Gérard, F., Jourdan, C., Laclau, J.P., Le Cadre, E., Jaillard, B., and Plassard, C. (2011). Acquisition of phosphorus and other poorly mobile nutrients by roots. Where do plant nutrition models fail? Plant Soil **348**: 29–61.

Hiratsu, K., Mitsuda, N., Matsui, K., and Ohme-Takagi, M. (2004). Identification of the minimal repression domain of SUPERMAN shows that the DLELRL hexapeptide is both necessary and sufficient for repression of transcription in Arabidopsis. Biochem. Biophys. Res. Commun. 321: 172–178.

Hirota, A., Kato, T., Fukaki, H., Aida, M., and Tasaka, M. (2007). The Auxin-Regulated AP2/EREBP Gene PUCHI Is Required for Morphogenesis in the Early Lateral Root Primordium of Arabidopsis. Plant Cell Online 19: 2156–2168.

Hochholdinger, F., Park, W.J., Sauer, M., and Woll, K. (2004). From weeds to crops: Genetic analysis of root development in cereals. Trends Plant Sci. 9: 42–48.

Hochholdinger, F. and Zimmermann, R. (2008). Conserved and diverse mechanisms in root development. Curr. Opin. Plant Biol. 11: 70–74.

Hocking, P.J. and Jeffery, S. (2004). Cluster-root production and organic anion exudation in a group of old-world lupins and a new-world lupin. Plant Soil 258: 135–150.

Hodge, A. (2004). The plastic plant: Root responses to heterogeneous supplies of nutrients. New Phytol. 162: 9–24.

Hofhuis, H., Laskowski, M., Du, Y., Prasad, K., Grigg, S., Pinon, V., and Scheres, B. (2013). Phyllotaxis and rhizotaxis in Arabidopsis are modified by three plethora transcription factors. Curr. Biol. 23: 956–962.

Hufnagel, B. et al. (2019). Genome sequence of the cluster root forming white lupin. bioRxiv: 708917.

I

Ilina, E.L., Kiryushkin, A.S., Semenova, V.A., Demchenko, N.P., Pawlowski, K., and Demchenko, K.N. (2018). Lateral root initiation and formation within the parental root meristem of Cucurbita pepo: Is auxin a key player? Ann. Bot. 122: 873–888.

Ivanchenko, M.G., Coffeen, W.C., Lomax, T.L., and Dubrovsky, J.G. (2006). Mutations in the Diageotropica (Dgt) gene uncouple patterned cell division during lateral root initiation from proliferative cell division in the pericycle. Plant J. 46: 436–447.

Ivanchenko, M.G., Muday, G.K., and Dubrovsky, J.G. (2008). Ethylene-auxin interactions regulate lateral root initiation and emergence in Arabidopsis thaliana. Plant J. 55: 335–347.

Ivanov, V.B. and Dubrovsky, J.G. (2013). Longitudinal zonation pattern in plant roots: Conflicts and solutions. Trends Plant Sci. 18: 237–243.

Jain, A., Poling, M.D., Karthikeyan, A.S., Blakeslee, J.J., Peer, W.A., Titapiwatanakun, B., Murphy, A.S., and Raghothama, K.G. (2007). Differential Effects of Sucrose and Auxin on Localized Phosphate Deficiency-Induced Modulation of Different Traits of Root System Architecture in Arabidopsis. PLANT Physiol. 144: 232–247.

J

Jansen, L., Roberts, I., de Rycke, R., and Beeckman, T. (2012). Phloem-associated auxin response maxima determine radial positioning of lateral roots in maize. Philos. Trans. R. Soc. B Biol. Sci. 367: 1525–1533.

Jenik, P.D. and Barton, M.K. (2005). Surge and destroy : the role of auxin in plant embryogenesis. Development 132: 3577–3585.

Johnson, J.F., Vance, C.P., and Allan, D.L. (1996). Phosphorus deficiency in Lupinus albus. Altered lateral root development and enhanced expression of phosphoenolpyruvate carboxylase. Plant Physiol. 112: 31–41.

K

Kang, N.Y., Lee, H.W., and Kim, J. (2013). The AP2/EREBP gene PUCHI co-acts with LBD16/ASL18 and LBD18/ASL20 downstream of ARF7 and ARF19 to regulate lateral root development in arabidopsis. Plant Cell Physiol. 54: 1326–1334.

Karas, I. and McCully, M.E. (1973). Further Studies of the Histology of Lateral Root Development in Zea mays. Protopl 269: 243–269.

Karimi, M., Inze, D., and Depicker, A. (2002). {GATEWAY} vectors for \textit{Agrobacterium}-mediated plant transformation. Trends Plant Sci. 7: 193–195.

Kasahara, H. (2016). Current aspects of auxin biosynthesis in plants. Biosci. Biotechnol. Biochem. 80: 34–42.

Katoh, K. and Standley, D.M. (2013). MAFFT multiple sequence alignment software version 7: Improvements in performance and usability. Mol. Biol. Evol. 30: 772–780.

Kepinski, S. and Leyser, O. (2005). The Arabidopsis F-box protein TIR1 is an auxin receptor. Nature 435: 446–451.

Kim, J., Harter, K., and Theologis, A. (1997). Protein-protein interactions among the Aux/IAA proteins. Proc. Natl. Acad. Sci. U. S. A. 94: 11786–91.

Kögl, F., Erxleben, H., and Haagen-Smit, A.J. (1934). Über die Isolierung der Auxine a und b aus pflanzlichen Materialien . Hoppe-Seyler´ s Zeitschrift für Physiol. Chemie 225: 215–229.

Komatsu, M., Chujo, A., Nagato, Y., Shimamoto, K., and Kyozuka, J. (2003). Frizzy panicle is required to prevent the formation of axillary meristems and to establish floral meristem identity in rice spikelets. Development 130: 3841–3850.

Korasick, D.A., Enders, T.A., and Strader, L.C. (2013). Auxin biosynthesis and storage forms. J. Exp. Bot. 64: 2541–2555.

Korasick, D.A., Westfall, C.S., Lee, S.G., Nanao, M.H., Dumas, R., Hagen, G., Guilfoyle, T.J., Jez, J.M., and Strader, L.C. (2014). Molecular basis for AUXIN RESPONSE FACTOR protein interaction and the control of auxin response repression. Proc. Natl. Acad. Sci. 111: 5427–5432.

Křeček, P., Skůpa, P., Libus, J., Naramoto, S., Tejos, R., Friml, J., and Zažímalová, E. (2009). The PIN-FORMED (PIN) protein family of auxin transporters. Genome Biol. 10: 249.

Krogan, N.T., Hogan, K., and Long, J.A. (2012). APETALA2 negatively regulates multiple floral organ identity genes in Arabidopsis by recruiting the co-repressor TOPLESS and the histone deacetylase HDA19. Development 139: 4180–4190.

Kumpf, R.P., Shi, C.-L., Larrieu, A., Sto, I.M., Butenko, M.A., Peret, B., Riiser, E.S., Bennett, M.J., and Aalen, R.B. (2013). Floral organ abscission peptide IDA and its HAE/HSL2 receptors control cell separation during lateral root emergence. Proc. Natl. Acad. Sci. 110: 5235–5240.

Kurihara, D., Mizuta, Y., Sato, Y., and Higashiyama, T. (2015). ClearSee: a rapid optical clearing reagent for whole-plant fluorescence imaging. Development 142: 4168–4179.

Kuusk, S., Sohlberg, J.J., Long, J.A., Fridborg, I., and Sundberg, E. (2002). STY1 and STY2 promote the formation of apical tissues during Arabidopsis gynoecium development. Development 129: 4707–4717.

L

Lambers, H., Clements, J.C., and Nelson, M.N. (2013). How phosphorus-acquisition strategy based on carboxylate exudation powers the success and agronomic potential of lupines (Lupinus,Fabaceae). Am. J. Bot. 100: 263–288.

Lambers, H., Cramer, M.D., Shane, M.W., Wouterlood, M., Poot, P., and Veneklaas, E.J. (2003). Structure and functioning of cluster roots and plant responses to phosphate deficiency. Plant Soil 248.

Lambers, H., Finnegan, P.M., Jost, R., Plaxton, W.C., Shane, M.W., and Stitt, M. (2015). Phosphorus nutrition in Proteaceae and beyond. Nat. Plants **1**: 1–9.

Lambers, H. and Shane, M.W. (2007). Role of Root Clusters in Phosphorus Acquisition and Increasing Biological Diversity in Agriculture. In Frontis, pp. 237–248.

Lambers, H., Shane, M.W., Cramer, M.D., Pearse, S.J., and Veneklaas, E.J. (2006). Root structure and functioning for efficient acquisition of phosphorus: Matching morphological and physiological traits. Ann. Bot. **98**: 693–713.

Lambers, H. and Teste, F.P. (2013). Interactions between arbuscular mycorrhizal and non-mycorrhizal plants: Do non-mycorrhizal species at both extremes of nutrient availability play the same game? Plant, Cell Environ. **36**: 1911–1915.

Lamont, B.B. (2003). Structure, ecology and physiology of root clusters - A review. Plant Soil **248**: 1–19.

Laplaze, L. et al. (2007). Cytokinins Act Directly on Lateral Root Founder Cells to Inhibit Root Initiation. Plant Cell Online **19**: 3889–3900.

Larrainzar, E. et al. (2015). Deep sequencing of the Medicago truncatula root transcriptome reveals a massive and early interaction between nodulation factor and ethylene signals.

Laskowski, M., Biller, S., Stanley, K., Kajstura, T., and Prusty, R. (2006). Expression profiling of auxin-treated Arabidopsis roots: Toward a molecular analysis of lateral root emergence. Plant Cell Physiol. **47**: 788–792.

Laskowski, M.J., Williams, M.E., Nusbaum, H.C., and Sussex, I.M. (1995). Formation of lateral root meristems is a two-stage process. Development **121**: 3303–3310.

Di Laurenzio, L., Wysocka-Diller, J., Malamy, J.E., Pysh, L., Helariutta, Y., Freshour, G., Hahn, M.G., Feldmann, K.A., and Benfey, P.N. (1996). The SCARECROW gene regulates an asymmetric cell division that is essential for generating the radial organization of the Arabidopsis root. Cell **86**: 423–433.

Lavenus, J., Goh, T., Roberts, I., Guyomarc'h, S., Lucas, M., De Smet, I., Fukaki, H., Beeckman, T., Bennett, M., and Laplaze, L. (2013). Lateral root development in Arabidopsis: Fifty shades of auxin. Trends Plant Sci. **18**: 1360–1385.

LeClere, S. (2004). IAR4, a Gene Required for Auxin Conjugate Sensitivity in Arabidopsis, Encodes a Pyruvate Dehydrogenase E1 Homolog. Plant Physiol. **135**: 989–999.

Lee, H.W. and Kim, J. (2013). EXPANSINA17 Up-Regulated by LBD18/ASL20 promotes lateral root formation during the auxin response. Plant Cell Physiol. **54**: 1600–1611.

Lee, H.W., Kim, N.Y., Lee, D.J., and Kim, J. (2009). LBD18/ASL20 Regulates Lateral Root Formation in Combination with LBD16/ASL18 Downstream of ARF7 and ARF19 in Arabidopsis. Plant Physiol. **151**: 1377–1389.

Lee, S., Sundaram, S., Armitage, L., Evans, J.P., Hawkes, T., Kepinski, S., Ferro, N., and Napier, R.M. (2014). Defining binding efficiency and specificity of auxins for SCF TIR1/AFB-Aux/IAA Co-receptor complex formation. ACS Chem. Biol. **9**: 673–682.

Lefort, V., Desper, R., and Gascuel, O. (2015). FastME 2.0: A comprehensive, accurate, and fast distance-based phylogeny inference program. Mol. Biol. Evol. **32**: 2798–2800.

Lemoine, R. et al. (2013). Source-to-sink transport of sugar and regulation by environmental factors. Front. Plant Sci. **4**: 1–21.

Li, H., Shen, J., Zhang, F., Marschner, P., Cawthray, G., and Rengel, Z. (2010). Phosphorus uptake and rhizosphere properties of intercropped and monocropped maize, faba bean, and white lupin in acidic soil. Biol. Fertil. Soils **46**: 79–91.

Li, S.-B., Xie, Z.-Z., Hu, C.-G., and Zhang, J.-Z. (2016). A Review of Auxin Response Factors (ARFs) in Plants. Front. Plant Sci. **7**: 1–7.

Li, X., Mo, X., Shou, H., and Wu, P. (2006). Cytokinin-mediated cell cycling arrest of pericycle founder cells in lateral root initiation of Arabidopsis. Plant Cell Physiol. **47**: 1112–1123.

Liao, C.Y., Smet, W., Brunoud, G., Yoshida, S., Vernoux, T., and Weijers, D. (2015). Reporters for sensitive and quantitative measurement of auxin response. Nat. Methods **12**: 207–210.

Lie Sevin-Pujol, A., Sicard, M., Rosenberg, C., Auriac, M.-C., Lepage, A., Niebel, A., Gough, C., and Bensmihen, S. (2017). Development of a GAL4-VP16/UAS trans- activation system for tissue specific expression in Medicago truncatula.: 1–14.

Liu, W., Yu, J., Ge, Y., Qin, P., and Xu, L. (2018). Pivotal role of LBD16 in root and root-like organ initiation. Cell. Mol. Life Sci.

Livak, K.J. and Schmittgen, T.D. (2001). Analysis of Relative Gene Expression Data Using Real-Time Quantitative PCR and the 2−ΔΔCT Method. Methods **25**: 402–408.

Ljung, K. (2013). Auxin metabolism and homeostasis during plant development. Development **140**: 943–950.

Ljung, K., Bhalerao, R.P., and Sandberg, G. (2001). Sites and homeostatic control of auxin biosynthesis in Arabidopsis during vegetative growth. Plant J. **28**: 465–474.

Ljung, K., Hull, A.K., Celenza, J., Yamada, M., Estelle, M., Normanly, J., and Sandberg, G. (2005). Sites and regulation of auxin biosynthesis in Arabidopsis roots. Plant Cell **17**: 1090–104.

Lloret, P.G., Casero, P.J., Pulgarin, A., and Navascués, J. (1989). The Behaviour of Two Cell Populations in the Pericycle of Allium cepa, Pisum sativum, and Daucus carota During Early Lateral Root Development. Ann. Bot. **63**: 465–475.

Long, J.A., Ohno, C., Smith, Z.R., and Meyerowitz, E.M. (2006). TOPLESS regulates apical embryonic fate in Arabidopsis. Science (80-.). **312**: 1520–1523.

López-Bucio, J., Hernández-Abreu, E., Sánchez-Calderón, L., Nieto-Jacobo, M.F., Simpson, J., and Herrera-Estrella, L. (2002). Phosphate availability alters architecture and causes changes in hormone sensitivity in the Arabidopsis root system. Plant Physiol. **129**: 244–256.

Łotocka, B., Kopcińska, J., and Skalniak, M. (2012). Review article: The meristem in indeterminate root nodules of Faboideae. Symbiosis **58**: 63–72.

Lucas, M. et al. (2013). Lateral root morphogenesis is dependent on the mechanical properties of the overlaying tissues. Proc. Natl. Acad. Sci. **110**: 5229–5234.

Lucas, M. et al. (2011). SHORT-ROOT Regulates Primary, Lateral, and Adventitious Root Development in Arabidopsis. Plant Physiol. **155**: 384–398.

Luo, J., Zhou, J.J., and Zhang, J.Z. (2018). Aux/IAA gene family in plants: Molecular structure, regulation, and function. Int. J. Mol. Sci. **19**: 1–17.

Lynch, J.P. and Brown, K.M. (2001). Topsoil foraging - An architectural adaptation of plants to low phosphorus availability. Plant Soil **237**: 225–237.

M

Mähönen, A.P., Tusscher, K., Siligato, R., and Smetana, O. (2015). PLETHORA gradient formation mechanism separates auxin responses. **515**: 125–129.

Malamy, J.E. and Benfey, P.N. (1997). Organization and cell differentiation in lateral roots of Arabidopsis thaliana. Development **124**: 33–44.

Mallory, T.E., Chiang, S.-H., Cutter, E.G., and Gifford, E.M. (1970). Sequence and Pattern of Lateral Root Formation in Five Selected Species. Am. J. Bot. **57**: 800–809.

Marchant, A., Bhalerao, R., Casimiro, I., Eklöf, J., Casero, P.J., Bennett, M., and Sandberg, G. (2002). AUX1 promotes lateral root formation by facilitating indole-3-acetic acid distribution between sink and source tissues in the Arabidopsis seedling. Plant Cell **14**: 589–97.

Marquès-Bueno, M.M., Morao, A.K., Cayrel, A., Platre, M.P., Barberon, M., Caillieux, E., Colot, V., Jaillais, Y., Roudier, F., and Vert, G. (2016). A versatile Multisite Gateway-compatible promoter and transgenic line collection for cell type-specific functional genomics in Arabidopsis. Plant J. **85**: 320–333.

Marschner, H., Kirkby, E.A., and Cakmak, I. (1996). Effect of mineral nutritional status on shoot-root partitioning of photoassimilates and cycling of mineral nutrients. J. Exp. Bot. **47**: 1255–1263.

Marschner, H., Römheld, V., and Cakmak, I. (1987). Root-induced changes of nutrient availability in the rhizosphere. J. Plant Nutr. **10**: 1175–1184.

Massonneau, A., Langlade, N., Léon, S., Smutny, J., Vogt, E., Neumann, G., and Martinoia, E. (2001). Metabolic changes associated with cluster root development in white lupin (Lupinus albus L.): Relationship between organic acid excretion, sucrose metabolism and energy status. Planta **213**: 534–542.

McSteen, P. and Leyser, O. (2005). Shoot Branching. Annu. Rev. Plant Biol. **56**: 353–374.

Meng, Z.B., Chen, L.Q., Suo, D., Li, G.X., Tang, C.X., and Zheng, S.J. (2012). Nitric oxide is the shared signalling molecule in phosphorus- and iron-deficiency-induced formation of cluster roots in white lupin (Lupinus albus). Ann. Bot. **109**: 1055–1064.

Meng, Z. Bin, You, X. Di, Suo, D., Chen, Y.L., Tang, C., Yang, J.L., and Zheng, S.J. (2013). Root-derived auxin contributes to the phosphorus-deficiency-induced cluster-root formation in white lupin (Lupinus albus). Physiol. Plant. **148**: 481–489.

Moreno-Risueno, M.A., Van Norman, J.M., Moreno, A., Zhang, J., Ahnert, S.E., and Benfey, P.N. (2010). Oscillating gene expression determines competence for periodic Arabidopsis root branching. Science. **329**: 1306–1311.

Muday, G.K., Rahman, A., and Binder, B.M. (2012). Auxin and ethylene: Collaborators or competitors? Trends Plant Sci. **17**: 181–195.

N

Nacry, P., Canivenc, G., Muller, B., Azmi, A., Onckelen, H. Van, Rossignol, M., and Doumas, P. (2005). A Role for Auxin Redistribution in the Responses of the Root System Architecture to Phosphate Starvation in Arabidopsis. Plant Physiol. **138**: 2061–2074.

Nakajima, K., Sena, G., Nawy, T., and Benfey, P.N. (2001). Intercellular movement of the putative transcription factor SHR in root patterning. Nature **413**: 307–311.

Nanao, M.H. et al. (2014). Structural basis for oligomerization of auxin transcriptional regulators. Nat. Commun. **5**: 3617.

Negi, S., Ivanchenko, M.G., and Muday, G.K. (2008). Ethylene regulates lateral root formation and auxin transport in Arabidopsis thaliana. Plant J. **55**: 175–187.

Neumann, G., Massonneau, A., Langlade, N., Dinkelaker, B., Hengeler, C., Römheld, V., and Martinoia, E. (2000). Physiological aspects of cluster root function and development in phosphorus-deficient white lupin (Lupinus albus L.). Ann. Bot. **85**: 909–919.

Neumann, G. and Martinoia, E. (2002). Cluster roots - An underground adaptation for survival in extreme environments. Trends Plant Sci. **7**: 162–167.

Nibau, C., Gibbs, D.J., and Coates, J.C. (2008). Branching out in new directions: the control of root architecture by lateral root formation. New Phytol.

O

O'Rourke, J. a., Yang, S.S., Miller, S.S., Bucciarelli, B., Liu, J., Rydeen, a., Bozsoki, Z., Uhde-Stone, C., Tu, Z.J., Allan, D., Gronwald, J.W., and Vance, C.P. (2013). An RNA-Seq Transcriptome Analysis of Orthophosphate-Deficient White Lupin Reveals Novel Insights into Phosphorus

Acclimation in Plants. Plant Physiol. 161: 705–724.
Ohta, M., Matsui, K., Hiratsu, K., Hideaki, S., and Masaru, O.-T. (2001). Repression Domains of Class II ERF Transcriptional Repressors Share an Essential Motif for Active Repression. Plant Cell 13: 1959–1968.
Okushima, Y., Fukaki, H., Onoda, M., Theologis, A., and Tasaka, M. (2007). ARF7 and ARF19 Regulate Lateral Root Formation via Direct Activation of LBD/ASL Genes in Arabidopsis. Plant Cell Online 19: 118–130.
Olsen, A.N., Ernst, H.A., Leggio, L. Lo, and Skriver, K. (2005). NAC transcription factors: Structurally distinct, functionally diverse. Trends Plant Sci. 10: 79–87.
Op den Camp, R.H.M., De Mita, S., Lillo, A., Cao, Q., Limpens, E., Bisseling, T., and Geurts, R. (2011). A Phylogenetic Strategy Based on a Legume-Specific Whole Genome Duplication Yields Symbiotic Cytokinin Type-A Response Regulators. Plant Physiol. 157: 2013–2022.
Orman-Ligeza, B., Parizot, B., Gantet, P.P., Beeckman, T., Bennett, M.J., and Draye, X. (2013b). Post-embryonic root organogenesis in cereals: Branching out from model plants. Trends Plant Sci. 18: 459–467.
Overvoorde, P. et al. (2005). Functional genomic analysis of the AUXIN/INDOLE-3-ACETIC ACID gene family members in Arabidopsis thaliana. Plant Cell 17: 3282–3300.

P

Paponov, I.A., Paponov, M., Teale, W., Menges, M., Chakrabortee, S., Murray, J.A.H., and Palme, K. (2008). Comprehensive transcriptome analysis of auxin responses in Arabidopsis. Mol. Plant 1: 321–337.
Park, J., Lee, Y., Martinoia, E., and Geisler, M. (2017). Plant hormone transporters: What we know and what we would like to know. BMC Biol. 15: 1–15.
Pattison, R.J., Csukasi, F., and Catalá, C. (2014). Mechanisms regulating auxin action during fruit development. Physiol. Plant. 151: 62–72.
Peñaloza, E., Gutierrez, A., Martínez, J., Muñoz, G., Bravo, L. a, and Corcuera, L.J. (2002). Differential gene expression in proteoid root clusters of white lupin (Lupinus albus). Physiol. Plant. 116: 28–36.
Péret, B. et al. (2012). AUX/LAX Genes Encode a Family of Auxin Influx Transporters That Perform Distinct Functions during Arabidopsis Development. Plant Cell 24: 2874–2885.
Péret, B., Clément, M., Nussaume, L., and Desnos, T. (2011). Root developmental adaptation to phosphate starvation: Better safe than sorry. Trends Plant Sci. 16: 442–450.
Péret, B., Larrieu, A., and Bennett, M.J. (2009a). Lateral root emergence: A difficult birth. J. Exp. Bot. 60: 3637–3643.
Péret, B., De Rybel, B., Casimiro, I., Benková, E., Swarup, R., Laplaze, L., Beeckman, T., and Bennett, M.J. (2009b). Arabidopsis lateral root development: an emerging story. Trends Plant Sci. 14: 399–408.
Petrasek, J. and Friml, J. (2009). Auxin transport routes in plant development. Development 136: 2675–2688.
Poo, M. and Cone, R.A. (1974). Proteoid roots are microbially induced. Nature 251: 316–317.
Porco, S. et al. (2016). Lateral root emergence in *Arabidopsis* is dependent on transcription factor LBD29 regulation of auxin influx carrier *LAX3*. Development 143: 3340–3349.
Prát, T., Hajný, J., Grunewald, W., Vasileva, M., Molnár, G., Tejos, R., Schmid, M., Sauer, M., and Friml, J. (2018). WRKY23 is a component of the transcriptional network mediating auxin feedback on PIN polarity. PLoS Genet. 14: 1–18.
Purnell, H.M. (1960). Studies of the family proteaceae i. Anatomy and mophology op the boots op some victorian species. Aust. J. Bot. 8: 38–50.

Q

Quan, R., Wang, J., Yang, D., Zhang, H., Zhang, Z., and Huang, R. (2017). EIN3 and SOS2 synergistically modulate plant salt tolerance. Sci. Rep. **7**: 1–11.

R

Rampey, R.A., Leclere, S., Kowalczyk, M., Ljung, K., Bartel, B., Biology, C., and Texas, R.A.R. (2004). A family of auxin-conjugate hydrolases that contributes to free indole-3-acetic acid levels during Arabidopsis germination. Plant Physiol. **135**: 978–988.

Riechmann, J.L. and Meyerowitz, E.M. (1998). The AP2/EREBP family of plant transcription factors. Biol. Chem. **379**: 633–646.

Rubio, V., Bustos, R., Irigoyen, M.L., Cardona-López, X., Rojas-Triana, M., and Paz-Ares, J. (2009). Plant hormones and nutrient signaling. Plant Mol. Biol. **69**: 361–373.

Ruiz Rosquete, M., Barbez, E., and Kleine-Vehn, J. (2012). Cellular auxin homeostasis: Gatekeeping is housekeeping. Mol. Plant **5**: 772–786.

De Rybel, B. et al. (2010). A novel Aux/IAA28 signaling cascade activates GATA23-dependent specification of lateral root founder cell identity. Curr. Biol. **20**: 1697–1706.

S

Sabatini, S., Beis, D., Wolkenfelt, H., Murfett, J., Guilfoyle, T., Malamy, J., Benfey, P., Leyser, O., Bechtold, N., Weisbeek, P., and Scheres, B. (1999). An auxin-dependent distal organizer of pattern and polarity in the Arabidopsis root. Cell **99**: 463–472.

Dos Santos Maraschin, F., Memelink, J., and Offringa, R. (2009). Auxin-induced, SCFTIR1-mediated poly-ubiquitination marks AUX/IAA proteins for degradation. Plant J. **59**: 100–109.

Sas, L., Rengel, Z., and Tang, C. (2001). Excess cation uptake, and extrusion of protons and organic acid anions by Lupinus albus under phosphorus deficiency. Plant Sci. **160**: 1191–1198.

Sas, L., Zed, R., and Tang, C. (2002). The effect of nitrogen nutrition on cluster root formation and proton extrusion by Lupinus albus. Ann. Bot. **89**: 435–442.

Sato, A., & Yamamoto, K. T. (2008). Overexpression of the non-canonical Aux/IAA genes causes auxin-related aberrant phenotypes in Arabidopsis. Physiologia plantarum, *133*(2), 397-405

Sbabou, L., Bucciarelli, B., Miller, S., Liu, J., Berhada, F., Filali-Maltouf, a., Allan, D., and Vance, C. (2010). Molecular analysis of SCARECROW genes expressed in white lupin cluster roots. J. Exp. Bot. **61**: 1351–1363.

Scarpella, E., Barkoulas, M., and Tsiantis, M. (2010). Control of leaf and vein development by auxin. Cold Spring Harb. Perspect. Biol. **2**: a001511.

Secco, D., Shou, H., Whelan, J., and Berkowitz, O. (2014). RNA-seq analysis identifies an intricate regulatory network controlling cluster root development in white lupin. BMC Genomics **15**: 230.

Shane, M.W., De Vos, M., De Roock, S., and Lambers, H. (2003). Shoot P status regulates cluster-root growth and citrate exudation in Lupinus albus grown with a divided root system. Plant, Cell Environ. **26**: 265–273.

Shimizu-Mitao, Y. and Kakimoto, T. (2014). Auxin sensitivities of all arabidopsis aux/IAAs for degradation in the presence of every TIR1/AFB. Plant Cell Physiol. **55**: 1450–1459.

Shishkova, S., Rost, T.L., and Dubrovsky, J.G. (2008). Determinate root growth and meristem maintenance in angiosperms. Ann. Bot. **101**: 319–340.

Shu, L., Shen, J., Rengel, Z., Tang, C., and Zhang, F. (2007). Cluster root formation by Lupinus albus is modified by stratified application of phosphorus in a split-root system. J. Plant

Nutr. **30**: 271–288.

Sitbon, F., Åstot, C., Edlund, A., Crozier, A., and Sandberg, G. (2000). The relative importance of tryptophan-dependent and tryptophan-independent biosynthesis of indole-3-acetic acid in tobacco during vegetative growth. Planta **211**: 715–721.

Skene, K.R., Kierans, M., Sprent, J.I., and Raven, J.A. (1996). Structural aspects of cluster root development and their possible significance for nutrient acquisition in Grevillea robusta (Proteaceae). Ann. Bot. **77**: 443–451.

Skene, K.R. (1998). Cluster roots: some ecological considerations. J. Ecol. **86**: 1060–1064.

Skene, K.R. and James, W.M. (2000). A comparison of the effects of auxin on cluster root initiation and development in Grevillea robusta Cunn. ex R. Br. (Proteaceae) and in the genus Lupinus (Leguminosae). Plant Soil **219**: 221–229.

Skene, K.R. (2000). Pattern Formation in Cluster Roots: Some Developmental and Evolutionary Considerations. Ann. Bot. **85**: 901–908.

Skene, K.R. (2001). Cluster roots: model experimental tools for key biological problems. J. Exp. Bot. **52**: 479–485.

Skene, K.R. (2003). The evolution of physiology and development in the cluster root: Teaching an old dog new tricks? Plant Soil **248**: 21–30.

De Smet, I. et al. (2007). Auxin-dependent regulation of lateral root positioning in the basal meristem of Arabidopsis. Development **134**: 681–690.

De Smet, I. et al. (2010). Bimodular auxin response controls organogenesis in Arabidopsis. Proc. Natl. Acad. Sci. **107**: 2705–2710.

De Smet, I. (2012). Lateral root initiation: one step at a time. New Phytol. **193**: 867–873.

De Smet, I., Vanneste, S., Inzé, D., and Beeckman, T. (2006). Lateral root initiation or the birth of a new meristem. Plant Mol. Biol. **60**: 871–887.

Smolarkiewicz, M. and Dhonukshe, P. (2013). Formative cell divisions: Principal determinants of plant morphogenesis. Plant Cell Physiol. **54**: 333–342.

Sozzani, R., Murray, J.A.H., Busch, W., Cui, H., Vernoux, T., Van Norman, J.M., Dewitte, W., Brady, S.M., Moreno-Risueno, M.A., and Benfey, P.N. (2010). Spatiotemporal regulation of cell-cycle genes by SHORTROOT links patterning and growth. Nature **466**: 128.

Ståldal, V., Cierlik, I., Landberg, K., Myrenås, M., Sundström, J.F., Eklund, D.M., Chen, S., Baylis, T., Ljung, K., and Sundberg, E. (2012). The Arabidopsis thaliana transcriptional activator STYLISH1 regulates genes affecting stamen development, cell expansion and timing of flowering. Plant Mol. Biol. **78**: 545–559.

Swarup, K. et al. (2008). The auxin influx carrier LAX3 promotes lateral root emergence. Nat. Cell Biol. **10**: 946–954.

Swarup, R. and Péret, B. (2012). AUX/LAX family of auxin influx carriers—an overview. Front. Plant Sci. **3**: 1–11.

Szemenyei, H., Hannon, M., and Long, J.A. (2008). TOPLESS mediates auxin-dependent transcriptional repression during Arabidopsis embryogenesis. Science (80-.). **319**: 1384–1386.

T

Tang, H., Shen, J., Zhang, F., and Rengel, Z. (2013). Interactive effects of phosphorus deficiency and exogenous auxin on root morphological and physiological traits in white lupin (Lupinus albus L.). Sci. China Life Sci. **56**: 313–323.

Tian, H., De Smet, I., and Ding, Z. (2014). Shaping a root system: Regulating lateral versus primary root growth. Trends Plant Sci. **19**: 426–431.

Tiwari, S.B., Hagen, G., and Guilfoyle, T. (2003). The roles of auxin response factor domains in

auxin-responsive transcription. Plant Cell **15**: 533–43.

Torres-Martínez, H.H., Rodríguez-Alonso, G., Shishkova, S., and Dubrovsky, J.G. (2019). Lateral Root Primordium Morphogenesis in Angiosperms. Front. Plant Sci. **10**.

Toyokura, K. et al. (2018). Lateral Inhibition by a Peptide Hormone-Receptor Cascade during Arabidopsis Lateral Root Founder Cell Formation. Dev. Cell: 1–12.

Trinh, C.D., Laplaze, L., and Guyomarc'h, S. (2018). Lateral Root Formation: Building a Meristem *de novo*.

U

Uhde-Stone, C., Gilbert, G., Johnson, J.M.F., Litjens, R., Zinn, K.E., Temple, S.J., Vance, C.P., and Allan, D.L. (2003). Acclimation of white lupin to phosphorus deficiency involves enhanced expression of genes related to organic acid metabolism. Plant Soil **248**: 99–116.

Uhde-Stone, C., Liu, J., Zinn, K.E., Allan, D.L., and Vance, C.P. (2005). Transgenic proteoid roots of white lupin: A vehicle for characterizing and silencing root genes involved in adaptation to P stress. Plant J. **44**: 840–853.

Ulmasov, T., Murfett, J., Hagen, G., and Guilfoyle, T. (1997). Aux/IAA proteins repress expression of reporter genes containing natural and highly active synthetic auxin response elements. Plant Cell **9**: 1963–1971.

V

Vance, C.P., Uhde-Stone, C., and Allan, D.L. (2003). Phosphorus aquisition and use: critical adaptations by plants for securing a nonrewable resource. New Phytol. **157**: 423–447.

Van Mourik, H., van Dijk, A. D., Stortenbeker, N., Angenent, G. C., & Bemer, M. (2017). Divergent regulation of Arabidopsis SAUR genes: a focus on the SAUR10-clade. *BMC plant biology*, *17*(1), 245.

Venuti, S., Zanin, L., Marroni, F., Franco, A., Morgante, M., Pinton, R., and Tomasi, N. (2019). Physiological and transcriptomic data highlight common features between iron and phosphorus acquisition mechanisms in white lupin roots. Plant Sci.

Vermeer, J.E.M. and Geldner, N. (2015). Lateral root initiation in Arabidopsis thaliana: a force awakens. F1000Prime Rep. **7**: 1–7.

Vermeer, J.E.M., von Wangenheim, D., Barberon, M., Lee, Y., Stelzer, E.H.K., Maizel, A., and Geldner, N. (2014). A Spatial Accommodation by Neighboring Cells Is Required for Organ Initiation in Arabidopsis. Science (80-.). **343**: 178–183.

Vert, G., Walcher, C.L., Chory, J., and Nemhauser, J.L. (2008). Integration of auxin and brassinosteroid pathways by Auxin Response Factor 2. Proc. Natl. Acad. Sci. **105**: 9829–9834.

Vieten, A., Sauer, M., Brewer, P.B., and Friml, J. (2007). Molecular and cellular aspects of auxin-transport-mediated development. Trends Plant Sci. **12**: 160–168.

Villalobos, L.I. a C. et al. (2012). A combinatorial TIR1/AFB-Aux/IAA co-receptor system for differential sensing of auxin. Nat. Chem. Biol. **8**: 477.

Vorster, P.W. and Jooste, J.H. (1986). Potassium and phosphate absorption by excised ordinary and proteoid roots of the Proteaceae. South African J. Bot. **52**: 277–281.

W

Wang, Z., Rahman, A.M., Wang, G., Ludewig, U., Shen, J., and Neumann, G. (2015a). Hormonal interactions during cluster-root development in phosphate-deficient white lupin (Lupinus albus L.). J. Plant Physiol. **177**: 74–82.

Wang, Z., Shen, J., Ludewig, U., and Neumann, G. (2015b). A re-assessment of sucrose signaling involved in cluster-root formation and function in phosphate-deficient white lupin

(Lupinus albus). Physiol. Plant. **154**: 407–419.

Wang, Z., Straub, D., Yang, H., Kania, A., Shen, J., Ludewig, U., and Neumann, G. (2014). The regulatory network of cluster-root function and development in phosphate-deficient white lupin (Lupinus albus) identified by transcriptome sequencing. Physiol. Plant. **151**: 323–38.

Von Wangenheim, D., Fangerau, J., Schmitz, A., Smith, R.S., Leitte, H., Stelzer, E.H.K., and Maizel, A. (2016). Rules and self-organizing properties of post-embryonic plant organ cell division patterns. Curr. Biol. **26**: 439–449.

Watt, M. and Evans, J. (1999a). Linking Development and Determinacy with Organic Acid Efflux from Proteoid Roots of White Lupin Grown with Low Phosphorus and Ambient or Elevated Atmospheric CO2 Concentration. Plant Physiol. **120**: 705–716.

Watt, M. and Evans, J.R. (1999b). Proteoid Roots. Physiology and Development. Plant Physiol. **121**: 317–323.

Willemsen, V., Bauch, M., Bennett, T., Campilho, A., Wolkenfelt, H., Xu, J., Haseloff, J., and Scheres, B. (2008). The NAC Domain Transcription Factors FEZ and SOMBRERO Control the Orientation of Cell Division Plane in Arabidopsis Root Stem Cells. Dev. Cell **15**: 913–922.

Wisniewska, J. (2006). Polar PIN Localization Directs Auxin Flow in Plants. Science (80-.). **312**: 883–883.

Wright, A.D.S., M. B., N., M. G., M., L., Slovin, J.P., and Cohen, J.D. (1991). Indole-3-acetic acid biosynthesis in the mutant maize orange pericarp, a tryptophan auxotroph. Science (80-.). **254**: 998–1000.

X

Xiao, T.T., Schilderink, S., Moling, S., Deinum, E.E., Kondorosi, E., and Franssen, H. (2014). Fate map of Medicago truncatula root nodules. Development **141**: 3517–3528.

Xuan, W., Audenaert, D., Parizot, B., Möller, B.K., Njo, M.F., De Rybel, B., De Rop, G., Van Isterdael, G., Mähönen, A.P., Vanneste, S., and Beeckman, T. (2015). Root cap-derived auxin pre-patterns the longitudinal axis of the arabidopsis root. Curr. Biol. **25**: 1381–1388.

Y

Yan, F., Zhu, Y., Mu, C., Zo, C., and Schubert, S. (2002). Adaptation of H-Pumping and Plasma Membrane H ATPase Activity in Proteoid Roots of White Lupin under Phosphate Deficiency 1. Plant Physiol. **129**: 50–63.

Yoshida, S., BarbierdeReuille, P., Lane, B., Bassel, G.W., Prusinkiewicz, P., Smith, R.S., and Weijers, D. (2014). Genetic control of plant development by overriding a geometric division rule. Dev. Cell **29**: 75–87.

Z

Zanin, L., Venuti, S., Marroni, F., Franco, A., Morgante, M., Pinton, R., and Tomasi, N. (2019). Physiological and RNA sequencing data of white lupin plants grown under Fe and P deficiency. Data Br. **25**: 104069.

Zazímalová, E., Murphy, A.S., Yang, H., Hoyerova, K., and Hosek, P. (2010). Auxin Transporters — Why So Many ? Cold Spring Harb. Perspect. Biol. **2**: a001552.

Zhao, Y. (2012). Auxin biosynthesis: A simple two-step pathway converts tryptophan to indole-3-Acetic acid in plants. Mol. Plant **5**: 334–338.

Zhou, K., Yamagishi, M., Osaki, M., and Masuda, K. (2008). Sugar signalling mediates cluster root formation and phosphorus starvation-induced gene expression in white lupin. J. Exp. Bot. **59**: 2749–2756.